

Project MANTIS

Final Report

Group 2



Project MANTIS

Final Report

by

Group 2

in completion of the fourth deliverable of the DSE Fall 2019 in order to obtain the degree of
Bachelor of Science
at the Faculty of Aerospace Engineering at Delft University of Technology.

Project duration: 11 November 2019 - 31 January 2020

Version	Date	Comment	Responsible	Approved by
1.0	12 - 12 - 19	Document created	Yannick	QC
1.1	16-12-19	Functional Analysis & Design Concepts added	Thomas	QC
1.1.1	9 - 01 - 20	Subsystems chapter added	Lars	QC
1.2	22 - 01 - 20	PM/SE Draft NOT final Draft	Thomas	QC
1.3	23 - 01 - 20	Final Draft	Thomas	QC
2.0	28 - 01 - 20	Final Report for DSE	Thomas	QC

Student:	Y.	Jannette Walen	4231678
	T.	Janz	4352777
	L.	Peschke	4471857
	M.	Rehbein	4460936
	N.	Voß	4550749
	D. C.	Saadeldin	4163672
	C. P.	Tranquille	4444841
	M. M. M.	D'heer	4557476
	L. C. J.	Haagh	4550366
R. F. A.	Wassenaar	4549074	

Tutor:	Ir.	M. C.	Naeije	TU Delft
Coach:	M.Sc.	F. K.	Leverone	TU Delft
Coach:	Ir.	J.	Sinke	TU Delft
Client:	Ir.	H.	Cruijssen	AIRBUS D&S NL

Acknowledgements

The group would like to thank our tutor Marc Naeije for the tremendous support during the project. He guided us throughout the whole project in technical and managerial ways. Furthermore, we would like to thank our coaches Jos Sinke and Fiona Leverone as well. They helped us a lot by giving feedback on the report and coach us in, especially, the management aspect. This team of three experts in their own fields joined us in the weekly status meetings and gave us feedback on the status of the project. This helped us a lot in going into the right direction.

We would also like to thank our client, Airbus Defence & Space NL, especially Henk Cruijssen, for providing us with the opportunity to work out this project. He guided us during (nearly) weekly video meetings and helped us in finding literature for our research. Furthermore, we want to thank his colleague, Lex Meijer who answered our questions regarding the ADCS subsystem.

Lastly, we would like to thank the experts present at the TU Delft. Erwin Mooij helped us a lot in setting up the project through his lectures and expertise in Project Management & Systems Engineering (PM/SE). Jasper Bouwmeester helped us a lot in designing the assembly and docking system. Eddy van den Bos also helped us in visualising Project MANTIS by assisting us with CATIA software. He also arranged a Virtual Reality session, where we could virtually 'walk around' the CATIA drawings we made. This helped us a lot in visualising the assembly methods.

Abstract

Assembly, Integration and Verification (AIV) in space makes launching geosynchronous satellites faster and significantly cheaper in the long term. A space-tug is launched into space to perform AIV there. It assembles a standardised satellite consisting of several modules. The modules are designed in such a way that the required subsystems for a communication satellite are incorporated in the modules. Examples of these modules are a propulsion module, a solar array module and a computer module. Due to the standardised modules, testing time and costs can be reduced significantly. This ensures a delivery time of maximum one year, which is the time from order until operations in space. The modules are efficiently packed and connected to external beams in the launch vehicle, to make sure that two satellites can be launched simultaneously. The external beams take up the extreme loads that occur during launch. This decreases the dry mass of the satellite, as the modules do not need as much structural mass. The subsystem design and structural analysis result in a dry mass of 1847 kg per satellite. Next to the two satellites, a refuelling tank is added in the launch vehicle to refuel the tug. The tug requires 2921 kg of fuel to transfer the two satellites and go back to its initial state. Due to the modularity of the satellites, the lifetime of the satellites can be increased. Regarding the economic feasibility of the mission, a full return on investment is expected after 15 years of operations in base case scenario.

Key words: Assembly in space, Communication satellite, Verification & Validation, Modularity, Standardisation, short lead time, Mid Life Update

Executive Overview

The space industry has evolved a lot over its short history. From the initial experiments with rocketry, to the first artificial satellite in space, all the way to a multinational and truly global collaboration on the building of the ISS, this industry always strives to evolve.

For GEO telecommunication satellites, and the assembly of satellites in general, the next evolutionary step has to be made. Rather than designing, developing, building and testing on Earth prior to launch, the next step is to minimise and eliminate the inefficiencies and financial losses that originate from this process. The next step is to assemble, integrate and verify in orbit.

This evolution of the satellite manufacturing sector was brought about as the aim of the bachelor graduation project Design Synthesis Exercise (DSE) which describes this Assembly, Integration & Verification (AIV) system. Therefore, a Mission Need Statement (MNS) and Project Objective Statement (POS) were created, namely,

Mission Need Statement: *"Define a business case and create a space-born architecture able to perform assembly, integration and verification of spacecraft in space."*

Project Objective Statement: *"Develop an AIV design with 10 Students in 10 weeks that will be featured as a concept at the 71st International Astronautical Congress 2020, by invitation, on behalf of Airbus D&S NL."*

Design Concepts and Trade-off

In the previous phase of the project, several design concepts have been created, all capable of providing AIV in space. Four concepts have been generated.

RE²:The first concept was the RE² the Re-Assemble & Re-Use. It makes use of an assembly station located in a LEO orbit. The assembly is done via two robotic arms on a rail system. The satellite modules are sent up by a box carrier system. This box is sent up by the LV close to the station and with ADCS of the box carrier it docks to the station. After assembly, the telecommunication satellite transfers to its GEO mission orbit using electrical propulsion. This concept is adaptable to different markets being situated in LEO it has the possibility to assemble satellites for all orbits not just for GEO. A drawback is the high initial cost next to the modular satellite a whole assembly station and the box carrier system have to be developed. Another drawback is the throughput time due to the electrical propulsion of the telecommunication satellite the transition to GEO takes a long time (5 month) with that the requirement of one year throughput time is barely met.

TUG&PLAY: This concept entails a mobile assembly platform, the tug. The assembly is done by two robotic arms. The assembly takes place in an orbit a few 100 km below a GEO orbit. Prior to the assembly the modular satellite is launched as a module package into a GTO orbit where the TUG will rendezvous with the package and transfer to the assembly orbit. After assembly the telecommunication satellite reaches its final mission orbit on its own propulsion. This concept is a multi purpose system. It is a mobile platform capable of reaching orbits from LEO to GEO that does mean that all kinds of assembly missions in that orbit range are possible. Additionally it provides the possibility to add a space debris removal system to the tug. It could take back an old geo satellite to burn up in the atmosphere when it picks up the next satellite package in GTO.

SASSY: The third concept is SASSY the Self Assembling Space System. In comparison to the other concepts, the SASSY concept is assembling itself and does not need an additional assembly structure in space. The assembly will be done by a "walking" robotic arm. The satellite module package will be launched into GTO where the assembly of the necessary subsystems for the transfer is carried out first. The rest of the assembly is done during the transfer. The main advantage is the possibility to change the design of the modular satellite for every new mission however this flexibility also increases the cost of SASSY. Every satellite would need

its own robotic arm whereas the other concepts only need two robotic arms to assemble several satellites this increases the cost per satellite.

SAUS: The last concept SAUS the sub assembly unification station would make use of the ISS structure after its decommissioning in 2025. The satellites are launched with the already existing ISS resupply vehicles. Sub-assembly of satellites is done inside using a ring rail system with robotic arms. These sub parts will be put together outside the ISS. After assembly the Satellite transfers to its final GEO mission orbit on its own electrical propulsion. The main advantage of this concept is the fact that an already existing structure would be used which makes it the concept with the highest determined sustainability factor. Next to that it has some major disadvantages which are for one the high operating cost of the ISS. Additionally there are too many uncertainties when it comes to the ISS there is not a clear plan of what will happen after 2025 this imposes some high business risks for this concept.

As the detailed design phase requires the selection of a single concept to be pursued in more detail, a trade-off was performed. This trade-off evaluated the different options as shown in table 1.

The chosen weights can be seen under the respective criteria, with the final score being calculated as the sum of each score multiplied with the weight, which is then divided by the sum of weights. The highest score wins.

Table 1: Trade summary table; Upgr. = Upgradability, MA = Market Adaptability, TPT = Throughput Time, Sust. = Sustainability

Criterion Concept	Cost [10]	Sust. [7]	Upgr. [6]	Risk [6]	MA [5]	TPT [4]	Average Score
RE ²	4	3	3	4	4	1	3.3
TUG&PLAY	3	3	5	4	3	4	3.6
SASSY	2	1	1	3	5	2	2.2
SAUS	1	4	3	2	4	1	2.4

Based on the trade-off results various conclusions can be drawn. First of all an order of best performing concepts can be determined. Consequently the ranking is from best to worst: TUG&PLAY, RE², SAUS and lastly SASSY. Secondly, quantitatively, the best concept has a lead of 0.3 average score points. To make this difference more understandable, this means RE²'s score in a medium important category like upgradability or technical risk would have to increase by two points.

A local sensitivity analysis was performed. The major conclusion of this analysis was that the order of ranking does not change. Therefore it can be said with confidence that the trade-off is not sensitive to changing the weights and the decision to continue the design process with TUG&PLAY is justified. For these reasons and on account of the average scores the decision was made to continue the detailed design phase with TUG&PLAY now called Project MANTIS.

Detailed Design Approach

Having established a concept to be pursued in the final phase of the project, the team set about to design the system in more detail. Again, teams were formed to investigate the subsystems and develop the individual designs to a sufficient level that functionality can be reasonably analysed. Resources were also diverted to analyse other mission related topics and an overview of all the findings will be given in this section.

This report aims to present the approach to the detail design in a logical and stepwise manner of which the most important results will be presented in the following paragraphs. For an overview of where to the specific topics of the report, please refer to either chapter 1 or the table of contents.

Modular Assembly Network of Technology in Space(MANTIS)

As the tug had been selected as the most viable option to pursue, it was decided to get off to a somewhat fresh start, by naming the concept "MANTIS", as the looks of the spacecraft, equipped with two robot arms somewhat resemble the insect. For the arms, several existing technologies have been investigated, including a system designed by DARPA, whose mission objective is very similar to that of the tug. Additionally, work has been put into the design of ADCS, propulsion, communication, power, command and data handling, thermal control and structures subsystems and most importantly: the launch vehicle integration and assembly process. Also the management, sustainability and business aspects have been considered, coming together to form the design proposal that is being put forward.

MANTIS is a precursor of modern in space assembly technology and as such aims to make space access easier and more affordable. The demonstrator is designed to be capable of bringing communication satellite modules into geostationary orbit and assemble them into a functional system. To compete with current solutions it was decided to aim for a delivery time of one year from order to operational system in space. The basic staging of such a mission can be seen in fig. 1. In the first stage, the tug is waiting for a module package to be sent up. A rendezvous point is communicated and the tug approaches this point as dictated per schedule. As there will always be orbital discrepancies, the tug will be guided towards the package via ground radar, which is shown in stage two. Stage three consists of the tug and package, now being docked to each other, performing a maneuver to end up in GEO-. Once in that orbit, the tug will begin assembly of the satellite, as can be seen in stage four.

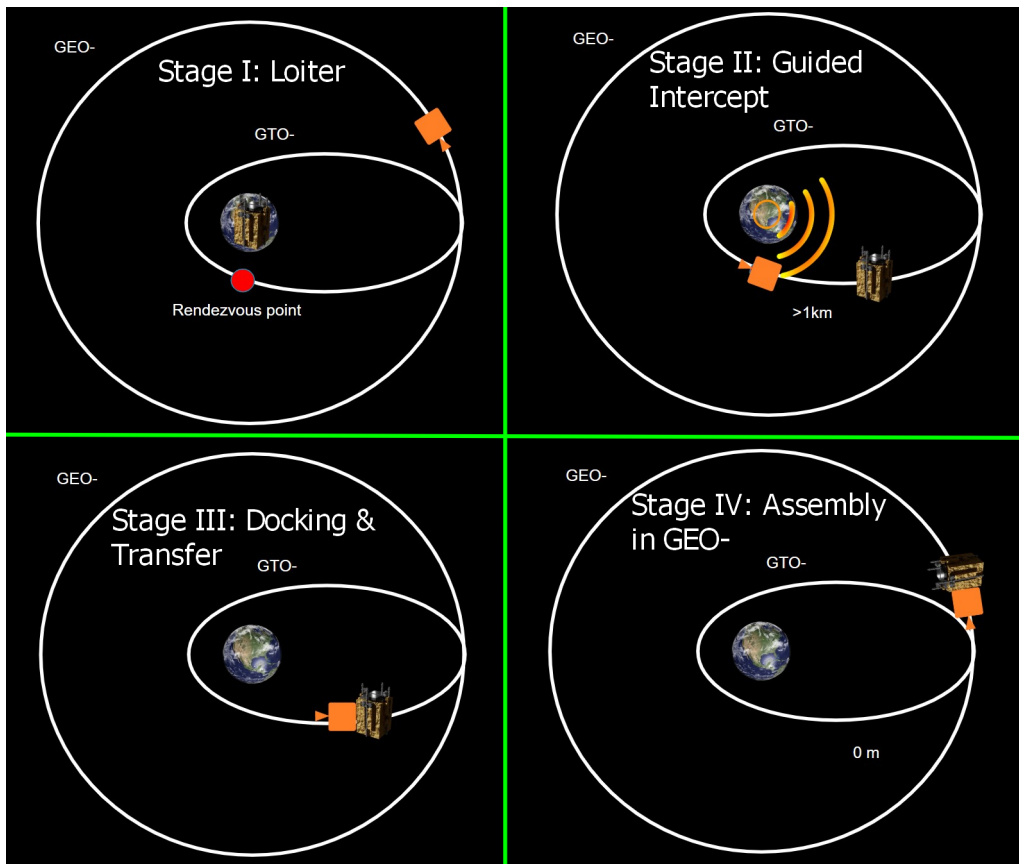


Figure 1: Mission Stages of MANTIS

MANTIS - Components

The system is based on two major hardware components. These are the tug and the modularised satellite components. We aim to show the technical and financial feasibility of the system by elaborating on the conceptual design and building a preliminary business case. For this, the components will be integrated into a Falcon 9 fairing, with the possibility of using the Ariane 5 in mind, with the individually discussed subsystems integrated as sized modules. Those are then rearranged into functional configuration once

the tug has successfully intercepted and transitioned the component package to GEO-. After completing assembly and verification the satellite will then ascend to the final GEO slot on its own power, using the same ionic thrusters that are utilised for ADCS and station keeping.

Requirements

As a first step before adding detail to the system, a set of requirements is devised and confirmed by the client. With this, boundary conditions are imposed on the design process, guiding it in the direction the customer desires. The most important requirements are briefly mentioned below.

IKEA-TECH-AIV-MOD-T2: "The modules shall make use of a standardised link."

The way that standardisation of parts and interfaces is achieved will be a major driver in this project. The way of connecting mechanically, power, and data will impose constraints on many other parts of the S/C. For example the way assembly is done, storing in the launch vehicle and subsystem sizing.

IKEA-TECH-AIV-ASM-T2: "The AIV system shall assemble different modules."

This requirement is driving because of the novelty of AIV in orbit. It is not possible to fall back to proven concepts and therefore a considerable amount of resources have to go into meeting the requirement.

Subsystem Investigation

A short summary of the different subsystem designs will be given, to provide an overview of design detail and team progress. The presentation includes the steps taken and selections made, based on existing components as far as those were available.

Communication

The Communication subsystems of tug and satellite have been analysed by utilising a link budget tool. Currently used technology has been investigated and a preliminary selection has been made on what components will be used in the assembly. Using the specifications of these components, the link budget tool was utilised to confirm that the system would indeed be feasible.

From the technical side it has been decided to make use of the following components:

- Set of 52 Tesat-Spacecom Ku-Band Receiver and Transmitter
- Set of 4 Airbus Large Ku-band Multi-spot Feed Array (LMFA)
- Set of 4 HPA Large Deployable Antenna (LDA) for beam focus and relay
- Set of 4 steerable spot-beam units

These will be arranged in two different kinds of modules, of which there will be four of each on the reference communication satellite. These are detailed in the following paragraphs:

Static Spot Module This module implements a set of 12 Tesat-Spacecom Transponders that are connected to a 12 horn antenna feed array for the attached LDA antenna. This antenna will be stored in a folded manner and deploy from the satellite once all modules have been assembled.

Steerable Spot Module A considerably smaller module was devised for the steerable spot beams, where a single Transponder feeds a horn antenna, that uses a double reflector system to redirect and focus the signal on the desired regions by having them rotate on a gimbal system. During launch, the larger reflector is folded into the module, deploying once the satellite has been assembled.

Propulsion

For the propulsion design, different solutions have been considered for the tug and the satellite. As transition times in the design trade-off have been identified as a major design driver, guaranteeing on time delivery, it has been decided to make use of a chemical liquid oxygen / liquid hydrogen propulsion unit for the tug. The satellite is equipped with an ionic propulsion unit that is used for ADCS, station keeping and eventual deorbit of the decommissioned system. For GEO, The tug will require refuelling after each trip, which will be done by attaching a refuelling tank to the module package. Both the propulsion system and refuel tank have also been sized and put into the CATIA collaboration space to integrate it into the LV configuration.

The most important findings are summarised below:

Table 2: Final propulsion systems selection

Characteristics	TUG	Satellite
TRL	9 [79]	6 (in 2017 [40])
Engine	RL10A-4-2	Qinetiq T-6
Number of engines	1	4
Thrust per engine [N]	105,978.9	0.145
Thruster dry mass [kg]	167.8	8.5
Specific impulse [s]	451	4300
Dry mass [kg]	1348.9	1847.0
Fuel mass [kg]	2920.9	249.3
Wet mass [kg]	4269.7	2096.3

ADCS

Again, both spacecraft have been considered in the design of this subsystem, yielding a layout and component selection for both tug and satellite, based on system characteristics found from the arrangement in 3D space via CATIA and the subsystem design and component selection. Both systems have to perform in a set of modes that can be summarised as:

Acquisition mode: Initial determination of attitude and position just after launch. May also needs to be performed for recovery from emergencies and unscheduled power-ups.

Detumbling mode: While separating from first stage or satellites to keep the S/C as steady as possible.

Safe mode: Used in case of emergency if one of the nominal modes fails. Runs on the bare minimum of functions to keep the points of failure and the power consumption down.

Orbital, transfer and maintenance mode: Period during and after transferring orbits. To counter the disturbance torques caused by the burn of the main engine in order to not waste fuel or even fail mission.

Slew mode: Rotate the S/C around its axes in a certain time period.

Docking mode: While docking with the satellite packages, space debris or satellites in need of maintenance with a certain attitude and ΔV

Standby mode: Most of the time the S/C runs with minimum functionality to save power.

The layout that has finally been selected for the tug consists of a Space Propulsion thruster system of four arrays with four thrusters each arranged as shown in the following figure:

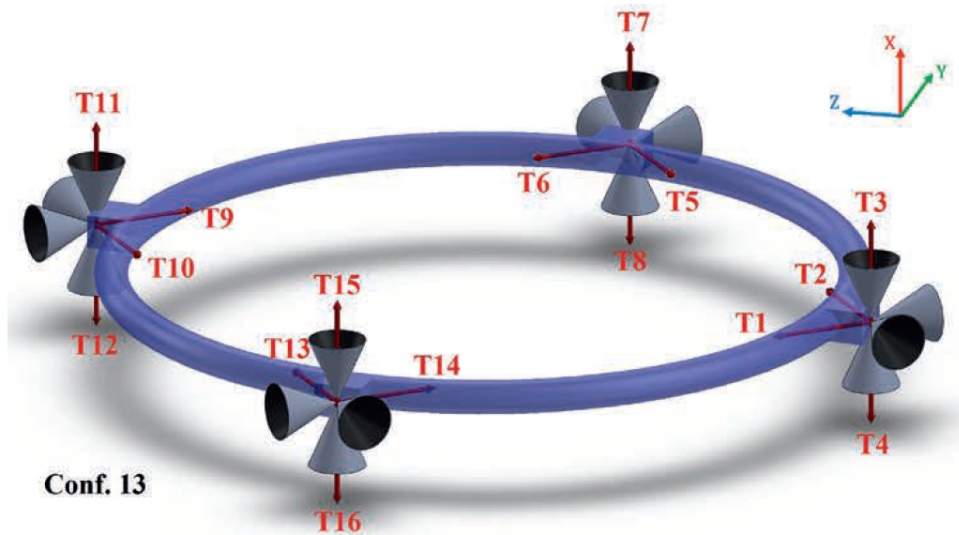


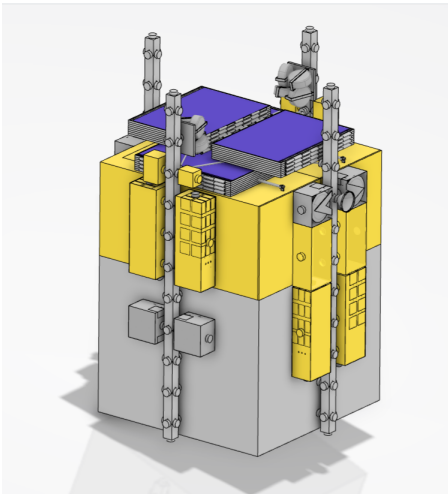
Figure 2: Tug thruster configuration [47]

In addition a set of four Rockwell reaction wheels, one Airbus Astrix 120 IMU, two TNO sun sensors and two Adcole star trackers will be used to determine the orientation and position via onboard measures.

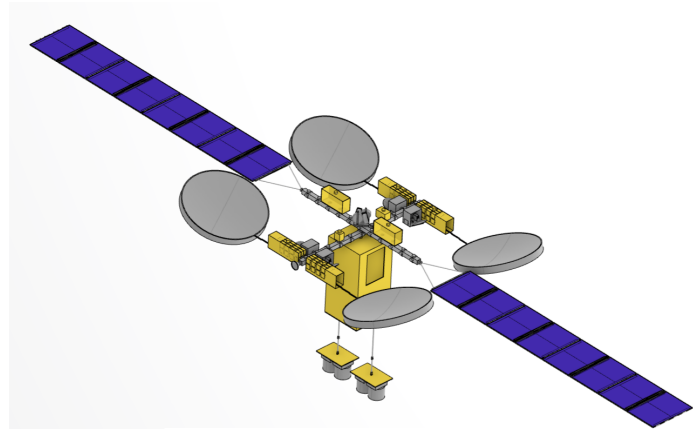
For the satellite, the ionic propulsion will be used as ADCS thrusters as previously mentioned, whilst the selection of other components is one Airbus Astrix 200 IMU, two TNO sun sensors and two Leonardo star trackers.

Modules, Structures & Layout

The layout of the satellite, satellite package and the tug are all interconnected due to assembly and modularity. After designing the subsystems and choosing components the modules themselves were created. To find a workable layout a lot of iterating was done between structural analysis, layout, assembly and these modules. The layout of the satellite package needed to be able to carry all launch loads. The tug also needed to be able to assemble this package into two satellites. This led to a lot of constraints for the structures connecting all the modules. After some analysis it was decided that the satellite would consist of two beams in a plus shape. These beams will double as structural components during launch. The final layouts can be seen in fig. 3a and fig. 3b.



(a) Final layout satellite package LV



(b) Final satellite layout

Figure 3: Final layout satellite package LV and satellite

The structural analysis also showed that the module connection on its own is possibly too weak to withstand certain loads that will occur during the mission. To mitigate this risk a module support was designed that can be placed over the crucial module connections.

Mission & Operations

The preliminary mission operations plan outlines the top-level operations functions, operation phases and a detailed plan of how the routine operations will operate. This is part of the bigger mission operation plan that will eventually include the overall operations overview, staff & training plans, and procedure development for data management. It is determined that for an efficient and effective mission operations, mission operation management will be vital. The most important conclusion is that tug operation engineers should be trained in satellite operation roles so that they can be reassigned to satellite operations when the tug is between its assembly tasks. This way costs can be reduced and the learning curve increased.

Assembly and the Robotic Arm

There are different methods for assembling the satellite, and this begins by either berthing, or docking with the payload sent into orbit. It was ultimately decided that, due to the uncooperative nature of the payload, berthing would be the only viable option. This does raise the issue that a robotic arm is needed.

The robotic arm is a 6.9 m, three link design capable of reaching the extreme edges of the payload once the tug and payload are berthed and coupled, to the extremes of the final assembled design of the desired satellite. An optimisation model, calculating the optimal angles for the different links allow the arm to reach the target destination with remarkable accuracy, as well as the possibility of an assembly time of approximately 37 hours.

To get a clear idea of assembly, Catia was used to render certain steps of assembly. It starts off by moving the free docking port from the satellite package to the opposite side of the tug where the satellite will be assembled and moving all parts to the tug buffer storage so as to free up the first beam. Subsequently, the free beam is assembled, followed by any free parts that attach to the beam and the next beam is freed up using the buffer storage. The free beam is then assembled followed by the remaining parts of the first satellite. As the first satellite is complete, it is released from the tug. For the second satellite, the first beam of the second satellite is loosened and this beam is assembled, followed by all relevant parts. Finally, the second beam is freed up and the second satellite is fully assembled.

Business Considerations

To define a profitable business case for Project MANTIS, the market, costs and return on investment have been analysed in detail.

Over the previous decade, the space economy has registered significant growth, currently positioning itself as one of the most lucrative industries globally. During 2012-2017, the number of satellites in orbit increased from 994 to 1,459, and this number is expected to increase exponentially over the coming years. Moreover, the global space economy is forecast to exceed \$1 trillion by 2040 according to Morgan Stanley. The space economy offers aerospace companies strong growth potential in the coming decades, though the market is characterised by high entry barriers through significant investments and end-to-end value chain coverage. Currently holding a leading position in the space market, Airbus Defence & Space is therefore positioned excellently to reap the fruits of its continuous investments in space technology.

Key market trends are:

- An expanded demand for satellite systems, driven by the expansion of emerging markets and additional capacity required for communications
- Increased commercial value of space, driven by new business models and vertical integration
- Reduced costs, driven by technological advancements such as increased satellite constellation capacity and declining launch costs
- Increased risk appetite, driving shorter-term projects and rapid renewal

The global space economy is currently valued at \$360bn, and is set to grow at a Compound Annual Growth Rate (CAGR) of 5.6% to a value of \$558bn in 2026. From the \$360bn space economy, approximately \$277bn corresponds to the global satellite industry. In terms of size, the global satellite has registered gradual growth, increasing from \$246bn to \$277bn gradually in 2014-2018.

While commercial GEO order in 2018-2017 are in total valued at approximately \$40bn (for 140 satellites), an additional 210 satellites are projected to be manufactured and launched to GEO in 2018-2027, comprising approximately \$60bn. From correspondence with the client, the target quantity of orders to process was set at approximately 3 per year. Considering Airbus' market share and the projected number of satellite orders, this is considered an achievable goal on the relatively shorter term.

Airbus interacts with numerous stakeholders including investors, commercial clients, (quasi)governments, competitors, employees, suppliers, and society, driving the company to create value in many ways. Project MANTIS is designed to fit Airbus' stakeholder management by defining a sustainable and profitable business case that complies with the division's strategy.

The costs are broken down in four phases that together make up the full process of the MANTIS project. The first phase is Development, starting from the very first thought of an AIV system in space until the moment all tests have run and a qualification unit has been manufactured. This phase naturally includes analysis, verification & validation and other software and hardware development costs, as well. Compared to the others, this is the most expensive and time consuming phase. This phase (and its cost) is non-recurring, unless the end product is in need of new development over the years.

After Project MANTIS has completed this phase, the tug and its modular satellites are ready for the Production phase. The cost of production is presented per spacecraft. Over time, these costs might decrease because of routine fabrication and new technologies. In between Production and Operations is the launch to bring the spacecraft into orbit. Satellites are scheduled to be launched, cutting the launching cost per satellite in half. Both the Production as Launch phase are recurring costs that are to be expected for every product.

Once in orbit, the spacecraft will start its operational life. The costs to keep it operational is also presented in table 3. These costs are estimated per year of service.

Finally, the return of investment is projected with financial model, projecting the financial throughout the lifetime of Project MANTIS. Herein, a base case was defined using assumptions for price, volume, and costs. This resulted in an average ROI of 8.9% and a break-even point after 15 years of operations. This is considered a profitable and realistic business case.

To further project the financial viability of this project, two multi-parameter sensitivity analyses were con-

Table 3: Final cost estimations

All costs	Tug	Satellite
Development	\$280,000,000	\$630,000,000
Production	\$150,000,000	\$188,000,000
Launch (per device)	\$90,000,000	\$45,000,000
Operations (per year)	\$15,000,000	\$19,000,000

ducted. The first sensitivity analysis altered a range of prices charged for the AIV-service (ranging from \$30m to \$60m) and the annual Research & Development (R&D) costs for the tug and satellite system (ranging from 3% to 5% of the initial development costs). The second sensitivity analysis altered the initial development costs of the tug and satellite system (ranging from \$80m to \$480m and from \$480 to \$780m respectively). The analyses show that Project MANTIS remains a profitable business case, unless AIV-price is reduced to very low prices. The findings in terms of average ROI are presented in tables 4 and 5.

Table 4: Multi-parameter sensitivity analysis of the recurring R&D costs versus AIV price in terms of ROI

		Recurring R&D (% of initial costs)				
		3.0%	3.5%	4.0%	4.5%	5.0%
AIV price (\$m)	30	4.9%	4.5%	4.1%	n/a	n/a
	35	6.5%	6.1%	5.7%	5.3%	4.9%
	40	8.1%	7.7%	7.3%	6.9%	6.5%
	45	9.7%	9.3%	8.9%	8.5%	8.1%
	50	11.3%	11.0%	10.6%	10.2%	9.8%
	55	13.0%	12.6%	12.2%	11.8%	11.4%
	60	14.6%	14.2%	13.8%	13.4%	13.0%

Table 5: Multi-parameter sensitivity analysis of the preliminary development costs in terms of ROI

		Preliminary Tug R&D					
		(\$m)	80	180	280	380	480
Preliminary Satellite R&D	480	14.6%	12.5%	11.0%	9.5%	8.4%	
	530	13.5%	11.7%	10.2%	8.9%	7.9%	
	580	12.5%	10.9%	9.5%	8.4%	7.4%	
	630	11.7%	10.2%	8.9%	7.9%	7.0%	
	680	10.9%	9.5%	8.4%	7.4%	6.6%	
	730	10.2%	8.9%	7.9%	7.0%	6.3%	
	780	9.5%	8.4%	7.4%	6.6%	5.9%	

Even with multi-parameter sensitivity analyses considering costs and pricing, Project MANTIS remains a promising business case for Airbus D&S. Moreover, Project MANTIS creates value in several other ways, making it a promising business case for Airbus:

- Project MANTIS puts Airbus ahead of the competition by creating value through AIV for its customers. By offering the new generation of telecommunication satellites with attractive advantages, Airbus can distinguish itself.
- Project MANTIS offers Airbus additional financial benefit through cross-selling its services (launching the modules, manufacturing the modules, etc.) and extra business through additional services such as debris-removal and refuelling are also possible.
- Project MANTIS will enable Airbus to further develop in-space AIV for various other purposes besides GEO telecom satellites. Consequently, Airbus can roll-out this technology on a larger scale and thus serve a larger customer base.

Sustainable Development Strategy

Sustainability is a key aspect in current projects. The approach followed in this project incorporates the three sustainability pillars, environmental, social and economic, on every level of the project. The design, manufacturing, testing, lifetime and End-Of-Life. In order to quantify this strategy a sustainability factor is created. This factor shows in percent how much more sustainable this project is than the chosen reference

case in terms of the chosen parameters. The reference case is chosen to be the Eutelsat 172b. Multiple parameters are defined to make up this factor. All of these parameters are found and the results are shown in the following table, with Human Development Index (HDI) and CPI (Corruption Perception Index):

Table 6: Overview table of the sustainability factor

<i>Spacecraft (4)</i>	Use of Earth Resources	Carbon Emissions	Pollution	HDI	CPI
Sustainability factor	3.55	23.84	610.2	0.59	5.33
Weight	4	3	5	3	3
Total Spacecraft	175.25				
<i>Launcher (5)</i>	Use of Earth Resources	Ozone Depletion	HDI	CPI	
Sustainability factor	640.77	-179.33	5.89	1.72	
Weight	3	5	3	3	
Total Launcher	74.89				
MANTIS TOTAL	125.07				

Further Project Development

The next phases of Project MANTIS will entail a final product. To get to the final product further analysis and design is necessary. The first phase, the transition phase, is for assembling the new design team with a group of experts and assessing the current design of Project MANTIS. In the next phase the design is improved with help of the expert group. For that the main focus lays on the design of the module connection and the assembly system. These designs will be verified by manufacturing and testing prototypes. After verification and validation of the prototypes the development phase starts. During this phase the planning of the production and qualification of the tug and modular satellite is done. In the implementation phase the actual systems are manufactured, qualified and assembled. This is followed up by the operation phase during which the first assembly tug and the first modular satellites are launched followed by the assembly of the modules. The project is concluded with the follow-up phase in which the overall project and the first mission are assessed.

Conclusion & Recommendations

The design of a functional AIV system has reached another milestone towards a functional modular satellite and an assembling tug. Even though the scope and time constraints of this project did not allow to establish a fully functional system in all its detail and intricacies, the result is a feasible concept. Project MANTIS implements initial sizing and component selection, space mission requirements, power and mass budgets, a business case, sustainability considerations and manufacturing approaches. One of its great benefits is the modularity and the subsequent opportunities that follow. Upgrading or reusing launched satellites will be standardised much more when Project MANTIS will enter the production phase and further research will explore new possible functionalities of the tug such as cleaning the graveyard orbit.

For now, the initial method to perform Assembly, Integration and Verification (AIV) in space is believed to work. It even seems, be it preliminary, effective to compete with conventional spacecraft. It is however recommended that this scientific research should continue as well as optimising both the tug as the modular satellite in the near future. Furthermore, a more thorough business case could be conducted with Airbus' own experience at hand that would result in a deeper insight of the market and thus Project MANTIS' prospects.

Nomenclature

Initialisms

ADCS Attitude Determination and Control System
 ADDT Atmospheric Drag Disturbance Torque
 AIV Assembly, Integration & Verification
 AVGS Advanced Video Guidance Sensor
 BFN Beam Forming Network
 BOL Beginning of Life
 CAGR Compound Annual Growth Rate
 CBD Cost Breakdown Structure
 CDH Command & Data Handling
 COCOMO 81 Cost Construction Model 1981
 Corruption Perception Index CPI
 CSS Coarse Sun Sensors
 DLR Deutsches Zentrum für Luft- und Raumfahrt
 DoD Depth of Discharge
 DSE Design Synthesis Exercise
 EBD Electrical Block Diagram
 ECSS European Cooperation for Space Standardisation
 EOL End of Life
 FBS Functional Breakdown Structure
 FFBD Functional Flow Block Diagram
 FHPA Falcon Heavy Payload Adapter
 GEO Geostationary Orbit
 GGDT Gravity Gradient Disturbance Torque
 GTO Geostationary Transfer Orbit
 HDI Human Development Index
 iBOSS intelligent Building Blocks for On-Orbit Satellite Servicing and Assembly
 IMU Inertial Measurement Unit
 iSSI intelligent Space System Interface
 L-BFGS-B Limited Memory Broyden Fletcher Goldfarb Shanno bounded
 LDA Large Deployable Antenna
 LEE Latching End Effector
 LEO Low Earth Orbit
 LMFA Large Ku-band Multi-spot Feed Array
 LR Level of Redundancy
 MAIV Manufacturing, Assembly, Integration & Validation
 MANTIS Modular Assembly Network of Technology in Space
 MER Mass Estimating Relations
 MFB Multiple Feed per Beam
 MFDT Magnetic Field Disturbance Torque
 MIB Minimum Impulse Bit
 MLI Multilayer insulation
 MMOI Mass Moment of Inertia
 MNS Mission Need Statement
 MOP Mission Operations Planning
 NICM NASA Instrument Cost Model
 PMU Power management unit
 POS Project Objective Statement
 PPU Power Processing Unit
 R&D Research & Development
 RAMS Reliability, Availability, Maintainability and Safety

RDT Requirement Discovery Tree
 RE² Re-Assemble & Re-Use
 ROI Return on Investment
 S/C Spacecraft
 SASSY Self-Assembling Space System
 SAUS Sub-Assembly Unification Station
 SCCM Small Satellite Cost Model
 SFB Single Feed per Beam
 SMU Spacecraft Management Unit
 SNR Signal to Noise Ratio
 SRDT Solar Radiation Disturbance Torque
 TT&C Telemetry, Track & Command
 USCM8 Unmanned Space Vehicle Cost Model, version 8

Symbols

α absorbtivity [-]
 α_{acc} Angular Acceleration [rad/s^2]
 ΔV Delta V [m/s]
 η Antenna Efficiency [-]
 η_{sol} Solar cell efficiency [-]
 λ Function of magnetic latitude [-]
 μ Earth's Gravitational Constant [m^3/s^2]
 ω Rotational Speed [deg/s]
 Φ Solar Constant [W/m^2]
 ρ Density [kg/m^3]
 ρ_{sol} Solar cell density [kg/m^2]
 σ_{crc} Theoretical buckling stress for a thin-walled cylindrical shell [MPa]
 σ_{crs} Theoretical buckling stress for thin-walled spherical spherical cap [-]
 σ Stefan-Boltzmann constant [-]
 τ_{al} aluminium 7025 yield shear [Pa]
 Θ Half Power Bandwidth [deg]
 Θ Maximum Angle between Principal Axis and Local Vertical [deg]
 Θ_{ec} Eclipse Angle [$^\circ$]
 ε emissivity [-]
 A_r Ram Area [m^2]
 A_s Sunlit Surface Area [m^2]
 A_{sol} Solar panel area [m^2]
 A_{sus} Inverted abundance [mpp]
 C Coverage Area [deg^2]
 c Speed of Light [m/s]
 $C/N0$ Carrier-to-Noise-Density-Ratio [$dB - Hz$]
 C_d Drag Coefficient [-]
 cm Center of Mass-
 cp_a Center of Atmospheric Pressure-
 cp_s Center of Solar Pressure
 D Residual Dipole Moment [$A \cdot m^2$]
 d Dish Diameter [m]
 d_{pin} pin depth [m]
 E Youngs modulus [GPa]
 E_{pk} Package Young's Modulus [Pa]
 $E_b/N0$ Energy per Bit to Noise Power Spectral Density Ratio [dB]
 F Thruster Force [N]
 f Frequency [Hz]
 F_D Thruster Force for Disturbance Counter [N]
 F_{bx} Beam total force in x direction [N]

F_{by}	Beam total force in y direction [N]	M_{sol}	Solar panel mass[kg]
F_{bz}	Beam total force in z direction [N]	MF	Margin Factor [-]
F_{lat}	lateral force in module [N]	N_s	System Noise Temperature [K]
F_{pin}	Lateral force in pin [N]	N_{bats}	Number of batteries [-]
F_{slew}	Thruster Force for Fast Slew[N]	N_{pins}	number of pins [-]
G	Gravitational Constant [m/s^2]	P	Orbital Period [s]
G/T	Gain-to-Noise Temperature [dBK]	P_{EIRP}	Equivalent Isotropic Radiated Power [W]
g_0	standard gravity [m/s^2]	P_{re}	Battery charge power [W]
G_{rx}	Gain of Receiver Antenna [dB]	P_{rx}	Received Power [dBW]
G_{tx}	Gain of Transmitter Antenna [dB]	P_{tx}	Transmitter Power [dBW]
h	Momentum[Nms]	q	Reflectance Factor [-]
$h_{disturbance}$	Momentum Storage due to Disturbance Torque[Nms]	R/t	Radius to thickness ratio [-]
h_{slew}	Momentum Storage for Slewing[Nms]	r_e	Radius of Earth [m]
I	Moment of Inertia[kgm^2]	r_{geo}	Radius of geostationary orbit [m]
I_x	Mass Moment of Inertia around X-Axis [$kg \cdot m^2$]	T_a	Atmospheric Drag Disturbance Torque[Nm]
I_y	Mass Moment of Inertia around Y-Axis [$kg \cdot m^2$]	T_c	Control Torque[Nm]
I_z	Mass Moment of Inertia around Z-Axis [$kg \cdot m^2$]	T_g	Gravity Gradient Disturbance Torque[Nm]
I_{pk}	Package second moment of inertia [m^4]	T_m	Magnetic Field Disturbance Torque[Nm]
I_{sp}	Specific impulse [s]	T_s	Solar Radiation Disturbance Torque[Nm]
I_{sus}	Single index [-]	t_{bm}	beam wall thickness [m]
K_c	Buckling coefficient [-]	T_{ec}	Eclipse time [s]
K_{cf}	Buckling coefficient for a thin flat plate [-]	T_{orb}	Orbit time [s]
L	Moment Arm [m]	t_{pin}	pin thickness [m]
L_{bm}	beam length [m]	T_{slew}	Slew Torque[Nm]
L_{pk}	Package CoM distance [m^4]	T_{sun}	Sun time [s]
L_{sus}	Amount of material [-]	TA_{sus}	Total abundance [ppm]
L_{tx-rx}	Path Loss [dB]	$TotI_{sus}$	Total index [-]
M_e	Mass of Earth [kg]	ν	Poissons ratio [-]
M_f	Fuel mass [kg]	W_{sus}	Index weight [-]
m_{bats}	Mass of batteries [kg]	Z_c	curvature parameter cylindrical shell [-]
m_{bm}	beam mass [kg]	A_{IR}	area exposed to infrared [m^2]
M_{dry}	Dry mass [kg]	A_p	projected area toward sun [m^2]
m_{pk}	Package wet mass [kg]	A_R	area exposed to reflected irradiance [m^2]
		IR	irradiance of infrared energy from Earth [W]
		Q_{in}	internal heat generated [W]
		R	percentage of solar irradiance reflected [%]

Contents

Executive Overview	1	7.2 Satellite ADCS	39
1 Introduction	1	7.2.1 System modes.	39
Project Description	1	7.2.2 Requirements.	39
2 Requirements	2	7.2.3 Disturbance Environment	40
2.1 Requirements.	2	7.2.4 ADCS Components Type Selection	40
2.2 Subsystem Requirements	3	7.2.5 Reaction Wheel and Thruster Sizing	40
2.3 Key Requirements	4	7.2.6 ADCS Components.	41
2.3.1 Driving Requirements	4	7.2.7 Conclusion	42
2.3.2 Conflicting Requirements	4	8 Command & Data Handling	43
3 Design Concepts & Trade-Off	5	8.1 Telemetry, Tracking & Command	43
3.1 Design Concepts	5	8.1.1 Requirements.	43
3.2 Trade-Off	8	8.1.2 Design	43
4 Project MANTIS	9	8.2 On-board Computer Module	43
4.1 MANTIS Mission	9	8.2.1 Requirements.	43
4.2 Functional Analysis of the Tug and the Modular Satellite	10	8.2.2 Design	43
Detail Design	15	8.3 Command & Data Handling unit	44
5 Communications	15	8.3.1 Requirements.	44
5.1 Technology	15	8.3.2 Design	44
5.2 Possible Implementation	16	8.4 Conclusion	45
5.3 Check System Viability - Link Budget . .	17	9 Electric Power System	46
5.4 Digital Encoding Techniques	21	9.1 Power Generation	46
5.5 Chapter Conclusion	21	9.2 Power Storage.	46
6 Propulsion	23	9.3 Battery Sizing	47
6.1 Astrodynamics Characteristics	23	9.4 Solar Array Sizing.	48
6.2 Propulsion Requirements	23	9.5 Conclusion	49
6.3 Satellite	24	10 Thermal Control	50
6.3.1 Power	24	10.1 Thermal Control Subsystem.	50
6.3.2 Mass	24	10.2 Thermal Control System Components .	51
6.4 Tug	25	10.3 Thermal Control Analysis	51
6.4.1 Tug mission stages	26	10.3.1 Thermal Analysis for tug	51
6.4.2 Fuel tank design	26	10.3.2 Thermal Analysis for modular Telecommunication Satellite . .	53
6.4.3 Trade-off Thruster	27	10.4 Conclusion & Recommendations for the Thermal Control System.	54
6.4.4 Sensitivity analysis	27	11 Satellite Modules	55
6.4.5 Cleaning up graveyard orbit . . .	27	11.1 Module Contents	55
6.5 Conclusion	29	11.1.1 Module Box Mass.	55
7 ADCS	30	11.2 Module Connection	57
7.1 Tug ADCS	30	11.2.1 Business Analysis	57
7.1.1 System Modes.	30	12 Structure	58
7.1.2 Requirements	30	12.1 Design Loads	58
7.1.3 Disturbance Environment	31	12.1.1 Structural Requirements.	58
7.1.4 ADCS Components Type Selection	33	12.2 Materials	59
7.1.5 Reaction Wheel and Thruster Sizing	33	12.3 Beam Sizing.	59
7.1.6 ADCS Components Trade-Off . .	35	12.3.1 Forces	59
7.1.7 Conclusion	38	12.3.2 Bending	60
		12.3.3 Verification	61

12.4 Refuel Tank	61	18 Market Analysis	99
12.4.1 Determining refuel tank radius	61	18.1 At a Glance	99
12.4.2 Determining tank supporting structure.	62	18.2 Market Concepts & Trends.	99
12.5 Module Support	63	18.3 Market Sizing	99
12.6 Final Structure Mass	64	18.3.1 Global Market.	99
12.6.1 Structural Components	64	18.3.2 Target Market	101
12.6.2 Wiring	64	18.4 Stakeholder Analysis	101
12.6.3 Final Mass.	64	18.4.1 Shareholders & Investors.	101
12.7 Vibrations.	65	18.4.2 Commercial Clients	101
12.8 Stability and Control Characteristics	65	18.4.3 Governments	101
12.8.1 CG	65	18.4.4 Competitors.	102
12.8.2 ADCS thrusters moment arms.	66	18.4.5 Other Stakeholders	103
12.8.3 Mass Moment of Inertia	66	18.5 Strategic Fit with Airbus Defence & Space	103
12.9 Conclusion	67	18.6 Conclusion & Design Drivers	103
13 Layout & Configuration	68	19 Sustainable Development Strategy	104
13.1 Layout LV	68	19.1 Vision	104
13.2 Layout Satellite	69	19.2 Strategy	105
13.3 MANTIS layout	69	19.3 Assessment	106
13.4 Hardware Diagrams	71	19.3.1 Spacecrafts	106
13.5 Resource Allocation & Budget Break-down	72	19.3.2 Launcher	109
13.6 Conclusion	73	19.4 Conclusion	110
14 Assembly	74	20 Mission Operations	111
14.1 Rendezvous.	74	20.1 Mission Operations Planning	111
14.1.1 Far Range	74	20.2 Real-Time Routine Operations	112
14.1.2 Close Range	74	21 Project Design & Development Logic	113
14.2 Mating.	75	21.1 Project Design & Development Logic.	113
14.2.1 Docking and Berthing	75	21.2 Project Gantt Chart.	113
14.2.2 Mating System Design	75	22 Manufacturing, Assembly, Integration & Validation Plan	116
14.3 Robotic Arms	75	23 Cost Breakdown Structure	118
14.3.1 Requirements and Design	75	23.1 Cost Estimation Model.	118
14.3.2 Simulation and Modelling	76	23.1.1 Development	119
14.3.3 Collision Detection	78	23.1.2 Production	119
14.3.4 TRL	78	23.1.3 Operations	120
14.3.5 Verification and Validation.	78	23.2 Conclusion	120
14.4 Tools.	79	24 Return on Investment	122
14.5 Sequence	79	24.1 Model Characteristics and Use Case	122
14.6 Performance Analysis	81	24.2 Assumptions & Base Case Scenario	122
14.7 Conclusion	81	24.2.1 Revenues	122
15 Mission Risk Assessment	83	24.2.2 Costs.	123
15.1 Risk Identification	83	24.3 Sensitivity Analysis	123
15.2 Risk Mitigation	88	24.3.1 Sensitivity Analysis 1	123
15.3 Conclusion	91	24.3.2 Sensitivity Analysis 2	123
16 Reliability, Availability, Maintainability and Safety	93	24.4 Model Outputs	123
17 Compliance Matrix	95	24.5 Value Creation for Airbus Defence & Space	125
Business Case	99	25 Conclusion & Recommendations	127
		References	128

Introduction

As of 2020, satellites are manufactured, assembled and tested on Earth. Advances in robotics are revolutionising the way automobiles and aircraft are built here on Earth but as of now, that did not have a significant influence on space-borne architecture. This project, will transform the way satellites are built by incorporating Assembly, Integration and Verification (AIV) in Space. This disruptive technology has many upsides. It will decrease the throughput time from order to functional satellite operation while extending the lifetime by having a modular design. This will make the replacement of older components in space possible and therefore extends the lifetime and capabilities of satellites in orbit. This decreases cost and is increasingly sustainable. Furthermore, current satellites and space structures are heavily constrained by the limitations of existing launch systems. With AIV in space the final satellite geometry and configuration is not limited by the launcher geometry - this means that any satellite could expand, fold out, and even be reorganised after it is launched into orbit.

Further, this section gives a summary of the design and iteration process for Project MANTIS, a system which assembles, integrates and verifies a payload sent into GTO- orbit, transferred to GEO- (and ultimately GEO). These custom orbits, explained more in detail in section 6.1.

Firstly, different management aspects of the project are discussed, starting from the requirements which drove the design, a functional analysis, as well as the different concepts which were conceived and the trade off which ultimately resulted in Project MANTIS. This is seen in chapters 2, 3 and 4 respectively.

This is followed by a detail design of Project MANTIS which is split into two angles. Firstly, the design process was started by setting up the design process for each subsystem as found in chapters 5 to 10. In chapter 11 these subsystems were then put into modules required for assembly.

This is followed by a discussion of the general structure and layout in chapters 12 and 13. Here the created modules are used to analyse the required structure during launch. From this a layout for the satellites in the launch vehicle and after assembly could be determined.

The second angle concerns the robotic arm located on the tug. In chapter 14, the assembly and assembly methods are considered and discussed, ultimately affecting how the satellite will cooperate with the tug and robotic arm. In section 14.3, the robotic arm itself is discussed, heavily focusing on the computer model used to simulate its behaviour.

In the later chapters, a design analysis is performed, which highlights the performance of the system, as well as risks, the reliability, availability, maintainability and safety of the system, as well as a summary of the system with regard to complying with the requirements set. These chapters are chapters 15 to 17, respectively.

Consequently the business case is presented. This starts off with a market analysis in chapter 18, which is followed by the sustainability strategy in chapter 19. The last few chapters incorporate items for the operations and logistics as well as any future intentions for the project (chapters 20 and 21).

The report concludes with a plan concerning how the different components of the product are manufactured and assembled, integrated and validated (chapter 22), followed by a Cost Breakdown Structure and Return on Investment (chapters 23 and 24). This reports finishes with chapter 25, concluding the entire project.

Requirements

This chapter investigates how the system has to perform by identifying and understanding the stakeholder requirements and wishes and translating them into system requirements. By talking to the client, the importance of most of these can be estimated and killer requirements mitigated. Influence might also come from information gained during the market analysis in chapter 18 as well as the functional analysis in chapter 4.

2.1. Requirements

Following the Requirement Discovery Tree (RDT), the different requirements are designed. These requirements contain pre-defined requirements by the stakeholder and the ones discovered through use of the RDT.

First of all, the constraints for the mission are stated below. These constraints are divided into project & management constraints and engineering constraints.

IKEA-CONS: Perform mission within constraints

- **IKEA-CONS-PM:** Project and Management Constraints
 - **IKEA-CONS-PM-LEG:** Legal
 - ◊ **IKEA-CONS-PM-LEG-T1:** The AIV shall be following the International Space Law.
 - ◊ **IKEA-CONS-PM-LEG-T2:** The mission shall obey European law.
 - ◊ **IKEA-CONS-PM-LEG-T3:** The production shall obey the respective production country's laws.
 - **IKEA-CONS-PM-CO:** Cost
 - ◊ **IKEA-CONS-PM-CO-T1:** The spacecraft development cost shall not be more than \$700m.
 - **IKEA-CONS-PM-SCHE:** Schedule
 - ◊ **IKEA-CONS-PM-SCHE-T1:** Space-borne architecture construction shall start in 2028.
 - ◊ **IKEA-CONS-PM-SCHE-T2:** First operation of space-borne architecture shall begin in 2032.
 - ◊ **IKEA-CONS-PM-SCHE-T3:** Once in operation, the system shall assemble a new satellite within one year.
 - **IKEA-CONS-PM-STA:** Stakeholder Deliverables
 - ◊ **IKEA-CONS-PM-STA-T1:** The design study shall incorporate a profitable business plan.
 - ◊ **IKEA-CONS-PM-STA-T2:** The final design shall incorporate a cost assessment.
 - ◊ **IKEA-CONS-PM-STA-T3:** The final design shall incorporate a risk assessment.
 - ◊ **IKEA-CONS-PM-STA-T4:** The design study shall incorporate an operations plan which details further concepts for the system's end-of-life strategy.
 - ◊ **IKEA-CONS-PM-STA-T5:** AIV design shall integrate Airbus' IKEA-Sat Idea.
 - ◊ **IKEA-CONS-PM-STA-T6:** AIV design shall be technically feasible.
- **IKEA-CONS-ENG:** Engineering Constraints
 - **IKEA-CONS-ENG-RESA:** Reliability and safety
 - ◊ **IKEA-CONS-ENG-RESA-T1:** Safety shall be considered in the trade-off process.
 - ◊ **IKEA-CONS-ENG-RESA-T2:** Reliability shall be considered in the trade-off process.
 - ◊ **IKEA-CONS-ENG-RESA-T3:** The IKEASPACE system shall have a minimum success rate of 95% after 3 years of use on a new or serviced satellite.
 - ◊ **IKEA-CONS-ENG-RESA-T4:** The launcher used shall have a minimum launch success rate of 94%.
 - **IKEA-CONS-ENG-SUS:** Sustainability
 - ◊ **IKEA-CONS-ENG-SUS-T1:** Sustainability shall be integrated in the design trade-off process.
 - ◊ **IKEA-CONS-ENG-SUS-T2:** The product shall ensure that applicable systems adhere to the internationally recognised ISO 140001 certification for energy management systems.
 - ◊ **IKEA-CONS-ENG-SUS-T3:** The product shall ensure applicable systems implement an energy management system based on the ISO 5001 standard.

- ◇ **IKEA-CONS-ENG-SUS-T4:** The use of at least TRL5 items shall be considered first for use in the design.
- ◇ **IKEA-CONS-ENG-SUS-T5:** The product shall have a sustainability factor higher than 50.
- **IKEA-CONS-ENG-ENBU: Engineering Budgets**
 - ◇ **IKEA-CONS-ENG-ENBU-T1:** The maximum mass of the AIV system shall be 9364 kg.
 - ◇ **IKEA-CONS-ENG-ENBU-T2:** The maximum power use of the AIV system shall be 22600 W.
 - ◇ **IKEA-CONS-ENG-ENBU-T3:** The maximum payload volume during launch will be «TBD» m³.
 - ◇ **IKEA-CONS-ENG-ENBU-T4:** The maximum number of recurring (resupply) launches shall be «TBD».
 - ◇ **IKEA-CONS-ENG-ENBU-T5:** The maximum number of non-recurring launches shall be 2.
 - ◇ **IKEA-CONS-ENG-ENBU-T6:** The data storage shall have 360 Gb size.
 - ◇ **IKEA-CONS-ENG-ENBU-T7:** The on-board processing shall be 300 Mb/s.
 - ◇ **IKEA-CONS-ENG-ENBU-T8:** The minimum SNR at the ground receiver shall be 8 dB.
 - ◇ **IKEA-CONS-ENG-ENBU-T9:** The minimum SNR at the space receiver shall be 8 dB.

Next to the mission constraints, there are requirements regarding the technical side of the project. These requirements are stated below.

IKEA-TECH: Perform mission technically

- **IKEA-TECH-PROD: Production**
 - **IKEA-TECH-PROD-T1:** The production cost of one satellite shall be below \$200m.
 - **IKEA-TECH-PROD-T2:** Only sustainable production techniques shall be used.
 - **IKEA-TECH-PROD-T3:** At least 15 % of the energy usage for manufacturing will be green energy.
 - **IKEA-TECH-PROD-T4:** The sub-assemblies shall be able to be transported to the launch site.
- **IKEA-TECH-LAU: Launch**
 - **IKEA-TECH-LAU-T1:** The AIV system shall physically fit into the selected launcher.
 - **IKEA-TECH-LAU-T2:** The selected launcher shall be available 1 times per year.
 - **IKEA-TECH-LAU-T3:** The selected launcher shall be able to bring the S/C to GTO-Orbit.
 - **IKEA-TECH-LAU-T4:** The selected launcher shall have a reliability of 94%.
- **IKEA-TECH-AIV: Assembly, integration and verification.**
 - **IKEA-TECH-AIV-MOD: Client Modules**
 - ◇ **IKEA-TECH-AIV-MOD-T1:** The modules shall communicate with the AIV system.
 - ◇ **IKEA-TECH-AIV-MOD-T2:** The modules shall make use of a standardised link.
 - ◇ **IKEA-TECH-AIV-MOD-T3:** The modules shall communicate with each other.
 - ◇ **IKEA-TECH-AIV-MOD-T4:** The modules shall be mechanically coupled.
 - ◇ **IKEA-TECH-AIV-MOD-T5:** The modules shall be electrically coupled.
 - ◇ **IKEA-TECH-AIV-MOD-T6:** The modules shall be thermally coupled.
 - ◇ **IKEA-TECH-AIV-MOD-T7:** The modules shall connect the data bus.
 - ◇ **IKEA-TECH-AIV-MOD-T8:** The modules shall verify whether the links are correctly connected.
 - ◇ **IKEA-TECH-AIV-MOD-T9:** The modules shall be packageable in a condensed way so that the modularity proves to have an advantage over traditional launch-configurations.
 - ◇ **IKEA-TECH-AIV-MOD-T10:** The modules shall be able to be assembled in 48 hours time.
 - ◇ **IKEA-TECH-AIV-MOD-T11:** The modules shall be coupled fluidly.
 - ◇ **IKEA-TECH-AIV-MOD-T12:** The modules shall be replaceable / upgradable.
 - **IKEA-TECH-AIV-ASM: Assembly system**
 - ◇ **IKEA-TECH-AIV-ASM-T1:** The AIV system shall communicate with the modules.
 - ◇ **IKEA-TECH-AIV-ASM-T2:** The AIV system shall assemble different modules.
 - ◇ **IKEA-TECH-AIV-ASM-T3:** The assembled modules shall be verified by the AIV.
 - ◇ **IKEA-TECH-AIV-ASM-T4:** The AIV systems shall reconfigure assembled modules.
 - ◇ **IKEA-TECH-AIV-ASM-T5:** The AIV systems shall assemble the modules in less than 48 hours time.

2.2. Subsystem Requirements

The subsystem requirements are outlined in the individual subsystem; chapters 5 to 12.

2.3. Key Requirements

Requirements can differ in priority. Therefore it is of significance to identify key requirements. These are requirements that are of primary importance to the user. They can be requirements that drive the design to an unacceptable extent, requirements that drive the design more than average and last but not least requirements that need more attention because they are conflicting with each other. They are described more thoroughly in sections 2.3.1 and 2.3.2, respectively.

2.3.1. Driving Requirements

IKEA-TECH-AIV-MOD-T2: "The modules shall make use of a standardised link."

The way that standardisation of parts and interfaces is achieved will be a major driver in this project. The way of connecting mechanically, power, and data will impose constraints on many other parts of the S/C. For example the way assembly is done, storing in the launch vehicle and subsystem sizing.

IKEA-TECH-AIV-ASM-T2: "The AIV system shall assemble different modules."

This requirement is driving because of the novelty of AIV in orbit. It is not possible to fall back to proven concepts and therefore a considerable amount of resources have to go into fulfilling the requirement.

2.3.2. Conflicting Requirements

Some of the requirements can be conflicting as well. This causes that at least one of the requirements cannot be met in the end of the project. Therefore, these couples of requirements can be seen as killer requirements as well. At this stage, the conflicting requirements will still be limited.

IKEA-CONS-PM-SCHE-T1 vs. IKEA-TECH-PROD-T2

These two requirements conflict in terms of scheduling. According to the first requirement, the space-borne architecture assembly should be started in 2024. However, the second requirement states that only sustainable production techniques shall be used. As the current production techniques are not all sustainable, these two requirements are conflicting. This conflict can be resolved by changing one of the requirements. Either delay the schedule or choose for less sustainable production techniques. As mentioned above, the requirement regarding the schedule is a killer requirement and was negotiated upon. Therefore the conflict has been solved for these two requirements.

IKEA-TECH-PROD-T1 vs. IKEA-TECH-PROD-T2

The requirements regarding production could become conflicting in the future once the production costs are determined. The first requirements could limit the sustainable techniques that should be used. This is due to the reason that sustainable techniques are more expensive at the moment. This could be overcome by researching cheaper sustainable techniques, but this would again conflict with requirement **IKEA-CONS-PM-SCHE-T1** like in the conflict above. Now it can be seen that the use of sustainable production techniques only is conflicting twice. Therefore, this requirement was changed in consultation with the sustainability officer. The updated requirement is stated below.

IKEA-TECH-PROD-T2: The use of sustainable production techniques shall be maximised.

So to conclude, the killer and conflicting requirements are solved by the means mentioned above. Next to that, the driving requirements are listed which shows a good overview of the most important requirements that will drive the design.

Design Concepts & Trade-Off

This chapter summarises the viable concepts that have been generated for the AIV mission, in section 3.1, and gives insight into the trade-off results, in section 3.2, of each of the systems. The following criteria were assessed for the trade-off: cost, sustainability, upgradeability, technical risk, market adaptability and throughput time. They are elaborated on in section 3.2. A better performance correlates with a higher score.

3.1. Design Concepts

During the concept generation phase, four concepts have been developed. They are outlined in the following sections.

Concept 1 - RE²

The means of assembly in the Re-Assemble & Re-Use (RE²) concept is an expandable assembly station. A render of the concept is presented in fig. 3.1. By placing the station in Low Earth Orbit (LEO), the payload that can be brought up with LVs is increased. Furthermore, locating the system in LEO provides the possibility of assembling satellites for orbits other than Geostationary Orbit (GEO). A carrier vehicle is created to rendezvous with the assembly station, after having separated from the LV. This "box carrier" will provide a structural rack for the modules during launch and possesses Attitude Determination and Control System (ADCS) to approach the station and dock. From this point the station begins the assembly process by (re-)connecting the modules on a secondary port using its robotic arms and the connection interfaces on the modules. During assembly and after construction, tests are run to verify the satellites' functionality. In case a component is faulty, a replacement can be sent up. Having passed final checks, the satellite is released and ascends to GEO on its own ionic propulsion.

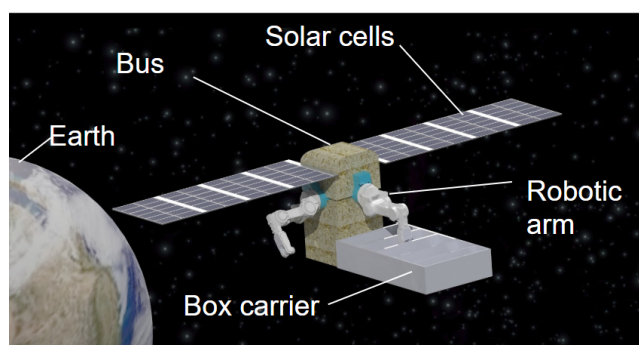


Figure 3.1: RE² concept drawing [52]

For the trade-off RE² wins in the cost category, as slightly higher initial costs are mitigated by low recurring costs. In addition, RE² can adapt to different market needs, giving it a high grade in market adaptability. Being situated in LEO and having its characteristic hub function, it could provide services to other customer groups and easily change to manufacturing lower orbit satellites. The technical risk scores high by comparison, as proven and tested technologies can be utilised and the orbit allows for possible maintenance. The throughput time is high when compared to the concepts making use of a chemical propulsion for transfer, as the utilised ionic propulsion has a longer orbit transfer, causing the system to score low in this category. Upgradeability scores relatively low, as satellites that are active in GEO would have to return to LEO in order to be serviced and this will take a long time with electric propulsion. Whilst the newly manufactured ones could do that, current telecommunication satellites are not equipped to do that and cannot be upgraded by the station. Finally, the sustainability of the system is relatively low as the station uses a lot of resources in the set-up phase as well as on the disposable carrier vehicles.

Concept 2 - TUG&PLAY

This concept involves a tug that picks up modules of up to two satellites inserted into Geostationary Transfer Orbit (GTO) and brings them to an orbit with a slightly lower orbital altitude than GEO where it assembles them. When successfully assembled the satellites will raise their orbit independently using electric propulsion to the final mission orbit in GEO. The tug vehicle has different tools available to its robot arms that can perform various tasks from refuelling to upgrading. Example of tools are a torquer, welder, a tool for grasping and berthing, cutters and a fuel valve connection. The connection system, however, is not permanent. It makes use of interlocking screw joints, that include data and power connectors.

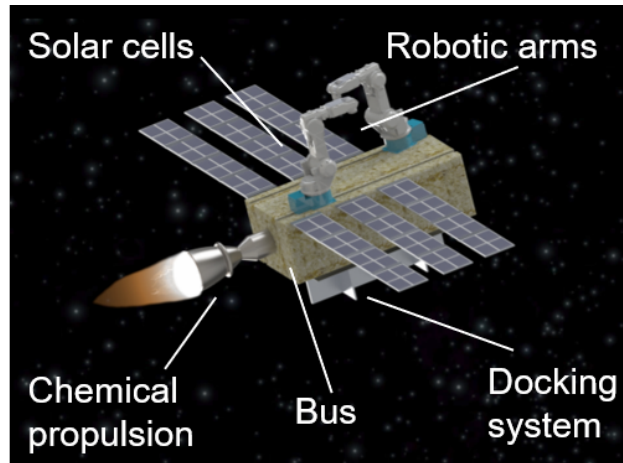


Figure 3.2: TUG&PLAY concept drawing [52]

In the trade-off TUG&PLAY scores high in upgradability because it is already in GEO and is able to attach itself to satellites. For example, it can also refuel and repair satellites in need of extension of life. Paired with the relatively low cost and risk and an acceptable market adaptability, this concept proves to have a strong business case. Last but not least this concept also scores high on sustainability because extension of life practices mean that fewer satellites need to be built and the dedicated propulsion on the tug leads to a decrease in fuel needed on the satellites.

Concept 3 - SASSY

The Self-Assembling Space System (SASSY) illustrated in fig. 3.3 comes as a complete package in which the modules connect to each other by using three on-board robotic arms. One of these robotic arms assembles the modules needed for the transfer to GEO first, such as the power generation and propulsion units. In order to reduce the throughput time the assembly of the satellite is conducted during the transfer to the final mission orbit. This is needed, as it uses an ionic propulsion system to transfer to GEO, which takes longer than chemical propulsion. Once the transfer is finished, this robotic arm will change its end-effector into an ADCS system. The second robotic arm will perform the ADCS as well to couple with the first arm. The last robotic arm is used as a redundant arm, in case of any failure with the other arms. At the end of life the satellite will decrease altitude and eventually burn up in the atmosphere.

In the trade-off, SASSY scores relatively low in terms of costs, sustainability and upgradability. This is due to the fact that the reusability of the system is very low. The costs of the concept rise significantly due to the fact that for every launch the robotic arms has to be adjusted. Furthermore, the sustainability is low, because the end of life can not be extended and at the end of life nothing can be recycled. On the other hand, the market adaptability is high due to the new robotic arms that needs to be designed for every mission. Therefore, it can adapt to changes in the market as well. Lastly, the throughput time scores relatively high as the assembly stage coincides with the transfer to GEO.

Concept 4 - SAUS

The Sub-Assembly Unification Station (SAUS) as shown in fig. 3.4 is an assembly bay onboard the ISS. When the ISS begins commercialisation in 2024 [65], satellite modules will dock to ISS docking port PMA2 aboard a conventional cargo resupply vehicle. The modules are transferred autonomously to a buffer storage area

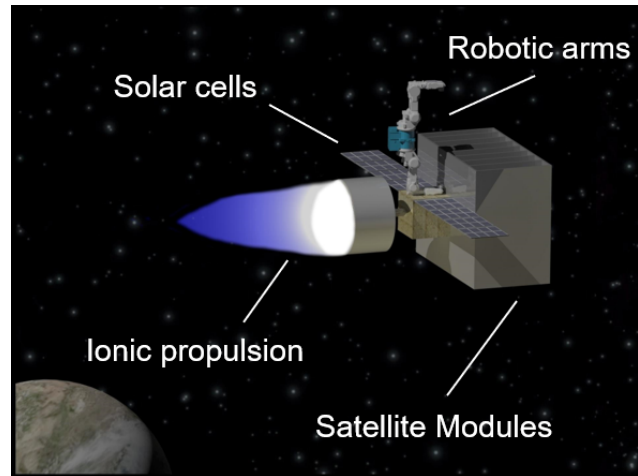


Figure 3.3: SASSY concept drawing [52]

from which two robot arms on a circular rail extract and assemble the necessary modules to create a sub-assembly. The sub-assembly is then transferred through the Quest airlock and manipulated by Canadarm2 to a temporary storage area outside the ISS, where preliminary testing can begin. Meanwhile, the robot and rail system repeats the process until all sub-assemblies are tethered outside the ISS. Finally, the Canadarm2 with a suitable Latching End Effector (LEE) assembles all sub-assemblies to create the final satellite. When all the necessary testing is completed the satellite propels itself, once the robotic arm releases it, into a trajectory towards GTO and then GEO using electric propulsion.

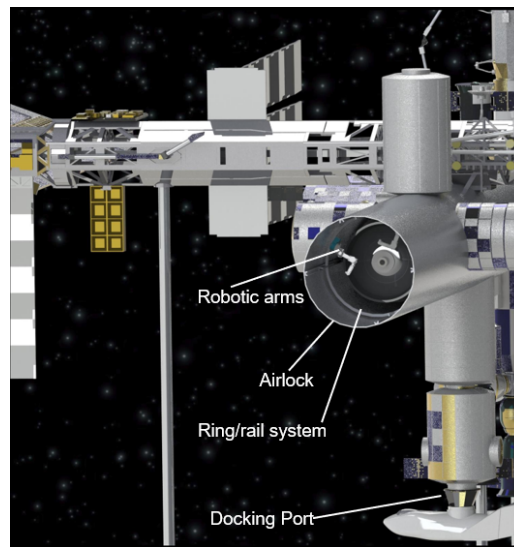


Figure 3.4: SAUS concept drawing on ISS template [51, 52]

By eliminating the need for costly new developments, qualification campaigns and using existing infrastructure of the ISS, SAUS scores the highest in sustainability. Likewise, due to its orbit system and the fact that final assembly takes place outside the ISS, the system can assemble any spacecraft regardless of size, thereby scoring high in market adaptability. On the other hand, while non-recurring costs are relatively low compared to other concepts, the annual operating fee and dependency on external space agencies that makes SAUS score lower in cost and risk.

3.2. Trade-Off

In order to select the concept for the detail design phase a trade-off was performed. The trade-off criteria were determined in such a way that they clearly show how well a concept meets key requirements. Some initial weights were determined, also using key requirements. Afterwards, the trade-off weights and criteria were discussed with and confirmed by the client, Airbus D&S. A guideline was defined that specifies the justification of scores for each criteria. The criteria of the trade-off were as follow: **Cost** - Based on recurring and non recurring costs of a concept. **Sustainability** - Mainly based on the sustainability of End of Life (EOL) strategies of a concept. **Upgradability** - Based on the ability of a concept to upgrade designed and existing satellites. **Risk** - The technical risk of a concept. **Market Adaptability** - The ability for a concept to adapt to a different type of satellite. **Throughput Time** - The time required from ordering a satellite till it is operational in space.

Good	5
	4
Moderate	3
	2
Low	1

Figure 3.5: Trade-off colour key

Table 3.1: Concept trade-off summary table; Upgr. = Upgradability, MA = Market Adaptability, TPT = Throughput Time, Sust. = Sustainability

Criterion Concept	Cost [10]	Sust. [7]	Upgr. [6]	Risk [6]	MA [5]	TPT [4]	Average Score
RE ²	4	3	3	4	4	1	3.3
TUG&PLAY	3	3	5	4	3	4	3.6
SASSY	2	1	1	3	5	2	2.2
SAUS	1	4	3	2	4	1	2.4

Based on the trade-off results various conclusions can be drawn. First of all an order of best performing concepts can be determined. Consequently the ranking is from best to worst: TUG&PLAY, RE², SAUS and lastly SASSY. Secondly, quantitatively, the best concept has a lead of 0.3 average score points. To make this difference more understandable, this means RE²'s score in a medium important category like upgradability or technical risk would have to increase by two points.

In an ideal case, a winning concepts should not only have the best average score but also perform consistent. Comparing TUG&PLAY and RE², it can be seen that the latter performs poorly on throughput time. It is a key requirement to have a throughput time of 1 year and RE² just makes that. As there is still some uncertainty at the preliminary design phase this poses a big risk for the project and therefore gives an additional reason for not choosing RE².

In order to evaluate the trade-off result a local sensitivity analysis was performed. The major conclusion of this analysis was that the order of ranking does not change. Therefore it can be said with confidence that the trade-off is not sensitive to changing the weights and the decision to continue the design process with TUG&PLAY is justified. For these reasons and on account of the average scores the decision was made to continue the detailed design phase with TUG&PLAY now called Project MANTIS.

Conclusion

After defining a trade-off method and determining useful criteria based on stakeholder requirements, a complete trade-off was executed. TUG&PLAY ended up having the highest score in the trade-off. Even after performing a sensitivity analysis where the weight of each criteria was changed and the average score recalculated, TUG&PLAY remained the top candidate. That is why TUG&PLAY has been selected as the best choice for the final design phase of this project. For the final design phase TUG&PLAY has been renamed to Project MANTIS.

Project MANTIS

Project MANTIS, or Modular Assembly Network of Technology In Space, is the design that was selected based on the concept trade-off in the midterm report [28]. This concept entails an extra assembly structure that assembles the modular satellite in space. Prior to the assembly this structure brings the satellite modules to a dedicated assembly orbit which is close to the final GEO mission orbit. In this chapter the mission of Project MANTIS is outlined in section 4.1. The functionality of the MANTIS tug and the modular telecommunication satellite are described in section 4.2.

4.1. MANTIS Mission

Project MANTIS consists of two spacecraft designs, the tug and the modular satellite. Firstly the tug is launched into orbit. When idle, the tug stays in GEO- orbit. This GEO- orbit is the assembly orbit it is roughly about 1000 km below GEO. This GEO- orbit is further elaborated on in section 6.1. Whenever satellites are ordered, they are sent up in a Falcon Heavy rocket in to GTO- orbit. GTO- orbit is the transfer orbit to GEO-. Along with the spacecraft package a refuel tank is launched. At this point the tug will move from GEO- orbit to GTO- orbit to rendezvous with the second stage of the Falcon Heavy. The tug first refuels itself while the satellite package is still attached to the second stage. Afterwards the tug docks to the satellite package, signals the refuel tank and second stage to release, these will then slowly de-orbit due to atmospheric drag.

The tug then takes the satellite package to GEO- using bipropellant liquid propulsion system propulsion. Once in a stable GEO- orbit, the tug begins the assembly. After the satellites are assembled and their functionality has been verified, they ascend to their designated GEO orbits to begin their missions. The tug then sits idle again in GEO- orbit awaiting its next mission.

Further operations the tug can carry out are upgrading, repair, service and refuelling of the modular satellites. There is the possibility to add space debris removal as an additional function for the tug.

When the tug reaches EOL it de-orbits itself using chemical propulsion. When the satellites reach EOL they de-orbit themselves using electrical propulsion.

In an ideal case the tug assembles two satellites per assembly mission, however if the demand at that time does not allow for a two satellite mission it is possible to take only one satellite. This would increase the cost for the satellite.

These mission stages for both the tug and the satellite are shown in figs. 4.1 and 4.2 respectively.

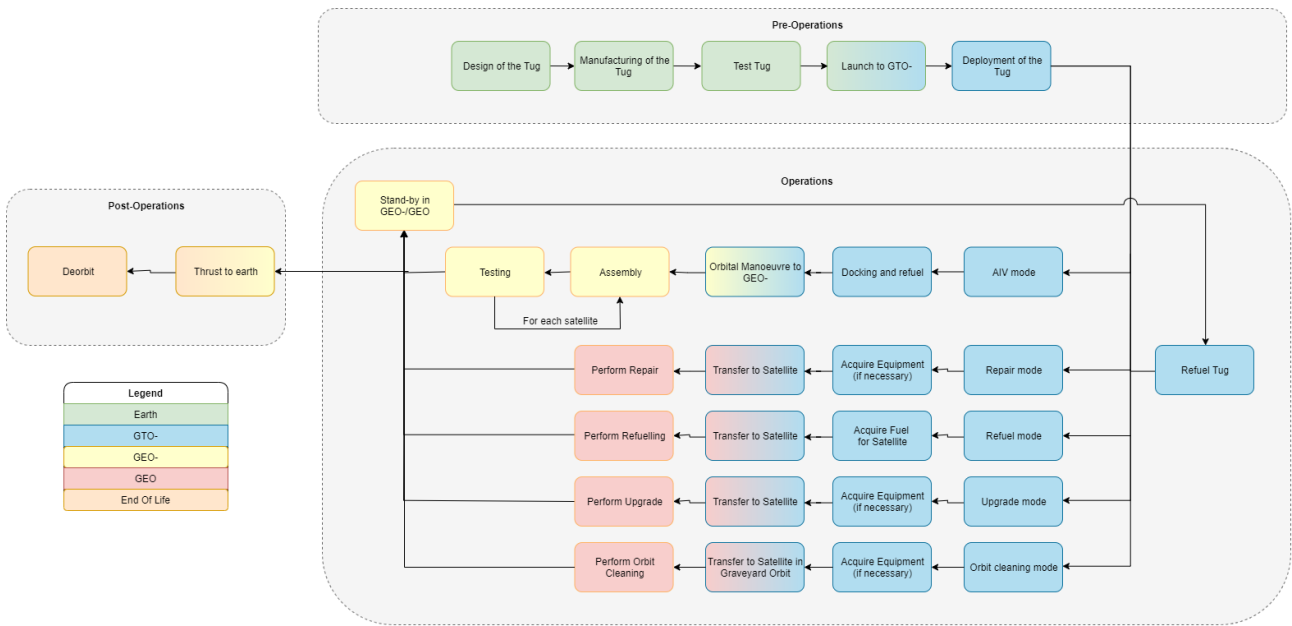


Figure 4.1: Mission stages of the tug

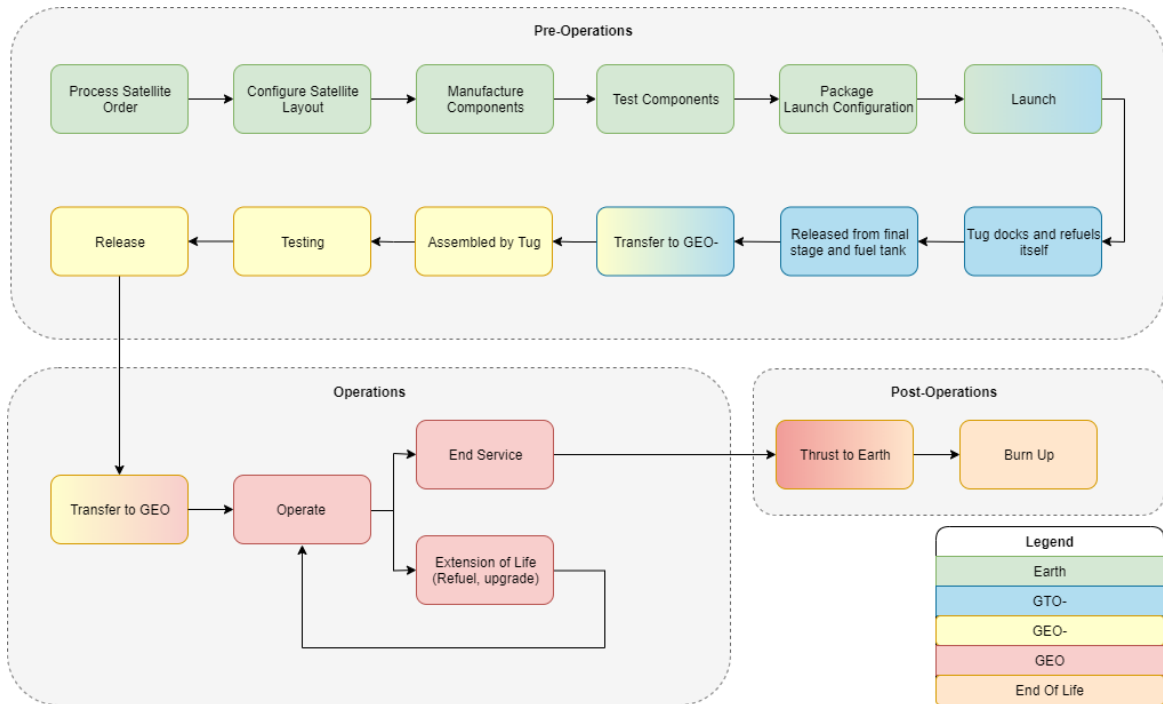


Figure 4.2: Mission stages of the satellite

4.2. Functional Analysis of the Tug and the Modular Satellite

For the functional analysis of the tug a Functional Flow Block Diagram (FFBD) and a Functional Breakdown Structure (FBS) have been established. They are tools used in the functional analysis and help to prepare the step-by-step operations sequence of the system. The Functional Breakdown Structure includes all functions of the FFBD and includes a lower level to most functions. The Functional Breakdown structure thus provides more detail on the functions of the system. A first version of the FFBD and the FBS for AIV missions have been established at an earlier stage of the project. For the detail design of Project MANTIS these have been updated in order to use them as a guideline during the detail design process. The FFBD and FBS for the tug are depicted in figs. 4.3 and 4.4 respectively. For the modular satellite the same design tools have been established. The FFBS and FBS of the satellite are depicted in figs. 4.5 and 4.6 respectively.

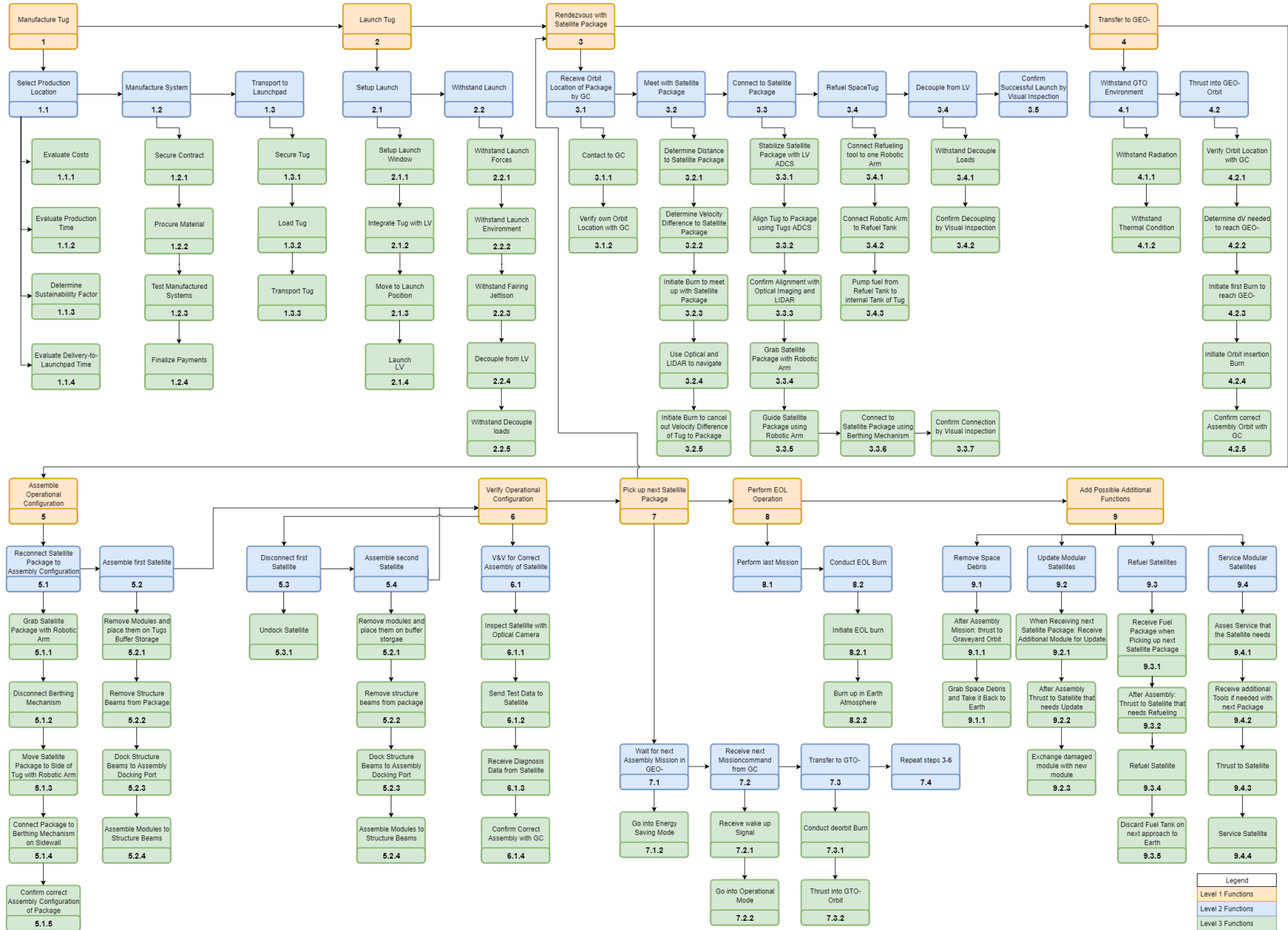


Figure 4.3: FFBD for the tug

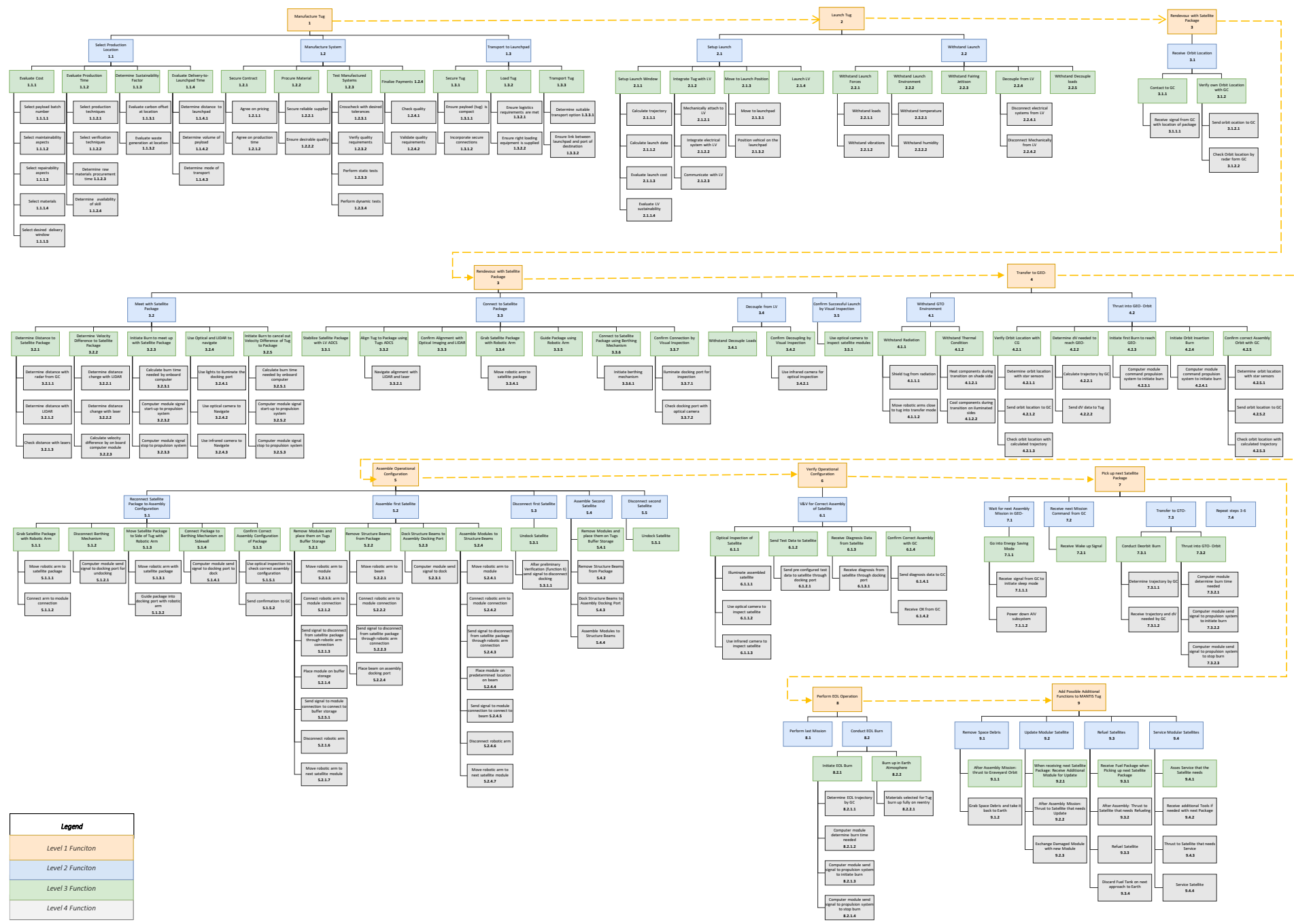


Figure 4.4: FBS for the tug

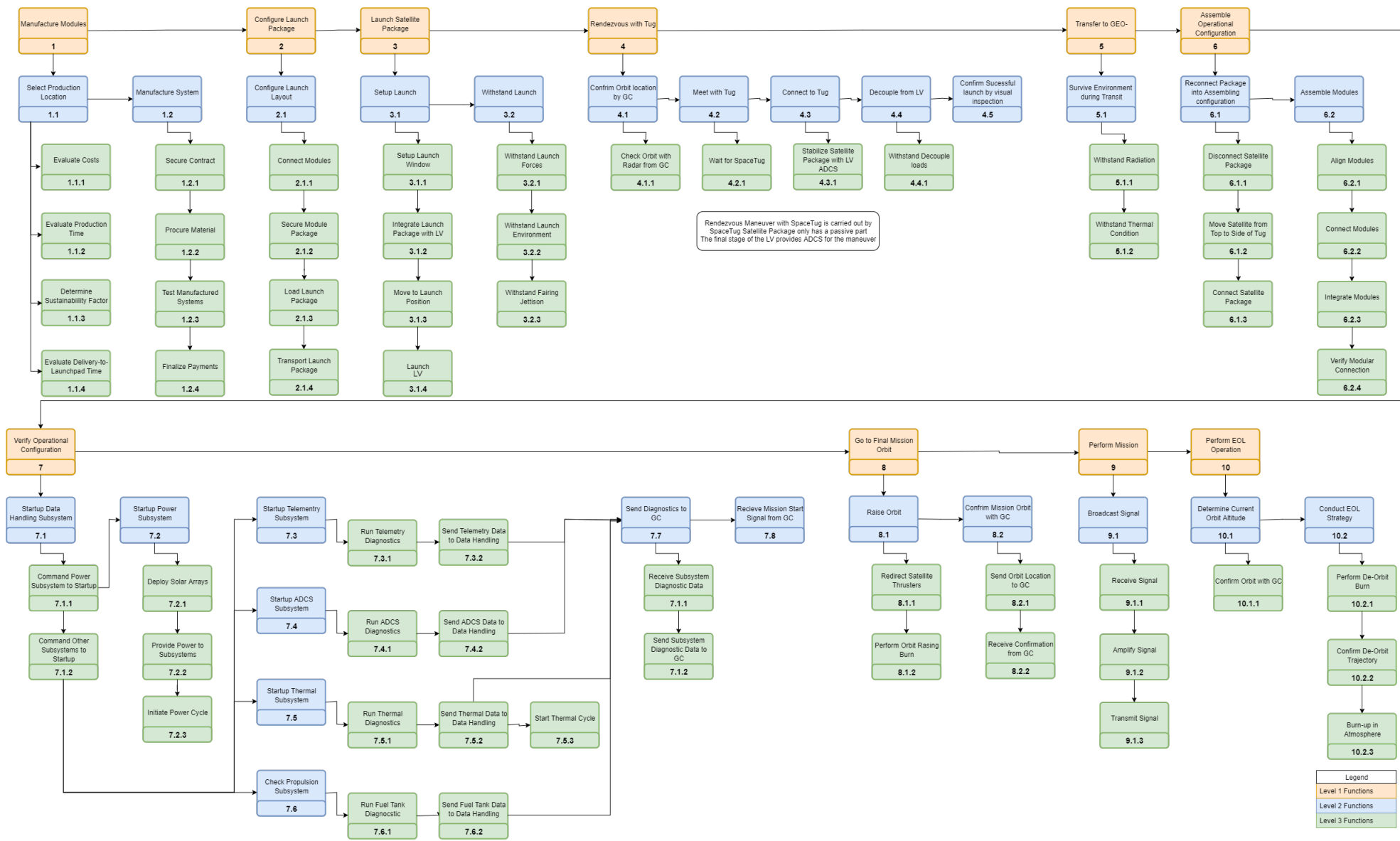


Figure 4.5: FFBD for the satellite

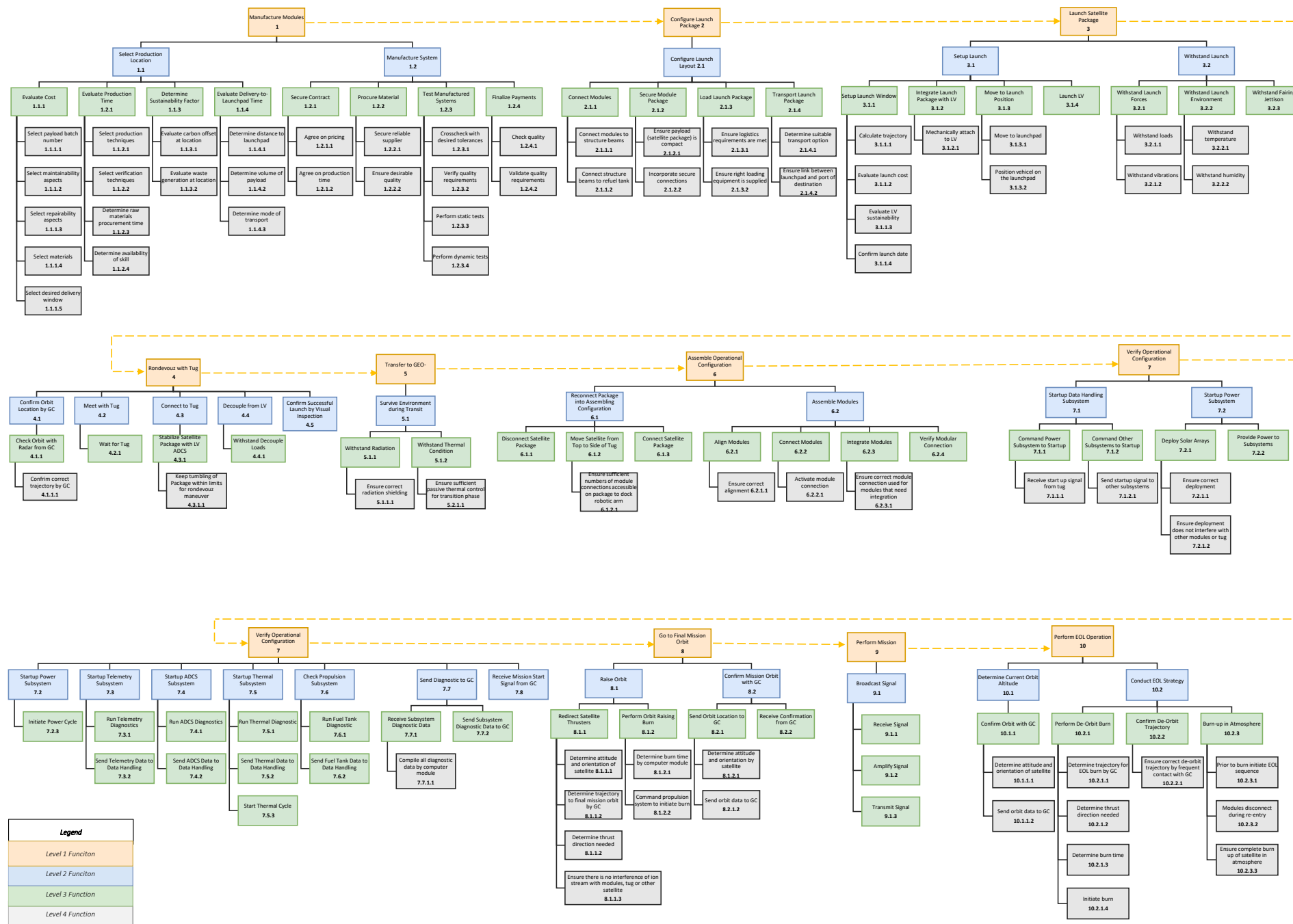


Figure 4.6: FBS for the satellite

Communications

A reliable communication with the spacecraft is crucial for any mission. This chapter will investigate the issue at hand by providing an overview of the purpose, sizing and implementation of communication systems for both the tug and the constructed satellite. The major difference between the two systems is the amount of data that needs to be transferred and the number of ground stations that are in contact at a given time. For the tug this number, representative of the amount of users is going to be much smaller and specialised on command and telemetry transmission. Ground stations dedicated to this can be much more powerful and sensitive than the average user terminals for a telecommunication satellite.

To get an initial idea of the communication link parameters a link analysis is performed. In this, the most important tool is the link budget, that takes a variety of system specific inputs and gives feedback on whether a given link closes with the selected parameters. This tool can be very useful to explore different methods of achieving this goal, based on the requirements previously set for the system.

Listing the previously formulated [27] and complied with relevant requirements (see chapter 17) to be fulfilled, that have been slightly modified in this subsection to account for the detailed architecture:

- **IKEA-CONS-PM-STA-T6:** AIV design shall integrate Airbus' IKEA-Sat Idea.
- **IKEA-CONS-ENG-SUS-T4:** The use of at least TRL5 items shall be considered first for use in the design.
- **IKEA-CONS-ENG-ENBU-T8 - 1:** The minimum E_b/N_0 at the ground receiver for the tug shall be 8 dB.
- **IKEA-CONS-ENG-ENBU-T8 - 2:** The minimum E_b/N_0 at the ground receiver for the satellite shall be 8 dB.
- **IKEA-CONS-ENG-ENBU-T9 - 1:** The minimum E_b/N_0 at the space receiver for the tug shall be 8 dB.
- **IKEA-CONS-ENG-ENBU-T9 - 2:** The minimum E_b/N_0 at the space receiver for the satellite shall be 8 dB.
- **IKEA-TECH-PROD-T4:** The sub-assemblies shall be able to be transported to the launch site.
- **IKEA-TECH-OPE-TTC-T3:** The data transfer shall be done in the Ku-Band frequency range.

These were refined and now specify actual operational parameters which were derived from operational systems. Separate trade-offs were performed to decide on exact values that will be explained in the following sections, whilst chapter 17 is dedicated to evaluate the full system requirement fulfillment. Additional content of this chapter includes the different possible options of implementing a communication system in terms of hardware and a short overview of digital signal encoding.

5.1. Technology

One of the most used technologies nowadays is the usage of spot beams. The reason for this is on one hand achieving higher gain over the full coverage area, by avoiding gain fall-off on larger single beam fringe regions, and on the other hand more optimised coverage areas to facilitate communication. For this, different regions can reuse the same frequency with different data, optimising the use of the available bandwidth and increasing possible throughput. An exemplary visualisation can be found in fig. 5.1b. In order to achieve good spot beam coverage technology like the Multiple Feed per Beam (MFB) "MEDUSA" projector [88] in combination with a reflector or more conventional Single Feed per Beam (SFB) solutions (e.g. Airbus LMFA [32]) can be used. For a comparison of their appearance take a look at figs. 5.2a and 5.2b. The advantages of a Beam Forming Network (BFN) like the "MEDUSA" include the possibility of using a single reflector aperture to create overlapping beams, making it possible to reduce the spacecraft mass by reducing the amount of reflectors [75]. The state-of-the-art single feed per beam solution makes use of multiple reflectors, depending on the number of spot channels or "colours" [75]. Thus a common four colour system would need four reflector dishes, weighing its less complicated design against a higher payload mass. Considering the customer wishes and currently available technology, the latter system is going to be used in the satellite design.

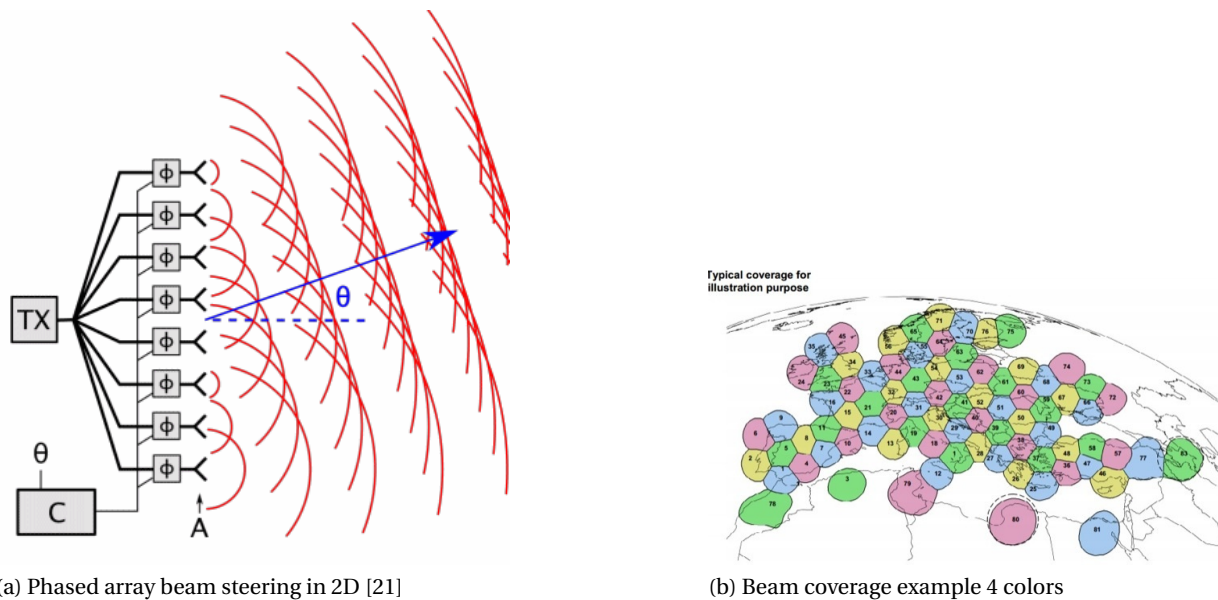
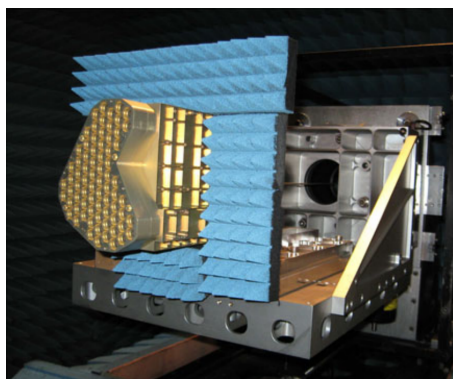
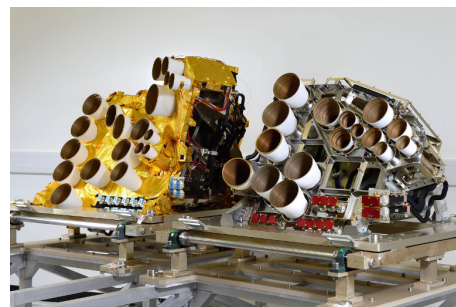


Figure 5.1: Visualisation of electronic beam steering in phased arrays and spot beam coverage

Steerable beams can be implemented by either making use of phased array technology utilising electrical steering (see fig. 5.1a), or a mechanically steered transmitter-antenna combination. To an extent it is also possible to utilise phased arrays for multiple spot broadcasting, but this technology currently has no major play in the market. In general, a phased array consists of several antennas that are arranged in a pattern and form beams by feeding the different antennas with a certain delay as shown in fig. 5.1a. The layout of the communication system and satellite are detailed in chapters 11 and 13 respectively. It shall already be stated that it was decided to make use of the more conventional steerable dish solution, as phased arrays are still being developed and ususally possess lower gain figures. In case of JAXA's Kizuna/WINDS satellite, the array radiated power was approximately 13dBW lower than the conventional multibeam array [31]. Of course, due to the modular nature of the system as a whole, it is possible to design a steerable beam or even static coverage via phased arrays at a later point and either upgrade existing missions or simply attach it to newly commissioned satellites.



(a) MEDUSA MFB array



(b) LMFA SFB array

Figure 5.2: Topology Comparison of MFB & SFB Arrays

5.2. Possible Implementation

The customer desires to have 50 - 70 transponders on the satellite, four of which possess the ability of adjustable coverage by beam steering. Besides that, a set of four main reflector antennas is to be implemented serving the remaining 48 transponders. Efforts to procure technical specifications are ongoing and the data that has been found so far will be used to create a preliminary hardware layout and link analysis.

TESAT-Spacecom has been most helpful in providing detailed information on their transponder technology and estimates, so their components will be used as a reference [59]. In addition, General Dynamics

makes technical information available on their website [53], providing another source of reasonable system characteristics. Other suppliers include Mitsubishi Electric and NEC Corp. However, most companies providing the satellite bus seem to make use of proprietary hardware. For the reflector dishes and steerable spot beams antenna technology provided by HPS is used, resulting in four unfoldable Large Deployable Antennas and four top-deck steerable beam assemblies.

The physical hardware layout will be shown in more detail in chapter 11. The power, mass, size and module arrangement will be presented there.

5.3. Check System Viability - Link Budget

Generally speaking, a communication satellite has four directions of signal links: The up- and down-link from the first user (forward) and the up- and down-link from the second user (return). Link analysis is always performed on an end-to-end basis, from ground transmitter to the user receiver and vice versa. This holds true for all back and forth communication systems. In case of the tug, there is only one user, which is the mission control station. The principal result of the link analysis is the E_b/N_0 ratio. To interpret the result, this value is compared to the operating parameters threshold. The required detection threshold on the receiving side is referred to as the link margin, which has to be positive for a successful “closing” of the link. To ensure robustness this margin needs to be designed to be larger than 0, by how much depends on mission critically, where typical values are around 3 dB [30].

The signal power at the receiver can be expressed as a function of the transmitter power, the gains of both antennas and the total loss as follows [58]:

$$P_{rx} = P_{tx} + G_{tx} + G_{rx} - L_{tx-rx} \quad (5.1)$$

Here P_{rx} is the power that arrives at the actual receiver, having passed through the antenna and initial stages of the input section of the receiver side. G_{rx} is the gain of the receive antenna and G_{tx} is the gain of the transmitter antenna. As a side note: it is always interesting to have higher gain antennas, as the transmitter needs to be less powerful. However, this greatly increases the directivity of the signal and thus reduces the achievable coverage.

Continuing with the terms of the equation, P_{tx} is the power radiated from the transmitter amplifier and L_{tx-rx} represents all losses on the link, including free space loss, atmospheric effects, line losses and pointing losses.

The equation seems easy at first glance, but especially the loss term requires analytical effort. Several link details need to be investigated to understand the different contributions to the budget. A working Microsoft Excel[®] sheet has been created to come up with a full link budget and has been verified by checking it against a given calculation [58]. The entered reference date perfectly reproduced the given result.

The most important formulas to be used as derived by current literature [58] are:

$$\Theta = \frac{21}{f \cdot D} \quad (5.2)$$

The Half Power Bandwidth angle Θ in degrees as a functional parameter of the antenna, where f is the frequency in GHz and D is the diameter of a parabolic dish in meters.

$$G = 20.4 + 20 \cdot \log(f) + 20 \cdot \log(d) + 10 \cdot \log(\eta) \quad (5.3)$$

The gain of an antenna in dB operating at frequency f in GHz with a diameter of d meters and an efficiency of η .

$$P_{EIRP} = 10 \cdot \log(P_{tx}) + G + L_{tx} \quad (5.4)$$

The P_{EIRP} is calculated by transforming the transmitter power into dB, adding the gain of the antenna and subtracting the line loss. The unit of measure is dBW.

The biggest contribution to the link budget is the Free Space Loss [dB], which is calculated as a function of the communication frequency in GHz and the distance between transmitter and receiver in km.

$$L_{FS} = -(92.45 + 20 \cdot \log(r) + 20 \cdot \log(f)) \quad (5.5)$$

The next equation calculates the gain of the satellite antenna based on the coverage area C in deg^2 and the antenna efficiency η . The dB value of this can be calculated according to the following formula.

$$G_s = 10 \cdot \log\left(\frac{41253}{C}\right) + 10 \cdot \log(\eta) \quad (5.6)$$

Another important value is the Gain-to-Noise Temperature of the system G/T in $\frac{\text{dB}}{\text{K}}$, which is easily calculated from the dB values of gain and the system noise temperature N_s as shown.

$$\frac{G}{T} = G_s - N_s \quad (5.7)$$

The second to last important formula describes the bandwidth independent Carrier-to-Noise ratio at the receiver, which is a special form of the Signal to Noise Ratio (SNR) for modulated signals in dB-Hz.

$$\frac{C}{N_0} = P_{EIRP} + \frac{G}{T} + 228.6 + L_{FS} + L_S \quad (5.8)$$

Finally the last formula, that is used to determine if the SNR is sufficient for a given encoding, calculates the E_b/N_0 at the receiver by subtracting the logarithmic value of the data rate in dB-Hz from the C/N_0 .

$$\frac{E_b}{N_0} = \frac{C}{N_0} - 10 \cdot \log_{10}(f[\text{Hz}]) \quad (5.9)$$

Link Budget Calculation Results

In the following a full Link Budget Calculation will be performed for a GEO telecommunication satellite, going from sender to satellite to recipient. Equations (5.2) to (5.9) will be used to compute the relevant parameters, whilst input is based on available data and references. In combination with the creation of the previously mentioned link budget Excel sheet, research has been carried out on available components, whose parameters can be used to make a meaningful calculation. The inputs for the satellite link are shown in tables 5.1 and 5.2, with the outputs following in tables 5.3 and 5.4. It has been decided that the 16APSK will be used for the satellite link, which requires an E_b/N_0 ratio of roughly 8 dB. Most Ku-Band satellites that provide communication services nowadays aim for 10-12 dB link margin, with exceptions that lay even higher up to 20 dB for urban coverage [73]. However, the desired mission is designed for slightly larger terminals such as on ships or aircraft, resulting in the given ground station parameters. Meanwhile, the Ku-Band has been chosen, because the impact of atmospheric attenuation is lower when compared to the Ka-Band, but the possible throughput much higher than lower frequency bands. Additionally, information could be procured on existing hardware originating in the European area, giving a more detailed impression on this otherwise rather rough first sizing.

Table 5.1: Link Budget inputs for up-link (left) and down-link (right)

	General Inputs	Value	Unit		General Inputs	Value	Unit
Ground	Uplink Frequency	13	GHz	Satellite	Downlink Frequency	12	GHz
	Uplink Antenna Diameter	1.5	m		Downlink Antenna Diameter	3	m
	Antenna Efficiency	0.55	%		Antenna Efficiency	0.5	%
	Power Output TX	50	W		Power Output TX	47	W
	Line Losses	-6	dB		Line Losses	-5	dB
	Propagation Range UP	35786	km		Propagation Range DWN	35786	km
	Atmospheric Loss	-10	dB		Atmospheric Loss	-9	dB
	Satellite	Satellite Antenna Diameter	3		m	Ground	Downlink Antenna Diameter
Antenna Efficiency		0.5	-	Antenna Efficiency	0.55		%
Line Losses		-2	dB	Line Losses	-3		dB
System Noise Temperature		29	dB-K	System Noise Temperature	28		dB-K

Performing a detailed sensitivity analysis for each of the parameters would go beyond the scope of the current project, as this subsystem is not the focus of the research. However, the most impactful parameters include the size and efficiency of the antennas, the data rate and the amount of users per channel.

Table 5.2: Additional input parameters for link budget calculation

Additional Inputs	Value	Unit
Carrier Bandwidth	28	MHz
User Data Rate	0.5	Mbps
Users/Carrier	4	-
Required Eb/N0	8	dB

Table 5.3: Output data for up-link

	Link Parameter	Output	Units	Comments
Ground User	Beamwidth Half Power	1.077	deg	eq. (5.2)
	Gain of Antenna	43.6	dBi	eq. (5.3)
	EIRP Power	54.6	dBW	eq. (5.4)
	EIRP Power/User	48.6	dBW	eq. (5.4)
	Free Space Loss	-205.8	dB	eq. (5.5)
	Path Loss	-215.8	dB	Add Atmospheric
Satellite	Beamwidth Half Power	0.538	deg	eq. (5.2)
	Gain of Antenna	49.2	dBi	eq. (5.3)
	Received Carrier Power	-114	dBW	eq. (5.1)
	Received Carrier Power/User	-120	dBW	eq. (5.1)
	G/T satellite	20.2	dB/K	eq. (5.7)
	RX (User) C/N0	79.6	dB-Hz	eq. (5.8)
	Data Rate	56.99	dB-Hz	Requirement/Input
Available Bit Energy/N0, Uplink	22.6	dB	eq. (5.9)	

Table 5.4: Output data for down-link

	Link Parameter	Output	Units	Comments
Satellite	Beamwidth Half Power	0.583	deg	eq. (5.2)
	Gain of Antenna	48.5	dBi	eq. (5.3)
	EIRP Power	60.2	dBW	eq. (5.4)
	EIRP per User	54.2	dBW	Requirement/Input
	Free Space Loss	-205.1	dB	eq. (5.5)
	Path Loss	-214.1	dB	Add Atmospheric
Ground	Beamwidth Half Power	1.167	deg	eq. (5.2)
	Gain of Antenna	42.9	dBi	eq. (5.3)
	Received Carrier Power/User	-120	dBW	eq. (5.1)
	G/T ground	14.9	dB/K	eq. (5.7)
	RX C/N0	80.6	dB-Hz	eq. (5.8)
	Data Rate	56.99	dB-Hz	Requirement/Input
	Eb/N0 per User, Downlink	23.6	dB	eq. (5.9)
	Link Margin	15.6	dB	
Link Closes?	YES			

For the tug, a ground station with a dish diameter of 13 m is considered based on information provided about ESTRACK [35]. We will assume a relatively low ground antenna efficiency of 50% [30] and a link frequency of 11 GHz [73]. Again the worst case scenario is when the spacecraft is located in GEO. The spacecraft will be equipped with a high gain Gregorian type antenna, similar to the one employed on the TESS spacecraft [66], which will be used to optimise the use of the limited on-board transmitter power. A diameter of 0.7 m with an efficiency of 70% will be used for calculations, assuming we make use of a single channel with a data rate of 1 Mbps. The transmit power of the ground station is assumed to be 200 W whilst the satellite has 2 W. Atmospheric losses are estimated at 8 dB, and total line losses one way of 8 dB are accounted for. The system noise temperature for the ground station and the tug are 28 and 29 K respectively. Finally, the required Eb/N0 is 8 dB. The results are presented in table 5.5, where it is visible, that the tug link is indeed very robust as well.

Table 5.5: Tug link budget

	Link Parameter	Output	Units	Comments
Ground TX	Gain of Antenna	60.9	dBi	eq. (5.3)
	EIRP Power	77.9	dBW	eq. (5.4)
	Free Space Loss	-204.4	dB	eq. (5.5)
	Path Loss	-212.4	dB	Add Atmospheric
Satellite RX	Gain of Antenna	36.6	dBi	eq. (5.3)
	Received Carrier Power	-99.9	dBW	eq. (5.1)
	RX(user) C/N0	99.7	dB-Hz	eq. (5.8)
	Data Rate	56.99	dB-Hz	Requirement/Input
	Available Bit Energy/N0, Uplink	42.8	dB	eq. (5.9)
Satellite TX	Gain of Antenna	36.6	dBi	eq. (5.3)
	EIRP Power	37.6	dBW	eq. (5.4)
	Free Space Loss	-204.4	dB	eq. (5.5)
	Path Loss	-212.4	dB	Add Atmospheric
Ground RX	Gain of Antenna	60.9	dBi	eq. (5.3)
	Received Carrier Power/User	-119.9	dBW	eq. (5.1)
	RX C/N0	80.7	dBW	eq. (5.8)
	Data Rate	56.99	dB-Hz	Requirement/Input
	Available Eb/N0, Downlink	23.8	dB	eq. (5.9)
	Link Margin	15.8	dB	
	Link Closes?	YES		

5.4. Digital Encoding Techniques

Using the link budget tool, the results as shown in table 5.5 are calculated. From this it is easily visible that the much larger receiver station for ground control makes it possible to use relatively small transmitters on the spacecraft with enough bit energy to make use of even 16APSK, if supported by the on-board hardware [30, 58]. These acronyms refer to digital encoding methods used to increase the data throughput by mapping bit combinations to certain phase and amplitude combinations of the carrier signal, when polarising the signal. A visual representation is given in fig. 5.3. Here I stands for the horizontal reference components, so the non polarised part of the signal. Q on the other hand stands for the signal component that is rotated by 90 degrees. The combined amplitude and phase of the received signal enable the receiver to distinguish between a set of symbols, each representing a series of bits. QPSK is also shown, to be able to see that distinction of symbols is easier, when less are used. This is also the background, to why higher density encoding requires better signal to noise results, as the uncertainty "areas" around a specific symbol don't allow for much deviation before the transmitted symbol is impossible to reliably identify.

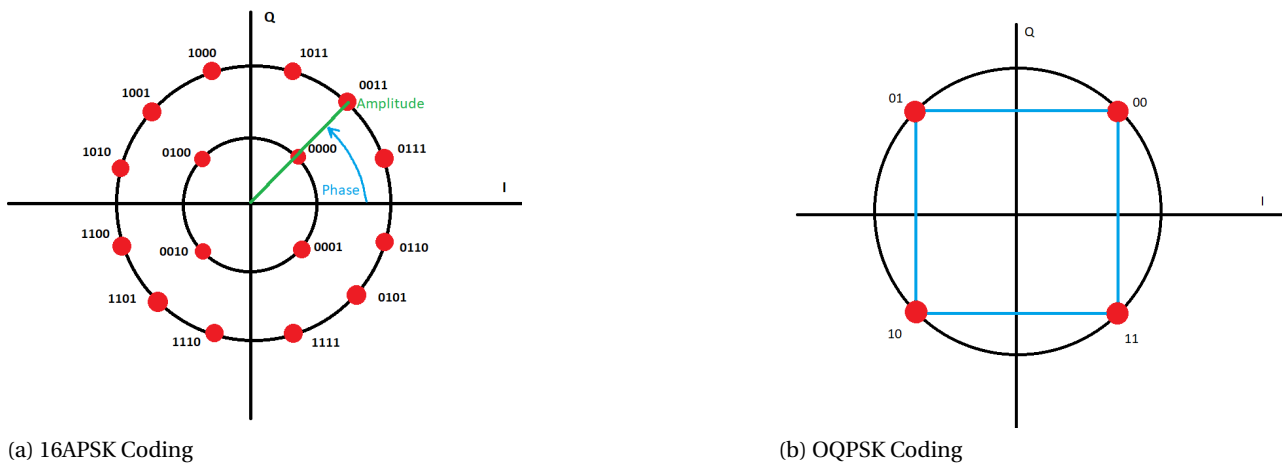


Figure 5.3: Coding methods for digital communication links

5.5. Chapter Conclusion

This section ends with the preliminary selection of components to be used and an explanation of the module layout. Components that have been selected for the architecture are:

- 52 Tesat-Spacecom Ku-Band Transponders
- 4 Airbus LMFA
- 4 HPS Large Deployable Antennas for beam focus and relay
- 4 steerable HPS spot-beam units

These components are then grouped as follows, to allow for a modularised system.

Static Spot Module

This module uses 12 Tesat-Spacecom Transponders that are connected to a feed array for the attached LDA.

Steerable Spot Module

A much smaller module, where a single Transponder feeds a horn antenna, that uses a double reflector system to redirect and focus the signal on the desired regions. It is also folded into a box shape during launch.

Requirement Compliance

The requirements previously mentioned in the introduction to this chapter have been proven to be complied with all around. The modules have been designed to be used in the MANTIS system, with all considered components being TRL5 or higher. The current layout vastly exceeds the required Eb/N0 ratio, making it possible to either serve more users or increase the data rate. Transport to the launch site is hardly an issue for these modules, due to their comparatively small size and the frequency used complies with the requirement of making use of the Ku-Band.

Finally a simplified TT&C Communication flow diagram for the actual assembly mission has been created with fig. 5.4.

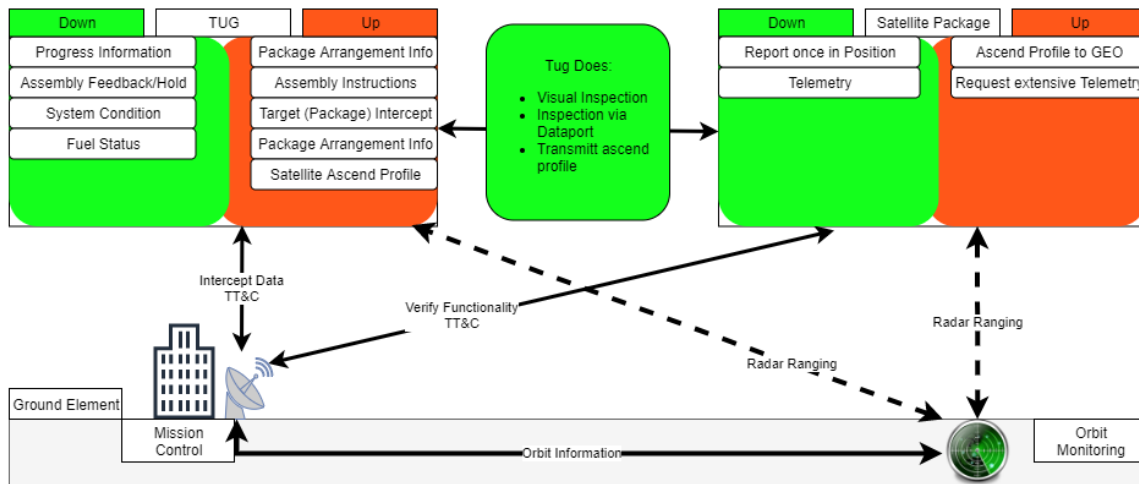


Figure 5.4: TT&C Communication Flow Diagram

Propulsion

To design the propulsion module, first the astrodynamics characteristics need to be determined to see for what orbits and transfers the propulsion system is designed for, which is done in section 6.1. After that, the boundaries and requirements of the system are set for the system in section 6.2. Lastly, the propulsion system is designed for the satellite and tug in sections 6.3 and 6.4 respectively.

6.1. Astrodynamics Characteristics

For the project, launchers and orbits play a vital role in the success of the mission. One important characteristic is the launcher that is used.

In the space industry, there are certain main companies which produce launchers suitable for the mission. These launchers include the Falcon series from SpaceX, the Ariane series from Arianespace, and the Soyuz series used by Roscosmos to launch payloads to the ISS.

In order to select a launcher, there are several characteristics that differ in importance. For this project, two characteristics are most important - namely sustainability and cost. It goes without saying that any launcher incapable of reaching the desired orbit was automatically discarded.

Based on the above criteria, the Falcon Heavy launcher was chosen. This is relatively cheap, especially since the first stage of this launcher is fully reusable [98]. This is also a large advantage over the other launchers regarding sustainability, which is further discussed in section 19.3.2.

For Project MANTIS, three orbits are used. First, any satellite payload enters a GTO- orbit. This is an orbit comparable to GTO, however its perigee is at 7131 km, while its apogee is at 41164 km. This is the orbital radius of the second orbit, GEO-. This orbit is 1000 km lower in orbital radius than GEO, which is the final orbit for the assembled satellite.

In order to get into the above orbits, the following ΔV values are required (table 6.1). These values were calculated using eq. (6.1) [104]. In this formula, G stands for the Gravitational constant, M_e is the mass of the Earth and, r_1 and r_2 stand for the radii of the perigee and apogee respectively.

$$\Delta V = \Delta V_1 + \Delta V_2 = \sqrt{\frac{G \cdot M_e}{r_1} \left(\sqrt{\frac{2r_2}{r_1 + r_2}} - 1 \right)} + \sqrt{\frac{G \cdot M_e}{r_2} \left(1 - \sqrt{\frac{2r_1}{r_1 + r_2}} \right)} \quad (6.1)$$

Table 6.1: ΔV values to get to desired orbits

Orbit	ΔV [km/s]
GEO- $\xrightarrow{\text{from/to}}$ GTO-	1.421
GEO- $\xrightarrow{\text{to}}$ GEO	0.037

For GEO- the orbital velocity is 3.11 km/s, with an eclipse time of approximately 68 minutes and 30 seconds in a total orbital period of 23 hours and 5 minutes. Finally, the orbital velocity for GEO is 3.074 km/s, with an eclipse period of approximately 69 minutes and 25 seconds in a total orbital period of 23 hours and 56 minutes.

6.2. Propulsion Requirements

The propulsion system is one of the main subsystems of the mission. This is the case due to the high mass which it contributes to the total wet mass. A trade-off has been conducted for both the chemical propulsion

system of the tug and the electric propulsion system of the satellite. This trade-off is based on the requirements as stated below. First, the fuel mass of the satellite and its propulsion system have been calculated in section 6.3. Secondly, this has been done for the tug as well in section 6.4.

- **IKEA-TECH-OPE-PROP-T1:** The propellant of the AIV system shall fit in the launch vehicle together with two satellites
- **IKEA-TECH-OPE-PROP-T6:** The tug propulsion system shall be able to cope with all ΔV requirements throughout the mission.
- **IKEA-TECH-OPE-PROP-T7:** Only non-toxic propellants shall be used.
- **IKEA-TECH-OPE-PROP-T8:** The propulsion system shall be able to cope with all thrust requirements throughout the mission.
- **IKEA-TECH-LAU-T1:** The AIV system shall physically fit into the selected launcher.
- **IKEA-CONS-PM-SCHE-T3:** Once in operation, the system shall assemble a new satellite within one year.

6.3. Satellite

Looking at the electric propulsion of the satellite, there are two main characteristics that are used for a trade-off between different engines. This is the power needed to thrust (section 6.3.1) and the specific impulse (section 6.3.2).

6.3.1. Power

The power is limited by the power that all other subsystems need during operation, as the solar panels will be designed for the power consumption while the satellite is in operational state in GEO. As will be explained later in chapter 9, the power budget of the satellite is 10.5 kW at Beginning of Life (BOL) and 9.2 kW at EOL. As the transfer from GEO- to GEO is at the beginning of the mission, there is 10.5 kW available for the thrusters. As an electric propulsion system requires four engines, of which two are redundant [34], this power should be divided by two to find the power available per engine. This results in a power budget of 5.3 kW at BOL and 4.6 kW at EOL. This limits the size of the ion electric engine that can be used. Engines in the range of 0 to 10 kW per engine are taken into consideration, as the engines can be throttled down and use less power. So, from now on all engines that require more than 10 kW are disregarded in the trade-off. In contrast to that, the required power should not be too low, as the thrust will decrease as well. This results in increasing the travel time too much and eventually, it will not comply with **IKEA-CONS-PM-SCHE-T3**. This results in a power budget of 1 to 10 kW per engine.

6.3.2. Mass

Next to the available power, the specific impulse and therefore fuel mass influences the choice of engine. The trade-off is based on the wet mass of the tug. Hence, the lowest wet mass is chosen within the, above determined power budget, to meet requirement **IKEA-TECH-OPE-PROP-T1**.

Most of the ion engines present require less than 1 kW [58]. There are five engines that operate in the previously set power budget. These are the XIPS-25 (L3), NSTAR (L3/NASA), NEXT (NASA), T-6 (Qinetiq) and RIT-XT (Astrium). The RIT-XT, NEXT and T-6 engines have specific impulses above 4000 s, so these three are regarded into the trade-off. Initially, the RIT-XT was even tested to reach a specific impulse up to 5000 s [60]. However, the company that was designing the engine, Astrium, emerged to become Airbus Defence & Space. As a result of the merge, the RIT-XT is not manufactured anymore. Secondly, the T-6 engine manufactured by Qinetiq can reach a specific impulse of 4300 s at 4.5 kW. This is reached by adding an Optimized Neutralizer, throttled to 145 mN [91]. Lastly, the NEXT thruster reaches a specific impulse of 4310 s at 4.2 kW, by throttling back to 134 mN.

Due to the specific impulses that are that close to each other, the dry mass of the propulsion system is taken into consideration as well. The two main masses are the engine itself and the Power Processing Unit (PPU). The dry masses of the engines used to calculate the final wet mass of the satellite are shown in table 6.2.

Beside the engine, the fuel tank plays a roll in the mass budget as well. For the xenon tanks that are needed in the electric propulsion system, an off-the-shelf product has been chosen. The fuel that needs to be stored

in the fuel tank weighs 249.3 kg. Cobham has developed a tank that can store up to 450 kg of xenon [22]. This tank has a dry mass of 22 kg which is added to the total dry mass.

Table 6.2: Trade-off electric thruster

Characteristics	Qinetiq, T-6	NASA, NEXT
Specific Impulse [s]	4300	4310
Required Power [W]	4500	4235
Thrust [mN]	145	134
Thruster mass [kg]	8.5	12.7
PPU mass [kg]	17.5	34.5
Dry mass [kg]	1847.0	1935.8
Fuel mass [kg]	249.3	260.6
Wet mass [kg]	2096.3	2196.4

These wet masses differ by only 100 kg. Therefore, a local sensitivity analysis has been conducted to see the impact of having a different dry mass for the satellite. This could happen due to slight changes in the design process. Therefore, these changes can not be too large, since it would change the whole design. For the sensitivity analysis, a range of 0 to 5000 kg dry mass has been used. This range is significantly higher than the allowable change, but it shows the validity of the choice well. The difference between the wet masses of the Qinetiq T-6 and the NEXT does not change much, as can be seen in fig. 6.1. Therefore, choosing the Qinetiq T-6 is validated for the MANTIS mission.

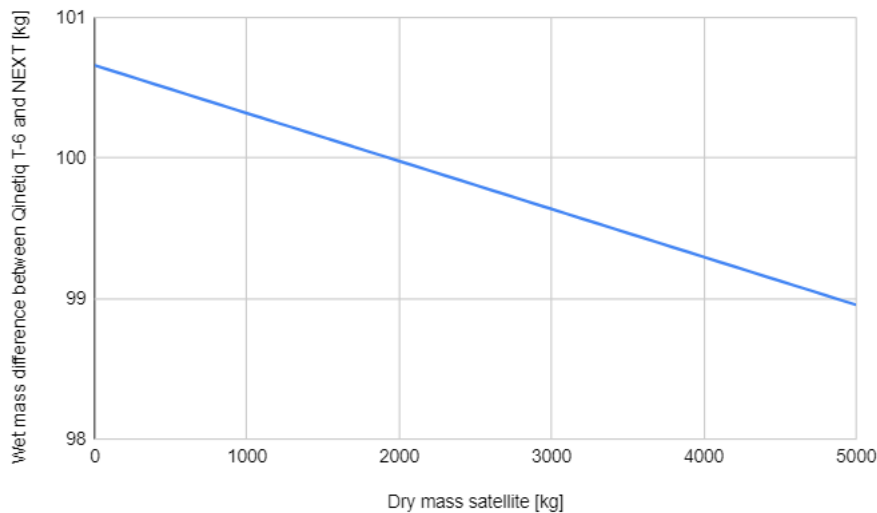


Figure 6.1: Difference in wet mass between Qinetiq T-6 and NEXT

6.4. Tug

The propulsion system of the tug should transfer the tug, along with two fully loaded satellites, as stated in requirement **IKEA-TECH-OPE-PROP-T6**. The most important characteristic of the propulsion system is the fuel mass that is needed for the mission. Therefore, a trade-off has been conducted between three different type of chemical engines, conducted in section 6.4.3. First of all, a choice has been made between a solid or liquid propellant engine. As the former can not be throttled, stopped or restarted [72], this type of engine is unsuitable for the mission. This led to the trade-off between three different engines in three different ranges of dry mass and specific impulse. These engines contain two upper stage engines (Raptor Engine by SpaceX [97] and RL10A-4-2 by Aerojet Rocketdyne [79]) and an apogee engine (AMBR 556 N (125 lbf) Dual Mode High Performance Rocket Engine by Aerojet Rocketdyne [78]). To calculate the tugs wet mass for each of the thrusters, the mission stages are defined to calculate the fuel mass per stage in section 6.4.1. The fuel mass of each stage is calculated using eq. (6.3), which is derived from eq. (6.2) [11].

$$\Delta V = I_{sp} \cdot g_0 \cdot \ln \left[\frac{M_f + M_{dry}}{M_{dry}} \right] \quad (6.2)$$

$$M_f = M_{dry} \cdot \left[\exp\left(\frac{\Delta V}{I_{sp} \cdot g_0}\right) - 1 \right] \quad (6.3)$$

In this equation, M_f stands for fuel mass, M_{dry} means dry mass, I_{sp} stands for the specific impulse of the engine and g_0 stands for the standard gravity, which is $9.80665 \frac{m}{s^2}$ for orbits around Earth.

6.4.1. Tug mission stages

When calculating the wet mass of the tug, it is necessary to calculate from the end of the mission towards the beginning, because the wet mass of a last stage is the dry mass of the prior stage. Therefore, the calculation starts with the tug going back from GEO- to GTO-. The required ΔV for this stage is 1420.7 m/s. In the ordinary mission, the tug does not carry any satellite. However, the tug can clean up the graveyard orbit and bring back satellites from there as a special mission. This case is calculated in section 6.4.5.

The orbit maintenance is calculated, as well. It is assumed that the tug will be in GEO- for one year. This is probably not the case, but it creates a safety factor for the fuel mass. In addition, it is assumed that the ΔV in GEO- is the same as in GEO, due to the small distance between them. Therefore, the ΔV that is counteracted is $50 \text{ m} / (\text{s} \cdot \text{y})$ for North-South correction and $5 \text{ m} / (\text{s} \cdot \text{y})$ for East-West corrections.

The first stage is the transfer from GTO- to GEO- of the tug together with two telecommunication satellites. During this stage, the tug brings up all the fuel mass for later stages, the dry mass of the tug and the wet mass of the two satellites. After calculating the propellant mass for this stage as well, the total fuel mass for the mission is known. Using this fuel mass, the fuel tank is designed in section 6.4.2.

6.4.2. Fuel tank design

Using the calculated propellant masses, the fuel tanks are designed [58]. This is done for the three different engines using its own propellant type. Each engine uses liquid fuel and liquid oxidizer. Therefore, two main fuel tanks are designed. However, the optimal ratio between the fuel and oxidizer, and the type of fuel and oxidizer are different for each engine. Using the separate densities of the propellant, the required tank volume are determined. Using eq. (6.8) the structural masses of the fuel tanks are calculated using Mass Estimating Relations (MER). For liquid hydrogen tanks, eq. (6.5) is used [71].

The fuel tanks that use cryogenic propellants need insulation as well. This is the case for two of the engines that use liquid oxygen and liquid hydrogen. Its insulation mass which is added to the tank mass is shown in eqs. (6.6) and (6.7), respectively. In these formulae, it is assumed that the fuel tanks are spheres to calculate the surface area of the tank.

$$M_{Prop} = 12.16 \cdot V_{Prop} \quad (6.4)$$

$$M_{LH_2} = 9.09 \cdot V_{LH_2} \quad (6.5)$$

$$M_{LOX_{insulation}} = 1.123 \cdot A_{tank} \quad (6.6)$$

$$M_{LH_2_{insulation}} = 2.88 \cdot A_{tank} \quad (6.7)$$

In the end, another 10% of structural mass is added as a safety factor. This all will contribute to a final dry mass of the propellant tanks using eq. (6.8). Finally, a fraction of 3% is added to the fuel mass which is needed for ADCS [58]. The ADCS subsystem will be further explained in chapter 7.

$$M_{tanks} = 1.1 \cdot (M_{ftank} + M_{Oxtank} + 2 \cdot M_{pr_{tank}}) \quad (6.8)$$

In the end, the dry mass of the fuel tanks will be added to the total dry mass of the tug. This initiates an iteration for the fuel tanks, because the increase in dry mass will increase the required fuel mass, which will increase the size of the fuel tanks again. As this relation is converging, the iteration will converge to a final value for the tank. This value will iterate until the difference between the two steps is less than 0.1 kg. This iteration will also be done for the structural mass of the satellite.

6.4.3. Trade-off Thruster

The fuel mass for the missions as calculated in section 6.4.1 and the dry mass of the tanks as calculated in section 6.4.2 are known, so this can be calculated for the three engines that are traded off. The main characteristics of the engines and its fuel are stated in table 6.3.

Table 6.3: Main characteristics engines for trade-off

Characteristics	Raptor	AMBR 556 N Dual Mode	RL10A-4-2
Dry mass [kg]	1500	4.9	167.83
Thrust [N]	3,500,000	556	105,978.88
I_{sp} [s]	382	329	451
Oxidizer	O_2	N_2O_4 , with 3% NO	O_2
Fuel	CH_4	N_2H_4	H_2
O/F ratio	1:1	3.4:1	5.5:1
ρ_{ox} [kg/m ³]	1141	1396.8	1141
ρ_f [kg/m ³]	422.62	1010	70.8
Dry Mass (excl. engine and propellant tanks)	1005.3	1005.3	1005.3
Dry Mass	2645.6	1084.3	1348.9
Fuel Mass	5170.7	4012.9	2920.9
Wet Mass	7816.3	5097.2	4296.7

Lastly, two pressurized tanks are added to keep the fuel and oxidizer tank pressurized once the ignition has started. Due to the fuel that is burned, the pressure will go down. However, the pressurized gasses will flow into these tanks to compensate for the power loss. This will make sure that the engine will keep running. There are two most common gasses used for in the pressurized tanks; nitrogen and helium. A tank design has been done [58] and it was found that the nitrogen tank weighs 156.3 kg and the helium tank weighs 31.3 kg, both including the gas itself as well. Therefore, two helium tanks are chosen.

These characteristics of the propellant and pressurized tanks are used separately for the three engines to calculate its wet mass. This is done by excluding the engine and fuel mass from the dry mass first. The dry mass of the engine and fuel tanks is then added to the dry mass per engine, separately. This dry mass is then used to calculate the fuel mass and wet mass. This is an iterative process due to the weight of the fuel tank again. Finally, the masses are stated in the bottom part of table 6.3, which show that the upper stage engine, RL10A-4-2 comes out to be the most suitable engine for the mission.

6.4.4. Sensitivity analysis

A local sensitivity analysis is conducted to validate the choice of engine. For a change in engine independent dry mass or a change in wet mass of the satellite, the wet mass of the tug is calculated again. This is shown in figs. 6.2 to 6.5. In these graphs, the dry mass of the tug is plotted on the horizontal axis against the wet mass of the tug on the vertical axis. In fig. 6.2, the actual designed dry mass of the satellite is shown. This shows what the most efficient engine would be if the real dry mass of the tug changes after the design process. The same is done for a changing dry mass of the satellite. Therefore, a dry mass of 1000, 2000 and 3000 kg are shown in figs. 6.3 to 6.5 respectively. Only in fig. 6.3, the RL10A-4-2 and AMBR 556N Dual Mode engines are touching. However, this is the case for the lowest dry mass of the satellite and tug, which is highly unlikely to happen. Therefore, looking at the results of this sensitivity analysis, it is concluded that the RL10A-4-2 engine is most efficient, also after changing all dry masses. Hence, the RL10A-4-2 engine is chosen to be used for the mission.

6.4.5. Cleaning up graveyard orbit

An extra part of the mission that could add a lot of value to the concept is cleaning up the graveyard orbit. This entails travelling to the graveyard orbit, docking to a satellite and bringing it back to GTO- to let it burn up in the atmosphere. This is done by decelerating at the graveyard orbit to get into an elliptical orbit with a perigee of 6781 km. Once this ΔV is reached, the tug will release the satellite and accelerate again towards a perigee of 7131 km. There are three different missions in which the tug can clean up the graveyard orbit.

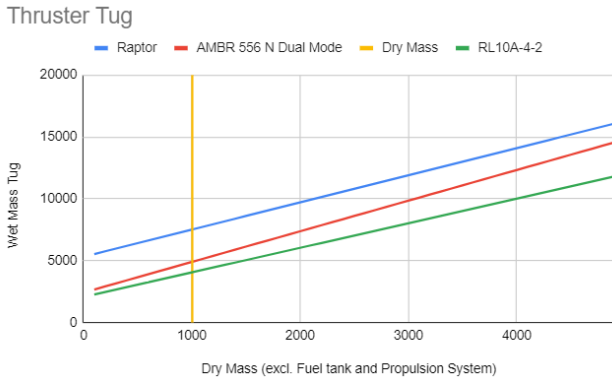


Figure 6.2: Actual dry mass satellite

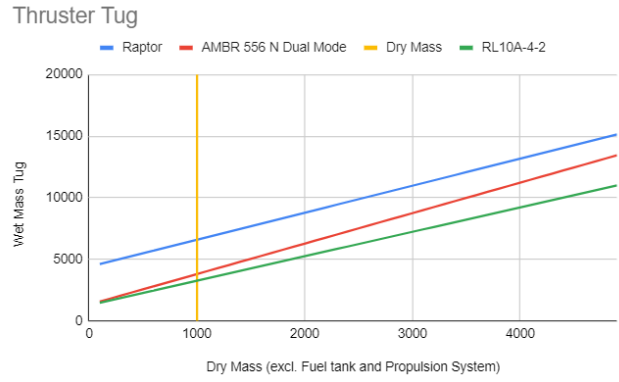


Figure 6.3: Dry mass satellite of 1000 kg

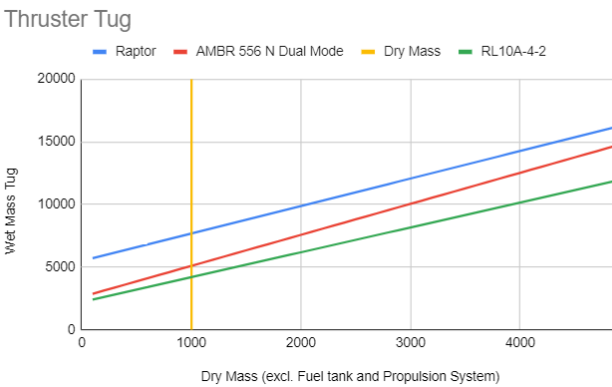


Figure 6.4: Dry mass satellite of 2000 kg

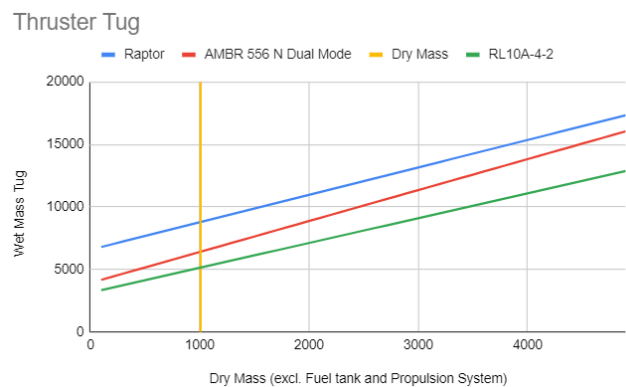


Figure 6.5: Dry mass satellite of 3000 kg

First of all, the tug can first bring two satellites to the GEO- orbit. Afterwards it will dock to a graveyard satellite and deorbit it into the atmosphere. This would be the most valuable trip, as it offers the most purposes. However, the tug needs to be over designed for all missions in which it does not clean up the graveyard, as this is an extra component. Using the same program and calculations, but adding the ΔV for the cleaning up mission, the wet mass of the tug has been calculated.

This calculation has also been produced in the case of delivering one or even zero satellites to the GEO-orbit. The masses calculated are shown in table 6.4. For these calculations, it is assumed that the dry mass of a satellite in the graveyard orbit is 2362 kg. This mass is estimated using the launched masses to GEO orbit stated in the UCS database [102]. A percentage of 72% is the propellant mass compared to the dry mass [58]. Using this relation, an average dry mass of 2362 kg is currently in GEO or in the graveyard orbit.

Table 6.4: Masses for clean up missions

Masses [kg]	Delivered Sats: 2 Clean up: NO (Regular Mission)	Delivered Sats: 2 Clean up: YES	Delivered Sats: 1 Clean up: YES	Delivered Sats: 0 Clean up: YES
Dry Mass	1348.9	1452.2	1395.5	1340.1
Fuel Mass	2920.9	4402.3	3550.6	2700.2
Wet Mass	4269.7	5854.5	4946.1	4040.3

This shows that for cleaning up the graveyard orbit and delivering at least one satellite, the tug needs to be increased in terms of mass. Therefore, this means that the tug will be over designed for regular missions, which is not efficient.

Therefore, taking down average sized satellites from the graveyard orbit is not suitable for the MANTIS mission. Smaller satellites are easier to transfer, as less fuel is needed for that. In fig. 6.6, the effect of the dry mass of the 'clean-up-satellites' on the wet mass of the tug is shown. It can be seen that the increase of the dry masses will increase the required fuel. The horizontal line shows the wet mass of the tug when the clean up mission is not performed. Therefore, the wet masses for any clean up mission should stay below this line, as the fuel tanks are designed for the regular mission. Looking at the cross-sections, the maximum dry mass that can be de-orbited into the atmosphere can be found. In the case of delivering one satellite into

GEO- first, the tug can take a satellite of maximum 2184.0 kg. Currently, there are over 100 satellites present in GEO or graveyard orbit below the 2000 kg [102]. Thus, it is feasible to clean up the graveyard orbit, while delivering one communication satellite to GEO-

Lastly, another mission could be performed by the tug to increase the value of the total mission. This is done by replacing and servicing the modules of already operating satellites in GEO. During this mission, the satellite package will be lighter, as there are not two full satellites in the launch vehicle. Therefore, the required fuel mass is less than during normal missions, which makes it a suitable mission as part of Project MANTIS.

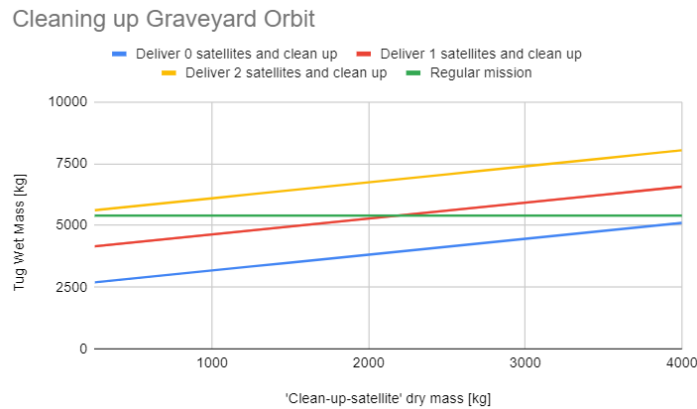


Figure 6.6: Tug wet masses per clean up mission

6.5. Conclusion

To conclude, the two propulsion systems are chosen for the MANTIS mission. A chemical engine transfers the tug, because of its high thrust and an electric engine is present on the satellites due to its high fuel efficiency. The final characteristics and masses are shown in table 6.5 for both the tug and satellite. Looking at the requirements stated in the introduction of chapter 6, all of them are met after designing the chemical and electric propulsion system.

Table 6.5: Final characteristics of the propulsion systems

Characteristics	TUG	Satellite
TRL	9 [79]	6 (in 2017 [40])
Engine	RL10A-4-2	Qinetiq T-6
Number of engines	1	4
Thrust per engine [N]	105,978.9	0.145
Thruster dry mass [kg]	167.8	8.5
Isp [s]	451	4300
Dry mass [kg]	1348.9	1847.0
Fuel mass [kg]	2920.9	249.3
Wet mass [kg]	4269.7	2096.3

The function of the ADCS is to perform small velocity changes, maintaining the orbit and most importantly obtaining and controlling the attitude of the spacecraft. In this chapter, the design of the ADCS of the tug is described in section 7.1 and of the satellite in section 7.2.

The tug as an AIV system is a concept that has not been realised before. Therefore the analysis for the tug is reported in detail to prove the feasibility of the project. On the other hand satellites with similar payload have already been built, although the required modularity to allow exchange and upgrading is new. Hence, the satellite ADCS design is calculated in similar fashion but reported in a less exhaustive way to match the scope of the project.

7.1. Tug ADCS

In this section the steps necessary to obtain a working ADCS concept for the tug are outlined. First the system modes are listed in section 7.1.1. Then the requirements are shown in section 7.1.2 and followed by calculating the disturbance torques in section 7.1.3. With this preparatory groundwork it is possible to select the component types needed for this mission which are presented in section 7.1.4. After that the actuators are sized in section 7.1.5 and a trade-off on component level is performed in section 7.1.6. Lastly, a conclusion is given in section 7.1.7.

7.1.1. System Modes

The first step in the ADCS design process is the definition of control modes based on mission goals and timeline. These control modes help with a better understanding of the actual needs of the mission and are designed to achieve sets of requirements.

- **Acquisition mode:** Initial determination of attitude and position after launch. Also need to be performed for recovery from emergencies and after unscheduled power-ups.
- **Detumbling mode:** While separating from first stage or satellites to keep the S/C as steady as possible.
- **Safe mode:** Used in case of emergency if one of the nominal modes fails. Runs on the bare minimum of functions to keep the points of failure and the power consumption down.
- **Orbital transfer and maintenance mode:** Period during and after transferring orbits. The ADCS has to counter the disturbance torques caused by the burn of the main engine in order to not waste fuel or even fail the mission.
- **Slew mode:** Rotate the S/C around its axes in a certain time period.
- **Docking mode:** This mode is active while docking with the satellites. It requires accurate attitude and velocity changes.
- **Standby mode:** Most of the time the S/C runs with minimum functionality to save power.

7.1.2. Requirements

The mission needs and control modes can be used to identify requirements for the ADCS. These mission needs impose different requirements for the individual stages. For example: For many Spacecraft (S/C) the ADCS shall control the attitude of the S/C while burning the main engine while it also needs to maintain a high pointing accuracy when the satellite is on station. Both will impose distinct requirements on the ADCS that will have to be satisfied by one system.

- **IKEA-TUG-TECH-OPE-ADCS-T1:** The spacecraft shall have full 3 dimensional attitude control.
- **IKEA-TUG-TECH-OPE-ADCS-T2:** The ADCS shall have a pointing accuracy of 0.5 degrees.
- **IKEA-TUG-TECH-OPE-ADCS-T3:** The spacecraft shall have an attitude determination accuracy of 0.05 degrees.
- **IKEA-TUG-TECH-OPE-ADCS-T4:** The bias drift of the Inertial Measurement Unit shall not exceed

the attitude determination accuracy in 4 hours without reference update.

- **IKEA-TUG-TECH-OPE-ADCS-T5:** The spacecraft shall be able to slew 180 degrees in 100 minutes when carrying 2 satellite packages.
- **IKEA-TUG-TECH-OPE-ADCS-T6:** For emergencies the spacecraft shall be able to fast slew 90 degrees in 5 minutes when carrying 2 satellite packages.
- **IKEA-TUG-TECH-OPE-ADCS-T7:** The ADCS of the tug shall have no single point of failure.
- **IKEA-TUG-TECH-OPE-ADCS-T8:** The reaction control thrusters of the tug shall have a Minimum Impulse Bit (MIB) no higher than 25 mNs to be able to control the S/C precisely.

7.1.3. Disturbance Environment

The environment the spacecraft operates in dictates which control methods will be effective. For example a S/C in LEO might be able to operate with magnetic torquers because of the relatively strong magnetic field. On the other side the same spacecraft is exposed to stronger magnetic disturbance torques than one in an orbit with a larger altitude. In this subsection the 4 major disturbance torques caused by solar radiation, atmospheric drag, magnetic field and gravity gradient are calculated. An overview of the inputs for the following calculations can be seen in table 7.1. The values are taken from literature[58] or are result from the structural and geometrical constraints explained in chapter 12 and section 13.2.

Table 7.1: Input parameters for ADCS sizing

Name	Symbol	Value	Unit
Solar Constant @ 1 AU	Φ	1.366	W/m ²
Speed of Light	c	3·10 ⁸	m/s
Distance Center of Solar Pressure - Center of Mass Tug	$cp_s - cm$	0.1	m
Distance Center of Solar Pressure - Center of Mass Sat	$cp_s - cm$	0.15	m
Sunlit Surface Area Tug	A_s	40	m ²
Sunlit Surface Area Satellite	A_s	45	m ²
Reflectance Factor	q	0.6	-
Density @300 km altitude	ρ	2.3E-11	kg/m ³
Drag Coefficient	C_d	2.2	-
Ram Area	A_r	16	m ²
Residual Dipole Moment	D	1	A·m ²
Function of magnetic latitude at equator	λ	1	-
Magnetic moment of the Earth times magnetic constant	M	7.8·10 ¹⁵	Nm/A· m ³
Distance S/C-Earth's Center (Tug @ Perigee)	R	6,771,000	m
Distance S/C-Earth's Center (Tug/Sat @ GEO)	R	42,164,000	m
Earth's Gravitational Constant (G· M)	μ	5.86·10 ²⁵	m ³ /s ²
Tug Mass Moment of Inertia around X-Axis	I_x	8,599.86	kg· m ²
Tug Mass Moment of Inertia around Y-Axis	I_y	11,407.98	kg· m ²
Tug Mass Moment of Inertia around Z-Axis	I_z	11,407.98	kg· m ²
Tug with Packages Mass Moment of Inertia around X-Axis	I_x	62,288.7	kg· m ²
Tug with Packages Mass Moment of Inertia around Y-Axis	I_y	44,325.04	kg· m ²
Tug with Packages Mass Moment of Inertia around Z-Axis	I_z	44,325.04	kg· m ²
Satellite Mass Moment of Inertia around X-Axis	I_x	12,184.07	kg· m ²
Satellite Mass Moment of Inertia around Y-Axis	I_y	4,149.92	kg· m ²
Satellite Mass Moment of Inertia around Z-Axis	I_z	9,977.35	kg· m ²
Maximum Angle between Principal Axis and Local Vertical	Θ	1	deg
Margin Factor	MF	3	-
Orbital Period GTO	P	37,345.22	s
Orbital Period GEO	P	86,160	s
Thruster Moment Arm (Satellite)	L	1.75	m
Thruster Moment Arm (Tug)	L	2.175	m

Solar Radiation Disturbance Torque (SRDT)

Sunlight carries momentum and therefore the absorbed sunlight exert a certain pressure on the S/C. In fact the solar radiation pressure is even twice as high if all of the sunlight is reflected. If the center of pressure

does not align with the center of mass of the spacecraft it would result in a torque. Assuming that the surfaces facing the sun are angled to the same degree and using a constant reflection factor the equation for the SRDT is as followed:

$$T_s = \frac{\Phi}{c} A_s (1 + q) (cp_s - cm) \cos \phi \quad (7.1)$$

The solar radiation disturbance torque, T_s , is a function of Φ , the solar constant with 1366 W/m^2 at 1 AU, c , the speed of light with $3 \cdot 10^8 \text{ m/s}$, $cp_s - cm$ which is the distance between the centers of solar radiation pressure and center of mass and is estimated to be 0.3 m , A_s is the sunlit surface area with 40 m^2 , q is the unitless reflectance factor that is 0.3 and ϕ is the angle of incidence of the Sun which in the worst case is 90° and is used to calculate the torque. The final values can be seen in table 7.2.

Atmospheric Drag Disturbance Torque (ADDT)

Just as photons can exert a pressure on the S/C, the particles of the atmosphere do this too. The resulting pressure force is called atmospheric drag. The center of atmospheric pressure is determined by the area, called ram area, exposed to the atmosphere in the direction of flight. When this center of pressure does not align with the center of mass, a torque results. This torque can be calculated as follows:

$$T_a = \frac{1}{2} \rho C_d A_r V^2 (cp_a - cm) \quad (7.2)$$

The Atmospheric Drag Disturbance Torque is T_a , ρ is the density of the atmosphere in kg/m^3 , C_d is the drag coefficient, A_r is the ram area in m^2 and V is the spacecraft's velocity in m/s .

Magnetic Field Disturbance Torque (MFDT)

Earth's magnetic field is a magnetic field that emerges from the Earth's liquid core. Most S/C have a residual magnetic moment which exerts a torque on the spacecraft to align with the local magnetic field. Earth's magnetic field is asymmetric and complex. However, for the ADCS design process it is sufficient to model it as a dipole. To determine the maximum torque acting on the S/C the following formulas are used:

$$T_m = D \cdot B \quad (7.3)$$

Where the Magnetic Field Disturbance Torque is T_m , D is the spacecraft's residual dipole moment in $\text{A} \cdot \text{m}^2$ and B is the magnetic field strength in Nm/A . The magnetic field strength is calculated as follows:

$$B = \frac{M}{R^3} \cdot \lambda \quad (7.4)$$

Here M is the magnetic moment of the Earth multiplied by the magnetic constant, R is the distance between the the S/C and the Earth's center in m and λ is the unitless function of the magnetic latitude.

Gravity Gradient Disturbance Torque (GGDT)

When the center of gravity of a spacecraft is not aligned with the center of mass with respect to the local vertical a GGDT acts. There is no gravity gradient torque if one of the principal axes of the S/C is aligned with the local vertical, however a torque raises with increasing angle between them. To calculate the GGDT the following simplified formula is used for a spacecraft with the minimum principle axis in its Z direction:

$$T_g = \frac{3\mu}{2R_{orbit}^3} |I_z - I_x| \cdot \sin(2\theta) \quad (7.5)$$

Where T_g is the gravity gradient torque, μ is the Earth's gravitational constant, R is the distance from the S/C to the center of the Earth, Θ is the angle between the local vertical and the Z principle axis, and I_z and I_y are the moments of inertia around their respective axis in $\text{kg} \cdot \text{m}^2$. As can be seen, the worst case gravity gradient is acting when the difference between the two moments of inertia is at its maximum. Therefore the gravity gradient is calculated for the package configuration.

Results

In this section, the results of the disturbance torque calculations are presented. An overview can be seen in table 7.2. As can be seen the solar radiation torque is the highest in GEO and the gravity gradient torque is the highest at GTO perigee. Hence the worst case torque of $1.03 \cdot 10^{-3}$ Nm will be considered in the actuator sizing in section 7.1.5.

Table 7.2: Disturbance torques for the tug at perigee and GEO

Type	GTO Perigee (500 km altitude)	At GEO
Solar Radiation Torque [Nm]	2.91E-05	2.91E-05
Atmospheric Drag Torque [Nm]	1.49E-05	-
Magnetic field Torque [Nm]	2.15E-05	1.04E-07
Gravity Gradient Torque [Nm]	1.03E-03	5.00E-06

7.1.4. ADCS Components Type Selection

From the requirements in section 7.1.2, it can be seen that the tug shall have full 3D axis control. Therefore, a configuration with thrusters and reaction wheels was chosen. The reaction wheels reduce the amount of fuel needed to counter disturbance torques and can change the altitude without using any propellant while providing high accuracy and precision.

The thrusters can be used to dump the momentum stored by the reaction wheels. Due to the higher torque the thrusters can deliver, they are also used to spin the spacecraft fast in case of emergency to satisfy the fast spin requirement. Finally and most importantly they accelerate the S/C translational, for example while docking or station keeping.

The tug will rely on a combination of sun sensors and star trackers as attitude reference. The sun sensors will give a less precise attitude reference that is used as a robust solution after a start up or in case of emergency. Furthermore this first estimation is used for the star trackers. They rely on a first estimate of attitude to deliver a high accuracy knowledge in return. Finally a Inertial Measurement Unit (IMU) is used to deliver high accuracy and frequency information to the satellite bus. The sizing and the selection of the components is described in the following sections.

7.1.5. Reaction Wheel and Thruster Sizing

Once the disturbance torques are known the preliminary sizing of the components can be started. In the following sections is explained how the parameters needed to select an actuator system are calculated. These parameters are: Control torque, slew torque, momentum storage and thruster force. The inputs used for the calculations can be found in table 7.1 and the outcome is shown in table 7.3. The moments of inertia have been calculated from the 3D arrangement of modules and their weights, with the help of Catia and an Excel sheet.

Control Torque

The control torque that the reaction wheels supply must equal the worst case disturbance torque times some margin.

$$T_c = T_D \cdot MF \quad (7.6)$$

As can be seen in table 7.2 the gravity gradient torque is the worst case disturbance. MF is the factor of margin. If the design is already at an advanced stage a factor 2 is usual[58]. Because this is at a preliminary stage where some inputs might be subject to iterations a MF of three is chosen. This results in a control torque of $3.1 \cdot 10^{-3}$ Nm.

Slew Torque for Reaction Wheels

For maximum acceleration slew the reaction wheel is accelerated half of the distance and then decelerated the second half. The following equation can be used, and then solving for T gives:

$$\frac{\phi}{2} = \frac{1}{2} \frac{T}{I} \left(\frac{t}{2} \right)^2 \quad (7.7)$$

$$T = 4\Phi \frac{I}{t^2} \quad (7.8)$$

Where ϕ is the angle that the S/C shall rotate, T is the reaction torque, I the moment of inertia and t the time for the maneuver. As can be read in the requirements in section 7.1.2 the tug has to be able to turn 180 degrees in 25 minutes in single-configuration and in 100 minutes when loaded with packages. The worst case moment of inertia will be considered for this calculation and can be read in table 7.1. The torque necessary to do this is 64 mNm for the single configuration tug and 22 mNm for the tug in package configuration.

Slew Momentum Storage for Reaction Wheels

With the torque calculated the momentum storage for this maneuver can be calculated:

$$h = T \cdot \frac{t}{2} \quad (7.9)$$

The momentum storage necessary for the single configuration is 47.79 Nms and 65.23 Nms for the package configuration.

Momentum Storage due to Disturbance Torque for Reaction Wheel

To estimate the momentum that the reaction wheels have to store the worst case disturbance torque can be integrated. For the gravity gradient, aerodynamic and solar radiation disturbance torque the maximum momentum accumulates in a quarter of the orbital period. For simplicity the momentum due to magnetic field torque is assumed to also build up in a quarter of a period. The equation looks as follows:

$$h_D = T_D \cdot P \cdot \frac{0.707}{4} \quad (7.10)$$

Where h_D is the momentum accumulated by the worst case disturbance torque, P is the orbital period and 0.707 is the rms average of a sinusoidal function.

As can be seen in table 7.2 the gravity gradient torque is the worst case. The calculated torque is the highest at the apogee of the GTO orbit and will be less over the rest of the quarter period. Assuming that the peak gravity gradient torque acts the whole time the resulting momentum storage needed is 6.82 Nms. Since the momentum storage needed due to the slew requirement is higher, no further research is required.

Thruster Force Level Sizing due to Disturbance Torques

The minimum force required for the thrusters to counter disturbance torques can be calculated as follows:

$$F = T_D \cdot MF/L \quad (7.11)$$

Where L is the moment arm of the thrusters. This results in a minimum thruster force of 1.77 mN. The factor of margin is 3 for the same reasons as explained in the control torque calculations. This relatively low value indicates that the fast slew requirements will determine thruster size.

Thruster Force Level Sizing due to Fast Slew

In case of emergency the S/C shall be able to turn faster than it does with reaction wheels. For this emergency case the thrusters shall be used and therefore need to be sized accordingly. As can be seen in section 7.1.2 the tug shall turn 90° in 300 seconds. Accelerating and decelerating 5% of the time and coasting the remaining 90% and assuming that the velocity after acceleration is carried through the whole maneuver the necessary thruster force can be calculated.

$$\omega = 90 \text{ deg}/300\text{s} = 0.3 \text{ deg/s} \quad (7.12)$$

To reach 0.3 deg/sec in 15 seconds requires an acceleration:

$$\alpha_{acc} = \omega/t = 0.02 \text{ deg/s}^2 = 3.5 \cdot 10^{-4} \text{ rad/s}^2 \quad (7.13)$$

Now that the necessary acceleration is known the required force can be calculated. It is assumed to rotate around the worst case axis which means the one with the highest moment of inertia. Because two thrusters are going to be acting on the S/C as can be seen in fig. 7.2 one needs to divide by two.

$$F = \frac{I\alpha_{acc}}{L \cdot 2} = \frac{62289 \cdot 3.5 \cdot 10^{-4}}{1.75 \cdot 2} = 6.21 \text{ N} \quad (7.14)$$

Results

Table 7.3: ADCS actuator sizing outputs tug

Type	Symbol	Value
Control Torque	T_c	3.1 E-03 Nm
Slew Torque, Single Configuration	$T_{slew, single}$	64 mNm
Slew Torque, Package Configuration	$T_{slew, package}$	22 mNm
Momentum Storage for Slewing, Single Configuration	$h_{slew, single}$	47,79 Nms
Momentum Storage for Slewing, Package Configuration	$h_{slew, package}$	65,23 Nms
Momentum Storage due to Disturbance Torque	$h_{disturbance}$	6.82 Nms
Thruster Force for Disturbance Counter	F_D	$1.77 \cdot 10^{-3} \text{ N}$
Thruster Force for Fast Slew	F_{slew}	6.21 N

7.1.6. ADCS Components Trade-Off

In this subsection the final components are selected with help of a trade-off. The components are graded from one till five. One (red) means that the component does not comply with the requirements or is performing inadequately and is therefore discarded. Two (brown) means it barely makes the requirements. A three (yellow) is an average performing component where a four (light green) corresponds to an over-performing component. A five (green) means the component has an outstanding performance in this criteria. The table is color coded and in every table one of the fields has the corresponding score to that color noted. The weights of the criteria are documented in last row of the table.

Thrusters

To select the right thruster a trade-off has to be performed. As can be seen in section 7.1.2 the MIB shall not be higher than 25 mNs, and they need to have a thrust of at least 6.21 N as can be seen in table 7.3. The thrusters shall if possible also consume little power, be light-weight and have a high specific impulse in order to save fuel mass. Thrusters considered are the "MR-106L 22N", "MR-107T 110N" and "MR-107S 275N" from Aerojet Rocketdyne [78], from Space Propulsion the 10 N Bipropellant Thruster [44] and the 1 N Bipropellant Thruster [45]. The trade-off matrix can be seen in table 7.4.

Table 7.4: Thruster trade-off

Thruster	Power [W]	Weight [kg]	MIB [Ns]	Thrust Range [N]	ISP	Final Score Sum (Score· CW)
Aerojet Rocketdyne MR-106L 22N	36	0.59	0,015	34 -10 Score: 3	235	3.3
Aerojet Rocketdyne MR-107T 110N	52 Score: 2	1.01	0,015	125-54 Score: 4	225	2.6
Aerojet Rocketdyne MR-107S 275N	52	1.01	0,015	360-85 Score: 5	236	3.2
Space Propulsion 10 N Bipropellant Thruster	17	0.65	0,015	12.5-6	292	4.2 Winner
Space Propulsion 1 N Bipropellant Thruster	10	0.29	0,01	0.32-1.1 Score: 1	220	Disqualified
Category Weight (CW)	0.1	0.2	0.1	0.2	0.4	

Reaction Wheels

The reaction wheel are crucial for a successful mission and since they contain moving parts they can be a source of reliability issues. Considering that the tug has to sustain at least 7 years, lifetime is one of the considered criteria for this trade-off to make sure that the reaction wheels will not sabotage mission-success. Hence reaction wheels with a higher lifetime score higher and additionally 4 reaction wheels are used for redundancy. The torque of 64 mNm and momentum storage of 65.23 Nms have to be satisfied as shown in table 7.3. Naturally power and weight are a criteria.

Two reaction wheels are considered from Rockwell Collins: The reaction wheel RDR 68-3 together with the "Wheel Drive Electrics" WDE 8-45 [23] and the already integrated solution RSI68-170/60 [24]. Furthermore the W45E from Bradford Space [15] and the RWA 15 from L3 Space & Navigation [69] were examed. The lifetime of the W45E was not advertised. It was used on the Rosetta mission which had a nominal lifetime of 11 years. Therefore this timeframe was assumed for the trade-off. The rating can be seen in table 7.5.

Table 7.5: Reaction wheel trade-off

Reaction Wheel	Power Usage Standby/Max [W]	Angular Momentum [Nms]	Torque [mNm]	Weight [kg]	Lifetime [years]	Final Score Sum (Score· CW)
Rockwell RDR 68-3/WDE 8-45	20/90 Score: 3	68 Score: 2	75	8.85	15 Score: 5	3.5
Rockwell RSI68-170/60	20/150	68	170 Score: 4	8.9	15	3.7 Winner
Bradford space W45E	29/168	45 Score: 1	248	9.785	11	Disqualified
L 3 Space & navigation RWA 15	17/230	20	680	14	7	Disqualified
Category Weight (CW)	0.1	0.2	0.1	0.2	0.4	

Sun Sensor

The sun sensors most important function is to supply a very robust and simple attitude determination. They provide a rough estimation of where the spacecraft is pointing to make the star trackers data useful. For example: When the S/C lost its attitude knowledge and starts in safe mode it shall start with minimal functions to minimise points of failure. If this happens the sun sensors shall provide a fast and reliable source of information.

Sun sensors that are analog, called Coarse Sun Sensors (CSS), are assumed to be more robust and cheaper than their more complex digital counterparts. Therefore only CSS are considered for the tug: From Lens' Research & Development (R&D) the Bison64-ET-B [76], from Bradford Space the Coarse Sun Sensor [16] and from TNO the Coarse Sun Sensor [100]. Their scoring can be seen in table 7.6.

Table 7.6: Coarse sun sensor trade-off

Coarse Sun Sensor	Accuracy [deg]	Weight [g]	Field of View [deg]	TRL Level	Final Score Sum(Score· CW)
Lens R/&D Bison64-ET-B	0,5 Score: 5	33	~60 Score: 2	9	3.5
Bradford Space Coarse Sun Sensor	1,5 Score: 3	215	180	9	4 Winner
TNO Coarse Sun Sensor	1 Score: 4	210	180	4 Score: 1	Disqualified
Category Weight (CW)	0.2	0.2	0.5	0.1	

Star Tracker

Star trackers will be used to satisfy the attitude determination accuracy of 0.05° as specified in section 7.1.2, which corresponds to 180 arcsec. This is not a very high accuracy for star trackers. Since an IMU is used to provide higher frequency information the refresh rate was not considered in the trade-off of the star trackers. Star Trackers compared are the ST200 [84] and ST400 [85] from Hyperion Technologies, the A-STR and AA-STR from Leonardo [61], the MAI-SS [64] from Adcole and the CT-2020 [10] from Ball Aerospace. The trade-off can be seen in table 7.7.

Table 7.7: Star tracker trade-off

Star Tracker	Power [W]	Accuracy(pitch,yaw,roll) [arcsec]	Weight [kg]	Final Score Sum (Score· CW)
Hyperion Technologies ST200	0.6 Score: 5	<30,<30,<200 Score: 1	0.042	Disqualified
Hyperion Technologies ST400	0.7	<10,<10,<120 Score: 3	0.28	3.7
Leonardo A-STR	8.9	<8.25,<8.25,<11.1	3.55	3
Leonardo AA-STR	5.6	<8.25,<8.25,<11.1	2.6	3.5
Adcole MAI-SS	1.5	<5.7,<5.7,<27 Score: 4	0.197	4 Winner
Ball Aerospace CT-2020	8 Score: 2	<1,<1,<1	3	3.5
Category Weight (CW)	0.2	0.5	0.3	

Inertial Measurement Unit

Finally the IMU of the tug has to be selected. This component consists of a group of gyrometers and accelerometers to provide high frequency information about the spacecraft's attitude as well as the position and velocity. Considered criteria are once more weight and power. Furthermore some of the IMUs have a configuration with three reaction wheels and some with four. A configuration with 4 reaction wheels means that the unit provides redundancy in itself. Therefore, if the configuration has only 3 reaction wheels, it is assumed that two units have to be taken and the mass is doubled.

The most important criteria is the bias stability since the IMU shall provide an accurate attitude for at least 4 hours even when the reference sensors are offline. As can be seen in section 7.1.2 the bias drift shall be smaller than the pointing accuracy in the course of 4 hours. That means the bias drift can not exceed 0.05° in 4 hours which is 0.00125 deg per hour. Examined were the Astrix 120, 200 and 1120 from Airbus Defense&Space [6], the Cirus [46] from L3 Space & Navigation, and the STIM300 [89] from Sensoror. The scoring can be seen in table 7.8.

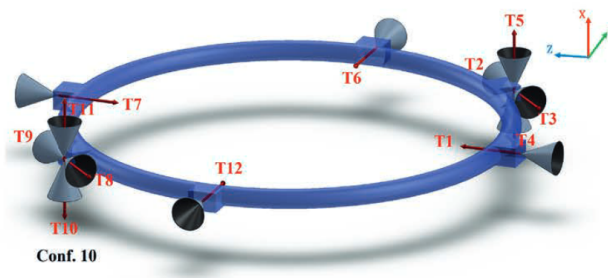


Figure 7.1: Configuration 10, potential constellation with 12 thrusters for MANTIS[47]

Table 7.8: Inertial Measurement Unit trade-off

IMU	Configuration	Power [W]	Bias Stability [deg/hour]	Weight [kg]	Final Score Sum (Score· CW)
Airbus Defense & Space Astrix 120	4 Score: 5	6 Score: 4	0.01 Score: 2	6.5 Score: 3	3.5 Winner
Airbus Defense & Space Astrix 200	4	5.5	0.0005	12.7 Score: 1	Disqualified
Airbus Defense & Space Astrix 1120 (two needed)	3	13.5	0.003	9 (4.5· 2)	3.1
L3 Space & Navigation Cirus	4	40	0.0003	15.4	Disqualified
Sensoror STIM300 (two needed)	3	1.5	0.3	0.11 (0.055· 2)	Disqualified
Category Weight (CW)	0.3	0.2	0.3	0.2	

Thruster Configuration

For the performance and functionality of the S/C it is important to find the optimal number of thrusters and in which configuration to place them. To find the best fitting configuration the article "A study of Spacecraft Reaction Thruster Configurations for Attitude Control System" [47] is used. It is assumed that, although the parameters of the S/C that the study is performed on are different, the results would be comparable. It is advised to revise the effect of the configuration on the mission with the parameters of the tug if this project continues.

The most important factor for the configuration is redundancy, therefore only configurations with 12 or 16 thrusters are considered. Configurations with 12 thrusters have a Level of Redundancy (LR) of 2 while configurations with 16 have a LR of 3.

Of the configurations studied in the article[47] configuration 10, which can be seen in fig. 7.1 and configuration 13, which can be seen in fig. 7.2 are considered. They have 12 and 16 thrusters respectively and do exceptionally good in using little fuel in the dynamic and static analysis.

In chapter 6 it is explained that roughly 3% of the fuel mass is used by the ADCS which equals to around 90 kg. Comparing the fuel consumption of the configurations in the static analysis it can be seen that the 16 thruster configuration uses 6% less fuel than the 12 thruster configuration. This equals to 5.4 kg less fuel used, outweighing the 2.6 kg more needed for the additional four thrusters. More importantly, while saving mass, an additional level of redundancy is achieved. Therefore the chosen configuration is configuration 13 with 16 thrusters.

7.1.7. Conclusion

The tug's ADCS consists of 16 "10 N Bipropellant Thrusters" from Space Propulsion, four reaction wheels from Rockwell to have sufficient redundancy, two "MAI-SS" star trackers from Adcole, one "Astrix 120" IMU from Airbus Defense & Space and two CSS from Bradford. With this setup there is no single point of failure and all requirements are met. An overview with component parameters can be found in table 7.9.

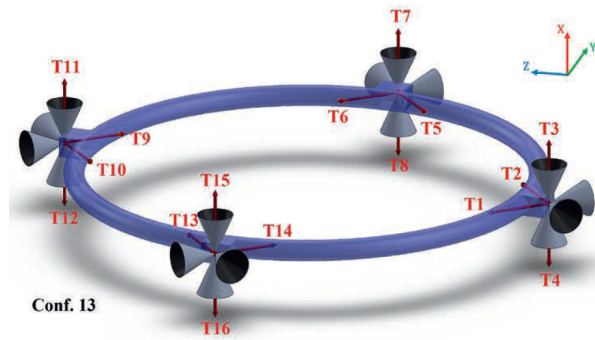


Figure 7.2: Configuration 13, final constellation with 16 thrusters for MANTIS[47]

Table 7.9: Tug ADCS component list

Component	Company Name	Amount	max Power Standby Power [W]	Total Weight [kg]	TRL	Operating Temperature [deg]	Specifications
Reaction Thruster	Space Propulsion 10 N Bipropellant Thruster	16	17 -	10.4	9	-	ISP 292 s MIB 0.015 Ns Hyrdazine/MON3
Reaction Wheel	Rockwell RSI68-170/60	4	150 20	35.6	9	-20 to 70	Torque 170 mNm Ang. Mom. 68 Nms Bias Stability 0.01 deg/hour Resolution 0.01 arcsec
IMU	Airbus Defense & Space Astrix 120	1	- 6	6.5	9	-20 to 60	Self-redundant configuration Accuracy 1 deg
Coarse Sun Sensor	TNO Coarse Sun Sensor	2	- -	0.42	9	-80 to 120	Field of View 180 deg Self-redundant configuration Accuracy 5,7,5,7,27 arcsec
Star Tracker	Adcole MAI-SS	2	1.5	0.4	9	-40 to 80	Radiation 75 krad Refresh Rate 4 Hz

7.2. Satellite ADCS

Other than the tug, the satellite operates most of the time in circular GTO orbit and therefore is subject to a different environment and has different requirements than the tug. This section explains the design process of the satellites ADCS. This will be performed in a more concise and shorter way than in the tug chapter but the intermediate steps are the same as in section 7.1. First the system modes are listed in section 7.2.1 and the requirements in section 7.2.2. Then the disturbance torques experienced by the satellite in GTO are show in section 7.2.3 and the type of ADCS components used are described in section 7.2.4. With this prework the reaction wheels can be sized in section 7.2.5. Lastly the selected components are presented in section 7.2.6 and the section concluded in section 7.2.7.

7.2.1. System modes

- **Acquisition mode:** Initial determination of attitude and position just after assembly in orbit. May also needs to be performed for recovery from emergencies and unscheduled power-ups.
- **Detumbling mode:** While separating from tug to keep the S/C as steady as possible and in case of a disturbance leading to sudden momentum change.
- **Safe mode** Used in case of emergency if one of the nominal modes fails. Runs on the bare minimum of functions to keep the points of failure and the power consumption down.
- **Deorbit mode:** After end of operations in GEO the S/C transfers back to earth to burn up in the atmosphere.
- **Slew mode:** Rotate the S/C around its axes in a certain time period.
- **Standby mode:** Most of the time the S/C runs with minimum functionality to save power.

7.2.2. Requirements

- **IKEA-TECH-OPE-ADCS-T1:** The spacecraft shall have full 3 dimensional attitude control.

- **IKEA-TECH-OPE-ADCS-T2:** The ADCS shall have a pointing accuracy of 0.05 degrees.
- **IKEA-TECH-OPE-ADCS-T3:** The spacecraft shall have an attitude determination accuracy of 0.005 degrees.
- **IKEA-TECH-OPE-ADCS-T4:** The bias drift of the Inertial Measurement Unit shall not exceed the attitude determination accuracy in 4 hours without reference update.
- **IKEA-TECH-OPE-ADCS-T5:** The spacecraft shall be able to slew 180 degrees in 25 minutes.
- **IKEA-TECH-OPE-ADCS-T6:** The ADCS of the satellite shall have no single point of failure.

7.2.3. Disturbance Environment

In the same way as described in section 7.1.3 the disturbance torques for the satellite can be calculated. The results of these calculations are displayed in table 7.10. The spacecraft experiences no atmospheric drag on station at GEO due to the lack of atmosphere. Therefore no atmospheric drag torque acts. Due to the high altitude the magnetic field torque and the gravity gradient torque are weak. As can be seen the highest disturbance torque is caused by solar radiation with $4.92 \cdot 10^{-5}$ Nm.

Table 7.10: Disturbance torques for the satellite on station (GEO)

Type	Value [Nm]
Solar Radiation Torque	$4.92 \cdot 10^{-5}$
Atmospheric Drag Torque	-
Magnetic field Torque	$1.04 \cdot 10^{-7}$
Gravity Gradient Torque	$1.74 \cdot 10^{-7}$

7.2.4. ADCS Components Type Selection

Just as the tug, the satellites control strategy is an active 3-axis stabilisation. Therefore reaction wheels and thrusters are chosen. Other than the tug, the satellites main propulsion is able to give small moment impulses. The four electric "Qinetiq T-6" engines have a thrust of 0.145 N per engine and a moment arm of 2.175 m. Further details are available in chapter 6. The thrusters are on gimbaled arms they can dump momentum about all 3 axis. Therefore the satellite can use its main propulsion also for attitude purposes and does not need additional reaction thrusters. As attitude determination sensors the spacecraft will use sun sensors because of their robustness while utilizing star trackers to comply with the high accuracy requirements need for the payload. An Inertial Measurement Unit is used to provide high frequency information about the attitude and to satisfy the bias drift requirement in case the star trackers are temporary non-functional.

7.2.5. Reaction Wheel and Thruster Sizing

After the prework in the previous sections the reaction wheels and thrusters can be sized in the same manner as in section 7.1.5.

Control Torque

The control torque that the reaction wheels supply must equal the worst case disturbance torque plus some margin. As can be seen in table 7.10 solar Radiation Torque is the worst case disturbance with $4.92 \cdot 10^{-5}$ Nm and the factor of margin, MF, is three. This gives a necessary control torque of $148 \cdot 10^{-4}$ Nm. This is negligible compared to the torque needed for slewing the satellite.

Slew Torque for Reaction Wheels

As can be seen in the requirements in section 7.2.2 the satellite has to be able to turn 180° in 25 minutes. Calculating with the worst case moment of inertia the necessary torque is 68 mNm.

Slew Momentum Storage for Reaction Wheel

The momentum storage necessary to perform the 180° slew maneuver is 51 Nms.

Momentum Storage due to Disturbance Torque for Reaction Wheel

Using the formula shown in section 7.1.5 and considering using the gravity gradient disturbance torque of $4.92 \cdot 10^{-5}$ Nm and the orbital period of the satellite in GEO of 86,160 seconds the momentum storage necessary is 0.75 mNms. This is much lower than the slew requirements.

Thruster Force Level Sizing due to Disturbance Torques

Using the equation displayed in section 7.1.5 and plugging in a moment arm for the gimbaled thrusters of 2.175 m, a factor of margin of 3 and assuming that two thrusters will counter the disturbance gives a necessary thrust of $3.39 \cdot 10^{-5}$ N for one thruster. Even for electric thrusters this is low and proves that the selected propulsion shown in table 6.5 satisfies the ADCS needs.

Results

In table 7.11 an overview of the parameters that the reaction wheel and the propulsion unit have to fulfill can be seen. Looking at the values it becomes obvious that the slew requirement is the driving factor for the sizing of the reaction wheels. For the electric propulsion it can be said that the selected engine in chapter 6 satisfies the requirements of the ADCS to control the spacecraft.

Table 7.11: ADCS actuator sizing outputs satellite

Type	Symbol	Value [Nm]
Control Torque	T_c	3.1 E-03 Nm
Slew Torque	T_{slew}	68 mNm
Momentum Storage for Slewing	h_{slew}	51.04 Nms
Momentum Storage due to Disturbance Torque	$h_{disturbance}$	4.92E-05 Nm
Thruster Force for Disturbance Counter	F_D	3.39E-05 N

7.2.6. ADCS Components

Like in section 7.1.6 a trade-off was performed to select the components used for the satellite. For the satellite however, the trade-off process is not reported but the results are shown. The momentum storage and slew torque required for the satellite is similar to the requirements of the tug. Therefore the same reaction wheel of Rockwell, the RSI68-170/68, is selected. Increasing the quantity of the order will decrease the cost per piece. Hence selecting this reaction wheel does not only meet the requirements but will also reduce cost.

The "Astrix 200" IMU from Airbus was selected, satisfying the high attitude determination accuracy of 0.005 degrees.

Table 7.12: Satellite ADCS component list

Component	Company Name	Nr.	Power (max/stby) [W]	Total Weight [kg]	TRL	Operating Temp. [deg]	Specifications
Reaction Wheel	Rockwell RSI68-170/60	4	150 20	35.6	9	-20 to 70	Torque 170 mNm Ang. Mom. 68 Nms
IMU	Airbus D&S Astrix 200	1	- 5.5	12.7	9	-20 to 60	Bias Stability 1.8 arcsec/h Resolution 0.001 arcsec Self-redundant configuration Accuracy 1 deg
Coarse Sun Sensor	TNO CSS	2	- -	0.42	9	-80 to 120	Field of View 180 deg Self-redundant configuration
Star Tracker	Leonardo AA-STR	2	5.6	5.2	9	-30 to 60	Accuracy 8.25,8.25,11.1 arcsec Refresh Rate 10 hz

7.2.7. Conclusion

The ADCS of the satellite makes use of the four Qinetiq T-6 thrusters for momentum dumping and to maneuver the spacecraft. If possible the S/C changes attitude with help of the four RSI68-170/60 reaction wheels from Rockwell. Attitude knowledge is provided by the two coarse sun sensors from Bradford and the two AA-STR star trackers from Leonardo. To supply high frequency attitude and altitude knowledge for the satellite, the Astrix 200 inertial measurement unit is used.

Together this system provides a highly accurate knowledge determination and pointing accuracy with no single point of failure. The requirements in section 7.2.2 are all met. An overview of the components and their specifications can be found in table 7.12.

Command & Data Handling

Another subsystem that is vital for the functioning of the satellite, is Command & Data Handling (CDH). In this chapter the Telemetry, Track & Command (TT&C) will be discussed first in the section 8.1. Next, the chosen on-board computer is explained in section 8.2 and the CDH unit will be elaborated on in section 8.3.

8.1. Telemetry, Tracking & Command

A conventional TT&C module is installed in a spacecraft to set up a downlink with GC in order to send collected data and have an uplink connection to receive commands from GC. An antenna would have to be set up as well to ensure the up- and downlink for these operations.

8.1.1. Requirements

There are some requirements that the TT&C of the satellite has to meet. They are listed below:

- **IKEA-TECH-OPE-TTC-T1:** The TT&C shall collect all measured internal data.
- **IKEA-TECH-OPE-TTC-T2:** The TT&C shall transfer all the telemetry data to the ground station with a maximum Bit Error Rate (BER) of 10^{-4} .

8.1.2. Design

The payload of the satellite consists of communications hardware, as elaborated on in chapter 5, and it is designed to send and receive the data and commands from GC during their operational life apart from their commercial purpose. This includes not only the antennas but also the transponders with its amplifiers and transmitters and other hardware used for both commercial enterprise use as well as the TT&C. The actual TT&C module to process the data and commands is integrated in the CDH unit which is explained in section 8.3.

8.2. On-board Computer Module

The satellite is dependent on a reliable on-board computer module. All subsystems send their data to this module to process and receive relevant processed outputs from the module to act upon. Data necessary for Ground Control will be processed by this module and subsequently be sent by the TT&C module in the CDH unit.

8.2.1. Requirements

The on-board Computer Module is designed according to the following requirements:

- **IKEA-TECH-OPE-DAHA-T1:** The spacecraft shall be equipped with a redundant data storage system.
- **IKEA-TECH-OPE-DAHA-T2:** The data storage shall be protected from the space environment.
- **IKEA-TECH-OPE-DAHA-T3:** All on-board system elements shall be connected to the control computer.

8.2.2. Design

To ensure all requirements are met, a fully redundant on-board computer module must be incorporated into the satellite that will store data and have enough ports to connect to all on-board system elements. The CREOLE ASIC module by RUAG was chosen because it can meet all above mentioned requirements and the manufacturer is very experienced in space hardware. Furthermore, it is also already a space-rated product

tested in orbit with TRL9. In fig. 8.1 the on-board computer module is shown [93].

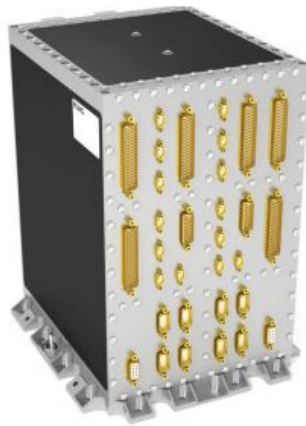


Figure 8.1: CREOLE ASIC module [93]

The CREOLE ASIC module is built fully redundant with all its functions installed at least twice. It also has a low mass and volume and only needs 23 W of power at most [93]. Furthermore, it has additional slots for possible expansion or changing modules and extra options to tailor the final module to the exact needs of a MANTIS satellite, even if the mission operations or the tug's design would change over the years.

8.3. Command & Data Handling unit

Whilst harbouring the TT&C module, the CDH unit should also be able to send and receive all commercial telecommunications that the payload will create. Apart from that, the module should also be able to store data if for whatever reason it cannot be sent directly to the intended ground station or the satellite's GC. The CDH unit directs and manages all subsystems, among which the on-board computer module from section 8.2.

8.3.1. Requirements

The CDH unit must meet the same requirements that were set for the on-board computer module in section 8.2.1, but also the TT&C requirements in section 8.1.1. These must be taken into account as well because the TT&C module is integrated in the CDH unit. Therefore, all requirements stated in this chapter apply to the CDH unit.

8.3.2. Design

In order to find an applicable CDH unit that would match perfectly with the on-board computer module, having the same manufacturing company is helpful. The Command, Data & Handling unit produced by RUAG, the Spacecraft Management Unit (SMU), has properties that fulfill the earlier listed requirements, provided that two of those are built in. For redundancy a third SMU is installed with the first two, weighing 16 kg per unit [94].

The SMU includes all interfaces for the ADCS devices and has inputs for digital, analog and pulse driven commands. In addition, the SMU also holds links that can send and receive up until 160 Mbps through SpaceWire links to ensure the full functioning of the whole satellite. Its mass and dimensions are small, weighing 16 kg in a box of $420 \times 270 \times 276$ mm and thus favourable for modular MANTIS satellites, as well. Lastly, because the SMU has functioned in multiple space missions before, it is rated TRL9 [94].

In order to visualise the CDH unit, a data handling block diagram is shown in fig. 8.3 including data flows and all the relevant subsystems incorporated in the CDH unit. The data handling block diagram is integrated in the hardware block diagram, shown in fig. 13.4.



Figure 8.2: RUAG Spacecraft Management Unit [94]

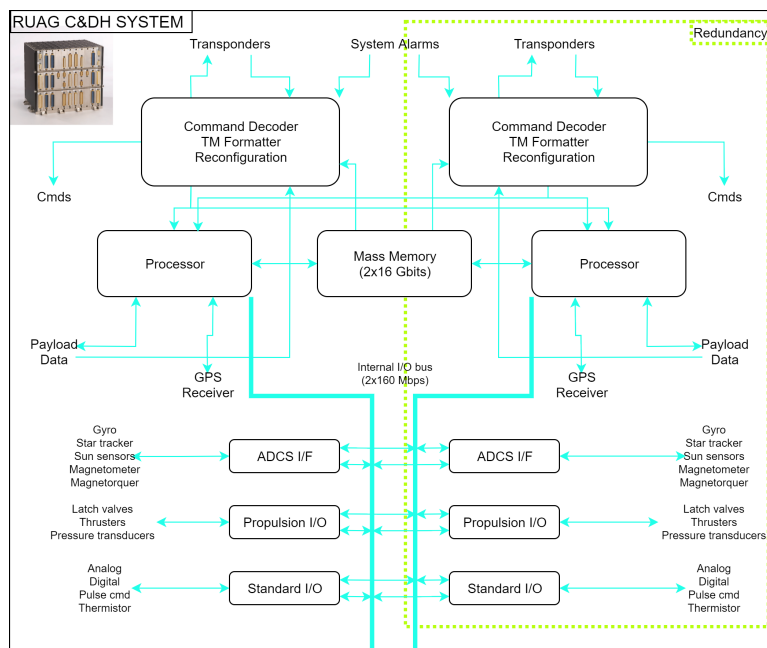


Figure 8.3: Data handling block diagram

8.4. Conclusion

The on-board computer module that was chosen meets all the requirements stated in section 8.2.1. Together with its extra features such as the expansion slots and its small dimensions, power usage and mass, the CREOLE ASIC is taken as the MANTIS satellite’s on-board computer module.

The chosen SMU built in three times per satellite will meet the requirements, including those brought along by the integrated TT&C module. The two SMU units combined have enough data links to send the collected data by the TT&C to Ground Control while simultaneously collecting, storing and distributing incoming data from all the connected modules.

The Computer Module is now designed as one box, the CREOLE ASIC and three SMU’s inside. In future research, an attempt to fit the different parts individually in the modular package might optimise this sub-system’s positioning even further. Different locations will also provide redundancy when subjected to a upsetting event.

Electric Power System

The following chapter analyses the different forms of power generation and power storage available for mission. After conducting an analysis the most suitable power system is chosen for tug and satellite. Based on this choice and the requirements, the modules masses and sizes are then calculated.

9.1. Power Generation

For power generation there are two main options: Fuel-based and Solar Energy based. Fuel-based energy was quickly disregarded due to the danger of having a high concentration of radioactive material on a spacecraft that will eventually burn up in the atmosphere.

There are a number of options when it comes to solar cells. In table 9.1 these options can be seen along with relevant information.

Table 9.1: Solar cells

Solar cell type	Efficiency [%]	Benefits
Gallium arsenide	31.6 - 42	Flexible, Temperature resistant
Crystalline Silicon	18 - 25	Maturity, Reliability, Abundance
Multi-Junction photovoltaic cells	30 - 40	Low cost materials, Easy to manufacture, low env. impact and robust

Based on this info it was determined that a gallium arsenide solar cell should be selected due to the high efficiency. The actual solar cell model that was selected is the Azur Space QJ Solar Cell 4G32C [92]. This cell was chosen due to its high efficiency and low mass. Also, it is a solar cell that is already used in space.

9.2. Power Storage

Secondary batteries are rechargeable batteries used to store energy and provide peak power generation. They have must have the following functions:

- Must be able to provide the spacecraft bus and payload with power during eclipse periods
- Must be able to charge to 100% by the solar array during sun time
- Must have enough life cycles at appropriate Depth of Discharge (DoD)
- Must withstand all phases of the mission

The following table presents different types of secondary batteries which are currently relevant to the commercial satellite industry. The energy density (e) indicates the amount of energy the battery can store. The charge efficiency (η_{charge}) is the ratio of the energy taken out of a battery divided by the energy you put in. The operating temperature ($T_{\text{operating}}$) is the temperature at which battery performs optimally [58]. Modularity refers to the ease of which batteries can be scaled up or down and Management refers to the operational maintenance required such as equalizing during eclipse periods and also includes severity of self-discharge [18].

Table 9.2: Comparison of battery types and their characteristics

Type	e_{sp} [Wh/kg]	η_{charge} [%]	$T_{\text{operating}}$ [°C]	Modularity	Management	Space Certified
Ni-Cd	30	72	0 - 40	No	High	Yes
Ni-H ²	60	70	-20 - 30	No	High	Yes
Li-ion	125 - 250	98	10 - 25	Yes	Low	Yes
Li-S	~350	-	-	Yes	-	In-Progress

When comparing Li-Ion batteries to Ni-Cd and Ni-H2 batteries the former has significantly higher energy density, higher charge efficiency, is scalable due to the introduction of cylindrical cells and requires almost no maintenance after launch. Evidently, lithium batteries are superior to nickel batteries which aligns with the current satellite market. Disadvantages of early lithium batteries such as low lifetime have seen significant technological improvement.

From table 9.2 it is evident that Li-S batteries have the highest specific energy density. While such batteries are not yet fully established in the space industry, they have been successfully tested on board Zephyr 7, a high altitude pseudo-satellite aircraft, operated by Sion Power in collaboration with Airbus in 2014. Given the rate of advancements in battery technology, it is not unreasonable to assume such batteries could be space-certified in time for the mission.

9.3. Battery Sizing

The main function of the batteries is to power the spacecraft during the longest possible eclipse. This means this eclipse time must be calculated. The longest eclipse occurs when the spacecraft's orbital plane is inline with the sun. Using this information fig. 9.1 was created. With this figure, eq. (9.1) the longest eclipse time can be calculated.

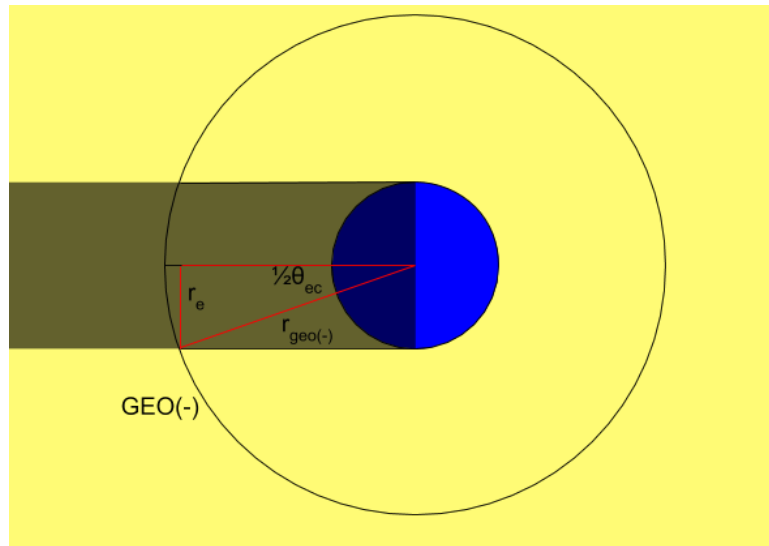


Figure 9.1: Satellite/Tug longest eclipse time

$$\frac{1}{2}\Theta_{ec} = \arcsin\left(\frac{r_e}{r_{geo(-)}}\right) \quad (9.1)$$

$$T_{ec} = T_{orb} \cdot \frac{\Theta_{ec}}{360} \quad (9.2)$$

Next the number of batteries needs to be calculated. For this the power needed during eclipse is required. Then, using eq. (9.3), a number of batteries can be calculated, from which a mass can be derived using eq. (9.4).

$$N_{bats} = \frac{T_{ec} \cdot P_{ec}}{3600 \cdot e_{cell} \cdot (1 - DoD)} \quad (9.3)$$

$$m_{bats} = \frac{T_{ec} \cdot P_{ec}}{3600 \cdot e_{sp} \cdot (1 - DoD)} \quad (9.4)$$

These batteries must be recharged during sun time. This means that the total power requirement of the solar panels increases to recharge the batteries while powering the rest of the satellite aswell. The ratio of

eclipse and sun time is equal to the ratio of the P_{ec} and P_{re} . This is because all the power used during eclipse must be charged during sun time. This leads to eq. (9.5) and gives a P_{re} of 402 W.

$$P_{re} = \frac{T_{ec}}{T_{sun}} P_{ec} \quad (9.5)$$

9.4. Solar Array Sizing

To determine the size and mass of the the solar arrays the maximum power requirement must be determined when the solar cells have degraded the most. Using the solar constant and solar cell efficiency[92] the size of the solar panels can be determined. This is done using eq. (9.6). From this the mass of the solar panels can be calculated using the solar cell mass [92], see eq. (9.7).

$$A_{sol} = \frac{P_{req}}{\Phi \cdot \eta_{sol}} \quad (9.6)$$

$$M_{sol} = \rho_{sol} A_{sol} \quad (9.7)$$

In table 9.3 the power requirement of each subsystem can be found. These values are at EOL and only of subsystem that must perform operations together. That is when the total power requirement is the highest.

Table 9.3: Power of subsystems

Subsystem	Power Req.
Payload	7184 W
ADCS	600 W
Command & Data Handling	120 W
Battery Recharge	402 W
Wiring Efficiency	923 W
Total (P_{req})	9229 W

From eqs. (9.6) and (9.7) and table 9.3 and using the solar cell parameters [92] a solar panel mass of 25.5 kg was calculated. The solar array module will be split into two so the module mass is half this plus the structural mass. This leads to a solar panel mass of 12.75 kg and structural mass of 19.9 kg per module. A robotic beam of 5 kg has been added to each module to be able to change the orientation of the array. It should be noted that the P_{req} value of 9229 W is at EOL, at BOL this will be equal to 10608 W.

In fig. 9.2 an electrical block diagram of the satellite can be found.

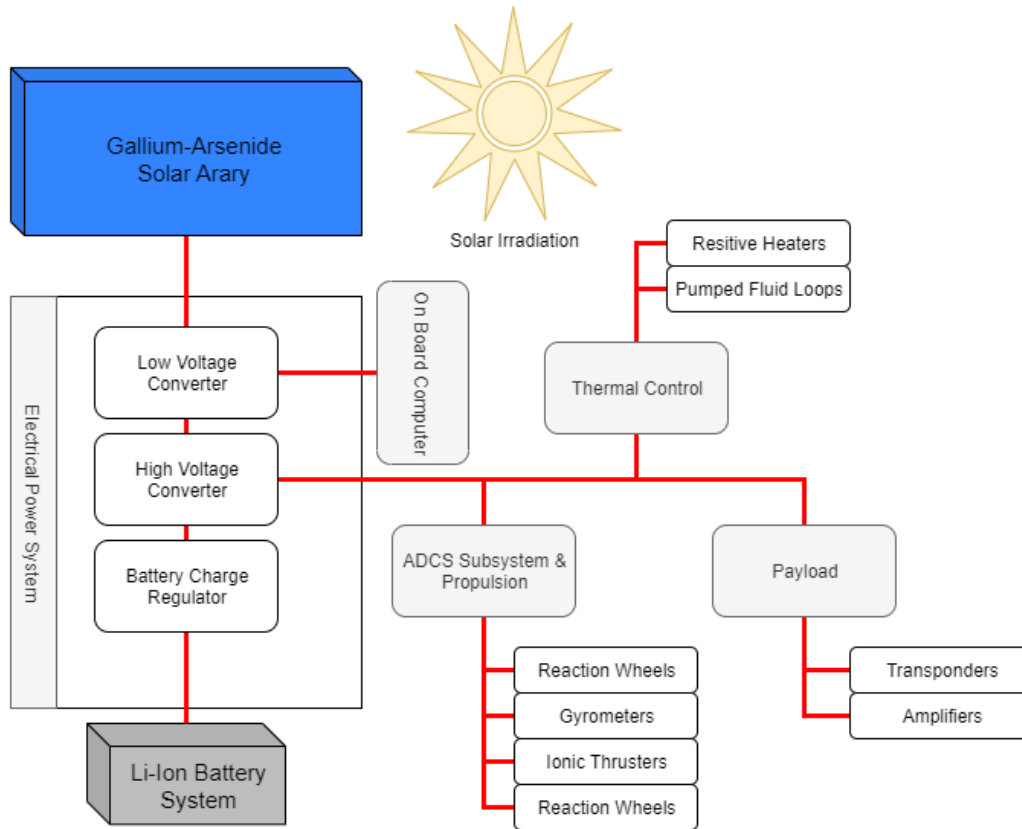


Figure 9.2: Electrical Block Diagram for satellite

9.5. Conclusion

In this chapter the power generation and power storage modules were designed. Each satellite will use two power generation and two power storage modules with the parameters found in tables 9.4 and 9.5 respectively. From this the Electrical Block Diagram (EBD) followed. In the future voltages and charge rates would have to be researched to ensure this set up works.

Table 9.4: Power generation

Component	Mass	N ^o	Total Mass
Solar Cells	13.3 kg	1	13.3 kg
Array Structure	19.0 kg	1	19.9 kg
Array Arm	5.31 kg	1	5.31 kg

Table 9.5: Power storage

Component	Mass	N ^o	Total Mass
Batteries	1.1 kg	40	44.0 kg
PMU	50.0 kg	1	50.0 kg

Thermal Control

In this chapter the thermal control system is outlined for the tug and for the modularised telecommunication satellite. A general overview of the functionality as well as the requirements of the thermal control system is given in section 10.1 additionally thermal control components are explained in section 10.2. The analysis of the control system is outlined in section 10.3 that of the tug in section 10.3.1 and that of the telecommunication satellite in section 10.3.2. The chapter is concluded in section 10.4 containing recommendations to further improve the thermal control system.

10.1. Thermal Control Subsystem

The purpose of the Thermal Control subsystem is to provide an environmental temperature in which all of the spacecraft's systems can function optimally. It needs to be able to remove and add heat when necessary. In space there are three main external sources responsible for temperature fluctuations:

- Infrared Radiation from Earth
- Reflected Sunlight from Earth
- Direct Solar exposure

In addition, the components within the satellite also radiate heat due to efficiency losses and cause internal heating. The combination of all these factors makes it necessary to properly control the spacecraft's temperature, as without the operating temperature limits would soon be exceeded.

Thermal Requirements

There are several requirements for the thermal control subsystem they are as follows:

- **IKEA-TECH-OPE-THE-T1:** The S/C thermal control systems shall cope with the subsystems thermal needs at any stage of the mission.
- **IKEA-TECH-OPE-THE-T2:** The thermal control system shall control the temperature of all components with an accuracy of 1°C
- **IKEA-TECH-OPE-THE-T3:** The thermal control system shall keep the temperature difference between individual components within the S/C below 5°C
- **IKEA-TECH-OPE-THE-T4:** The S/C thermal control system shall be a passive system if possible.
- **IKEA-TECH-OPE-THE-T5:** The S/C thermal control system shall keep all components within operating limits (table 10.1)

The operating and survival temperatures of individual components of the S/C are listed in table 10.1

Table 10.1: Temperature limits of S/C modules and equipment for operating and survival conditions [58]

Equipment	Operational	Survival
Battery Module	+10°C to +30°C	0°C to 40°C
Solar Array Module	-150°C to 110°C	-200°C to 130°C
Computer Module	0°C to 50°C	-20°C to 70°C
ADCS Module	-10°C to 40°C	-20°C to 50°C
Telecommunication Module	-100°C to 100°C	-120°C to 120°C
Propulsion Module	-80°C to +65°C	-100°C to 70°C

For the modular satellite the operating conditions of the components can be addressed individually as each module will be thermally controlled on its own. For the tug the lowest operational temperature range was taken to design the overall thermal control system. This range is +10° to +30°. To make sure these operational conditions are kept, several different methods of controlling and adjusting a spacecrafts temperature balance have been devised.

10.2. Thermal Control System Components

The S/C internal temperature can be controlled in different ways. The relevant thermal control components for the telecommunication satellite and the tug are the following:

- **Insulation:** Insulation is the most common thermal control elements [58]. They are used to prevent internal heat loss or to prevent external heating from environment. Multilayer insulation (MLI) has an effective emittance ε of 0.015 to 0.03.
- **Radiators:** Radiators are the most common component for rejection of waste heat. Radiators can be placed as S/C structural panels, as flat plate radiators attached to the S/C side wall or as deployable radiator panels. All these options emit the excess heat by IR radiation.
- **Heaters:** Heaters are used for active thermal control to prevent freezing of components. They are necessary due to orbital and seasonal variations of the environment as well as operational changes. For example the TUG will have a waiting period in GEO- with no operations this decreases the internal heat generated which needs to be compensated by heaters. Furthermore degradation of surface finish over time changes the emissivity and absorbtivity of the S/C this needs to be actively mitigated in order to keep the S/C at operating temperatures.
- **Louvers:** Louvers like radiators are used to emit excess heat into space or internally between S/C surfaces. In contrary to radiators they are active components. Louvers are commonly placed over radiators in order to regulate the heat emitted. They work like blinds that can be opened and closed. While closed the heat is kept inside the S/C, while opened the heat is emitted to space.
- **Heat Switches:** Mostly passive heat switches are used that activate the active thermal control elements if a certain temperature is reached.
- **Heat Pipes:** Heat pipes are used to distribute the heat internally. With the help of heat pipes the excess heat of e.g. the batteries can be used to heat other components of the S/C.

10.3. Thermal Control Analysis

To design the thermal control subsystem the following approach was taken:

- **Define Problem:** Identify temperature requirements and environment
- **Analysis:** Compute maximum and minimum orbit average temperature for the S/C using surface property estimates and average power dissipation when subjected to the maximum and minimum heating condition.
- **Design:** Adjust thermal coatings to see if passive design is possible.
- **Analysis:** Compute maximum and minimum temperature with added active thermal components
- **Design:** Adjust active thermal control components until operating temperatures are achieved

10.3.1. Thermal Analysis for tug

The thermal analysis was done with a MATLAB tool. The thermal analysis was based on steady state temperatures. The method used was the radiant energy heat balance where at equilibrium eq. (10.3) holds true. For a first estimate for the thermal control subsystem the spacecraft was considered as a lumped mass with 100% heat convection inside furthermore the surface properties and power dissipations were estimated. For the analysis all mission stages were considered. To analyse the thermal control of the GTO transfer orbit the internal temperature of the tug was assessed for the LEO orbit, a MEO orbit and the GEO orbit. The MEO orbit was chosen to be in between the LEO and GEO orbit with an orbit altitude of 17500 km. With these orbits all temperature ranges of the GTO orbit are covered.

The following has been included in the thermal control subsystem analysis:

- Infrared radiation from Earth
- Earth albedo
- Solar flux
- Estimation of internal heat generation

Equations (10.1) to (10.3) are used for the thermal analysis. The following parameters are included in the equations.

- α = absorptivity
- ε = emissivity
- Φ = Solar flux at Earth
- A_p = projected area toward sun
- R = percentage of solar irradiance diffusely reflected from Earth
- A_R = area exposed to diffusely reflected energy from the planet
- IR = irradiance of infrared energy from Earth
- A_{IR} = area exposed to the infrared
- σ = Stefan–Boltzmann constant
- Q_{in} = internal heat generated

$$Q_{env} = \alpha \cdot \Phi \cdot [A_p + R \cdot A_R] + \varepsilon \cdot IR \cdot A_{IR} \quad (10.1)$$

$$Q_{out} = \sigma \cdot T^4 \cdot \sum_1^n \varepsilon_n \cdot A_n \quad (10.2)$$

$$Q_{env} + Q_{in} = Q_{out} \quad (10.3)$$

The MATLAB tool was validated by checking the results with a given example calculation from SMAD[58]. The analysis was carried out with an initial estimate of the surface finish. For the internal heat generation an estimate was taken during transition 500 W during assembly and during waiting period 100 W. Following the first analysis the surface finish of the relevant S/C walls was upgraded until almost operating temperatures were reached by passive thermal control. Figure 10.1 shows that only passive thermal control will not be possible. During some mission stages the temperature range is outside of the predetermined operating temperatures for the batteries table 10.1. The surface finish used for this thermal analysis was vapor deposited aluminum which has an absorptivity α of 0.08 and a emissivity ε of 0.04. This was the surface finish which came closest to actual operating temperatures for passive thermal control. However the maximum reached temperature during the tugs assembly mission is 40°C which is 10°C over the operational limit for the batteries. Therefore the tug needs active thermal control components for heating and cooling.

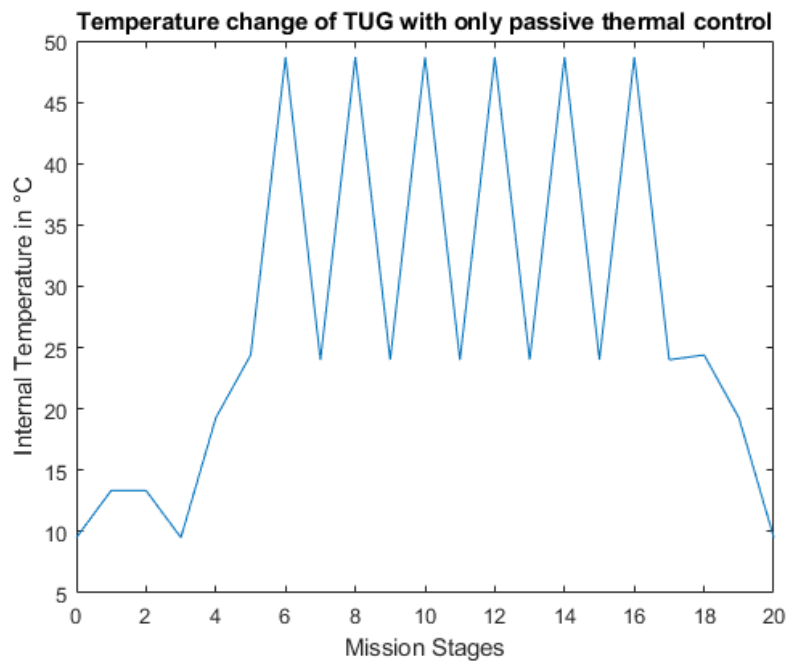


Figure 10.1: Steady state temperatures of the tug during the different mission stages

The following components have been selected for the thermal control subsystem of the tug.

- Radiators - to radiate the excess heat
- Heaters - to heat components when necessary
- Louvers - to control the radiated heat by the Radiators

- Heat Pipes - to distribute the heat internally

For a detailed design of the thermal control system of the tug further analysis in the following project stage is needed.

10.3.2. Thermal Analysis for modular Telecommunication Satellite

For the telecommunication satellite the thermal control subsystem was designed for the final mission orbit. During the transit to the mission orbit the individual satellite modules will not be operated thus increasing the acceptable temperature range of the components as can be seen in table 10.1. Furthermore the transit time is not long enough to thermally damage the modules, thus only passive thermal control of the satellite modules during transition is sufficient. The thermal analysis is carried out for two different module layouts. The first one during the transition to verify passive thermal control is sufficient for the satellite package and the second one during operation of the satellite. The same method was used as described in section 10.3.1 for the first case the whole satellite package was again considered as a lumped mass with one side considered insulated from the tug's side wall for the second case the individual modules were considered as lumped masses.

The outcome of the analysis shows that the passive thermal control is sufficient for the satellite package as can be seen in fig. 10.2.

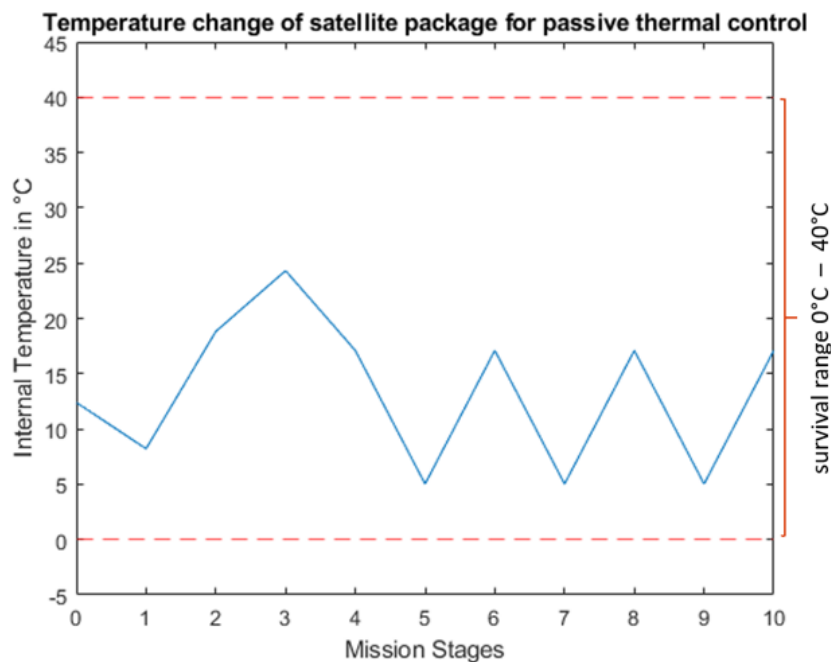


Figure 10.2: Steady state temperatures of the satellite package during the transition

The outcome of the thermal analysis for the operating configuration of the satellite shows that passive thermal control is not sufficient to keep all components in an operating temperature range fig. 10.3.

In order to operate the satellite sufficiently active thermal control components need to be added to the following modules. The other modules have a larger temperature range where passive thermal control can be achieved without adding to much risk of permanently damaging the modules due to temperature.

- Battery module
- ADCS module
- Computer module

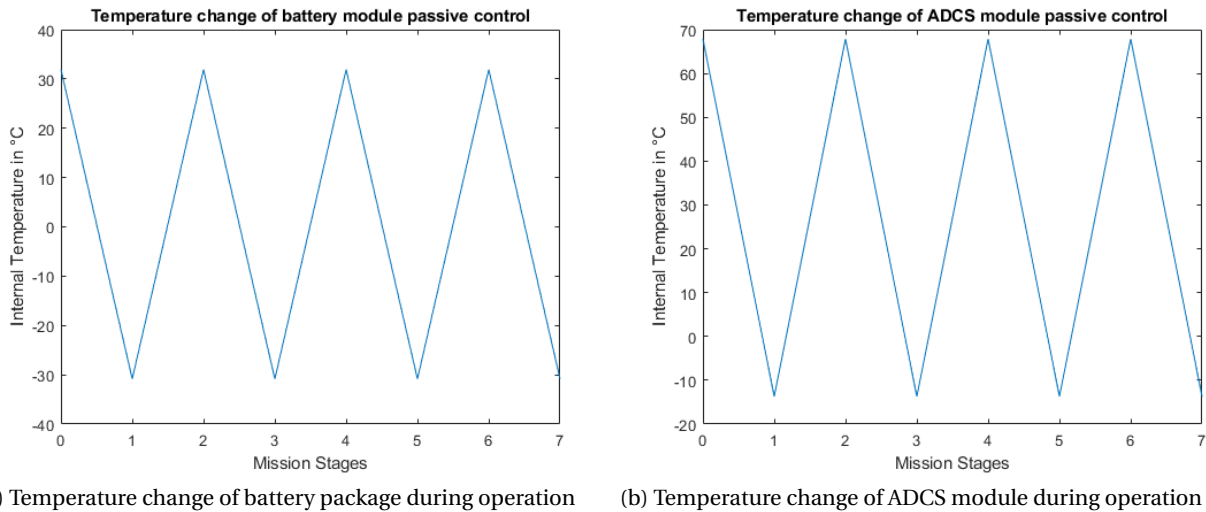


Figure 10.3: Thermal analysis of critical satellite modules

10.4. Conclusion & Recommendations for the Thermal Control System

In this chapter the thermal control system has been analysed, designed and validated for the tug and the individual satellite modules. The analysis showed that the thermal control of individual modules and thermal control for a spacecraft that operates in a variety of orbits is possible. For a more detailed design of the thermal control subsystem and in order to select the exact components for the subsystem another method should be used. The method used, radiant energy heat balance, was only for a proof of concept for the modular boxes of the telecommunication satellite and the tug. For a more thorough thermal analysis a multi node thermal model should be used to determine the internal heat convection and the temperature difference between individual modules. If the analysis of the multi node thermal model reveals that passive thermal control of the modules during transition is not possible the tug itself can act as an active thermal control component with the help of roll maneuvers throughout the transfer to GEO- the satellite package can be placed in sunlight or the shadow, whichever is needed. During the detailed design phase estimations for mass and power of the thermal control subsystems have been used with adherence to the SMAD estimations [58].

Satellite Modules

This chapter presents the module catalogue that explains the make-up of a single satellite's individual modules in terms of used components, hardware arrangement, quantity and mass. Furthermore, a brief list explaining the reasoning behind their physical appearance in the design is included. The layout in chapter 13 in contrast deals with the placement of these modules on the supporting structure. Finally, the module connection that forms the modular framework, is detailed separately.

11.1. Module Contents

As with regular satellites, certain components need to be present on the satellite. The content of these modules is based on the components selected during the subsystem design processes. Some modules were split in two for redundancy and to create a symmetrical final satellite layout. The sizes of modules is also based on the components within the module. For more detail regarding the contents of each module fig. 11.1 and fig. 11.2 should be consulted.

11.1.1. Module Box Mass

As can be seen in each module subsection, most modules have a box structure surrounding them. This structure is designed to both protect from radiation and carry loads. Designing each of these boxes in more detail would need to be done in the future. For now their mass has been estimated depending on the mass of each module. A percentage of 30% has been taken into account for the box masses as this is the percentage calculated for structures of a satellite [27]. For more detail regarding the mass of the contents of each module fig. 11.1 and fig. 11.2 should be consulted.

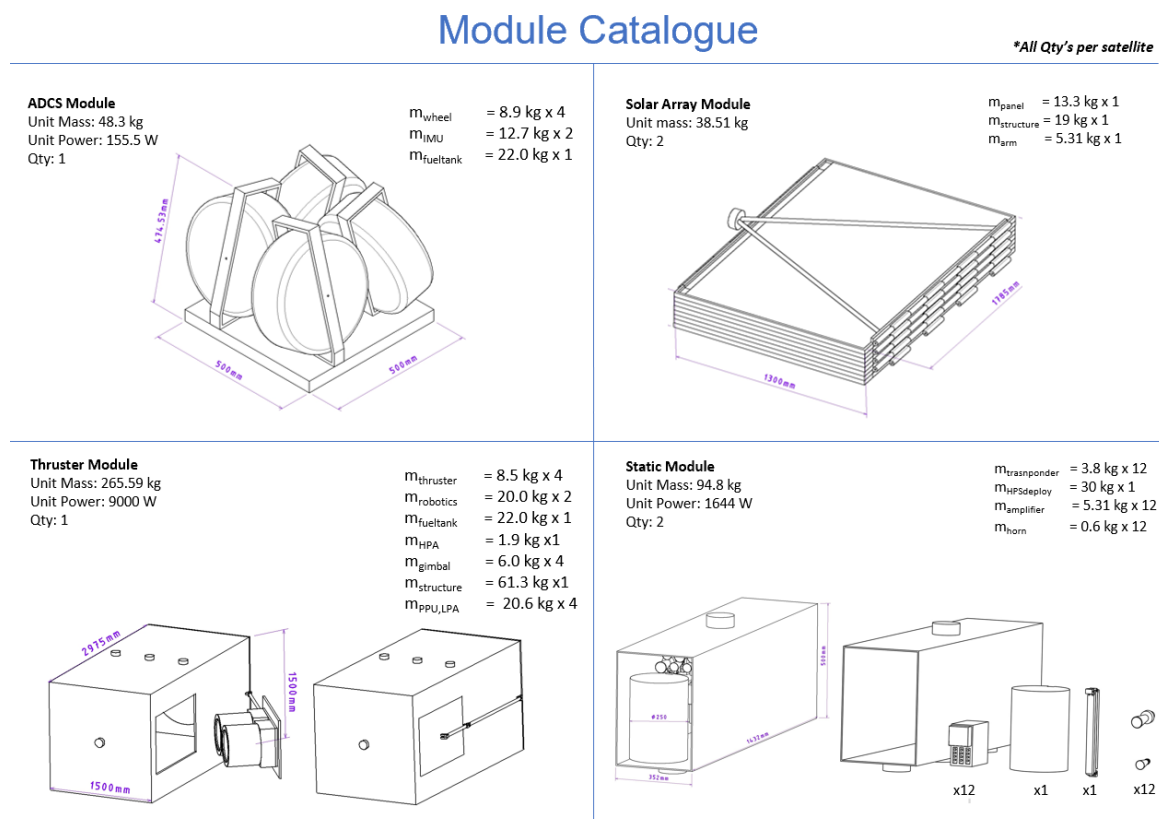


Figure 11.1: Module catalogue pt.1

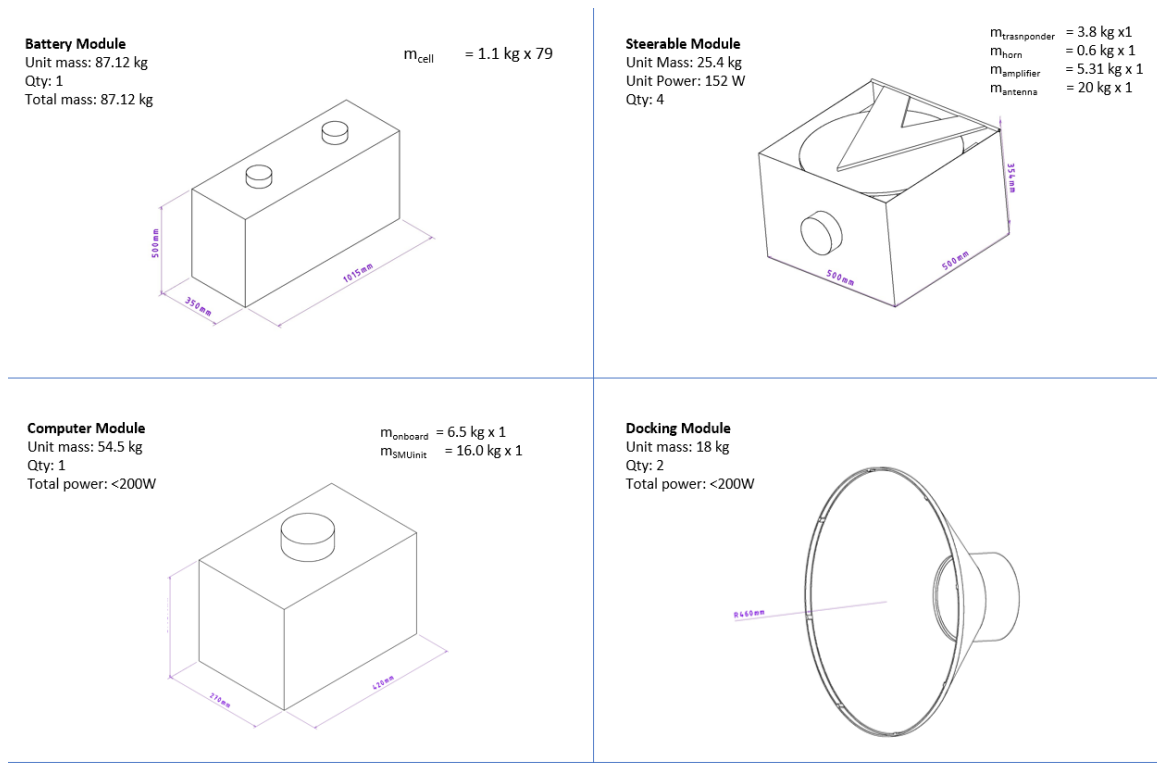


Figure 11.2: Module catalogue pt.2

ADCS Module: The ADCS module consists of the four reaction wheels and one inertial measurement unit. The reaction wheels are placed in a skewed formation to provide a 3 out of 4 redundancy. The IMU is placed inside the module itself as well, while the two coarse sun sensors and the Star Tracker have to be placed outside in order to have unobstructed view on the sun and stars. The catalogue can be seen in fig. 11.1 and detailed information about the chosen components can be found in chapter 7.

Solar Module: In fig. 11.1 a to-scale CAD Drawing of the solar array module can be found. There will be 2 of these modules per satellite which will unfold after assembly.

Propulsion Module: In fig. 11.1, the propulsion module is shown. This module consists of four electric thrusters, as was determined in chapter 6. The thrusters are placed on robotic arms in pairs. These robotic arms can steer the thrusters in the directions needed for the ADCS. Furthermore, every thruster is linked to a PPU, LPA and a Gimbal. These are together linked to the HPA and the Xenon fuel tank. All of these components are stored directly in the propulsion module.

Static Module: For this module, it has been decided to make use of four separate larger module blocks, each containing 12 transponders and a feed-array/dish combination. Additionally, four smaller modules will be considered, each being a functional spot beam assembly. For the bigger fixed spot beam modules, a combination of a feed array similar to Airbus' LMFA [32], transponders based on references from Tesat-Spacecom and General Dynamics and large deployable antennas from HPS [43] will be used.

Battery Module: The battery module is composed of multiple lithium ion battery cells housed in a protective metal casing and connected in an optimal configuration. There will be a venting port to mitigate the risk of gassing which could lead to the explosion. The scalability of batteries ensures the module itself can be easily scaled to fit the needs of the customer.

Steerable Module: For the steerable modules, a system as utilised in the Eutelsat 3b [42] will be considered. Here, the feed system is fixed to an extended position and a first reflector dish is mounted on a 2-axis precision gimbal to allow for mechanical steering.

Computer Module: The Computer Module consists of three Command, Data & Handling units manufactured by RUAG, called an SMU. Apart from the SMU, an on-board computer module is also included. This will be a product manufactured by the same company, internally designated as CREOLE ASIC. The specifics for these units about how they function and what properties and features they have, are further elaborated on in chapter 8.


Docking Module: The final module is the docking module, seen in fig. 11.2. It is a simple module consisting of the docking port and module connection. One module is optimised for pushing and the other for rotation.

11.2. Module Connection


In the following section the connection of the modules is outlined. The connection is not included into the catalogue because it requires more detailed attention. The connections are used to assemble the satellite modules into a fully integrated satellite. Furthermore, they are used to connect the modules into a ready-to-launch satellite package. The connection needs to be able to transfer data, transfer power and provide structural integrity. Some connections also need to have a thermal coupling to transfer heat. The module connection chosen for the system is the intelligent Space System Interface (iSSI) by iBOSS company [56]. The German Aerospace Center, known as the Deutsches Zentrum für Luft- und Raumfahrt (DLR), has founded a collaborative research program from 2010 until 2018 for the intelligent Building Blocks for On-Orbit Satellite Servicing and Assembly (iBOSS) [63]. The company iBOSS GmbH was founded in 2017 following the successful research program. The company continued the development of iSSI and achieved a TRL 6 in 2018 [55]. Rather than designing a completely new connection a collaboration of Airbus with the iBOSS company for this project is assumed. With their module connection iBOSS wants to be able to provide a standardised connection for all modular satellite systems: A USB for space. The company provides four different kinds of connection.

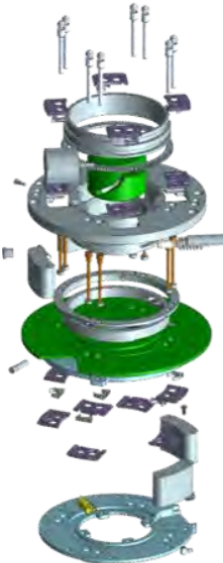
- passive connection: structure
- 2-in-1 connecting: structure and power
- 3-in-1 connection: structure, power and data
- 4-in-1 connection: structure, power, data and thermal

With these connections it is possible to fully assemble and integrate the MANTIS project satellite. A render and a photograph of the iSSI can be seen in fig. 11.3.



iSSI - Specifications





BASELINE (3-in-1)
Design Features

Geometry

Mass w Electronics/Harness Total

Coupling Sequence

Loads w/o Form Fit Axial / Lateral

Transfer Rates Bending / Torque

Power

Data

Heat

Temperature Range Operational

Misalignment Tolerance Radial/w FormFit

Angular/w FormFit

ADD-ON MODULES

(+) Passive Interface

(+) FormFit

(+) Dust Cover

(+) Launch Lock

SCALABLE DESIGN

Mechanical + Power + Data (+ Thermal = 4-in-1)

Androgynous w 90deg Rotational Symmetry

Fully-Retractable in Plain Surface

Fail-Safe System

Lubricant-Free

Diameter 119mm

Height 48mm

0.900kg

< 10s

6,000N / 400N

400Nm / 400Nm

5kW/100V

1Gbit/s

5W/K

-50°C / +70°C

3mm / 20°mm

15deg / 60deg

0.400kg

Easy Berthing

Planetary Missions

Launch Loads

CERTIFIED MANUFACTURING PROCESS

WIPO

WO/2015/150338

JP 6550690

US 15300940

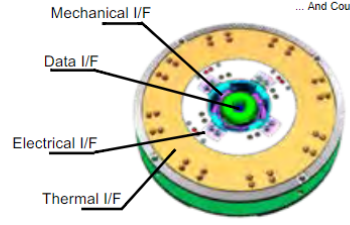

EP 2015713331

RU 2016138844

KR 1020167030560

CN 201550016403.1

... And Counting

PRODUCTION PARTNERS

HEGEMANN

DSI
Aerospace Technology

14019-03 28 6/24/2017 - Dec 2019
©2019 iBOSS - Deutsches Zentrum für Luft- und Raumfahrt. Copying and Distribution without Permission

Figure 11.3: iSSI TRL6 module connection data sheet [55]

11.2.1. Business Analysis

Assuming that iBOSS establishes itself as the market leader for modular satellite connection, it is beneficial for Airbus to use the same connection for their satellites. With that, there is the possibility of expanding the operations of the tug. Airbus could provide refuelling and servicing capabilities not only to their own satellites, but to all satellites using this iSSI connection. This would increase the market capability and could increase the return of investment. Therefore it was decided not to design a whole new connection for modular satellites but rather design the satellite to be able to use the already existing connection by the iBOSS company.

This chapter concerns structural analysis of the critical aspects of the telecommunications satellite in order to ensure the mission is completed successfully. Firstly, the main load cases are established. Then, the most critical structural elements are scrutinised to ensure they meet the structural requirements in accordance with ECSS standards. In parallel, materials are selected and mass estimates iterated accordingly.

12.1. Design Loads

There are various mechanical and environmental loads which influence the structural design. These include lifecycle design loads, launch loads, on-ground handling loads, transportation loads and EOL loads. Typically, the loads that drive the structural design are the launch loads. During launch the spacecraft experiences the highest dynamics loads in both the axial and lateral direction, the most vibrations, shock loads and thermal loads. For these reasons, the launch loads are designated as the design loads and will be verified with respect to the requirements. The load factor diagram for the chosen launch vehicle, the Falcon Heavy, is provided by the SpaceX and is presented in fig. 12.1.

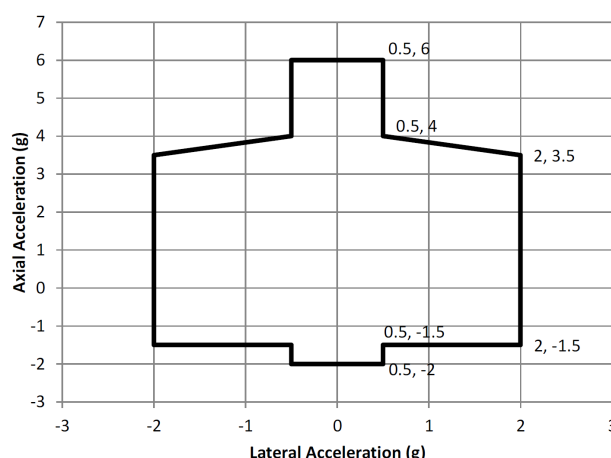


Figure 12.1: Falcon 9 and Falcon Heavy payload design load factors for "standard" mass (over 1820 kg) [83]

From this graph the design load cases for the structural analysis can be finalised. Namely, a maximum axial load factor of 6 times the gravitational acceleration and a maximum lateral load factor of 2 times gravitational acceleration [83].

Another crucial aspect of the structure that needs to be adhered to is the stiffness of the system so that the natural frequency requirements that are provided by the launch vehicle are met. Launch vehicles on their own are not perfectly rigid and have certain frequency at which they are designed most optimally. The natural frequency is therefore set by the manufacturer of the launch vehicle. For the Falcon heavy, the fundamental axial mode is 25Hz [29].

12.1.1. Structural Requirements

The requirements can therefore be formulated in accordance with the guidelines set by the European Cooperation for Space Standardisation (ECSS).

- **IKEA-TECH-OPE-THE-S1:** The designated design limit load in axial direction shall be 6g.
- **IKEA-TECH-OPE-THE-S1:** The designated design limit loads in lateral direction shall be 2g.
- **IKEA-TECH-OPE-THE-S1:** The structure shall withstand the design limit loads without failing or exhibiting permanent deformations that can endanger the mission
- **IKEA-TECH-OPE-STR-S2:** For metal structures or metal structure components local yielding may

- exist, provided it does not cause overall permanent set, instability or fatigue failure of the structure
- **IKEA-TECH-OPE-STR-S3:** The stability (i.e. no buckling) of the structure shall be verified for the design loads.
 - **IKEA-TECH-OPE-STR-S3:** The fundamental stiffness requirement of 25 Hz specified by the launch vehicle manufacturer shall be met.

12.2. Materials

For the structures there are a number of options when it comes to material selection. The main options identified are aluminium, steel and titanium. Due to the EOL strategy for all systems within Project MANTIS the selected material must be able to burn up in the atmosphere. This eliminates titanium and certain steels as an option.

According to initial layout and mass estimations the limiting property of the satellite package will be its mass and not its volume. Initial estimations show there will be room to spare within the fairing during launch while the mass is reaching the upper limit. That is why aluminium has been selected as the main material for all structures. It is lighter than steel while still having a adequately high yield strength and Young's Modulus.

In table 12.1 a few aluminium alloys have been researched along with relevant properties. All structural designs will use an alloy selected from this table.

Table 12.1: Aluminium for structures

Material	E [GPa]	Yield [MPa]	Density [kg/m ³]
AL 2014	10.6	58	2800
AL 5056	10.3	50	2640
AL 6061	10	35	2720
Al 7025	71.7	483	2800

12.3. Beam Sizing

In this section the beam structures that connect all modules during launch will be sized. This is based on the load cases during launch since these are by far the highest load cases.

12.3.1. Forces

The beam dimensions were preliminary estimated based on the modules described in chapter 11. This will be further elaborated in chapter 13.

The beams themselves are thin walled structures with harness wiring running through them. They are meant to connect all modules during launch and also after assembly. The thickness of the thin wall must be calculated based on launch forces because this is when the highest forces occur. In fig. 12.2 a coordinate system has been established and the relevant forces shown. The forces F_{bx} , F_{by} and F_{bz} are the total forces of all masses the beam must support, including its own.

The beam with the most mass attached to it includes the following modules: 1 × solar array module, 2 × battery module, 2 × static spot modules, 2 × spot beam modules, 1 × dock module and 44 × module connection. This is based on the layout described in chapter 13. Using the masses for these modules an initial value for F_{bx} , F_{by} and F_{bz} can be calculated using the launch loads in fig. 12.1, see eqs. (12.1) to (12.3). Note that m_{bm} is equal to 0 for the first iteration of this calculation.

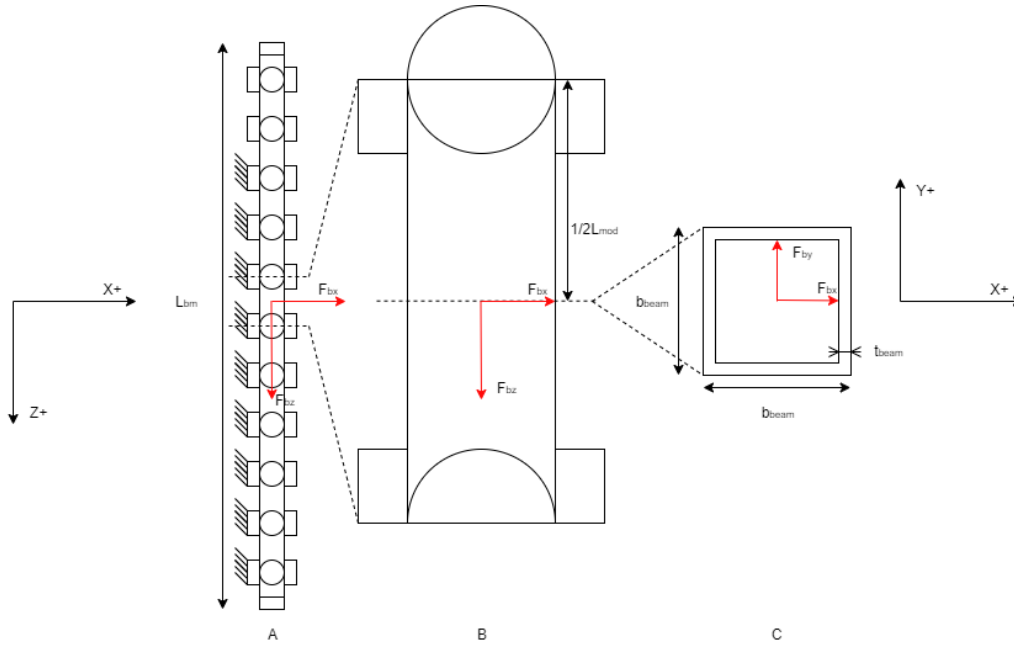


Figure 12.2: Beam total forces. A is the entire beam, B is a zoomed in and C is a cross section.

$$F_{bx} = A_{lx}(m_{sol} + 2m_{bat} + 2m_{sspot} + 2m_{spotb} + m_{dock} + 44m_{mod} + m_{bm}) \quad (12.1)$$

$$F_{by} = A_{ly}(m_{sol} + 2m_{bat} + 2m_{sspot} + 2m_{spotb} + m_{dock} + 44m_{mod} + m_{bm}) \quad (12.2)$$

$$F_{bz} = A_{lz}(m_{sol} + 2m_{bat} + 2m_{sspot} + 2m_{spotb} + m_{dock} + 44m_{mod} + m_{bm}) \quad (12.3)$$

12.3.2. Bending

In the case of this beam bending stress is the stress that needs to be designed for. Using the calculated loads a beam wall thickness (t_{bm}) can be calculated based on the bending stress equation seen in eq. (12.4).

$$\sigma_{bz} = \frac{(M_x I_{yy} - M_y I_{xy})y + (M_y I_{xx} - M_x I_{xy})x}{I_{xx} I_{yy} - I_{xy}^2} \quad (12.4)$$

As the cross section of the beam is symmetrical in all axes, see fig. 12.2 C, ($I_{xy} = 0$ and $I_{xx} = I_{yy}$), eq. (12.4) simplifies to eq. (12.5).

$$\sigma_{bz} = \frac{M_x y + M_y x}{I_{xx}} \quad (12.5)$$

The bending moments are equal over both axes ($M_x = M_y = F_{bx} L_{mod}$), so eq. (12.5) simplifies further into eq. (12.6).

$$\sigma_{bz} = \frac{M_x (x + y)}{I_{xx}} \quad (12.6)$$

I_{xx} can be calculated based on the cross section seen in fig. 12.2 C. This leads to eq. (12.7).

$$I_{xx} = \frac{b_{bm}(b_{bm}^3)}{12} - \frac{(b_{bm} - 2t_{bm})(b_{bm} - 2t_{bm})^3}{12} = \frac{b_{bm}^4 - (b_{bm} - 2t_{bm})^4}{12} \quad (12.7)$$

Since the only unknown in is t_{bm} , this value can be derived based on eqs. (12.6) and (12.7), see eq. (12.8).

$$t_{bm} = \frac{1}{2} \left(b_{bm} - \sqrt{b_{bm}^4 - 12 \frac{M_x(x+y)}{\sigma_{bm}}} \right) \quad (12.8)$$

From here an initial value for the beam mass (m_{bm}) can be determined using the cross section, the beam length (L_{bm}) and the density of the selected material. The material selected for the beam is aluminum 7025 due to its high yield stress.

Subsequently, the bending stress calculations must be repeated, but now accounting for the initial beam mass. This calculation is then iterated until a variation of only 0.1 kg is reached with each iteration. This leads to a final result: t_{bm} of 9.04 mm and m_{bm} of 43.2 kg.

12.3.3. Verification

The verification of the mathematical bending stress model was done according to the procedures set up in the Midterm Report [28]. Each entered equation was verified using unit tests. Then the integration and system tests were done by using similar cases where the bending stress was known. If the model calculated the same bending stress as the chosen example it proves the model works correctly.

12.4. Refuel Tank

The aim of this section is to size the refuel tank and the thin-walled box that will be protecting it. First, the refuel tank has to be sized. For this case a cylindrical thin-walled shell with thin-walled spherical caps on both ends was chosen. The spherical caps were chosen to handle the internal pressure. The refuel tank is located at the bottom of the satellite package. This location was chosen because it increases the stiffness of the overall construction and thereby increases the associated natural frequency. The thin walled box is necessary to offer additional protection for the tank, alleviate some loads and provide a flat surface on which other square modules can rest.

12.4.1. Determining refuel tank radius

Most conventional fuel tanks are cylindrical in shape because they are inherently part of the launch vehicle. However, in the case of Project MANTIS the refuel tank is not used during launch and just acts like another part of the payload. Furthermore, the radius is linked to the volume of fuel that needs to be carried and to the height of the tank. In order to determine the optimal shape of the refuel tank, the buckling strength a cylindrical tank with spherical end caps will be calculated for three unique radii; 0.8 m, 1.3 m and 1.75 m. The smallest radius represents the smallest radius possible as that is the radius of the Falcon Heavy Payload Adapter (FHPA). It is assumed that the fuel tank is securely bolted to FHPA during launch. The largest radius represents the largest footprint withing the walls of the fairing.

The buckling stress of a thin-walled cylindrical shell is given by the eq. (12.9) [17, 103].

$$\sigma_{crc} = \frac{K_c \cdot E \cdot \pi^2}{12(1-\nu^2)} \cdot \left(\frac{t}{L} \right)^2 \quad (12.9)$$

Herein, σ_{crc} is the theoretical buckling stress for thin-walled cylindrical shell, K_c is the buckling coefficient dependent on the boundary conditions, E is the Youngs modulus and ν is Poisson ratio.

As shown in fig. 12.3 the value for K_c can be derived from the intersection of the applicable curvature parameter, Z_c and the radius-to-thickness ratio, R/t . For the demonstratory calculations, Aluminum 7025 from table 12.1 was used.

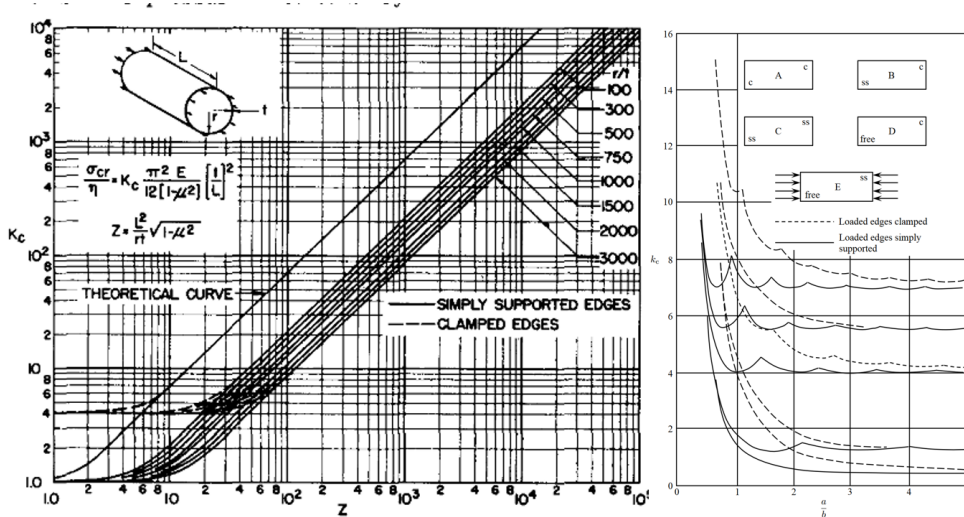


Figure 12.3: Buckling coefficient for thin-walled cylinders and buckling coefficients for flat plates.

For spherical caps the minimum buckling stress, σ_{crs} , can be calculated using eq. (12.10).

$$\sigma_{crs} = \frac{2}{\sqrt{3(1-\nu^2)}} \cdot E \cdot \left(\frac{t}{R}\right)^2 \tag{12.10}$$

Table 12.2: Buckling loads for different cylinder radii at various wall thicknesses

t [mm]	$P_{0.8}$ [kN]	$P_{1.3}$ [kN]	$P_{1.75}$ [kN]
1.0	9.8	12.79	11.34
1.5	33.35	38.53	19.09
2.0	79.05	91.32	45.25
3.0	266.8	308.21	152.73
3.5	423.67	489.43	242.20
4.0	632.42	730.58	362.029

It is clear that thickness and radius have a large influence on the buckling load since the buckling load increases with $\left(\frac{t}{L}\right)^2$. Verification of these through unit tests backs up these presumptions. In a study with similar variables, the buckling load versus thickness was observed where, similarly for a given radius, as thickness increased the buckling load increased. As a first selection for the structural iteration, a radius of 1.75 m with thickness of 3.5 mm was chosen because the Buckling Load of 242.20 kN is just under buckling load of 246.77 kN without the safety factor. With addition of the protective layer it is assumed the structure will fully sustain the load and including the 1.25 safety factor.

A radius of 1.75 m was also selected due to mass. Comparing two cylinders both able to sustain the buckling loads, one 1.75 m cylinder with 3.5 mm thickness and the other 0.8 mm radius with 3.0 mm, the latter has 5 times the mass. It is important to note that the internal pressure was not accounted for, however, it is feasible to assume that the external axial pressure is greater than the internal pressure and therefore the launch are still the design loads applicable to the selection.

12.4.2. Determining tank supporting structure

The supporting structure around it can be sized next. For a preliminary estimate the casing around the refuel tank will consist of a thin-walled rectangular box. Each side can be modelled as a flat plate for which the buckling stress is given by eq. (12.11) [17].

$$\sigma_{crf} = \frac{\pi K_{cf} E}{12(1 - \nu^2)} \left(\frac{t}{b} \right)^2 \quad (12.11)$$

Here, K_{cf} is the buckling coefficient for a thin flat plate and b is the length of the shortest side. K_{cf} can be read from fig. 12.3 by following the dashed line for exhibit C which stands for clamped on the loaded sides and simply supported on the remaining sides. The length of the shorter side is set to 1.75 m and 2.5 m for the long side there for the restraining ratio $2.5/1.75 = 1.42$. As before, at the intersection with the appropriate line for exhibit C, $K_{cf} = 4.3$. Once again, for the calculations Aluminium 7025 was used. The results showed that the thin walled structure on it's own could not sustain the launch loads because Euler buckling set in too early. As a result, a proposal will be made to include longitudinal X-stiffeners that should in theory be implemented in order to increase the effective area. Nonetheless, the protective box is still needed necessary in the design for supporting the modules above and offering a connection point for the beams. In addition, the thin wall will protect the refuel tank further from space debris and radiation as it make the journey to GTO.

12.5. Module Support

The module connection is not only a data and power port, it also has structural properties. These can be found in fig. 11.3. The connection is capable of withstanding axial loads of 6000 N, lateral loads of 400 N and moments of 400 Nm. This will be too weak in certain cases during launch. making it imperative to add structural support. The support will be a cylindrical cap around the module connection. This is because the support must take on lateral loads and bending moments and this shape allows for that. As can be seen in fig. 12.4 the support simply slides in to place. It is held in place by the module and the beam.

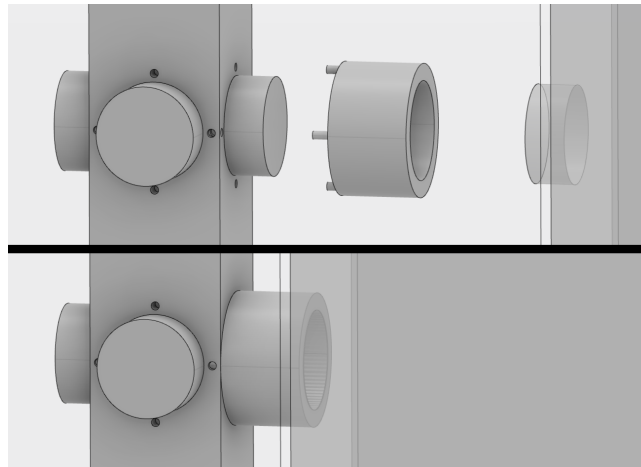


Figure 12.4: Module support connection

The driving variables of the module support are the number of pins (N_{pins}) and pin thickness (t_{pin}). Furthermore the pin depth (d_{pin}) and allowable shear (τ_{al}) determine the strength of the pin. Using fig. 12.5, F_{pin} can be determined based on the F_{lat} . This is done according to eq. (12.12). Then using eq. (12.13) a pin diameter can be determined.

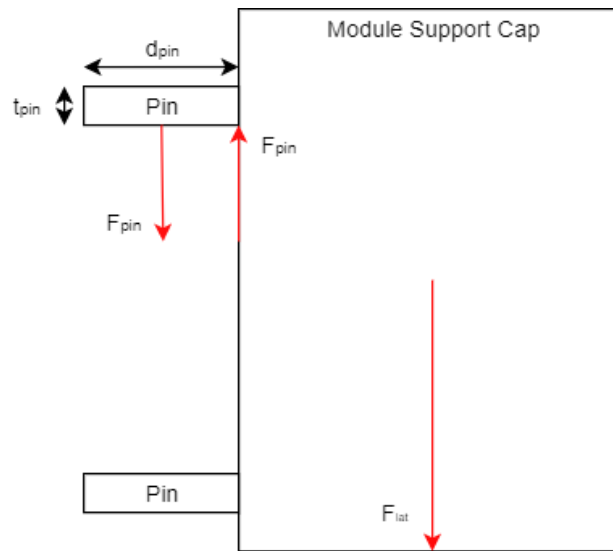


Figure 12.5: Pin forces

$$F_{pin} = \frac{F_{lat}}{N_{pins}} \quad (12.12)$$

$$t_{pin} = 2\sqrt{\frac{F_{pin}}{2\pi \cdot \frac{\tau_{al}}{SF}}} \quad (12.13)$$

Using the max value for F_{bz} for F_{lat} , as this is the worst case scenario, the pin thickness was determined to be 3.12 mm. This makes the total mass of the module support 4.09 kg. The module support will be added to each module connection where a module is actually connected and between the beams and the refuel tank. This totals to 36 module supports per satellite.

12.6. Final Structure Mass

Based on structural a final mass must be calculated. The mass of each module box must still be accounted for and also the wiring of the satellite.

12.6.1. Structural Components

Table 12.3: Structural components

Component	Mass	Nº	Total Mass
Beam	43.2 kg	2	86.5 kg
Module Connection	0.9 kg	88	79.2 kg
Module Support	4.09 kg	46	147 kg

12.6.2. Wiring

Wiring also adds to the mass of the satellite and has been found to be 4.5% according to SMAD [58]. This brings the total dry mass of a satellite up to 1847 kg.

12.6.3. Final Mass

The final mass of a single satellite and the satellite package and can now be calculated. These masses are found in table 12.4.

Table 12.4: Final masses

	Dry Mass	Wet Mass
Satellite	1847.0 kg	2096.3 kg
Package	-	7289.2 kg

12.7. Vibrations

During launch it is important to know the natural frequency of the satellite package. This is to prove the package does not resonate with launch vibrations. It is required to be higher than 25 Hz for modes in axial direction as specified in section 12.1.

To calculate the natural frequency the structure of the package is assumed to be a square beam. With this assumption the frequency can be calculated using eq. (12.14). Herein E_{pk} is the Young's Modulus of the package which can be assumed [58] to be equal to that of aluminium 7025 because this material is used for all structural components. The I_{pk} is the package second moment of inertia based on the adapter ring of the launch vehicle, which has an outer diameter of 1575 mm and thickness of 185 mm. m_{pk} is the package wet mass and L_{pk} is the distance from the fairing adapter to the center of mass of the satellite package based on the layout in section 13.1.

$$f_n = \frac{1}{2\pi} \sqrt{\frac{3E_{pk}I_{pk}}{m_{pk}L_{pk}^3}} \quad (12.14)$$

This amount to a natural frequency of 74.3 Hz far greater than the minimum requirement of 25 Hz. This is a simplified calculation and should be further elaborated in the future.

12.8. Stability and Control Characteristics

The following section summarises the relevant stability and control characteristics for the design of the ADCS subsystem in chapter 7.

Table 12.5: Size and mass properties of the tug and satellite

Parameter	TUG	Parameter	Satellite
Size in X [m]	4.5	Size in X [m]	2.5
Size in Y [m]	3.5	Size in Y [m]	3
Size in Z [m]	3.5	Size in Z [m]	3
Mass prior GEO-	4270 kg	Single Sat. Mass	2096 kg
Mass achieved GEO-	1860 kg	Mass Package	4192 kg

Table 12.6: CG locations over mission stages

Parameter	Value [m]
Tug/Sat CG min. distance	3.50
Before-burn Tug CG distance to combined CG	1.73
After-burn Tug CG distance to combined CG	2.42
After-burn Sat CG distance to combined CG	1.77
Before-burn Sat CG distance to combined CG	1.08

12.8.1. CG

For the stability and control analysis of the Tug with the satellite package the following assumptions were made.

- MANTIS tug and satellite package are cuboids with constant density
- CG of tug is in center of body
- CG of satellite package is in center of body

Once the tug is refueled and the satellite package is connected to it in the transition configuration, the CG of the whole structure shifts as can be seen in fig. 12.6. During the transition from GTO to GEO- the CG shifts again due to the propellant being used. The amount of propellant burnt is 2301.5 kg as was calculated in chapter 6. Thus, the new total mass of the tug once it arrives in GEO- is 1883.1 kg.

During the transition to GEO- the CG shifts a total of 700mm to the front this has an impact on the ADCS. This is all due to the fuel usage in this transition.

12.8.2. ADCS thrusters moment arms

Due to the shift in CG the moment arms of the Tugs ADCS thruster change. The new moment arms are depicted in fig. 12.7.

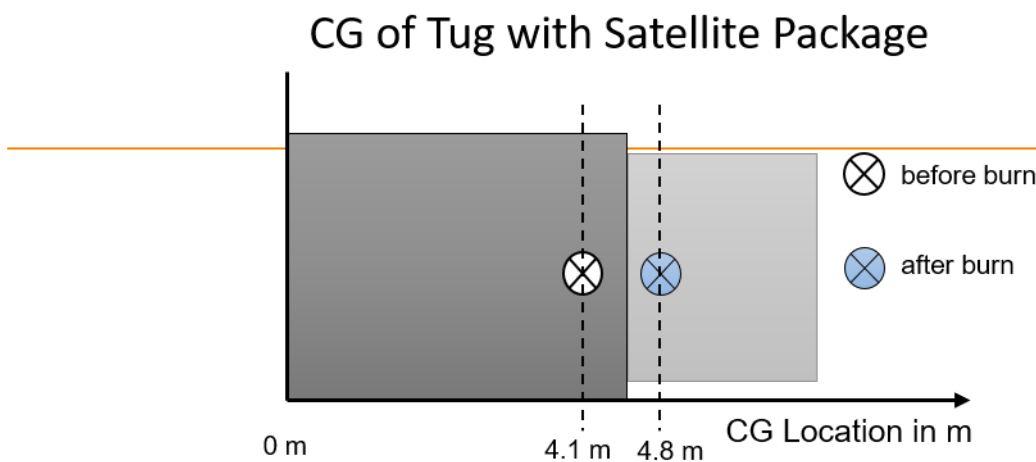


Figure 12.6: CG shift of tug with satellite package in transition configuration before transition burn and after transition burn

12.8.3. Mass Moment of Inertia

The moment of inertia of a solid cuboid of height h , width w , and depth d , and mass m is calculated using eqs. (12.15) to (12.17). The configurations' mass moments of inertia before and after burn are given in table 12.7.

The determined axis are

- yaw axis = z
- roll axis = x
- pitch axis = y

$$I_x = \frac{1}{12} \cdot m \cdot (h^2 + w^2) \quad (12.15)$$

$$I_y = \frac{1}{12} \cdot m \cdot (d^2 + w^2) \quad (12.16)$$

$$I_z = \frac{1}{12} \cdot m \cdot (w^2 + h^2) \quad (12.17)$$

For the satellite, the Mass Moment of Inertia (MMOI) also needs to be known, as this impacts the sizing of the ADCS thrusters. Using the sizes and masses of the different components, combined with the parallel axis theorem, ?? highlights the final MMOI of the assembled satellite.

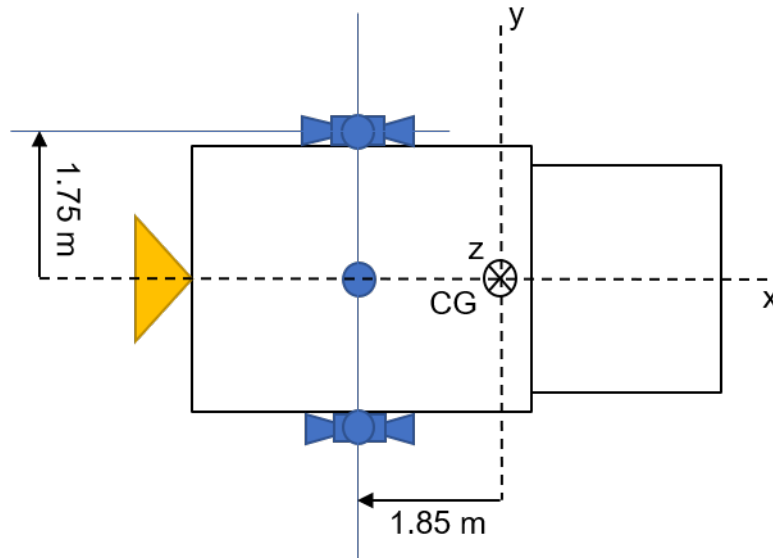


Figure 12.7: ADCS thruster moment arm with MANTIS connected to satellite package

Table 12.7: Mass moment of inertia for tug, the satellite package and tug together with the satellite package

Configuration	Axis	before burn	after burn
MANTIS	x	8599.86	3635.64
MANTIS	y	11407.98	4822.79
MANTIS	z	11407.98	4822.79
Satellite Package	x	6950.33	6950.33
Satellite Package	y	5888.48	5888.48
Satellite Package	z	5888.48	5888.48
MANTIS + Package	x	62288.7	45167.21
MANTIS + Package	y	44325.04	29567.19
MANTIS + Package	z	44325.04	29567.19

12.9. Conclusion

After some iteration, a layout based on structural analysis was selected. In this layout the beams carry most of the lateral loads while the refuel tank carries most axial loads. Aluminium 7025 was selected as the main material for all structures as it is a strong yet light material. The module connection was found to be too weak and needed to be supported to mitigate its risk of failing. This additional support carries most lateral loads of the module connection. The stability and control characteristics have been upgraded during the design process in order to accurately size and design the ADCS subsystem of the tug. In this chapter the final values were given.

In the future the structural analysis must be refined. The calculations done now are rough. This leads to an over designed structure meaning the structural mass could be lowered with more accurate calculations. Also, there is a possibility of designing a new module connection that already can withstand greater loads without the need of designing a workaround support structure.

Layout & Configuration

In this chapter the layouts of the LV, satellite and tug are described and the process that lead to them. Based on this the hardware diagram were made, shown in section 13.4. Also, the final technical budgets are shown in a clear overview.

13.1. Layout LV

Determining a final layout for the satellite package in the LV is a complicated process. Mainly due to the iteration required between the structural analysis, assembly and the layout itself. The first layout was designed based on very simplified initial structural calculations. This led to an initial layout seen in fig. 13.1. At this stage each module's mass and size was subject to change and the whole assembly process needed to be designed.

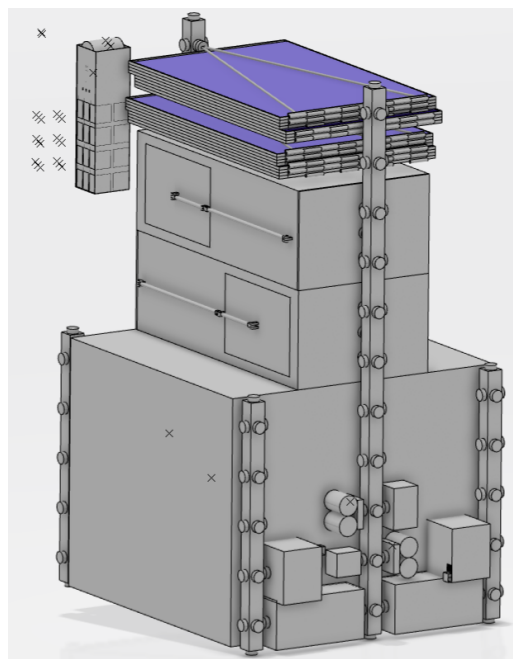
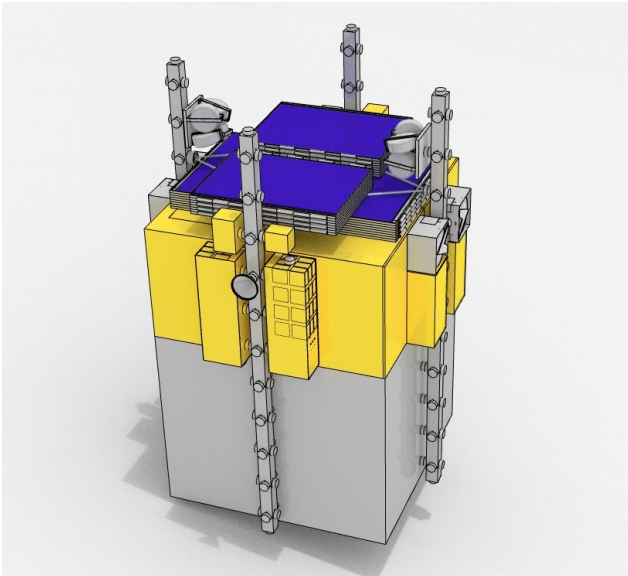


Figure 13.1: Initial layout satellite package LV

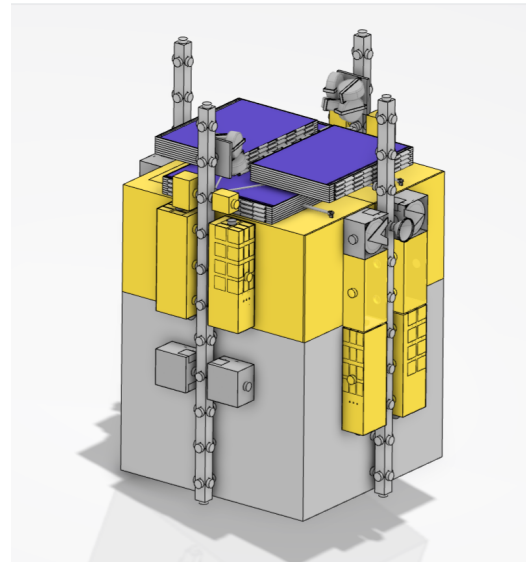
As described in section 12.4, this initial layout would not be able to handle the lateral launch loads. That is why the support beam needed to be changed. Through further analysis a different set up was chosen as seen in fig. 13.2a.

In this 2nd layout the package is structurally sound but assembly is still not entirely possible due to the order of assembly, as explained in section 14.5. This meant some minor changes needed to be made to the layout leading to a final configuration seen in fig. 13.2b.

This layout has been structurally verified, fits in the launch vehicle and is also suited for assembling two satellites as explained in section 14.5.



(a) 2nd layout satellite package LV



(b) Final layout satellite package LV

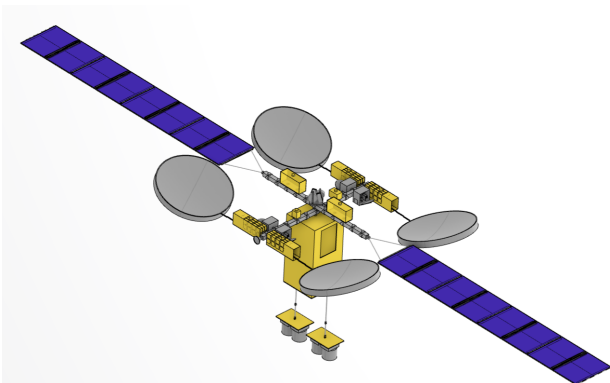
Figure 13.2: 2nd and final layout satellite package LV

13.2. Layout Satellite

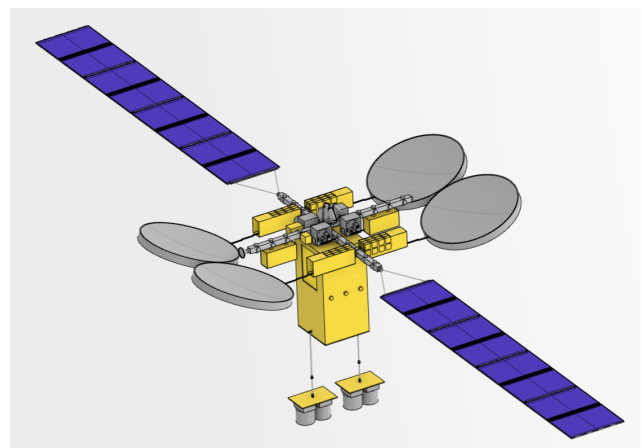
The driving properties for the layout of the satellite are based on the moment of inertia and the thermal properties. However the possible layouts are also very dependant on the satellite package layout and assembly limitations. For this reason the first suitable solution for the satellite layout has been used.

Due to the high amount of modular connections on the beams a very large number of layouts are possible. There is bound to be one that has the most benefits for all subsystems and it is definitely recommended to research this further after this stage in the project. For now the layout in fig. 13.3a has been chosen as the final layout and one alternative has been given, fig. 13.3b, just to show the capabilities of a modular satellite.

In both the layouts a plus structure is used but H structures [13] or spiderweb structures could also be possible.



(a) Final satellite layout



(b) Alternative satellite layout

Figure 13.3: Final satellite and alternative configuration

13.3. MANTIS layout

The actual layout and architecture of the MANTIS is not the focus of this DSE project. For now only a preliminary architecture of the spacecraft is needed in order to proof the AIV concept. As a first estimation

of the size and mass one of Airbus satellite bus platforms is used. ESA has been working on a SpaceTug for space debris removal with the e.Deorbit project. The Envisat satellite was considered as the object to be de-orbited by the ESA SpaceTug [33]. Envisat has a mass of about 8,000 kg [62]. Given that the satellite package with the refuel tank has a total mass of 7289.2 kg . Therefore it is a reasonable assumption that the e.Deorbit SpaceTug is capable of handling the satellite package and the e.Deorbit SpaceTug system in development can be used as an estimate for MANTIS. The e.Deorbit S/C platform is based on Airbus GEO satellite Eurostar-NEO [36]. The Eurostar-Neo platform is for the 3- to 6-tonne GEO satellite market [54]. The wet mass for the tug is 4269.7 kg thus within the range of the Eurostar-NEO platform mass budget. Only the following subsystems have been designed in more detail for the tug. These are the relevant subsystems to prove the AIV mission .

- Robotic Arm section 14.3
- Propulsion section 6.4
- ADCS section 7.1

For all other subsystems the estimation method by SMAD has been used to determine the dry mass of the subsystem [58]. The initial assumption of the tugs dry mass has been updated after the propellant and propulsion mass was determined in the midterm report[28].

13.4. Hardware Diagrams

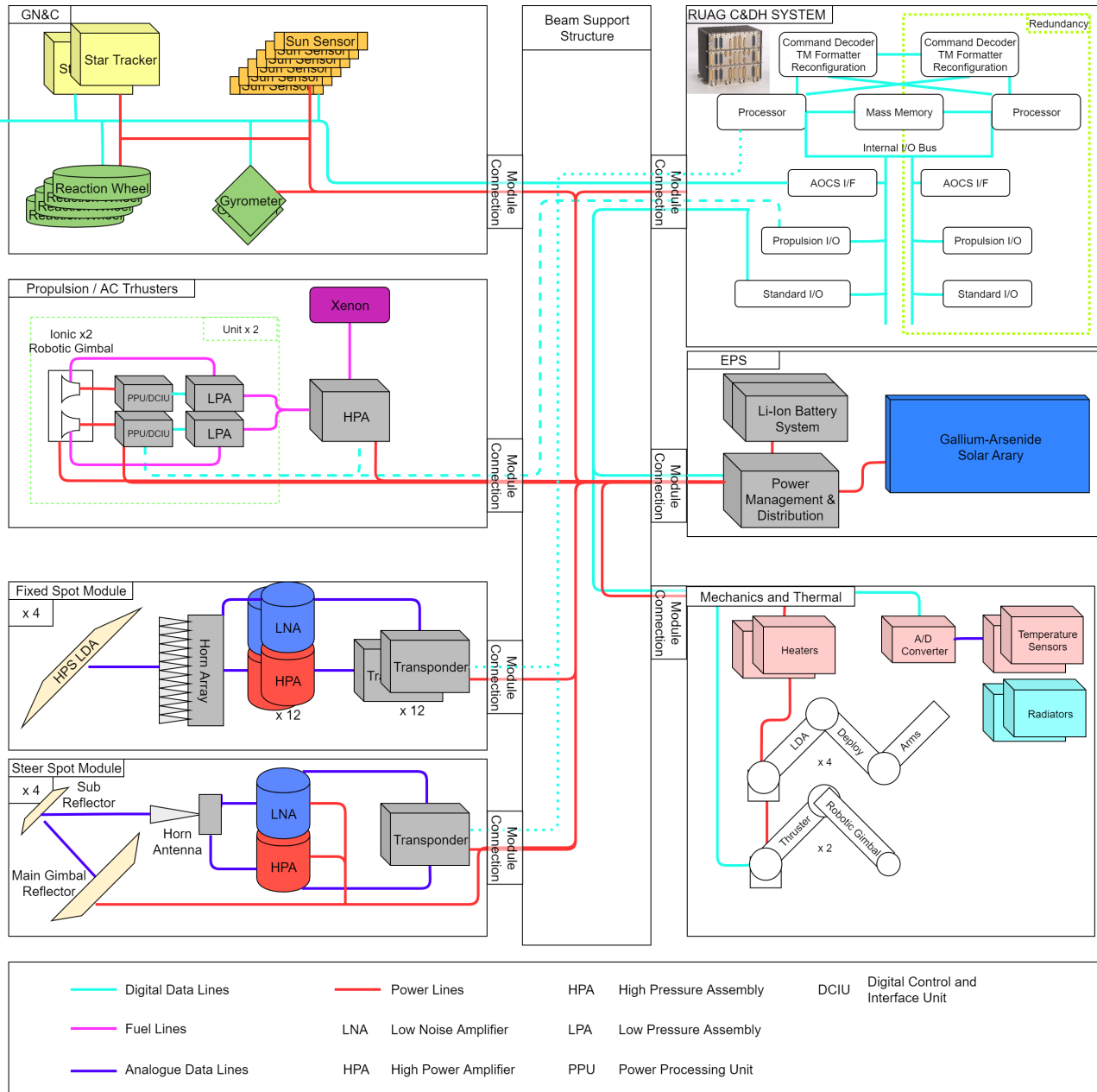


Figure 13.4: Hardware Diagram of operational satellite

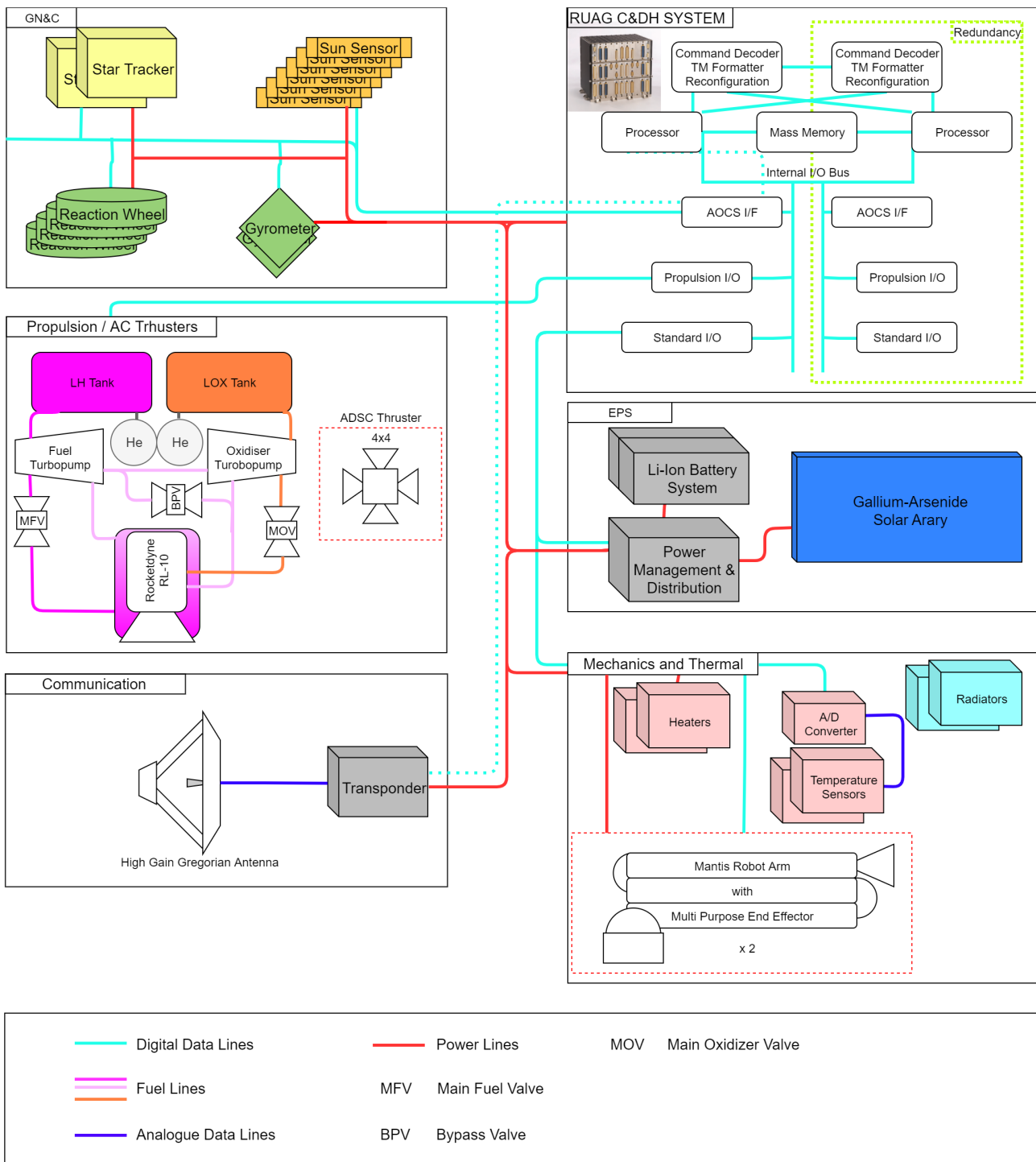


Figure 13.5: Hardware Diagram of the tug

13.5. Resource Allocation & Budget Breakdown

In the baseline report [27] a table allocating budgets to certain technicals aspects was created. This table has been copied and updated comparing the allocated budgets to the actual budgets, see table 13.1.

Table 13.1: Resource budgets

Safety Factor	Avg LM [kg]	Avg DM [kg]	Avg PM [kg]	Avg Power [kW]
Without Safety Factor	6243	3286	2970	15.0
Satellite	2102	1852	250	10.49

As can be seen, the satellite is way below the allocated budgets. This is because these budgets are max values

and also because the satellite uses electrical propulsion which saves immensely on propellant mass.

13.6. Conclusion

After iterating between subsystems and assembly a final layout was created for the satellite, tug and satellite package. This process was mainly based on structural, assembly and LV requirements. The hardware diagrams and final technical budgets followed from this..

Assembly

A concept central for Project MANTIS envelops the ability to assemble, as well as service and repair, satellites in orbit. The tug has been designed with its own robotic arms which have the capability to grab, construct and service satellites. This also aids in the first step for servicing satellites - during servicing the MANTIS needs to remain in the same reference frame as the target satellite, hence the need to grab the satellite with the robotic arm. In addition there also exists two distinct methods for servicing, namely docking and berthing.

14.1. Rendezvous

After the modules of the telecommunication satellite are launched into space, the modules must rendezvous and mate with the tug before the tug can transfer the module package to GTO-. Consequently, a rendezvous procedure is designed for clarity. The full procedure is given in fig. 14.1 and comprises multiple phases. Most importantly, rendezvous can be broken down in far range and close range.

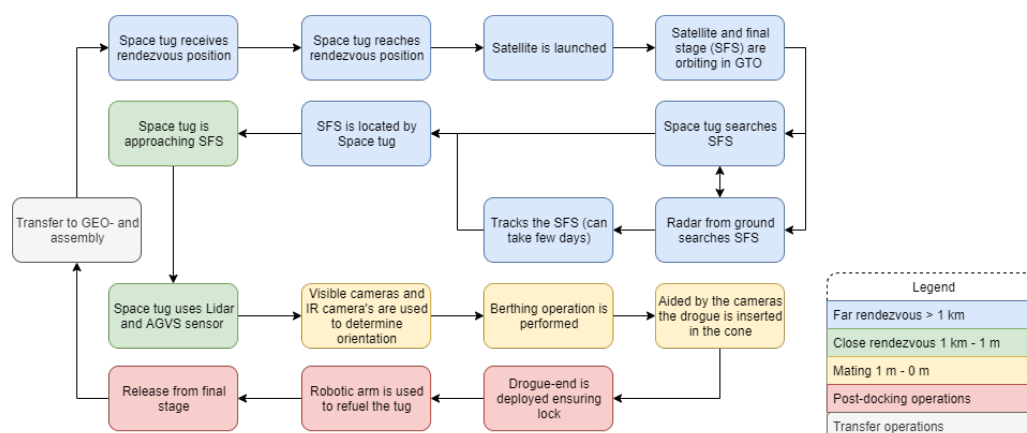


Figure 14.1: Docking flowchart

14.1.1. Far Range

As indicated before consist the rendezvous procedure out multiple stages. The stage where the relative distance between the chaser (tug) and the target (module package) is approximately 3000 km is named the far range.

The launcher is attempting to bring the satellite package closely to the rendezvous position. However, this does not always succeed. The first step in the rendezvous process is using the Lidar and a Advanced Video Guidance Sensor (AVGS) to determine the position of the packages. In case this fails is radar equipment on earth used to locate the package. This position is contacted to the space tug.

14.1.2. Close Range

The close range is defined as 1 km to 1 m. Whenever the space tug is in range of 1 km to 1 m is the Lidar and AVGS used to determine the position of the package and final stage combination more accurately. It is then autonomously approaching the target until 1m. For this maneuver is the RVS 3000-3D lidar of Jenaoptronik used as a reference.

14.2. Mating

After the tug has a rendezvous with the module package, the tug must mate with the module package before changing orbits. To acquire both the module package in space as well as space-born satellites, different acquisition techniques can be used to acquire these objects. The two main techniques are docking and berthing.

14.2.1. Docking and Berthing

While docking can only occur with cooperative targets, berthing offers a solution for non-cooperative targets. Herein, the system can then place satellite module packages and active telecommunications satellites. Though docking has been considered, berthing will be necessary for some of the operations which are meant to be performed by the tug. Since the module package will be delivered by the launcher (and only limited ADCS will be available) this is considered an uncooperative target. Consequently, the mating system has primarily been designed for berthing.

14.2.2. Mating System Design

There are multiple considerations to be made when designing a mating system for the tug. Firstly, a trade-off can be made between central and peripheral systems. A central mating system is advantageous in the sense that this enables effective alignment most easily. Moreover, the key disadvantage of central mating mechanisms prohibit a transfer tunnel, which is irrelevant in the situation of the tug. Therefore, a central mating system is designed. The mating system comprises a probe and drogue design with an asymmetric probe. Therefore, all module packages and satellites can only dock in one specific orientation [39].

Moreover, the drogue is designed with a 45° angle to guide the probe inwards. This enables the tug to conduct docking with cooperative systems such as active satellites. Docking is favoured over berthing, as this spares the robotic arm of being used and reduces use of resources (e.g. manpower, electricity).

For preliminary sizing of the mating system, separation forces, environmental vibrations, environmental disturbance torques, assemble forces, ADCS forces and acceleration forces are considered. With further sizing for the tug itself (which is out of scope), this can be completed.

14.3. Robotic Arms

For Project MANTIS, the arm's primary purpose is to grab a module, manoeuvre this module to the correct location and attach it to the existing structure. This process takes a significant amount of time, where the assembly of 20 modules would take up to 36 hours. This includes a period of down time to account for the eclipse period during orbit and assumes that the assembly starts once the eclipse finishes. Should assembly proceed later, this assembly time would increase by another hour if the tug and modules are eclipsed a second time.

For this design, the biggest consideration concerned the maximum length of the robotic arm. This impacts the maximum reach of the robotic arm, and is determined by multiple factors, mainly the size and configuration of the final assembly of the modular satellite. Due to the lack of versatility in the arm's ability to manoeuvre over the tug, this means also means that any modular satellite constructed is limited in size (in principle).

14.3.1. Requirements and Design

For the robotic arm, two major requirements had to be met. It was vital that any extension of the arm could reach all places where the satellite payload was, and move every module to its final location. It was ultimately concluded that three links, totalling 6.9 m in length was sufficient for this. In addition, it is required that the assembly takes no more than 48 hours, as seen in **TECH-AIV-ASM-T5**, chapter 17.

14.3.2. Simulation and Modelling

Prior to launch and further development work for the robotic arm, simulations have to be run. Therefore, two models for the robotic arm were made.

Assembly Time

Firstly, through Microsoft Excel[®], a spreadsheet was made consisting of basic assumptions, combined with some values from the DARPA arm [26], in order to estimate an order of magnitude for total assembly time. This ultimately resulted in an assembly time, including down time during any eclipse which occurs once per orbit for a duration of one hour, of 37 hours.

In order to estimate the assembly, several assumptions were made. It was assumed that the angular velocity of the robotic arm was about 1/360th the speed of the DARPA arm. This meant that assembly was considerably slowed down, while assembly still remained within the requirement.

The assembly time was calculated by using several values taken from [26]. The speed of the DARPA arm, after adjustment, was taken when the arm was extended by 75%, as well as 95% (as these values were the only values available for the DARPA arm), as well as the arm being loaded with the maximum payload mass for the propulsion module. Then, with an assumption of 20 modules, one trip was calculated for an unloaded and loaded arm, per module. It was also assumed that it took about three minutes for the arm to grab a module. In the table below are a summary of the values mentioned above, per module, as well as a total assembly time.

Table 14.1: Summary of robotic arm performance estimation

Load case	Duration [min]
75% extended, empty	30.2
75% extended, full	50.3
95% extended, empty	60.4
95% extended, full	100.7
Total	2201.7 (\approx 36.7 hours)

Computer Model

A computer model was coded in Python 3.6/3.7. The primary focus of this program was to generate the (initial and) final position of the robotic arm per movement request, while implementing a collision detection algorithm to determine if the path that the arm was following would not interfere with other modules already placed, as well as the tug and its peripherals such as solar panels. This meant that the model firstly generated the so-called "optimum" angles - this was the combination of the four angles that defined the robotic arm's geometry. "Optimum" indicated a particular combinations of angles which minimised the distance between the target point and the end of the robotic arm. One angle defined the "roll" angle (named θ), while the other three indicated pitch (named $\beta_1, \beta_2, \beta_3$). This does mean that the model is over defined, since there are three angles which would be used to define the arm's geometry within a plane. In principle, this means there are infinite solutions. This does allow extra flexibility, especially for object avoidance, but does complicate matters when first coding the model.

The above meant that the initial intentions to use inverse kinematics to solve for the "optimum" angles was quickly eliminated. Ultimately, a numeric solver from Python's SciPy module was used, which bounded all angles within particular ranges.

A Limited Memory Broyden Fletcher Goldfarb Shanno bounded (L-BFGS-B) algorithm [19] is used, an optimisation algorithm originally based on FORTRAN¹. There are cases where a global minimum was not found. In this case, this meant the above solver found a local minimum rather than the global minimum, or the arm could not reach the desired target. This is the case either because the desired point was too far for the arm to reach, or $\beta_1 = 45^\circ$ was too restrictive. In these cases, a Basin Hopping algorithm was employed rather than the minimisation solver².

¹This was the default solver for the bounded optimiser from SciPy.

²From verification and validation tests, since either solvers met the requirements for accuracy, as well as the solver completing the optimisation in around 0.1 seconds, no other solving methods were investigated.

θ had bounds between 0° and 360° , while β_2 and β_3 had limits between -180° and $+180^\circ$ (technically this is not possible due the robotic arms being rigid bodies, however this would only affect a small selection of points, thereby the bounds remaining in this range). β_1 was only allowed a range between 10° and 80° as this did consider the effects of the rigid body nature of the robotic arm³. It did not have negative angles as this would be the equivalent of θ rotating 180° .

For this computer model, fig. 14.2 was devised to illustrate the expected infrastructure in order to successfully code the model.

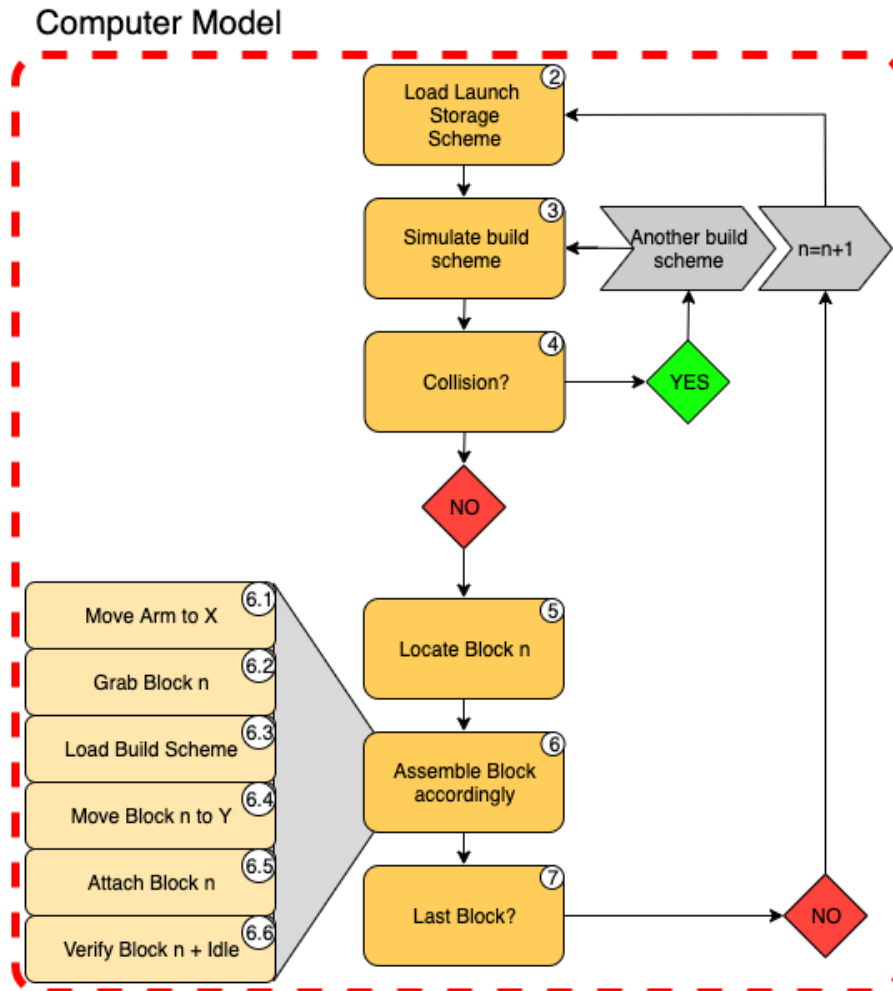


Figure 14.2: Software diagram - computer model segment

As a whole, the model takes as input, the dimensions of the tug, any peripheral items such as solar panels as obstacles, and then the target location. This would be either the start location of module n , and later on the end destination. For the model, the home location of the robotic arm are at all angles = 0° , except for β_1 which is 45° .

For this model, there are also plans to add further functionality as part of the PDD (detailed in chapter 21). The biggest feature would be the implementation of accurate determination of construction time. Whilst currently a first order estimation has been made, as mentioned previously, more details need to be investigated prior to modelling these characteristics into the computer model. Details such as exact weight distributions of the robotic arm links, the specific motors that would be used to mobilise the arm, as well as an optimised collision detection algorithm would need to be developed.

Furthermore, while the angle optimisation works as it is supposed to, it, as of yet, does not optimise the angles based on the arm's last position. This means that, using (2, 2, 2) again as an example, if the arm is in a particular configuration, the optimal angles that the solver produces might mean that the entire arm

³This mobility would only be needed in two distinct cases. Either if another pitch angle would be immobilised due to failure of the robotic arm, or this pitch angle causes the robotic arm to not be able to reach it's target location. In all other cases this angle is set to 45° .

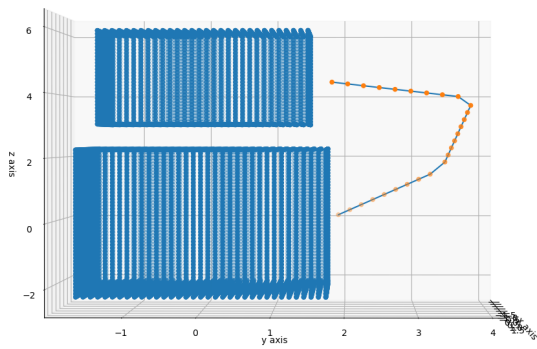


Figure 14.3: The robotic arm approaching the satellite payload pre-assembly

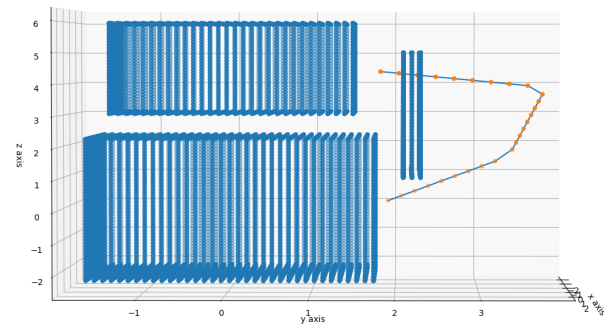


Figure 14.4: Collision with collision error message - the robotic arm is still plotted as the current state of the model separates the collision detection and plotting of the robotic arm

has to rotate 180°, while its previous position might mean that only one link has to rotate to get to the same position. This is a limitation of the model.

It is also for the above reason that a position of (2, 2, 2) might produce multiple angles all 45° off of center. Due to the arm's length being a total of 6.9 m, this is more than enough to reach this location with the desired accuracy

14.3.3. Collision Detection

One feature incorporated in the model is collision detection. This algorithm does angle-step calculations of the different permutations of the set angles that are possible. Should one permutation incorporate into a collision, another order will be checked. This means that there are a possible six total ways for the robotic arm to reach its desired destination.

There is also a final state of "no solution found". This error message is displayed when no combination of angle movements are possible to get to the destination.

Figures 14.3 and 14.4 illustrate two situations. One situation is where the arm is in the process of reaching the satellite payload, pre-assembly. The second image is if there is an obstacle. For the second image, the arm is still illustrated in the desired place (with an error of 10^{-9} m), however this was accompanied with a "no solutions found" error message.

14.3.4. TRL

In this project, the focus concerned the development of a model of a robotic arm that deals with the environment that it will be in. This is independent of any material and other technology choice. This is further reinforced by the fact that there are multiple robotic arms currently present in space. The fact that the currently existing robotic arms are all TRL 9, it is a safe assumption that the only research and development that would need to be done would be investigation of specific components regarding the mobility of the arm, rather than research in which materials are applicable. Additionally, since this arm would be launched in 2028, this allows further development time in the general robotic arm development, meaning integration into Project MANTIS will be, relatively speaking, straightforward.

14.3.5. Verification and Validation

The robotic arm model also requires verification and validation as this affirms whether the assumptions and calculations made are representative of the actual use case described in the project.

Verification

It is paramount to verify the computer model for the robotic arm, as well as begin to validate the model to the best of the team's abilities in the limited time and resources available.

For verification, simple tests were performed. This consisted of the arm in its default position, and then without any obstacles, the model should predict the precise angles the robotic arm should have. This was done firstly done with target points such as (2, 2, 2) - this should produce an angle that is 45° off from center.

Validation

Once these tests were completed, the model also had to be validated. This was done by using a robotic arm model in SolidWorks[®], where then the angles were inserted. The distance to the target point was then checked, as well as the end destination. Once both confirmed that the arm would reach the target point within the agreed-upon accuracy (to the order of 1 mm, slightly better than the DARPA arm accuracy of 2 mm [26]), the model would be deemed validated.

Additionally, once a working robotic arm is constructed, both verification and validation can also occur visually. This would mean, during testing, humans can visually inspect the arm's location, thereby adding another step in verification and validation.

In orbit this would also occur, however cameras would be used to construct a 3D computer model to verify the location of the arm. This would be a combination of image recognition and depth sensing with clear markers on the robotic arm to sense its location. This would also aid the computer model, however this step is beyond the scope of the project.

Recommendations

Though this program provides an initial model of the robotic arm, development towards an enhanced model would lead to possibilities for optimisation of the robotic arm (in terms of sizing), improvement of the module layout and, optimisation of the arm's trajectory. Moreover, more accurate time calculations could be made by implementing angular velocities and verification times in the model, better representing the capabilities of the robotic arm.

14.4. Tools

For versatility, the robotic arms should have different tools that can be attached to the ends. These tools are defined by the functional requirements of the arms. As a reference, the DARPA arm has been considered and used in analogous estimation.

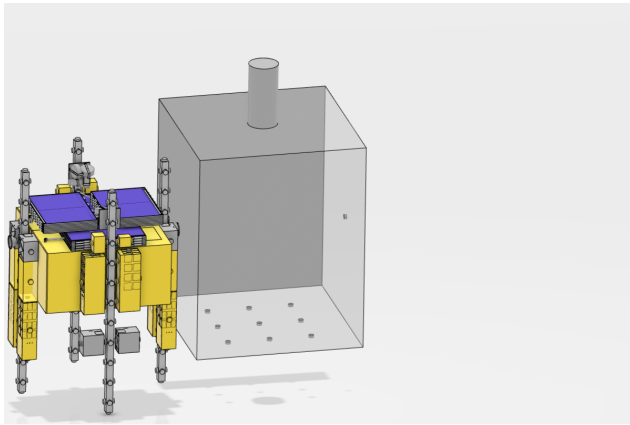
The DARPA mission is to provide services similar to those of the AIV mission in space. These services include inspection, repair, relocation and upgrading of satellites in GEO. Hence, the mission profile fits well with that of Project MANTIS.

In contrast to the DARPA mission however, the AIV mission is meant to complete various additional tasks. These tasks include AIV and deorbiting space debris. Therefore, three additional tools have been considered to cover these additional functions. Firstly, for AIV the module connection device is considered. This is simply a connection device which can lock in with the modules. Consequently, the arm can then move the modules in place and assemble the satellite. Secondly, mass estimations have accounted for a debris acquisition system. Herein, a netting system will be launched to catch space debris. Airbus has already designed such a system for prior space missions, and this tools therefore sized accordingly. Finally, a refuelling device has been accounted for, as this was not a mission objective in DARPA.

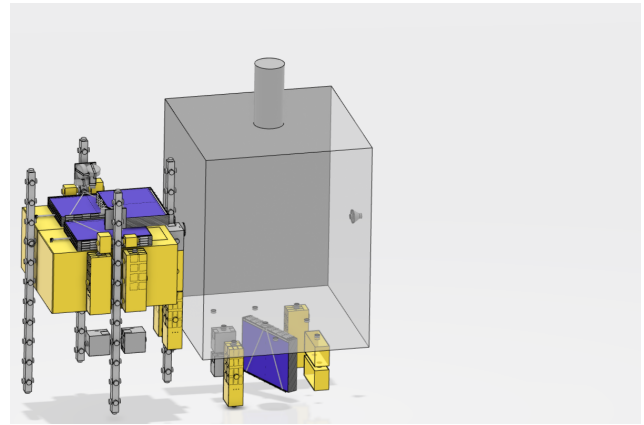
14.5. Sequence

Assembling the actual satellites from the satellite package is rather complicated. To get a clear idea of assembly Catia was used to render certain steps of assembly. During the iteration of the LV layout with respect to the structural analysis, the assembling was also accounted for. This consisted of constantly measuring distances and updating dimensions. The assembly starts off by moving the free docking port from the satellite package to the opposite side of the tug where the satellite will be assembled and moving all parts to the tug buffer storage so as to free up the first beam (figs. 14.5a and 14.5b). Subsequently, the free beam is assembled, followed by any free parts that attach to the beam (fig. 14.6a) and the next beam is freed up using the buffer storage (fig. 14.6b). The free beam is then assembled followed by the remaining parts of the first

satellite (fig. 14.7a). As the first satellite is complete, it is released from the tug (fig. 14.7b). For the second satellite, the first beam of the second satellite is loosened (fig. 14.8a) and this beam is assembled, followed by all relevant parts (fig. 14.8b). Finally, the second beam is freed up (fig. 14.9a) and the second satellite is fully assembled (fig. 14.9b).

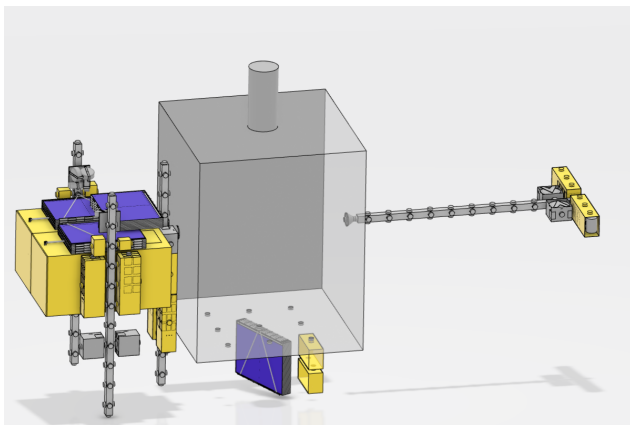


(a) Assembly step 1

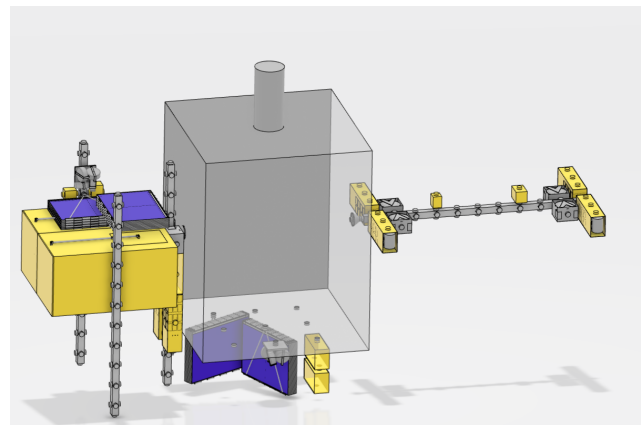


(b) Assembly step 2

Figure 14.5: Step 1 and 2 of assembly

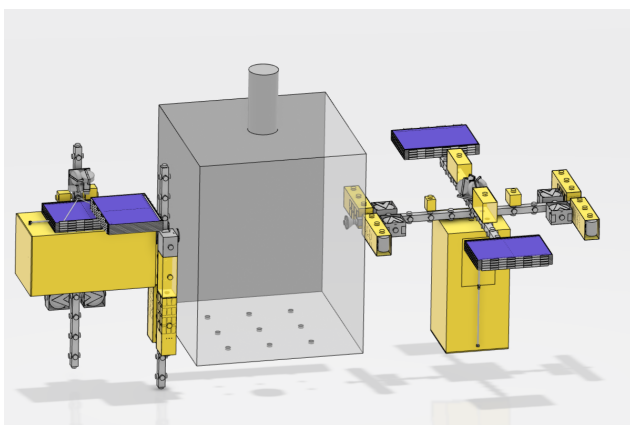


(a) Assembly step 3

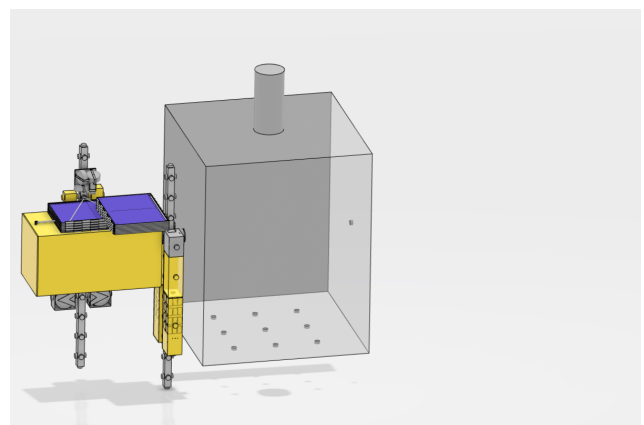


(b) Assembly step 4

Figure 14.6: Step 3 and 4 of assembly

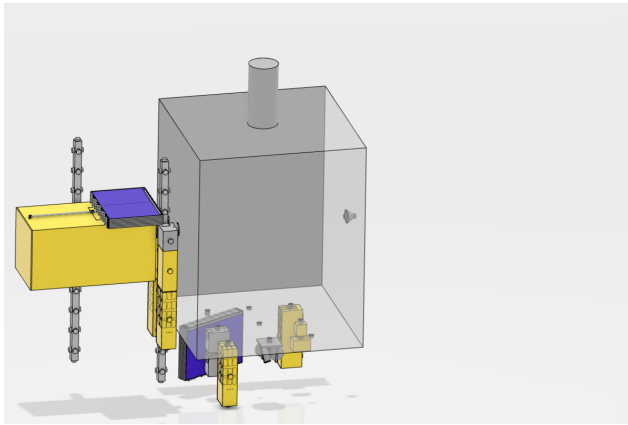


(a) Assembly step 5

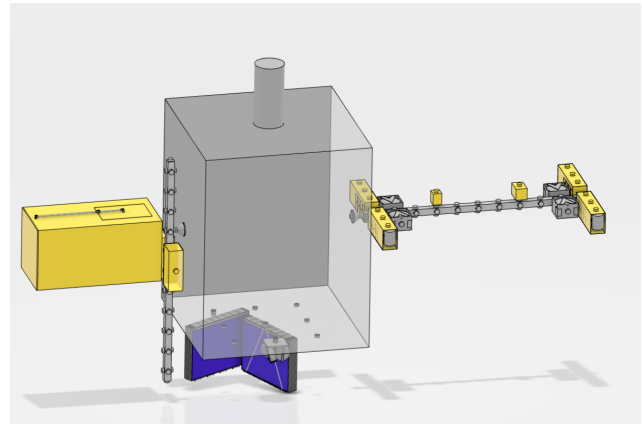


(b) Assembly step 6

Figure 14.7: Step 5 and 6 of assembly

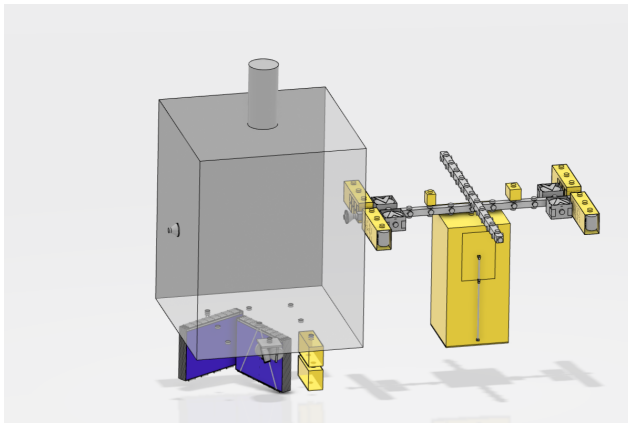


(a) Assembly step 7

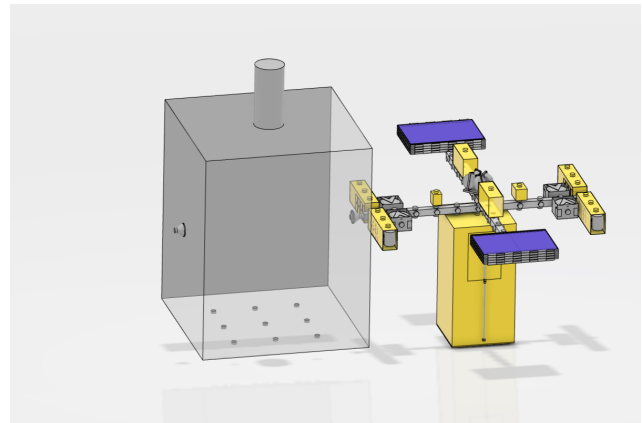


(b) Assembly step 8

Figure 14.8: Step 7 and 8 of assembly



(a) Assembly step 9



(b) Assembly step 10

Figure 14.9: Step 9 and 10 of assembly

14.6. Performance Analysis

With the modules that have been designed the AIV system has performance capabilities as shown in table 14.2.

Table 14.2: Performance analysis overview

Module	Resource	Amount	Reference Chapter
Solar Arrays	Power	7904 W	chapter 9
Batteries	Power Storage	9144.2 Wh	chapter 9
ADCS	Pointing Accuracy	$<0.05^\circ$	chapter 7
	Attitude Determination Accuracy	0.003°	chapter 7
	Rotation Speed	0.126 rad/min	chapter 7
	Communications	Eb/N0	15 dB
Assembly	Assembly Time	36.7 h	chapter 14

14.7. Conclusion

For the assembly of the telecommunication satellites, rendezvous, mating, the robotic arm, the tools and the assembly sequence has been designed. Firstly, the rendezvous will be executed with the module package through far-range and close-range rendezvous. Once this is completed, the robotic arm will berth with the module package using a asymmetric probe-and-drogue mating system. A model has been set up to

prove the viability of the robotic arm. Within this model, the arm uses numerical optimisation to determine the necessary angular displacements and check if these angles can be reached without causing a collision. Lastly, necessary tools have been considered and finally the assembly sequence is defined.

Mission Risk Assessment

Effective risk management and mitigation is key to successfully conducting the AIV project. During each phase of the project, a risk assessment has been conducted to adequately consider the risks and account for the corresponding mitigation where possible. This resulted in numerous (concept-specific) risk maps. For the detailed design phase of the project, in addition to those of the previous design phases, a detailed risk assessment has been conducted on system and sub-system level. Herein, risks have been identified for 11 different sections of the projects. These risks have then been elaborated on and ranked from 1 to 5 (increasing) in terms of probability (very unlikely, unlikely, possible, likely, very likely) and impact (negligible, marginal, substantial, critical, catastrophic). Following the identification of risks, mitigation has been considered for the corresponding risks when necessary. This mitigation has been implemented in the design, decreasing probability or impact of specific events and contributing to a successful mission.

15.1. Risk Identification

Several risks have been identified on both system and sub-system level, as shown in table 15.2. The risks are noted below with an elaboration on both the probability ranking and impact ranking. All risks have been given a unique code and have been mapped in table 15.1.

- **ADCS-1:** During the lifetime of the tug one of the star trackers could fail. This will result in some reduction in mission success since the tug then has to operate with less frequent and less accurate information solely from the sun sensors. The selected star tracker has a high reliability and therefore the risk to fail in only 7 years is highly unlikely.
- **ADCS-2:** During the lifetime of the tug one of the sun sensors could fail. This will result in questionable mission success because the tug now has to operate with only information from the star trackers. In safe mode the S/C relies on the sun sensors to keep the points of failure and power consumption down. The sun sensors are very robust and simple instruments. Therefore the chance of failure is unlikely.
- **ADCS-3:** During the lifetime of the tug one of the gyrometers could fail. This will have a large impact since the update rates of the sensors will be too low for effective manoeuvring. Therefore the spacecraft is not able to determine its attitude accurately anymore and will drift off. The selected gyrometers are flight proven and therefore it is unlikely that these will fail.
- **ADCS-4:** During the lifetime of the tug one of the thrusters could fail. If a thruster fails the spacecraft will have no full 3D-axis control and will not be able to dump momentum for the reaction wheels. Consequently, the spacecraft will not be able to be manoeuvred. The selected thrusters are very flight proven but the frequency of usage is high since the tug is moving a lot in its 7 years of lifetime. Therefore it is considered possible that one of the thrusters could fail.
- **ADCS-5:** During the lifetime of the tug one of the reaction wheels could fail. This would lead to questionable mission success because the tug now has to operate solely with the thrusters which will use up fuel at a much higher rate than accounted for. The reaction wheels contain moving parts which could become a problem for reliability. However, they are also designed for 15 years and are flight proven. Therefore, it is considered unlikely that these sensors will fail.
- **CMPT-1:** The CDH unit may not start due to internal or external factors. Failure of the CDH unit has a catastrophic impact, as the satellite cannot be overseen and/or commanded by ground control. Also, any data relevant to document or send directly to Earth cannot be sent anymore. This will result in a satellite not able to perform its original mission. The probability of a CDH unit refusing to start is highly unlikely after extensive testing on Earth. The dependency on other subsystems needs to be kept in mind though, resulting in more uncertainty and a slightly higher event probability.
- **CMPT-2:** The on-board computer may not start due to internal or external factors. When the computer fails, all subsystems are not able to collect their inputs and nor send their responsive outputs. This will make the satellite impossible to use effectively. As the on-board computer will have been tested extensively on Earth, it is considered highly unlikely that it would fail. Keeping the dependency on other subsystems in mind, this has been considered as a unlikely probability (in contrast to very unlikely).

- **CMPT-3:** The CDH unit may lose its direct connection with Ground Control unable to down- and upload any data. The data from the subsystems cannot be sent instantaneously and non-received commands will not be acted upon. Over the course of the tug's lifetime, it is considered very likely that Ground Control will lose connection with the satellites for a short period of time, possibly forced by weather conditions or faulty fine tuning of the antennas but also when parts of the connection (antennas, amplifier, etc.) are updated/upgraded.
- **DOC-1:** During the docking sequence, unexpected loads are introduced on the docking probe which could result in a fracture of the probe. Failure would be catastrophic, since the tug would not be able to dock to the satellite package which results in mission failure. The probability of this happening is highly unlikely as extensive calculations have been made and a safety factor is taken into account.
- **DOC-2:** As the package is treated as an uncooperative satellite, the tug is responsible for all of the attitude determination and does this autonomously. Approach could therefore be unsuccessful through e.g. disturbances. The tug would not be able to dock to the satellite package. Hence, approach failure would be catastrophic. The probability of this event occurring is unlikely. It is a relatively new concept of determining a object in space. However, the orbital express by DARPA [77] has shown proof of concept.
- **DOC-3:** As the package is treated as an uncooperative satellite, it has no ability to control its attitude. This could become a risk due to possible heavy angular velocities after separation. Failure would be catastrophic, as the tug would not be able to dock to the satellite package which means the mission is a failure. Heavy angular velocities will then make it impossible to dock. Since this has happened in the past, this is considered a possible risk.
- **DOC-4:** After the insertion of the probe in the drogue, the probe deploys itself in order to lock. As this is done through a specific mechanism, there is a possibility that interlocking the mating systems could fail, resulting in no locking at all. The impact will be high because not being locked will have catastrophic consequences for the mission: the module package cannot be moved to different orbits. Though this is unlikely to happen, there is always the possibility of failure. The locking system will be a mission-specific design, thus the risk of failure is higher. Also, this system will be used frequently, which increases the probability of failure. It is therefore considered unlikely.
- **OPR-1:** The launch operations could fail before the corresponding payload, a module package, reaches space. This would lead to a catastrophic mission as the modules are not delivered. With the two launchers which were considered most, the Falcon Heavy and Ariane 5, the probability of failure is unlikely.
- **OPR-2:** The final stage of the launch vehicle may fail to release its package correctly once in space. Due to this, the module will not be acquired and this will impact the mission catastrophically. Probability is considered highly unlikely since this event is considered less likely than conventional launch failure and this risk is associated with a simpler release system.
- **OPR-3:** Assembly, integration and verification procedures could take longer than initially planned, certainly when considering testing procedures. When delayed, this could lead to missing the required orbit phase for a manoeuvre to GEO. Therefore, this will have an impact though not considered substantial (as the delay will most likely comprise a handful of days). As testing is hard to estimate and prone to delays, this risk is considered likely.
- **PLO-1:** A transmit receive path of the satellite may become unavailable, resulting in loss of coverage for the respective spot covered by that unit. Loss of one of the many transponder units (up to several of hundreds) causes partial loss in global coverage. Depending on the spot size, this might have a harsh impact on the mission. However, the area usually covered is only a small fraction of the whole mission. The combination of these considerations sets the impact level of this event to substantial. The Static Spot Module would have to be replaced. Classic transponder technology is at a very high level of design maturity. It is a proven, quite simple and reliable system. Failure can however still occur in the hostile environment that is space.
- **PLO-2:** An LD-Antenna may become damaged or fail to deploy. This causes a severe loss in mission coverage, as each LDA supports a large number of spot beams. Assuming a 4 dish configuration, single failure would cause a coverage loss of 25%, borderlining on mission failure. Again, full module would likely have to be replaced. By the time of mission implementation, the LDA system is going to be at TRL8, pending successful integration into operational space missions. The risk of failure persists as it will be one of the first actual space deployments.
- **PLO-3:** The Gimbal of the steerable beams could fail, locking it in position. Spot beam coverage is an important part of the mission, as less spots are available when compared to the static coverage, but individual failure weighs more. Mission success is still not severely hindered, as spot modules are singular and replacement of this system is more "efficient" when compared to the above. Failure is

again unlikely as maturity is quite high and existing systems are very reliable, usually being designed for very high lifetime without replacement.

- **PLO-4:** The Interface between the Communication payload and the rest of the satellite does not close successfully. Similar to the above: in the worst case scenario one of the static modules may remain unpowered and non-functional, causing a substantial, possibly critical impact on mission success. Intensive testing has already been performed on the interface that has been selected. Successful connection in space is highly likely, however risks persist in integrating with a robotic arm assembly system.
- **PRJ-1:** For designing the first tug, an initial budget will be considered for both time and financial resources. This will result in a delay of the deployment of the AIV system and therefore its operations. In addition, Airbus is considered to have sufficient resources to maintain any necessary excesses in this project in terms of financial resources. Moreover, considering the project is designed for the longer term, time delays are not deemed critical. Through sufficient planning, this is considered a possible risk. Since the deadline has already been extended from the first phase of the project, this is deemed sufficient.
- **PRJ-2:** For redesign, an additional budget will be made and this could be exceeded. Since limited budgeting has been done for this activity, it is considered likely that this would occur. However, since the budget of the redesign is already considered a small component, the effects are estimated to be significantly less than PRJ-1.
- **PRJ-3:** A budget has been made for the cost of operations. These costs, however, are dependent on alterations in design which are made over the coming period. The impact will mean a larger cost for Airbus until improved. This will not impact the mission's functionality itself though. Considering that the current design phase is far from being realised, it is considered probable that this will occur.
- **PROP-1:** During any stage of the mission, (parts of the) the chemical propulsion engine could fail. Failure would be catastrophic, as the tug would not be able to travel to GTO- and GEO-. Therefore, the mission would fail. The reliability of LOX/LH2 engines is determined to be 80% at its first flight. [2]
- **PROP-2:** The electric propulsion is a less established technology and therefore it could fail during the orbit raising or the de-orbiting at end of life. Failure of the thruster will be catastrophic when it is still in GEO- as it can not reach GEO where it will operate. Once it is in GEO, the engine will maintain its orbit. Therefore it will be catastrophic on the long term. The probability of electric propulsion systems to fail is higher than chemical propulsion systems due to the less-proven technologies present in the system.
- **PROP-3:** Due to more degradation than expected, the available power will not be enough for the electric propulsion system to work on the telecommunication satellites. The impact is substantial as the electric propulsion system can be throttled down to use less power. However, the efficiency will decrease as well and therefore, the required propellant will increase. The probability of this is unlikely, since the degradation can be calculated quite accurately. However, sometimes unpredicted solar flares can occur.
- **PROP-4:** Space debris might damage the fuel tank due to its size. The impact of space debris hitting depends on the size of the debris. If the space debris is big enough it can rupture the fuel tank. Consequently, the liquid oxygen or liquid hydrogen will leak out and the cold liquid will freeze the whole satellite or tug. Moreover, the engine will stop working. The probability of this collision occurring at substantial levels is unlikely.
- **PROP-5:** Parts of the fuel tank or propulsion system could leak fuel or oxidizer. The engine will then stop working and therefore the mission will fail. It is unlikely that the pipes in the propulsion system or the fuel tank will leak, as they are produced by experienced manufacturers.
- **PWR-1:** During deployment of the solar arrays the systems responsible such as linear actuator, joints, hooks or connectors malfunction causing the solar to either unfold partially or not at all. Failure to deploy the solar cell leads to a significant loss in power output. The impact is not always catastrophic: Intelsat IS-19 which lost 25% of its power generation due to malfunctioning deployment, remained operational. A specific deployment mechanism failed three times on three separate satellites between 2004 and 2012 due to a manufacturing defect. Therefore, this is considered probable. [25]
- **PWR-2:** Solar cells may be punctured by small space debris, classified as debris smaller than 1mm. Impact into the cells will cause one cell or a series of cells to stop functioning, which reduces power output of the entire system. However, the entirety of the mission is not compromised. Only the usage of power will have to be re-evaluated. Several studies show the probability of losing a satellite due to a collision is in the order of magnitude of 5%. [14]
- **PWR-3:** The solar array could be punctured by medium and large space debris, which is classified as

debris larger than 1 mm and 10 cm respectively. Impact into the array could dismember the entire solar array and significantly cripple the available power to the critical subsystem required to continue the mission such as disrupting the center of gravity, causing the ADCS to fail and the satellite to lose control. Collisions among large objects are very seldom, taking place every 5 to 8 years depending on the models. [14]

- **PWR-4:** During the active mission of the satellite, batteries may begin discharging gases uncontrollably which causes fire or an explosion. Explosions or fires would have a severe impact on the mission. Current lithium-ion batteries for space have never been observed to break up in flight, but they may well explode if thermally, electrically or mechanically abused. [1]
- **RBA-1:** The base link for the arm attachment to the tug (which controls the roll of the arm) may fail. This would seriously hinder the angles reachable by the tug. The only factors which affect this would be those outside of human control (such as micrometeorites and other space debris). Substandard manufacturing of lubricant etc. for the joint is also possible but less likely. Therefore, this risk is considered unlikely.
- **RBA-2:** One of the joints along the arm, allowing pitch, may fail. Since one angle is already constrained, which means that there is one angle for redundancy which could be moved. This might limit accessibility slightly, depending on the joint (especially last joint in the robotic arm). Similar to RBA-1, this is most likely caused by space debris and is therefore considered an unlikely risk.
- **RBA-3:** Due to errors in modelling and simulations, the expected performance concerning the movement of packages from one location to another occurs slower and differently. This could seriously hinder the lifetime and performance of the robotic arm. Robotic arms are quite plentiful in orbit currently, meaning that there exists a lot of actual data concerning performance wherein the computer models and simulations can be verified and later on validated.
- **RBA-4:** One of the links which the arm comprises may snap, hereby fully incapacitating the robotic arm. If the robotic arm cannot be used, the tug's function will be heavily reduced since working with a reduced number of robotic arms (there will be at least one spare arm) would hinder the function of the tug significantly. This would be caused by space debris or another manoeuvre in which a collision of the robotic arm would cause a link to snap or break. This is considered unlikely.
- **RBA-5:** During launch, the robotic arm breaks or is caused damaged. This may limit the robotic arm's ability to function or result in failure. Since understanding of launch loads etc. is understood at this point in time, the chance that the robotic arm is designed incorrectly for the determined launch loads is small. Consequently, this means that the biggest source would be something incorrect fastening of the robotic arm during launch. This is considered highly unlikely.
- **STRC-1:** Failure could occur of the main support structure (refuel tank) of the payload during launch (where loads are most critical). If this structure fails, the entire package will be destroyed due to launch loads. Therefore, the impact is considered catastrophic. This structure's main function is to withstand launch loads and has thus been designed to do so with an added safety factor. Therefore the probability of this event is considered very unlikely.
- **STRC-2:** The module structure could fail during launch, as this is when it experiences the most critical loads. A structural analysis was done using assumptions to reduce complexity. Though these results have been confirmed it still means there may be errors in the design of the module structures. If a module structure fails, the components it contains may become partially or fully compromised. This results in a subsystem with limited functionality.
- **STRC-3:** Module connection reaction forces could exceed the limits throughout the mission. This is most likely to occur during launch. Due to simplifications in the structural analysis and the low force limit of the module connection, there is a high probability of a module connection failing. If a module connection fails, the module becomes unusable. This will have catastrophic consequences.
- **STRC-4:** Beside launch loads, high impulsive loads (shock loads) could be experienced during deployment or separation, damaging components that are not designed to handle such loads and vibrations. Combining the violent vibrations induced by pyrotechnics and the presence of pyrotechnics in separation bolts aboard the launch vehicles means shock loads are guaranteed and the probability they interfere with components is possible. If modules close to the final stage are not properly structurally protected then shock loads can affect the sensitive electronics. This is considered to have substantial impact.
- **TEM-1:** During operations one or more of the thermal sensors may fail to activate or deactivate the active thermal control component when necessary. Space graded temperature sensors have a high reliability. Occurrence of failure is highly unlikely, and therefore this event is considered highly unlikely. Failure to actively cool or heat a spacecraft component can lead to a decrease in efficiency of that component. In the worst case scenario, it leads to permanent damage of spacecraft components.

- **TEM-2:** One or more faulty thermocouples could be installed on the spacecraft. Thermocouples have a high reliability. Therefore, failure of these components is considered very unlikely. Failure to transfer heat within the spacecraft leads to overheating of spacecraft components. This decreases the efficiency of those components.
- **TEM-3:** During operation, one or more heaters of the spacecraft may fail. Failure to heat the spacecraft when necessary decreases the efficiency of the components. The decrease in temperature can lead to permanent damage of some spacecraft components. Just the sensors and couples, heaters have a high reliability and failure is very unlikely.
- **TEM-4:** One or more radiators may fail during operations, making heat rejection less efficient or impossible. Due to the high reliability of radiators, a failure is considered very unlikely. Failure to eject the excess heat leads to an overheating of the spacecraft. The efficiency of the components will decrease. The rise in temperature can lead to permanent damage of some spacecraft components.
- **TEM-5:** Insulation of one or more modules may fail during the transit to GEO- from GTO-. Insulation is highly unlikely to fail during the transit. It could however be that during the manufacturing the insulation is installed incorrectly. Failure could lead to freezing up of the module with the faulty insulation. Given that no components of the module are in operation freezing of the components does not lead to permanent damage. Once it is in operational stage the active thermal control components can counteract the insulation deficits.

Table 15.1: Risk map prior to mitigation

Consequence	Very unlikely	Unlikely	Probable	Likely	Very likely
Catastrophic	DOC-1 OPR-2 PWR-3 PWR-4 STRC-1	ADCS-3 CMPT-1 CMPT-2 OPR-1 PROP-5 RBA-4 RBA-5	ADCS-4 DOC-2 DOC-3 PROP-1	PROP-2 STRC-3	
Critical		ADCS-2 ADCS-5 DOC-4 PLO-2 PLO-4 RBA-1 STRC-2	PWR-1		CMPT-3
Substantial	ADCS-1 PLO-1 PROP-4	PLO-3 PROP-3 RBA-2 RBA-3	PWR-2		
Marginal	TEM-1 TEM-2 TEM-3 TEM-4		PRJ-1 PRJ-3 STRC-4 TEM-5	OPR-3	
Negligible				PRJ-2	

Table 15.2: Risks and assessment prior to mitigation

Code	Event description	Probability	Impact
ADCS-1	Star tracker failure	1	3
ADCS-2	Sun sensor failure	2	4
ADCS-3	Gyrometer failure	2	5
ADCS-4	Thruster failure	3	5
ADCS-5	Reaction wheel failure	2	4
CMPT-1	Command & Data Handling unit failure (RUAG SMU)	2	5
CMPT-2	On-board Computer failure (CREOLE ASIC)	2	5
CMPT-3	Sudden loss of power	5	4
DOC-1	Docking probe failure	1	5
DOC-2	Approach failure	3	5
DOC-3	Heavy rotation	3	5
DOC-4	Mechanism inter-locking failure	2	4
OPR-1	Launch Failure	2	5
OPR-2	Release Failure	1	5
OPR-3	AIV delays	4	2
PLO-1	Failure of Transponder Unit	1	3
PLO-2	Failure of LD-Antenna	2	4
PLO-3	Gimbal Failure	2	3
PLO-4	Attachement Failure	2	4
PRJ-1	Exceed preliminary R&D budget	3	2
PRJ-2	Exceed redesign budget	4	1
PRJ-3	Exceed operations budget	3	2
PROP-1	Chemical propulsion engine failure	3	5
PROP-2	Electric propulsion engine failure	4	5
PROP-3	Power shortage for propulsion	2	3
PROP-4	Fuel tank damage	1	3
PROP-5	Fuel leakage	2	5
PWR-1	Unfolding failure of solar panels	3	4
PWR-2	Small space debris collision with solar array	3	3
PWR-3	Medium or large space debris collision with solar array	1	5
PWR-4	Battery explosion during lifetime	1	5
RBA-1	Roll Joint failure	2	4
RBA-2	Pitch Joint failure	2	3
RBA-3	Significant difference in expected performance	2	3
RBA-4	Link breaking	2	5
RBA-5	Failure during launch	2	5
STRC-1	Supporting structure failure due to launch loads	1	5
STRC-2	Module structure failure due to launch loads	2	4
STRC-3	Module connection failure due to launch loads	4	5
STRC-4	Module damage due to shock loads	3	2
TEM-1	Temperature Sensor Failure	1	2
TEM-2	Thermocouple failure during operation	1	2
TEM-3	Heater failure during operation	1	2
TEM-4	Radiator failure during operation	1	2
TEM-5	Insulation failure during transit	3	2

15.2. Risk Mitigation

For each risk identified in the previous section, mitigation has been considered and actively incorporated in the final design. The mitigation and updates risk map are presented accordingly.

- **ADCS-1:** For mitigation, additional star trackers are accounted for in the design, making the previous star trackers redundant. Consequently, the impact of a star tracker failure will decrease to negligible.
- **ADCS-2:** Extra sun sensors are accounted for in the design for mitigation, making the initial number of sun sensors redundant. Impact of a failure will therefore comprise negligible effects.
- **ADCS-3:** The new design accounts for extra gyrometers. This renders the previous gyrometers as

redundant and decreases failure impact.

- **ADCS-4:** Extra thrusters are added for redundancy. Consequently, the impact of a thruster failure is set to decline. As this impact was already considered higher than the above, the new impact is considered marginal.
- **ADCS-5:** Similar to the mitigation above, reaction wheels will be added to the final design for redundancy. This will decrease the impact of ADCS-5 to marginal, similar to thruster failure.
- **CMPT-1:** It is foreseen a second CDH unit would be necessary for the satellite to work. For redundancy three CDH units are integrated in the final design. This mitigates the impact of failure. [93]
- **CMPT-2:** The on-board computer budget is increased so it can be manufactured by a well-established, reliable space company. The particular module will have its features (interfaces, buses, outputs/inputs, etc.) built in twice for redundancy. [94]
- **CMPT-3:** In order to cope with loss of connection, the on-board Computer has its built-in mass storage expanded to 2x374 Gb to store all data until the connection is restored.
- **DOC-1:** In order to reduce the impact, two fully redundant robotic arms have been incorporated in the design. The second arm could hold the module package (without a docking probe) in place. Though this will impact assembly time, it will also mitigate catastrophic consequences.
- **DOC-2:** To reduce the impact of a failed approach is chosen to use the berthing mechanism. As the robotic arm will help with the mating, this decreases the probability of failure.
- **DOC-3:** The only way to reduce the heavy rotation is by adding ADCS. However, that would increase complexity largely as power is also needed then. Therefore is chosen to stay docked to the final stage of the LV, dock with the tug to the package and then separate from the final stage.
- **DOC-4:** To reduce the impact, another robotic arm is integrated in the final design which can hold docking targets in place, as discussed in DOC-2.
- **OPR-1:** Launch failures cannot be mitigated. For future mitigation, the AIV modules could be launched with safer launch vehicles once these become available.
- **OPR-2:** Similar to failures in OPR-1, release failures cannot be mitigated in terms of launch vehicles. Moreover, considering the low probability, no consequence is considered necessary.
- **OPR-3:** For AIV, preliminary planning will be scheduled and optimised throughout the course of the orders which are realised. Though functions such as testing may still be hard to predict, the probability of such errors should decrease once planning can be improved. New probability: 3.
- **PLO-1:** Current transponders have high reliability and shielding. Extra attention is paid to providing the safest possible environment to the equipment by adding additional shielding the payload bay and sizing the environmental/thermal control system with significant safety margins. Fully cross-strapped redundancy is implemented to avoid single points of failure and re-route failed connections where possible.
- **PLO-2:** The antenna is already extensively tested on Earth. Possibilities for mitigation include single item space-test before launching the full system, reducing probability of failure. Additionally the robot arms of the TUG are able to assist in case of possible deployment issues. In case of failure, the impact remains the same.
- **PLO-3:** In addition to design maturity of implemented systems, the gimbal is made more robust by adding launch supports to reduce the chance of damage and adding redundancy (e.g. the gimbal implements a fully redundant set of motors to remain functional after single component failure).
- **PLO-4:** The robot arm observes the connection, reducing the chance of damaging connectors in fully pre-programmed assembly. Also, each module is equipped with several fully cross-strapped attachment points for increased throughput and redundancy
- **PRJ-1:** As a too short deadline has already been mitigated in previous phases, mitigation has already been accounted for and no further changes are deemed necessary.
- **PRJ-2:** With effective contingency management, the probability of exceeding redesign budgets will be less likely.
- **PRJ-3:** Financial analysis will be conducted in more detail when more detail is added to the mission. In addition, through effective contingency management, the chance of overshooting the budget will be limited.
- **PROP-1:** Flight proven engines will be used for the mission. That will make the probability of failure decrease to less than 2% after 13 flights. [2]
- **PROP-2:** Two redundant engines are added to the satellite. This means that there is a redundant engine per engine.
- **PROP-3:** The electric propulsion system is chosen in such a way that the highest specific impulse is below the available power. Therefore, the impact will decrease.
- **PROP-4:** An extra structural mass of 10% is added to the fuel tanks that make the impact of space

debris hitting it decrease.

- **PROP-5:** The fuel tank will be filled on the ground to check for leaking parts. Therefore, the probability will decrease.
- **PWR-1:** If a mechanical interface, such as a lug, is integrated into the solar array with which the robot arm can assist in unfolding in case the solar array fails to unfold autonomously then the impact of a solar array failing to unfold autonomously is reduced. The probability of malfunction decreases because the solar panels are connected to their final position using the robot arm meaning the final unfolding procedure requires one single axis rotation by means of hinges. This greatly simplifies the local solar array deployment system, therefore also decreasing the probability of failure which is associated with complex conventional unfolding systems.
- **PWR-2:** Installing bypass diodes allows the current in solar arrays to bypass shaded cells (which are essentially damaged cells) in order to avoid voltage losses that would otherwise be the cause for decrease in power output.
- **PWR-3:** This risk cannot be mitigated, though the chance of such a collision is extremely small.
- **PWR-4:** Enough separation will be installed between batteries so that one faulty battery does not affect its neighbour and heat sinks will be installed. For batteries connected in parallel which are at particular risk during thermal runaway, fuses are installed that trigger at the sign of increased temperatures. Lastly, a chimney or path for potential spewing gases to escape needs to be installed to relieve pressure. With these safety procedures, the probability of batteries exploding does not change but the impact of an explosion is mitigated by isolating a faulty cell therefore preventing catastrophic explosions.
- **RBA-1:** The joint will be extra reinforced. Additionally, the roll angle can then be compensated by the tug's own ADCS system. This would shorten and impact lifetime, but functionality should be somewhat comparable.
- **RBA-2:** Since one pitch joint is constrained, the robotic arm's design would incorporate the capability to rotate this joint. This means that some functionality might be limited, dependent on which pitch joint is affected, however this would not completely immobilise the robotic arm.
- **RBA-3:** Significant and extensive computer models must be verified and validated. Furthermore, once the tug is in orbit, the performance of the robotic arms should be monitored for a period of time with different arm configurations and load mass. This will then indicate early on any excessive wear on the moving components of the arm. This would then lead to alterations of the software for the arm to counterbalance this and prevent excessive wear.
- **RBA-4:** For mitigation, several methods should be combined. Firstly, the links should be designed with sufficient safety factors meaning that some impact would be manageable without failure. Secondly, verification and validation of the collision detection will be conducted extensively. Lastly, multiple arms should be used, at a minimum of two, resulting in redundancy.
- **RBA-5:** Significant time will be spent on accurately simulating launch conditions, allowing for designing the payload structure to account for these loads. This is aided with a abundant real world data on which models can be verified and validated. Additionally, two robotic arms are present for redundancy.
- **STRC-1:** This risk is already mitigated using a safety factor in design.
- **STRC-2:** Modules will be split up and will be made partially redundant. This lowers the impact of this risk significantly.
- **STRC-3:** The failure of the module connection in the lateral direction is most likely due to it only being able to resist 400 N compared to the 6000 N axially. To mitigate this risk each module connection on the support beams will have a female pin connection and on the module side a male connection. This will lower the probability of this risk occurring. Also the heavier modules will be connected using multiple module connections to reduce both impact and probability. Lastly, modules will be stacked on each other to transfer loads downward through the launch vehicle.
- **STRC-4:** The probability of inducing high shock loads is decreased by eliminating the use of pyrotechnics to separate with the final stage. Separation is instead performed with the help of the the tug which will activate the connectors holding the spent final stage and slowly eject it from the payload assembly.
- **TEM-1:** The number of temperature sensors is increased to make the temperature detection a highly redundant - the impact of a failure is therefore decreased.
- **TEM-2:** To mitigate this, the usage of thermocouples is reduced and the system is designed with each module individually thermally controlled.
- **TEM-3:** The number of heaters is increased for redundancy. The result of this is therefore a decreased impact of heater failure

- **TEM-4:** For sufficient redundancy, extra radiators will be accounted for in the final design. Radiators are furthermore controlled by louvers, which determine the amount of excess heat ejected.
- **TEM-5:** Thorough thermal vacuum testing prior to launch will be conducted. Insulation faults will be detected on ground and can be mitigated by reworking the insulation, therefore decreasing the probability of this occurring in space.

Table 15.3: Risks and assessment after mitigation

Code	Event description	Probability	Impact
ADCS-1	Star tracker failure	1	1
ADCS-2	Sun sensor failure	2	1
ADCS-3	Gyrometer failure	2	1
ADCS-4	Thruster failure	3	2
ADCS-5	Reaction wheel failure	2	2
CMPT-1	Command & Data Handling unit failure (RUAG SMU)	2	3
CMPT-2	On-board Computer failure (CREOLE ASIC)	1	5
CMPT-3	Sudden loss of power	5	2
DOC-1	Docking probe failure	1	3
DOC-2	Approach failure	2	5
DOC-3	Heavy rotation	1	5
DOC-4	Mechanism inter-locking failure	1	3
OPR-1	Launch Failure	2	5
OPR-2	Release Failure	1	5
OPR-3	AIV delays	3	2
PLO-1	Failure of Transponder Unit	1	2
PLO-2	Failure of LD-Antenna	1	4
PLO-3	Gimbal Failure	1	2
PLO-4	Attachement Failure	1	1
PRJ-1	Exceed preliminary R&D budget	3	2
PRJ-2	Exceed redesign budget	3	1
PRJ-3	Exceed operations budget	2	2
PROP-1	Chemical propulsion engine failure	1	5
PROP-2	Electric propulsion engine failure	4	1
PROP-3	Power shortage for propulsion	2	1
PROP-4	Fuel tank damage	1	2
PROP-5	Fuel leakage	1	5
PWR-1	Unfolding failure of solar panels	2	2
PWR-2	Small space debris collision with solar array	3	2
PWR-3	Medium or large space debris collision with solar array	1	5
PWR-4	Battery explosion during lifetime	1	4
RBA-1	Roll Joint failure	2	3
RBA-2	Pitch Joint failure	2	2
RBA-3	Significant difference in expected performance	2	2
RBA-4	Link breaking	1	3
RBA-5	Failure during launch	1	4
STRC-1	Supporting structure failure due to launch loads	1	5
STRC-2	Module structure failure due to launch loads	2	2
STRC-3	Module connection failure due to launch loads	2	3
STRC-4	Module damage due to shock loads	2	2
TEM-1	Temperature Sensor Failure	1	1
TEM-2	Thermocouple failure during operation	1	1
TEM-3	Heater failure during operation	1	1
TEM-4	Radiator failure during operation	1	2
TEM-5	Insulation failure during transit	1	2

15.3. Conclusion

In conclusion, the team has conducted an elaborate risk assessment on system and sub-system level. Herein, risks have been identified per subsystem. Subsequently, these risk have been mitigated, leading to substan-

Consequence	Very unlikely	Unlikely	Probable	Likely	Very Likely		
Catastrophic	CMPT-2 DOC-3 OPR-2 PROP-1 PROP-5 PWR-3 STRC-1	DOC-2 OPR-1					
	Critical	PLO-2 PWR-4 RBA-5					
		Substantial	DOC-1 DOC-4 RBA-4	CMPT-1 RBA-1 STRC-3			
			Marginal		ADCS-5 PRJ-3 PWR-1 RBA-2 RBA-3 STRC-2 STRC-4	ADCS-4 OPR-3 PRJ-1 PWR-2	CMPT-3
	Negligible			ADCS-1 PLO-4 PROP-3 TEM-1 TEM-2 TEM-3	ADCS-2 ADCS-3	PRJ-2	PROP-2

tial design changes, which increased the cost and weight of Project MANTIS . Though not each risk could be mitigated, the risk map post-mitigation illustrates acceptable risk for (all subsystems of) the project.

Reliability, Availability, Maintainability and Safety

This chapter deals with the operational characteristics of the system in terms of Reliability, Availability, Maintainability and Safety (RAMS). To start off, a short overview of the meaning of these terms [74] will be given, followed by a discussion of their application to Project MANTIS.

Reliability

"The probability of a system performing in a satisfactory manner for a defined period of time when used under specified operating conditions."

When applied to the system at hand, there are several factors playing into this attribute. A detailed analysis of technical risks has previously been performed in chapter 15, including mitigation strategies to minimise likelihood and impact of possible failure. Overall system reliability was improved significantly by considering redundancy and additional protection of existing systems, though it has had an increasing effect on mass and cost.

For Redundancy GEO missions usually employ fully cross-strapped redundancy for all mission critical components as part of their lifetime and location considerations [58]. Thus, this has been implemented into the current design, making it possible to re-route functional flows that would otherwise be blocked by a single point of failure, adding robustness to the system and improving its reliability even in the face of possible partial failure. This single chain avoidance is shown in fig. 16.1.

The tug itself is a relatively new idea, and as such has not successfully been proven to be reliable yet. Fault tolerance is taken into account as a main focus, as the system is per design going to operate without supervision for extended periods of time, far away from possible human intervention. Special attention is paid to the mission critical components, which in this case consist of the TT&C Link, the assembly mechanism and the main propulsion and ADCS units. Sufficient power generation is taken into account.

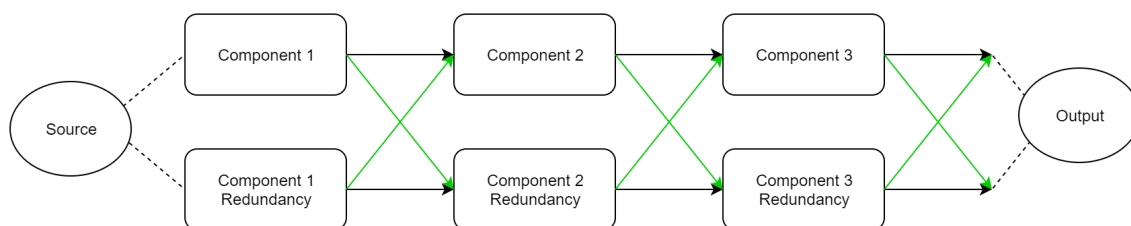


Figure 16.1: Visual representation of full cross-strapped redundancy

Availability

"The degree to which, percentage, or probability that a system will be ready or available when use is required."

As the up-time of the communication satellite is supposed to be 100% after commission of the system, the availability that is being designed for should at least approach this desired value. Current missions have availability figures of 99.9%, coming as close to the desired 24/7 availability as possible. To be competitive, the created satellite is designed to reach and if possible exceed these market standards, also being able to be repaired quickly.

This parameter is highly dependent on the further design of the mission planning after the initial design stage, which has yet to be clarified. However, it can be said that in the end, availability shall be high enough that satellites for GEO can be put into their designated slot within a year from being ordered at the customer

department.

Maintainability

"The ease, accuracy, safety, and economy in the performance of maintenance actions."

For space systems that are not man-rated, maintenance is usually not a focus of the design in so far that the system is design to operate maintenance free. Whilst the system is to maintain in operational state for it's entire lifetime, physical interaction with the product is limited to pre-launch activities and the possibility of replacing failed components with the space-tug. Plans for carrying out these activities will have to be made in later design stages, where the downtime of the satellite due to failure, amongst other impacts, has to be considered in the planning of maintenance activities.

Safety

"The freedom from hazards to human and equipment."

The system itself does not pose a major safety hazard to anyone once stationed in GEO, assuming it is functioning nominally and remains safely within the limits of its assigned slot. Safety risks remain during the launch phase, and the fact that additional objects are put into orbit, that have to be taken into account for collision avoidance. As the system is designed to carry several connectable components, they could create a debris cluster instead of a single out of control satellite. The procedure of burn-up in the atmosphere, depending on the final design of both tug and constructed satellite might pose additional safety hazards, but these are all comparable to existing systems.

Overall it can be said that all the previously mentioned and discussed aspects of the system design are related according to the scheme shown in fig. 16.2. Reliability and Maintainability are characteristics that are inherent to the design of the system, whereas Availability can be seen as a result of their combination. Safety may and generally does drive the amount of Reliability to be implemented in the design. Maintainability has a direct impact on safety, but as no direct maintenance of the tug system is part of the concept, this is a minor contribution. It has however be considered when taking into account the possibility of upgrading or re paring constructed satellites and possibly cleaning up uncooperative targets from graveyard orbit.

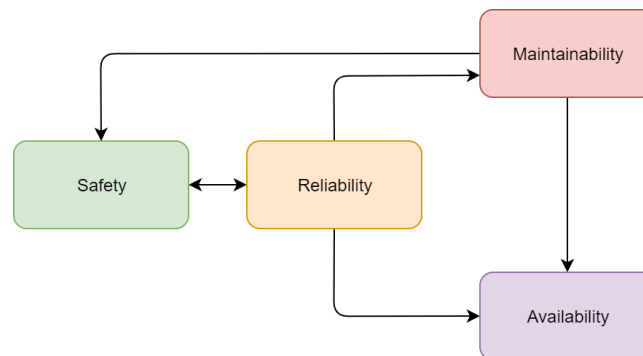


Figure 16.2: The RAMS relation

Compliance Matrix

This chapter will check, by means of a compliance matrix, if the previously postulated requirements are fulfilled by the system design. The compliance matrix can be seen in table 17.1. Requirements that are not satisfied because the solution space changed, or they will be researched in a later stage will have an explanation in the reference column. Subsystem requirements have been covered in their respective chapters. Therefore, only the top level requirements are displayed in the following table.

Table 17.1: Compliance Matrix

Requirement Identifier	Requirement	Compliance	Reference/Explanation
Legal			
CONS-PM-LEG-T1	The AIV shall be following the International Space Law.	✓	[67]
CONS-PM-LEG-T2	The mission shall obey European law.	✓	[67]
CONS-PM-LEG-T3	The production shall obey the respective production country's laws.	✗	Analysis: Investigated at a later stage
Cost			
CONS-PM-CO-T1	The spacecraft shall not cost more than \$240M.	✓	Chapter 23
Schedule			
CONS-PM-SCHE-T1	Space-borne architecture construction shall start in 2028.	✓	Chapter 20
CONS-PM-SCHE-T2	First operation of space-borne architecture shall begin in 2032.	✓	Chapter 20
CONS-PM-SCHE-T3	Once in operation, the system shall assemble a new satellite within one year.	✓	Chapter 20
Stakeholder Deliverables			
CONS-PM-STA-T1	The design study shall incorporate a profitable business plan.	✓	Chapter 18
CONS-PM-STA-T2	The final design shall incorporate a cost assessment.	✓	Chapter 18
CONS-PM-STA-T3	The final design shall incorporate a risk assessment.	✓	Chapter 15
CONS-PM-STA-T4	The design study shall incorporate an operations plan which details further concepts for the system's end-of-life strategy.	✓	Chapter 20
CONS-PM-STA-T5	AIV design shall integrate Airbus' IKEA-Sat Idea.	✓	Section 13.2
CONS-PM-STA-T6	AIV design shall be technically feasible.	✓	Chapter 14
Reliability and safety			
CONS-ENG-RESA-T1	Safety shall be considered in the trade-off process.	✓	Safety was considered as part of Mission Risk: Chapter 15 and Chapter 16
CONS-ENG-RESA-T2	Reliability shall be considered in the trade-off process.	✓	Reliability was considered as part of Mission Risk: Chapter 15 and Chapter 16
CONS-ENG-RESA-T3	The IKEASPACE system shall have a minimum success rate of 95% after 3 years of use on a new or serviced satellite.	✗	Demonstrated when IKEASPACE is in operations.
CONS-ENG-RESA-T4	The launcher used shall have a minimum launch success rate of 94%.	✓	[96]
Sustainability			
CONS-ENG-SUS-T1	Sustainability shall be integrated in the design trade-off process.	✓	Section 19.4, Chapter 3
CONS-ENG-SUS-T2	The product shall ensure that applicable systems adhere to the internationally recognised ISO 140001 certification for energy management systems.	✓	Section 19.4
CONS-ENG-SUS-T3	The product shall ensure applicable systems implement an energy management system based on the ISO 5001 standard.	✓	Section 19.4

Table 17.1 continued from previous page

Requirement Identifier	Requirement	Compliance	Reference/Explanation
CONS-ENG-SUS-T4	The use of at least TRL5 items shall be considered first for use in the design.	✓	Chapter 7, Section 11.2, Section 14.3.4, Chapter 6, Chapter 5, Chapter 9, Chapter 8
CONS-ENG-SUS-T5	The product shall have a sustainability factor higher than 50.	✓	Section 19.4
Engineering Budgets			
CONS-ENG-ENBU-T1	The maximum mass of the AIV system shall be 9364 kg.	✓	Section 13.5
CONS-ENG-ENBU-T2	The maximum power use of the AIV system shall be 22600 W.	✓	Section 13.5
CONS-ENG-ENBU-T3	The maximum payload volume during launch will be <<TBD>>m ³ .	✗	Fairing restrictions dictate the size. See: TECH-LAU-T1
CONS-ENG-ENBU-T4	The maximum number of recurring (resupply) launches shall be <<TBD>>.	✗	Number depends on orders of satellites
CONS-ENG-ENBU-T5	The maximum number of non-recurring (for initial build) launches shall be 4.	✓	Chapter 20 Concept Changed
CONS-ENG-ENBU-T6	The data storage shall have 360 Gb size.	✓	Chapter 8
CONS-ENG-ENBU-T7	The on-board processing shall be 300 Mb/s.	✓	Chapter 8
CONS-ENG-ENBU-T8	The minimum SNR at the ground receiver shall be 8 dB.	✓	Section 5.3
CONS-ENG-ENBU-T9	The minimum SNR at the space receiver shall be 8 dB.	✓	Section 5.3
Production			
TECH-PROD-T1	The production cost of one satellite shall be below \$300M.	✓	Chapter 23
TECH-PROD-T2	Only sustainable production techniques shall be used.	✓	Section 19.4
TECH-PROD-T3	At least 15% of the energy usage for manufacturing will be green energy.	✓	Chapter 19
TECH-PROD-T4	The sub-assemblies shall be able to be transported to the launch site.	✓	Chapter 20
Launch			
TECH-LAU-T1	The AIV system shall physically fit into the selected launcher.	✓	Chapter 13
TECH-LAU-T2	The selected launcher shall be available 1 times per year.	✓	[29]
TECH-LAU-T3	The selected launcher shall be able to bring the S/C to GTO-Orbit.	✓	[29]
TECH-LAU-T4	The selected launcher shall have a reliability of 94%.	✓	[96]
AIV-Client Modules			
TECH-AIV-MOD-T1	The modules shall communicate with the AIV system.	✓	Chapter 11
TECH-AIV-MOD-T2	The modules shall make use of a standardised link.	✓	Chapter 11
TECH-AIV-MOD-T3	The modules shall communicate with each other.	✓	Chapter 11
TECH-AIV-MOD-T4	The modules shall be mechanically coupled.	✓	Chapter 11
TECH-AIV-MOD-T5	The modules shall be electrically coupled.	✓	Chapter 11
TECH-AIV-MOD-T6	The modules shall be thermally coupled.	✗	Modules are individually controlled, however module connection is capable of coupling. see Chapter 11

Table 17.1 continued from previous page

Requirement Identifier	Requirement	Compliance	Reference/Explanation
TECH-AIV-MOD-T7	The modules shall connect the data bus.	✓	Chapter 11
TECH-AIV-MOD-T8	The modules shall verify whether the links are correctly connected.	✓	Chapter 11
TECH-AIV-MOD-T9	The modules shall be packageable in a condensed way so that the modularity proves to have an advantage over traditional launch-configurations.	✓	Chapter 11
TECH-AIV-MOD-T10	The modules shall be able to be assembled in 48 hours time.	✓	See TECH-AIV-ASM-T5
TECH-AIV-MOD-T11	The modules shall be coupled fluidly.	✗	No fuel fluid lines used
TECH-AIV-MOD-T12	The modules shall be replaceable / upgradable.	✓	Chapter 4
AIV-Assembly system			
TECH-AIV-ASM-T1	The AIV system shall communicate with the modules.	✓	Chapter 13
TECH-AIV-ASM-T2	The AIV system shall assemble different modules.	✓	Section 14.3
TECH-AIV-ASM-T3	The assembled modules shall be verified by the AIV.	✓	Chapter 22
TECH-AIV-ASM-T4	The AIV systems shall reconfigure assembled modules.	✓	Section 14.3
TECH-AIV-ASM-T5	The AIV systems shall assemble the modules in less than 48 hours.	✓	Section 14.3.2

Market Analysis

To assess the market in which Project MANTIS is positioned, an analysis has been conducted. Herein, an overview is given for the market, key concepts and trends are discussed, the market is sized, and the key stakeholders are discussed. Subsequently, the fit with Airbus Defence & Space is discussed. This chapter is then concluded and the design drivers which result from this analysis are discussed.

18.1. At a Glance

Over the previous decade, the space economy has registered significant growth, currently positioning itself as one of the most lucrative industries globally. During 2012-2017, the number of satellites in orbit increased from 994 to 1,459. This number is expected to increase exponentially over the coming years. Moreover, the global space economy is forecast to exceed \$1 trillion by 2040 according to Morgan Stanley [12, 57].

The space economy offers aerospace companies strong growth potential in the coming decades, though the market is characterised by high entry barriers through significant investments and longer-term contracts. In addition, many suppliers are driven toward end-to-end value chain coverage to create value. Currently holding a leading position in the space market, Airbus Defence & Space is therefore positioned excellently to reap the fruits of its continuous investments in space technology.

18.2. Market Concepts & Trends

The global space economy has been driven by the rapid commercialisation and technological advancement. With the global space economy estimated at approximately \$360 billion in 2018, three quarters of this revenue is generated by commercial business [9].

Key trends in the market are [87]:

- **Expanded demand:** Multiple drivers such as the expansion of emerging markets and the additional capacity required for connectivity, internet of things and 5G have increased the demand for earth orbiting satellites.
- **New business models:** Due to new business models, the commercial value of space has increased significantly. In addition, the space sector has seen vertical integration with major players such as Airbus D&S driving consolidation in the market. Through integration, these companies have more control over the components of the value chain. Consequently, companies can achieve higher operational efficiency by doing so.
- **Reduced costs:** Technological advancements such as increased satellite constellation capacity, declining launch costs and smaller solutions (e.g. Cubesats) have lowered the entry barriers into the space market. Consequently, this enables new business models.
- **Increased risk appetite:** Defence companies have shifted in terms of risk appetite (toward that of tech companies). The shift has occurred from long-term returns on large investments to shorter-term projects with rapid renewal.

18.3. Market Sizing

For a clear assessment of the market in which the MANTIS project should operate, the global market and target market have been sized accordingly in sections 18.3.1 and 18.3.2 respectively.

18.3.1. Global Market

The global space economy is currently valued at \$360b, and is set to grow at a Compound Annual Growth Rate (CAGR) of 5.6% to a value of \$558bn in 2026. From the \$360bn space economy, approximately \$277bn

corresponds to the global satellite industry. In terms of size, the global satellite has registered gradual growth, increasing from \$246bn to \$277bn gradually in 2014-2018, as seen in fig. 18.1.

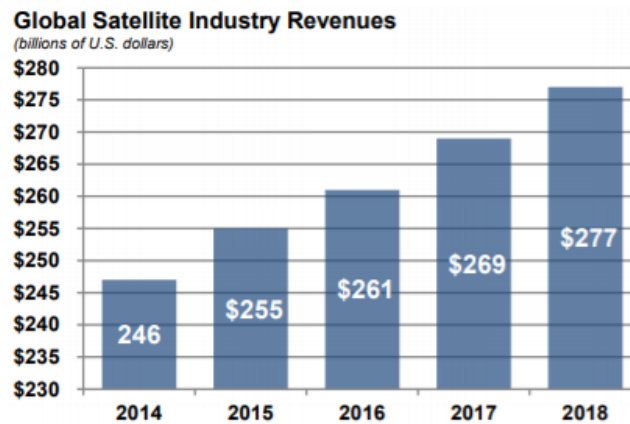


Figure 18.1: Global satellite industry revenues [9].

Herein, the industry is segmented in four key components [9]:

- **Satellite services (\$126.5bn):** the largest segment of the satellite industry; Services include telecommunications, remote sensing, space science and national security. Most of these revenues are accrued in the telecom business (e.g. television \$94.2bn, fixed \$17.9bn, radio \$5.8bn).
- **Ground equipment (\$125.2bn):** mainly includes GNSS Equipment (\$93.3bn), along with consumer equipment (\$18.1bn) and network equipment (\$13.8bn). 2017-2018, growth was mainly realised in the GNSS and network equipment segments.
- **Launch industry (\$6.2bn):** registered 34% growth in revenues with a record number of launches globally.
- **Satellite manufacturing (\$19.5bn):** registered 26% growth in terms of revenue 2017-2018. Herein, the majority of \$11.5bn is accountable to US orders.

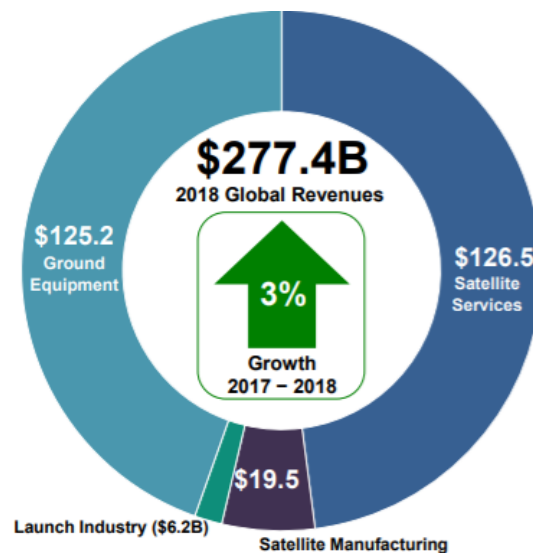


Figure 18.2: 2018 global revenues [9].

In terms of number of orders, Euroconsult forecasts an estimated 330 satellites per year to be built and launched with a mass larger than 50 kg during 2018-2027, representing a total of 3,300 satellites and a total value of \$284bn. Herein, most satellites are forecast to operate in LEO and MEO, approximately 2,300 satellites. Although GEO orbit seems less attractive due to the lower number of satellites being launched to this orbit, similar reports also note that the majority of LEO and MEO satellites will be small satellites (c.1,800 of the 2,300), mainly due to OneWeb, with a significantly lower value per satellite than those in GEO [20, 86].

18.3.2. Target Market

Airbus D&S has requested an AIV system for the development of GEO telecommunication satellites. Therefore, GEO telecommunication orders have become the main target market, and a market with significant importance toward the MANTIS project. Commercial GEO satellite orders have decreased drastically in 2009-2015 (from 39 to 17 orders) as shown in fig. 18.3, and executives of Airbus and Thales Alenia Space predict 10 to 18 GEO satellites to be ordered annually in the next years [49, 50].

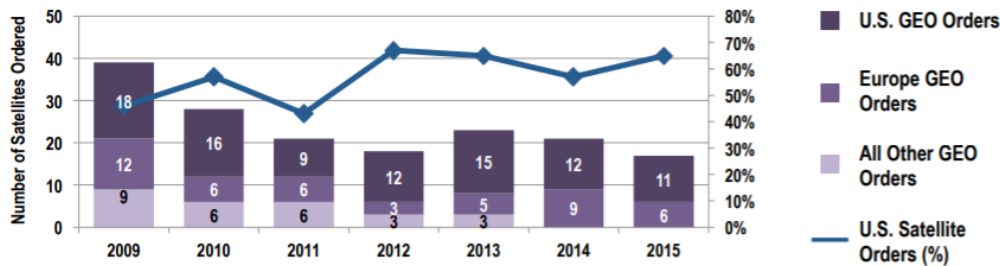


Figure 18.3: Commercial satellite manufacturing orders [9].

While commercial GEO order in 2018-2017 are in total valued at approximately \$40bn (for 140 satellites), an additional 210 satellites are projected to be manufactured and launched to GEO in 2018-2027, comprising approximately \$60bn.

From correspondence with the client, the target quantity of orders to process was set at approximately 3 per year. Considering Airbus' market share and the projected number of satellite orders, this is considered an achievable goal on the relatively shorter term. However, a relatively low number of orders on the longer term is considered a substantial business risk, and this will be accounted for in the design of the project.

18.4. Stakeholder Analysis

Within the space economy wherein Project MANTIS will operate, there are several key stakeholders which will constrain and drive different aspects of the design process. All essential stakeholders have been elaborated on below.

18.4.1. Shareholders & Investors

Arguably the most important stakeholders for Airbus are its shareholders and investors. As of 30 September 2019, the three key shareholders of Airbus are SOGEP (11%, French State), GZBV (11%, German State) and SEPI (4%, Spanish State). The remaining 74% of the shares are free float [5]. Additionally, Airbus holds billions of Euro's in long-term financing liabilities, mainly from debt investors [4]. Consequently, the majority of Airbus' financing is dependent on an for-profit investor base. Therefore, it is of high importance for Airbus to maintain its profitability and thus keep investing in profitable projects. Hence, to fit Airbus' strategy, the MANTIS project should provide Airbus with a profitable business case which contributes to the company's profitability.

18.4.2. Commercial Clients

One of the primary stakeholders on which Airbus is reliant, is its commercial customer base. This comprises the clients which order the GEO telecommunication satellites from Airbus which Project MANTIS aims to supply. Since this is a commercial stakeholder, it is of high importance to create value for these stakeholder. This could mainly be achieved by offering financially attractive solutions.

18.4.3. Governments

Besides commercial customers, the majority of GEO orders projected over the coming decade (c.60%) are non-commercial orders, largely driven by defence budgets. Thus, (quasi)governmental bodies will remain a

key stakeholder and customer for Airbus. In contrast to commercial clients, some governments (e.g. France, Spain and Germany) are also prominent shareholders in Airbus. Lastly, governments play a crucial role in determining relevant legislation. In conclusion, governments have a large impact on Airbus in various ways [20, 87].

18.4.4. Competitors

The competitive landscape of the space industry determines Airbus' success. In addition, new technology such as the MANTIS project will cause disruption, therefore altering the playing field in which Airbus is positioned. A handful of large players in the market offer full-service solutions, comprising e.g. manufacturing, launch, and ground services. More specifically, satellite manufacturing is dominated by some large companies in the US, Europe and Japan. Herein, key players are Airbus D&S, Lockheed Martin, Boeing, MELCO, SSL, OHB SE and Thales Alenia Space. Though information is limited, Airbus was forecast to hold a sizable 11% of the market share 2015-2019 in terms of manufacturing value, as shown in fig. 18.5. Considering that the project focuses on GEO satellite assembly, one should also consider the competitive landscape of GEO satellite manufacturing. As shown in fig. 18.6, Airbus D&S places itself as a leading satellite manufacturer.

To maintain its market position, it is of the essence for Airbus to keep innovating its product and service portfolio and to keep providing superior services. A SWOT-analysis has been conducted to emphasise Airbus' position in the market with respect to Project MANTIS.

Strengths	Weaknesses
<ul style="list-style-type: none"> - Globally leading position in space industry - End-to-end value chain coverage - Possible cross-sell and up-sell of assembly service - Capabilities to invest in R&D 	<ul style="list-style-type: none"> - No prior AIV designs developed by Airbus - Limited manpower in Airbus Innovation team
Opportunities	Threats
<ul style="list-style-type: none"> - Significant growth projected in space industry - First-mover advantage - Cost savings through efficiency gain 	<ul style="list-style-type: none"> - Competition could limit Airbus' GEO telecom orders - High market dependency on governmental budgets - LEO telecom solutions could drastically decrease GEO telecom satellite demand

Figure 18.4: SWOT analysis.

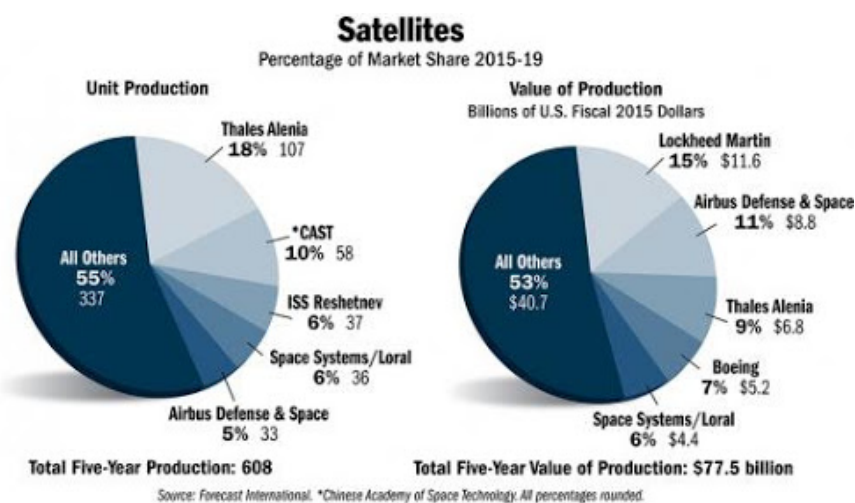


Figure 18.5: Value of production [105]

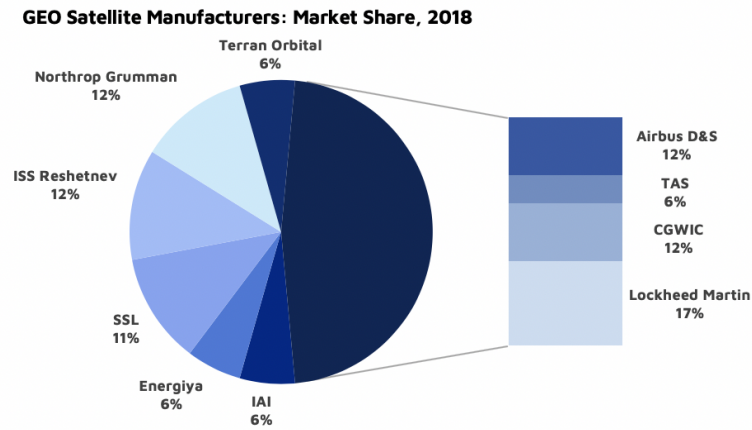


Figure 18.6: GEO satellite manufacturers: market share 2018 [81].

18.4.5. Other Stakeholders

In addition to the previously mentioned stakeholders, Airbus states its duties toward additional stakeholders in the annual report [4]. These groups, however, will have less of a direct impact on the Project MANTIS design than the previously mentioned stakeholders.

- **Employees:** Large aerospace companies such as Airbus will typically deal with a large number of employees. Therefore, such a company is tasked to manage these stakeholders correctly. This entails providing employees with sufficient benefits and development opportunities, to continuously attract talent.
- **Suppliers:** Airbus and its suppliers are dependent on each other. To benefit from each other, it is important that suppliers are dealt fairly with.
- **Society:** Finally, numerous communities can be affected by the activities of Airbus. It is therefore important to guarantee a sustainable approach to business.

18.5. Strategic Fit with Airbus Defence & Space

Airbus has established a clear growth strategy of strengthening core products and expanding its services business. The company states its key priorities for the D&S division in 2019 are the development for new businesses and accelerated deployment of digital solutions, focused on digital manufacturing among others. With Airbus's focus on strengthening its end-to-end solution, the AIV suits the company's portfolio excellently. Airbus can cross-sell and up-sell this service with its current offering and therefore provide integrated and modern solutions to its clients. Strategically, Airbus must continuously invest in R&D to maintain its leading market position. From the company's 3.2bn 2018 R&D expense, the company confirms its investments in future technology [4]. Consequently, Airbus is a good fit due to its end-to-end value chain coverage and capabilities to invest in sufficient R&D.

18.6. Conclusion & Design Drivers

In conclusion, the space industry is a promising business through several trends. Airbus is positioned excellently to take advantage of the market's potential. With a focus on GEO telecommunication satellites, Project MANTIS provides Airbus with a promising business case. However, all stakeholders should be considered extensively during design and the decline in commercial GEO orders over the previous years warrants inspection.

Therefore, Project MANTIS is designed to provide a broad range of services in a versatile manner. The project is made to offer additional services (e.g. clearing space debris, repair) and is not limited to a certain orbit. Therefore, MANTIS ensures numerous opportunities if no AIV is necessary. Finally, Project MANTIS is tailored toward the client strategy and creates value for numerous stakeholders of Airbus Defence & Space.

Sustainable Development Strategy

This chapter addresses the sustainability of this project. It will give an overview of the vision on sustainability which will be followed in this project. The strategy which is used to incorporate this vision is discussed. The main focus of this chapter is the assessment of the strategy.

19.1. Vision

Earth's climate has been changing for 13.8 billion years. This as can be observed in fig. 19.1, a large increasing trend in global temperature. Moreover, a large rise of atmospheric carbon dioxide, a loss of 127 billion tons of ice per year, an increase of 30 % in the acidity of the surface ocean waters, and more is observed [80].

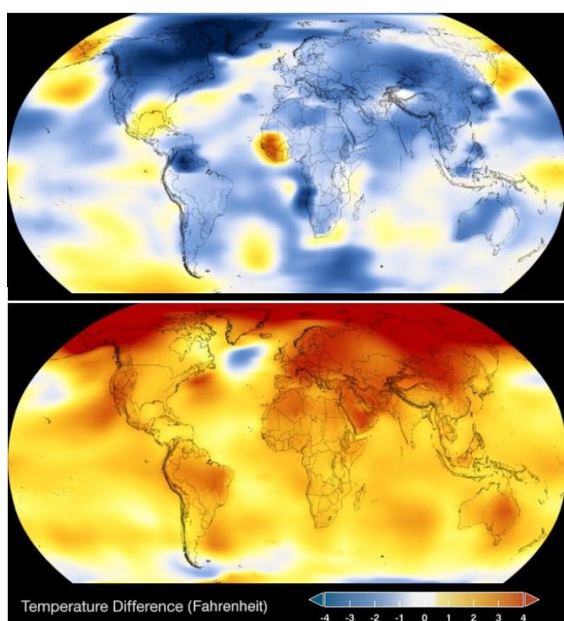


Figure 19.1: Change in global temperature from 1800 - 2018

These effects, in such large quantities in such short time span, have never been captured before. Evidence has shown (with an accuracy of higher than 95%) that these effects are caused by human activity. But, not only on our planet, also around our planet, humans are polluting. Currently is the amount of space debris estimated to be higher than 8000 tons which can be seen in fig. 19.2. This shows that now, more than ever, sustainability is imperative for the survival of the human race.

The philosophy incorporated in this project will consist of the three sustainability pillars: Environmental, Social and Economic. All of them should be represented in order to have a sustainable design. To make a project fully sustainable, it is necessary to incorporate sustainability on every level. During the design phase, the manufacturing, testing, ground control and end-of-life. Only then will a design be full sustainable. This vision on sustainability is coequal to the client's view on sustainability [3]. Together, there is strived to a more sustainable future.

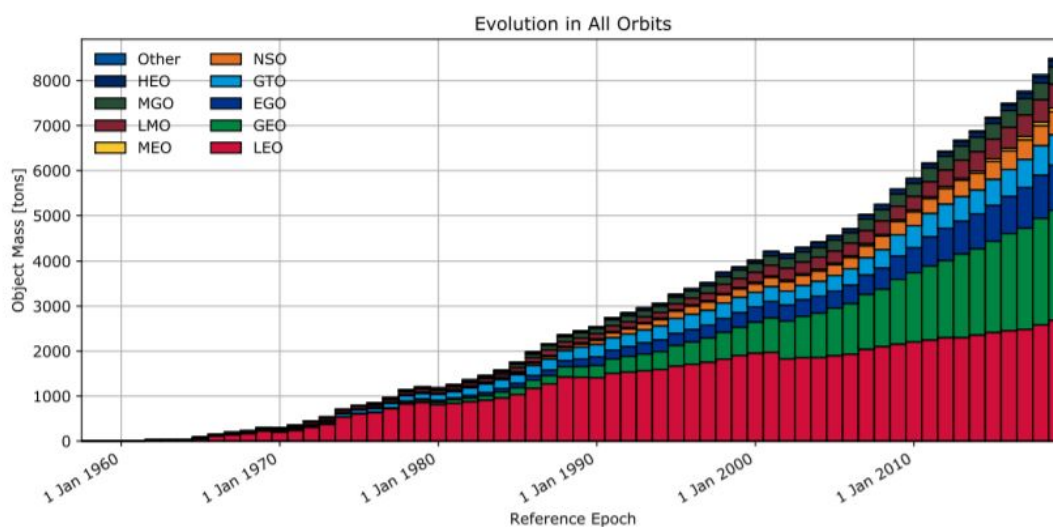


Figure 19.2: EESA estimation of space debris

19.2. Strategy

A vision without a strategy to implement it has no value. Consequently, this section is dedicated to the implementation of the vision discussed in section 19.1. The first step is narrowing the scope. Sustainability is a very broad topic, narrowing the scope is a necessity. To narrow the scope in a structural manner is the sustainability split up into two parts: the spacecraft which consist of the tug, telecom satellite and the launcher. For each will the three pillars will be considered. Each pillar is made up of different parameters. What each parameters incorporates can be found in the dotted boxes. An overview of this approach can be found in fig. 19.3.

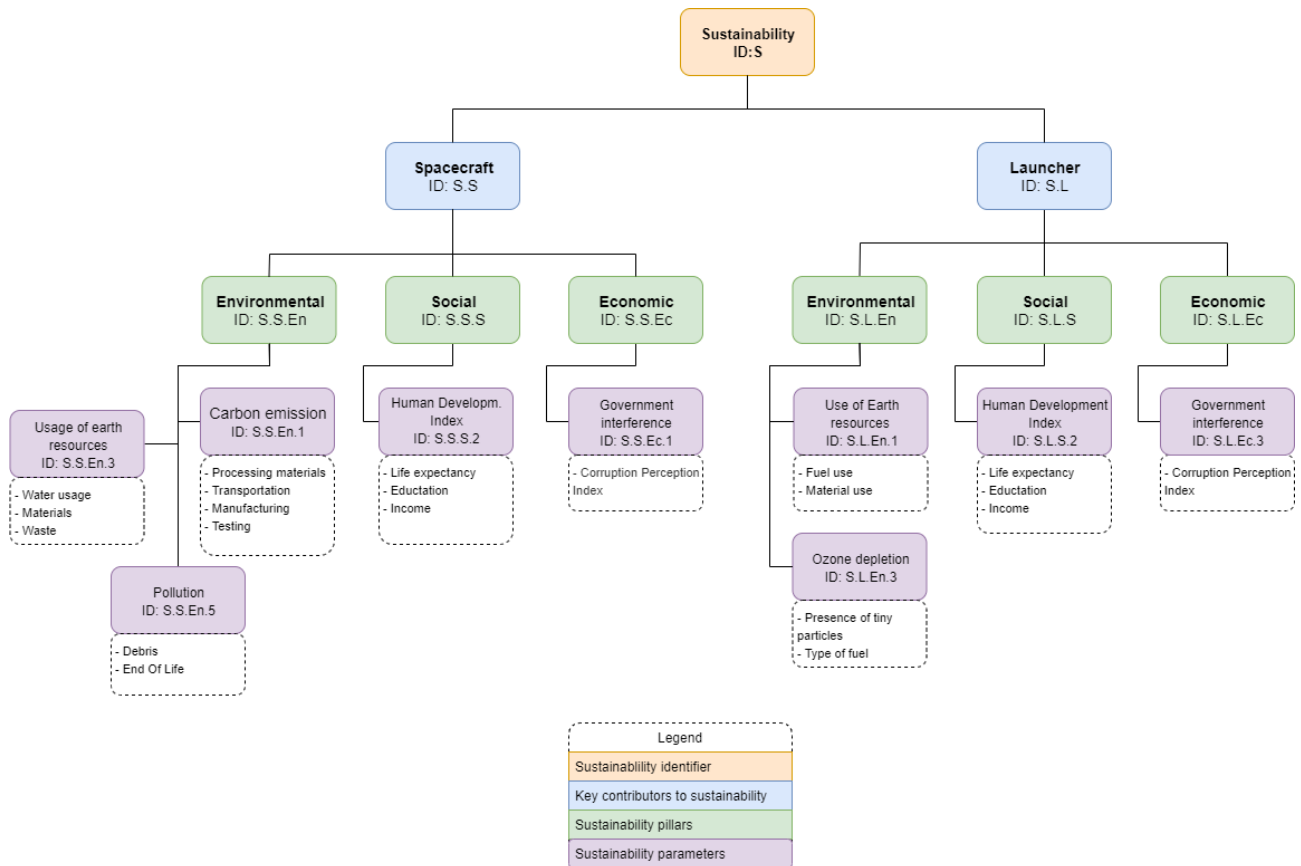


Figure 19.3: Overview sustainability factor

The second step is to quantify all these parameters and put them in a frame of reference. This is done by introducing the Sustainability Factor. This factor shows in percent how much more sustainable this project is than the chosen reference case in terms of the chosen parameters. The sustainability factor can be applied to each level of the flowchart. So the sustainability factor of the ozone depletion can be found, such as the sustainability factor for the spacecraft. The sustainability factor of each level shown in fig. 19.3 consists of the linear combination of the parameters combined with the assigned weights. Applying this for each level will result in the total sustainability factor. This strategy requires a reference case in order to succeed. This reference case should be a telecommunication satellite preferably using electrical propulsion which serves in the Geostationary Orbit and is not older than 5 years. The satellite meeting all these requirements is the Eutelsat 172B. It is a telecommunication satellite launched in 2017 by Airbus Defence and Space from Kourou with the Ariane V [95]. The Eutelsat was launched 3 years ago, which makes it very actual. An extra advantage of choosing the Eutelsat is the fact that the client, Airbus Defence and Space is one of the main designers and manufactures of this satellite [37].

This project is actively incorporating sustainability and will thus aim to show clear and quantified results of this integration. Project MANTIS has the ambition to show the space industry that sustainability is not only vital, but also very feasible, even without lowering the efficiency.

19.3. Assessment

The strategy is set. The resulting part of this section is dedicated to achieving the overall sustainability factor by assessing each parameter.

19.3.1. Spacecrafts

The spacecraft is the first part which is assessed. The spacecraft consist of the modular telecommunication satellite and the space tug. These two will be combined in the assessment. The parameters considered for the environmental are the usage of earth resources and carbon emission. To quantify the social pillar the Human Development Index (HDI) is used. The economic pillar is evaluated using the Corruption Perception Index (CPI) as this index gives an idea of the stability of a country. In order to quantify the aforementioned parameters in a mathematical manner the spacecrafts are divided into different subsystems which can be observed in table 19.1. These subsystems are assigned numbers based on the significance from 1 to 5, 1 being the lowest and 5 being the highest. The significance can be seen as how significant the subsystem is in terms of mass and complexity. Propulsion is assigned a 5 as it requires a considerate amount of fuel, both chemical and electrical. Also the telecommunication will take up a lot of mass as the antenna dishes will be very large. The power system is also very significant as telecommunication satellites have high power requirements.

The next step is to create the same table for the reference case. It is very hard to do it in the exact same fashion as not much information can be found about the different components and manufacturers. Eutelsat does not manufacture the telecommunication satellites themselves. The satellite is manufactured by its subsidiaries: Airbus Defence and Space (Airbus group), Orbital ATK Inc (Northrop Grumman group), Space/Systems Loral (MacDonald Dettwiler and Associates group) and Thales Alenia Space (Thales & Leonardo group) [37]. From these companies is determined where the satellite manufacturing locations are. It is assumed that each of these locations contributed the same amount to the reference case.

Table 19.1: Properties of the Project MANTIS subsystems

<i>Properties</i>	<i>Significance</i>	<i>Manufacturers</i>	<i>Critical Material</i>	<i>Country</i>
ADCS	3	ArianeGroup	Nitrogen	DE
Docking	2	IKEASpace	Aluminium	NL
Thermal Control	4	IKEASpace	Aluminium	NL
Assembly	3	IKEASpace	Carbon Fiber	NL
Propulsion	5	Aerojet rocketdyne/ NASA/ BOC	Xenon	USA/UK/ NL
Telecommunication	5	HPS GmbH/ Tesat/ Airbus	Carbon Fiber	HU/ DE/ NL
Brain	1	RUAG	Copper	CH
Power	5	Azurspace/ Saft	Gallium/lithion	DE/ FR
Structural	5	IKEASpace	Aluminium	NL

Use of Earth Resources

Every machine is made of materials. However, the space industry often uses the most innovative and rare materials which are not sustainable. To quantify this parameter is the abundance of elements in Earth's crust used. First of all, each subsystem given a weight in how much it needs the identified critical material shown in table 19.1. The critical material per subsystem is identified as a combination of rarity and amount. These weights can also be found in table 19.1.

Table 19.2: Abundance materials in Earth's crust [48]

<i>Abundance</i>	<i>Aluminium</i>	<i>Carbon</i>	<i>Copper</i>	<i>Lithium</i>	<i>Nitrogen</i>	<i>Gallium</i>	<i>Xenon</i>
Abundance (ppm)	8.23×10^4	200	60	20	19	19	3×10^{-5}
Abundance (mpp)	0.000012	0.005	0.0167	0.05	0.053	0.053	33 333.33

In order to calculate the use of earth resources eq. (19.1) is used. The total abundance (TA_{sus}) is equal to the amount of material (L_{sus}) times the bottleneck material abundance million per parts (A_{sus}). The values for these parameters can be found in table 19.2. Note that the first row is the abundance in part per million.

However, this is inverted to allow the most rare material have the largest value. With the use of eq. (19.1) a TA_{sus} value of 4065.06 can be found. This value shows how abundant the materials used in Project MANTIS are in Earth's crust.

$$TA_{sus} = \frac{\sum L_{sus_i} \cdot A_{sus_i}}{\sum L_{sus_i}} \quad (19.1)$$

The next step is to perform the same calculation for the reference case. However, not enough information is provided in order to do the exact same analysis. It is known that it will use mostly the same materials such as Xenon, Nitrogen and aluminum as they are both telecom satellites. But, the MANTIS project is replacing some of the telecommunication satellite task by the tug such as transfer to orbit. This tug is used for 7 years. Eventually less material will be used. The reference case will use more lithium and gallium as it is overdesigned to be able to meet the power requirements after degradation. Project MANTIS does not have this issue as components can be replaced eventually by more efficient ones. To calculate the TA value for the reference case the same materials are assumed, but using different weights. The power weight is set to 6 to account for degradation overdesign. The modular telecom satellite is also lighter than the reference case, resulting in less use of Xenon gas for transfer. This weight is set to 5.5. These changes result in a TA factor of 4214.58. This concludes a sustainability factor of 3.55 for this parameter.

Carbon Emission

The last decades, there has been a large rise in carbon dioxide in the atmosphere observed [80]. Therefore it is really important to lower the carbon emissions. To assess the carbon emission of the spacecraft is, to decrease complexity, only the transportation is considered. The following approach is used to determine the carbon emission of the MANTIS. First of all, the country of origin of each part is determined. Consequently the transportation distance is calculated of each component to the Airbus test location in France. An overview can be found in fig. 19.4. The emissions are calculated from those distances. Lastly, the components are shipped to the launch site in Florida. An overview can be found in table 19.3. A value of 100 g carbon emission per ton per km is used for transport by truck and 500 g for transport by plane. [70] These values are scaled to an estimation of each component its weight, resulting in the final column of table 19.3. The sum of these values is equal to 34.05 tons which is the total carbon dioxide emission due to transportation.

Table 19.3: Overview transportation distances and carbon emission for the MANTIS and the reference case

<i>MANTIS</i>	Distance	Mode of Transport	Carbon emission (in kg)
NL - FR	855	Truck	85.500
SW - FR	670	Truck	33.500
HU - FR	1665	Plane	832.500
DE - FR	9102	Truck	455.100
US - FR	7238	Plane	3619.000
UK - FR	1384	Truck	69.200
FR - US	7238	Plane	18095.0
<i>Reference case</i>	Distance	Mode of Transport	Carbon emission (in kg)
US - FR	7055	Plane	3527.50
KO - FR	8960	Plane	4480.0
IT - FR	1299	Truck	129.90
DE - FR	1040	Truck	104.00
CA - FR	5527	Plane	2763.50
FR - GY	7085	Plane	17712.50

The final step in determining the sustainability factor for this parameter is estimating the carbon emission for the reference case. The second part of table 19.3 is used for that. A total mass of 3551 kg is used which needs to be transported to achieve the values [95]. As little data is known, it is assumed that each location contributes the same amount of components. The sum of all the elements in the final column yields 28.71 tons. Thus, the MANTIS has a carbon emission which is 23.84 % lower than the reference case. Therefore, the sustainability factor is 23.84.



Figure 19.4: Map showing manufacture, assembly locations and launch sites for Project MANTIS (yellow) and the reference case (blue)

Pollution

Space debris is becoming a serious problem. Nowadays, more than 500,000 pieces of junk are orbiting our planet [41]. With the amount of space debris rising, so is the probability of collision with spacecraft in operation. The goal of Project MANTIS is to create no space debris. This will be achieved by the following plan.

The telecommunication satellite is sent up in a package together with a large fuel tank. The tug will dock to the package which is still connected to the final stage of the LV. Using its robotic arm, it will transfer the fuel from the fuel tank attached to the LV to its own fuel tank. After refuelling, the package will separate from the launch vehicle. The final stage will then de-orbit itself and burn up in the atmosphere.

The tug and telecommunication satellite both have the resources to de-orbit itself and burn up in the atmosphere at the end of life. The tug is refueled every journey and can therefore easily de-orbit itself. The telecommunication satellite is equipped with an electrical engine. This engine is used to de-orbit itself at end of life. In order to assure burn up, no ceramics or high melting point metals such as titanium are used.

This strategy makes sure that no pieces of junk are left behind by burning them up in the atmosphere. However, nothing actually disappears. It is only broken up into atoms. Not much research has been conducted on this, however, it is very hard to predict into what atoms it is split up and whether these are harmful.

In order to get the sustainability factor for pollution, this needs to be expressed in a percentage of the reference case. To have an accurate representation both the amount of mass which is left in space and the pollution caused by burning up in the atmosphere must be taken in account. Assuming that the pollution of burning the telecom satellite and tug up in the atmosphere is equivalent to leaving 500 kg in space. It means that the Project MANTIS is 610.2 % better than the reference case which is weighting 3551 kg. Resulting in a sustainability factor of 610.2.

HDI and CPI

The social and financial pillars of sustainability are discussed in the following section. In order to quantify these pillars the HDI and Corruption Perception Index (CPI) are considered. To determine these indices the spacecraft are split up into subsystems. Many subsystems are manufactured in different countries and these countries are thus involved in the project. For each country are the indices determined and multiplied by the significance value assigned to each subsystem. An overview is given in table 19.4. The last line shows

the weights for each country based on the significance of the part in the spacecrafts. The significance is determined based on the size and complexity of the components the country provides.

Table 19.4: Overview of HDI and CPI for both the MANTIS and the reference case [7, 68, 82, 101]

<i>MANTIS</i>	DE	NL	USA	UK	HU	FR	CH
HDI	0.939	0.933	0.92	0.92	0.845	0.891	0.946
CPI	80	82	71	80	46	72	85
Weights	4	5	3	3	2	4	2
<i>Reference case</i>	KR	CA	USA	UK	IT	FR	DE
HDI	0.906	0.922	0.92	0.92	0.883	0.891	0.939
CPI	57	81	71	80	52	72	80
Weights	1	1	1	1	1	1	1

Using table 19.4, the total indices can be found. I is the index and W is the weight. For the MANTIS, this yields a value of 0.917 for the HDI and 75 for the CPI. In order to calculate the indices for the reference case is second part of table 19.4 used. Resulting in a HDI of 0.911 and a CPI of 71. That shows that a sustainability factor of 0.59 is found for HDI and 5.33 for CPI. It can be concluded from this that the social and economic pillar are very similar for both cases.

$$TotI_{sus} = \frac{\sum I_{sus_i} \cdot W_{sus_i}}{\sum W_{sus_i}} \quad (19.2)$$

19.3.2. Launcher

A large (unsustainable) part of every space mission is the launcher. It can be compared to flying a Boeing 747 from London to New York, crashing it, only recovering the cockpit and doing this for every flight. This makes non recoverable launchers very unsustainable. For this reason a reusable launcher will be used for Project MANTIS. The Falcon Heavy of SpaceX is chosen. The result of this section will be dedicated to the reasoning why the Falcon Heavy was chosen (from a sustainability perspective) and to achieve the sustainability factor for the launcher.

Earth Resources

The two main parts which are Earth resource intensive are the launcher and the fuel therefore is this section split up in the aforementioned parts.

Launchers are very large machines which thus use a lot of materials, the dry mass of the Falcon heavy and Ariane V are approximated to be 72,300 kg and 80,900 kg respectively [29, 38]. The total recurring payload mass for Project MANTIS is estimated to be 6400 kg, as this is below 8000 kg, it is possible to recover all three boosters of the Falcon heavy. Resulting in only the final stage, which has a mass of approximated 4000 kg, is lost. Conclusively, 80,900 kg is lost for the reference case and only 4000 kg for the MANTIS Project. A falcon booster can be reused 10 times [90]. To have an accurate and correct comparison it is assumed that every flight 10 % of its mass is 'lost', which is equal to 7000 kg. Therefore the weight which is lost during every flight of the Falcon Heavy is estimated to be 11,000 kg.

The second part of this analysis is the fuel. The Falcon Heavy uses 1340800 kg of fuel. The reference cases uses 664900 kg of fuel, almost half of the fuel weight. However both launchers use different fuels. The reference case uses LH2 and the Falcon Heavy uses Rocket Propellant-1 which is highly refined kerosene [29, 38].

The final step is to express the Falcon Heavy use of earth resources in terms of the Ariane V. The values are known for the launcher and the fuel, however they are not in the same order. The launcher consists of complex high strength nozzles, combustion chambers, etc. Using the different weights can be found that the Falcon is 690.36 % better in terms of launcher material usage but 49.59 % worse in the fuel material. The fuel is less earth resources intensive, but is much larger in quantities to take that into account is assumed

that the launcher materials and fuel materials usage has equal importance. This results in a total of being 640.77 % better. And thus a sustainability factor of 640.77.

Ozone Depletion

Launching a large rocket can be responsible for burning 1,000,000 kg of fuel. All of this is burnt and entering the atmosphere. It is therefore important to consider how polluting each launcher is. The reference case is using 480,000 kg of solid propellant and 148,900 kg of liquid hydrogen. The Falcon Heavy is expelling 1,340,800 kg of Rocket Propellant-1 (RP-1) [29, 38]. As the hydrogen is converted into water vapor, it is not considered polluting. The Falcon heavy and reference case are using different fuels, however there can be assumed that they have the same polluting effect. Using the polluting fuel weights mentioned above it is found that the Falcon heavy is 179.33 % worse than the reference case. Resulting in a sustainability factor for this parameter of -179.33.

HDI and CPI

To assess the social and economic pillar are the human development index and corruption perception index used. SpaceX is only designing, testing and manufacturing in the US and is thus considered the only country involved. The reference case uses a Ariane V which is manufactured and operated by Arianespace. This company is involved in France, US, Japan, Singapore and French Guiana. There is assumed that each country has the same contribution to the company and thus the average will be taken for the HDI and CPI. The HDI and CPI for the Falcon Heavy is 0.92 and 71 respectively. Using table 19.5, the indices for the reference case are equal to 0.87 and 69.8 for the HDI and CPI respectively. The Falcon heavy is thus 5.89 % and 1.72 % better than the reference case in terms of HDI and CPI.

Table 19.5: Values for HDI and CPI [8, 68, 101]

Indices	Singapore	Japan	French Guiana
HDI	0.935	0.915	0.67
CPI	85	73	37

19.4. Conclusion

All the sustainability factors are defined. An overview can be found in table 19.6. The weights can be found in the same table. It can be concluded that the current design is 114% more sustainable than a reference case in terms of the parameters found in fig. 19.3 for a telecommunication mission over a few years.

Table 19.6: Overview table of the sustainability factor

<i>Spacecraft (4)</i>	Use of Earth Resources	Carbon Emissions	Pollution	HDI	CPI
Sustainability factor	3.55	23.84	610.2	0.59	5.33
Weight	4	3	5	3	3
Total Spacecraft	175.25				
<i>Launcher (5)</i>	Use of Earth Resources	Ozone Depletion	HDI	CPI	
Sustainability factor	640.77	-179.33	5.89	1.72	
Weight	3	5	3	3	
Total Launcher	74.89				
MANTIS TOTAL	125.07				

This chapter shows that all the requirements are met. As seen before, sustainability an important trade-off criteria. A clear overview was given in the chapter showing all the components. There can be observed that each partner company is doing efforts in order to decrease their emissions, thus complying to the ISO 50001:2018. In order to do so are sustainable manufacturing techniques used. By using green energy to manufacture the components [3].

This chapter has provided a clear overview of the sustainability of the MANTIS Project compared to the Eutelsat 172B mission using predominantly objective and quantifiable data.

Mission Operations

The following chapter explains the mission operations planning for the MANTIS system. The foundation of the missions operations plan is laid out and a detailed diagram representing the operations functions during routine operations of the tug and satellite are presented.

20.1. Mission Operations Planning

Mission Operations Planning (MOP) is vital to successful operations development. It summarises and lays a plan for what the different mission operations consist of, what the various goals of each operations segment is and how they will be accomplished. The final product culminates in a MOP Document that gives a system description, operations overview, staff & training plans (human logistics), phase detailing and procedures for data handling. Given that the MOP is too extensive for the scope of this project, efforts have been made to describe some of the fundamental points mentioned above [58]. It should also be noted that logistics not relating to humans but transportation of goods, such as payload, are usually not included in the missions operation plan. For information on what the country of origin of different modules are and how they are transported to their final destination, section 19.3 should be consulted.

As preliminary step in the mission operations plan, fig. 20.1 was created. The green ovals indicate the top-level operations functions. However, they represent only the tip of the ice-berg for the different roles that typically need to be filled. In addition, given that mission planning and operations is an extremely dynamic process that involves moving personnel between segments and phases, all operations functions are somehow intertwined with all phases of mission. The blue and green triangles therefore indicate that there is a clear distinctions between the satellite and tug, but that they still follow roughly the same operational steps. For example, as the tug is not a re-occurring spacecraft, the personnel responsible for its launch configuration can be re-assigned to a different department. Meanwhile, the team responsible for launching the customers payload needs to prepare the next launch configuration because it assumed there will be another customer waiting in line. For MANTIS there will be some flexibility margins to allow for changes to be made on the fly but most of the staff planning should be outlined in the MOP [58].

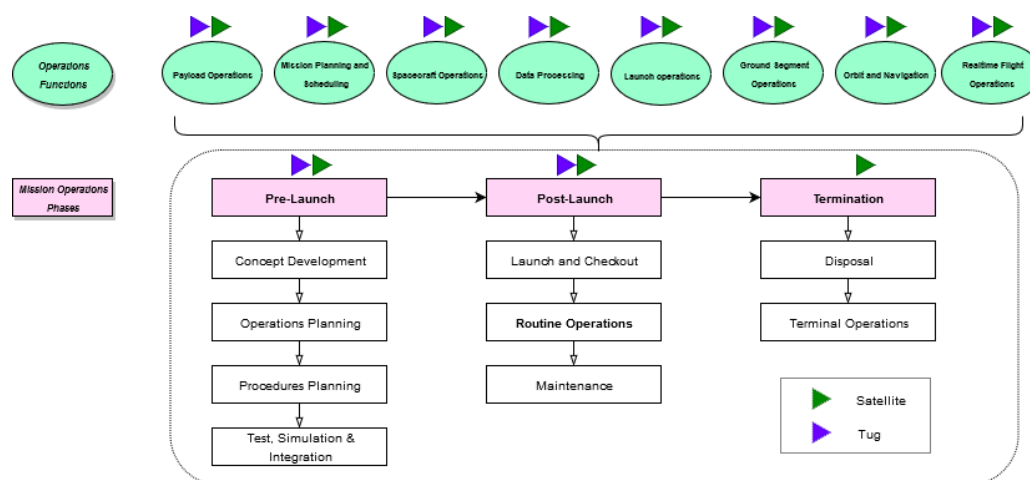


Figure 20.1: Mission operations phases and primary operations functions

Furthermore, the diagram above also shows the three key phases between which major re-shuffling of operations personnel takes place. The phases are: pre-launch, post-launch and termination. Below each are the different operation segments. The vertical order of these segments also roughly symbolises the timeline at which each segment has the most resources invest into it. Resources facilities, time slots, staff and training. For example, before customers satellites can be launched the majority of personnel will be assigned to operations concept development of the tug. This will be followed by the procedure development required for the

tug, then the testing of the data base procedures and so on. In the following section, a detailed description of how one of these segments operates will be discussed.

20.2. Real-Time Routine Operations

In fig. 20.2 a diagram showing the detailed execution of the routine operations is presented. Routine operations is a continuous and dynamic process that is part of the post-launch operations. It was decided to elaborate on routine operations because this is where the MANTIS system is different from conventional space missions. Launch operations themselves for example, are the responsibility of SpaceX and are virtually the same for all space-craft missions. Furthermore, routine operations also happen to be the longest in terms of duration. This make them particularly interesting because the operation functions and personnel tasks need to be efficiently divided and in order to do that the responsibilities need to be identified in detail.

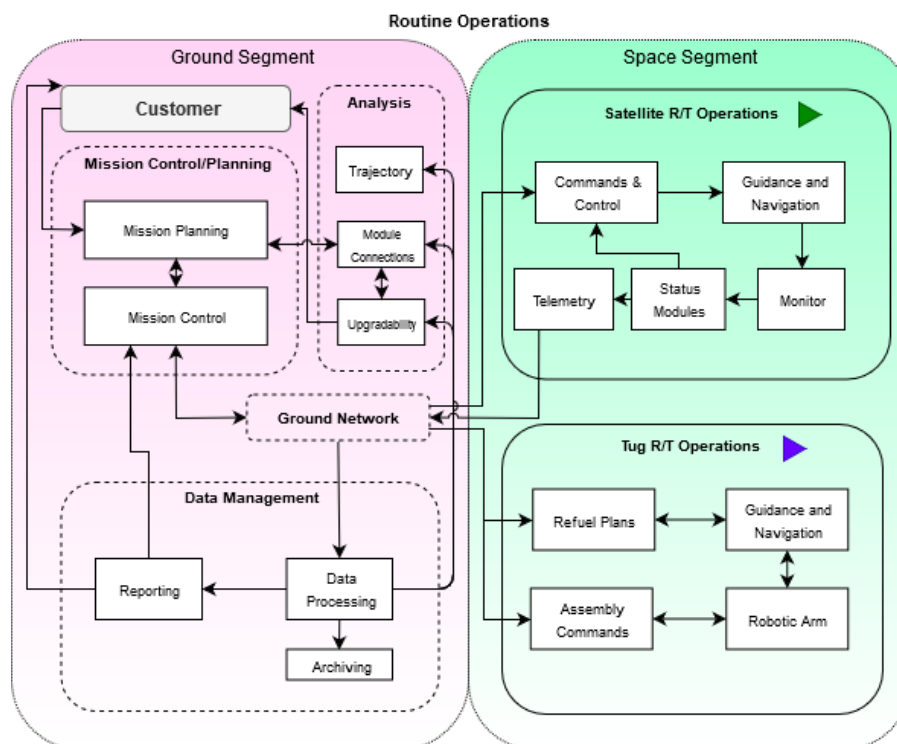


Figure 20.2: Mission operations functions and tasks during routine operations of the Om system

The bold headers of each box represent the sub-operations departments to which operations personnel are assigned. The white boxes represent the tasks and functions for which operations engineers are responsible. The arrows symbolise the flow of information and communication between them. The customer also plays a large role and is involved with potential upgrades and maintenance but is largely separated. The dashed lines of the ground segment indicate that the operational engineers operate similarly for both the tug and the satellite and therefore, when required, can be reassigned to the ground segment tug team. In contrast, the real time operations of the satellite and tug are very different. The filled lines mean that operators are pretty much dedicated to their functions and require specific skills. For example, the tug needs specialists in robotics that can send the correct assembly commands and are consistently busy with that task. On the ground, there is more flexibility. When there is a assembly operation, extra resources can be diverted from analysis to mission planning. Therefore, when the tug is waiting for a new assignment, some of the personnel from mission planning can assist in analysing data from the satellite or analysing the trajectory.

Project Design & Development Logic

In this chapter the project development logic is outlined in section 21.1. The project Gantt Chart is depicted in section 21.2.

21.1. Project Design & Development Logic

This section outlines the Project Design & Development Logic (PD&D) for Project MANTIS. The PD&D shows the logical order of activities to be executed in the post-DSE phases of the project and is shown in fig. 21.1. It starts with the "Detail Design Phase 2" in which the design is improved with the help of models, which are created and tested. Following that the "Development Phase" starts. During this phase the implementation phase is planned in detail. Furthermore all the contracts with the suppliers, subcontractors and the launch company are signed. Lastly clear instructions are given to the personnel. The next phase is the "Implementation Phase" during which the actual construction starts. Once module construction is finished they get tested and verified. Then the "Operational Phase" starts. The mission starts with launching the MANTIS assembly tug. After that the operational readiness of the tug is verified. Once the tug is fully operational the satellite packages are launched to GTO-. Once the modules are in space the assembly and integration starts, while the modules are assembled and integrated. Test data and optical inspection is used to verify correct assembly and integration. After completion of the verification process the satellite transfers to its final mission orbit. The tug goes into energy saving mode and waits for the next satellite package in GEO-. Once the telecommunication mission of the satellite is completed the satellite performs its EOL procedure. For the tug the same holds true. The last phase is the "Follow-up Phase" during which the project results are evaluated and possible improvements for the future are gathered.

21.2. Project Gantt Chart

The project Gantt Chart gives a timely order of the post DSE project tasks. It can be divided into six task categories. They are as follows:

- Organisational Tasks
- Detail Design Modules Tasks
- Detail Design TUG Tasks
- Prototype Tasks
- Production Tasks
- Launch and actual Mission Tasks

The Gantt chart is depicted in fig. 21.2. It provides a timely overview for the next phases of the project.

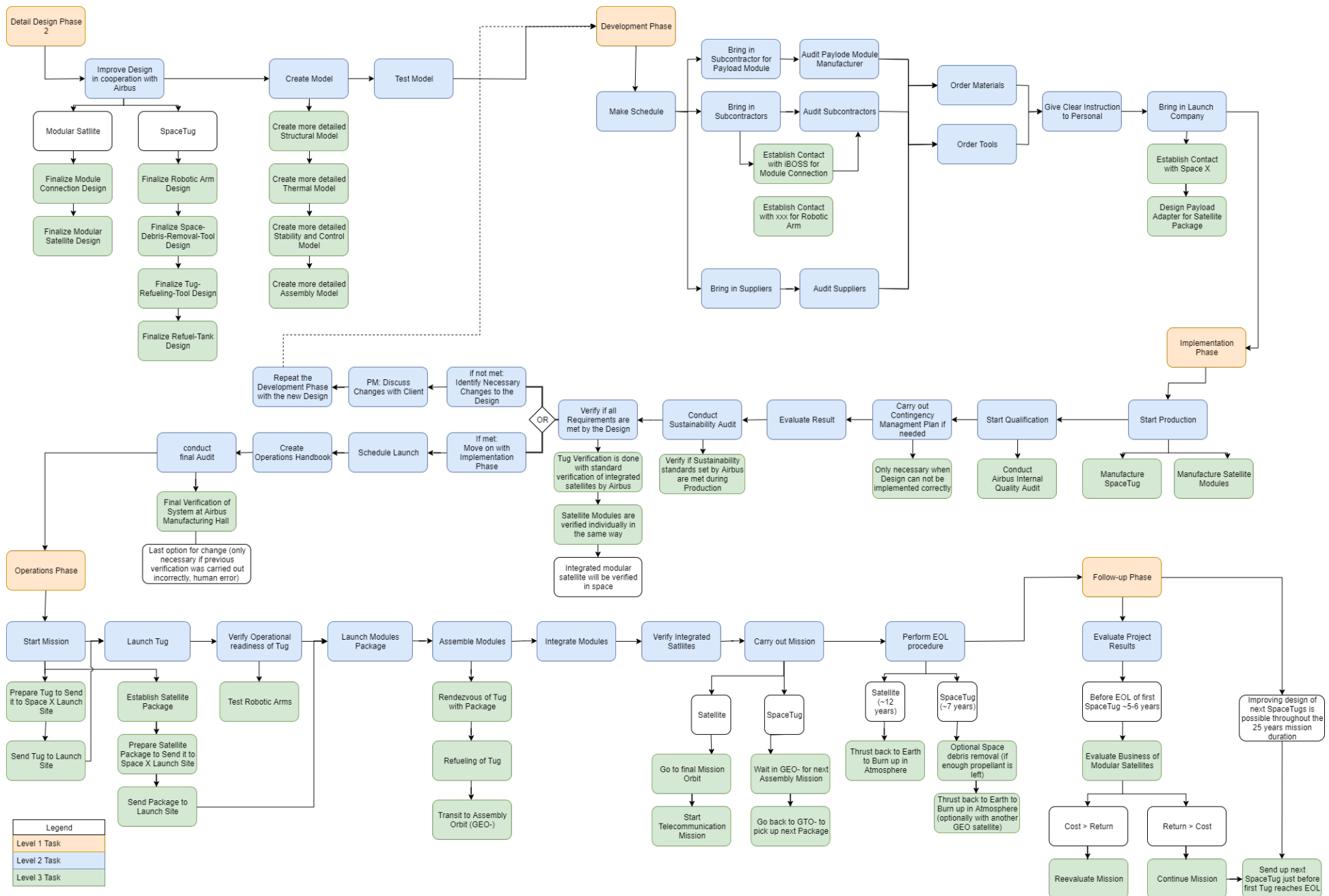


Figure 21.1: Project design & development logic for post DSE

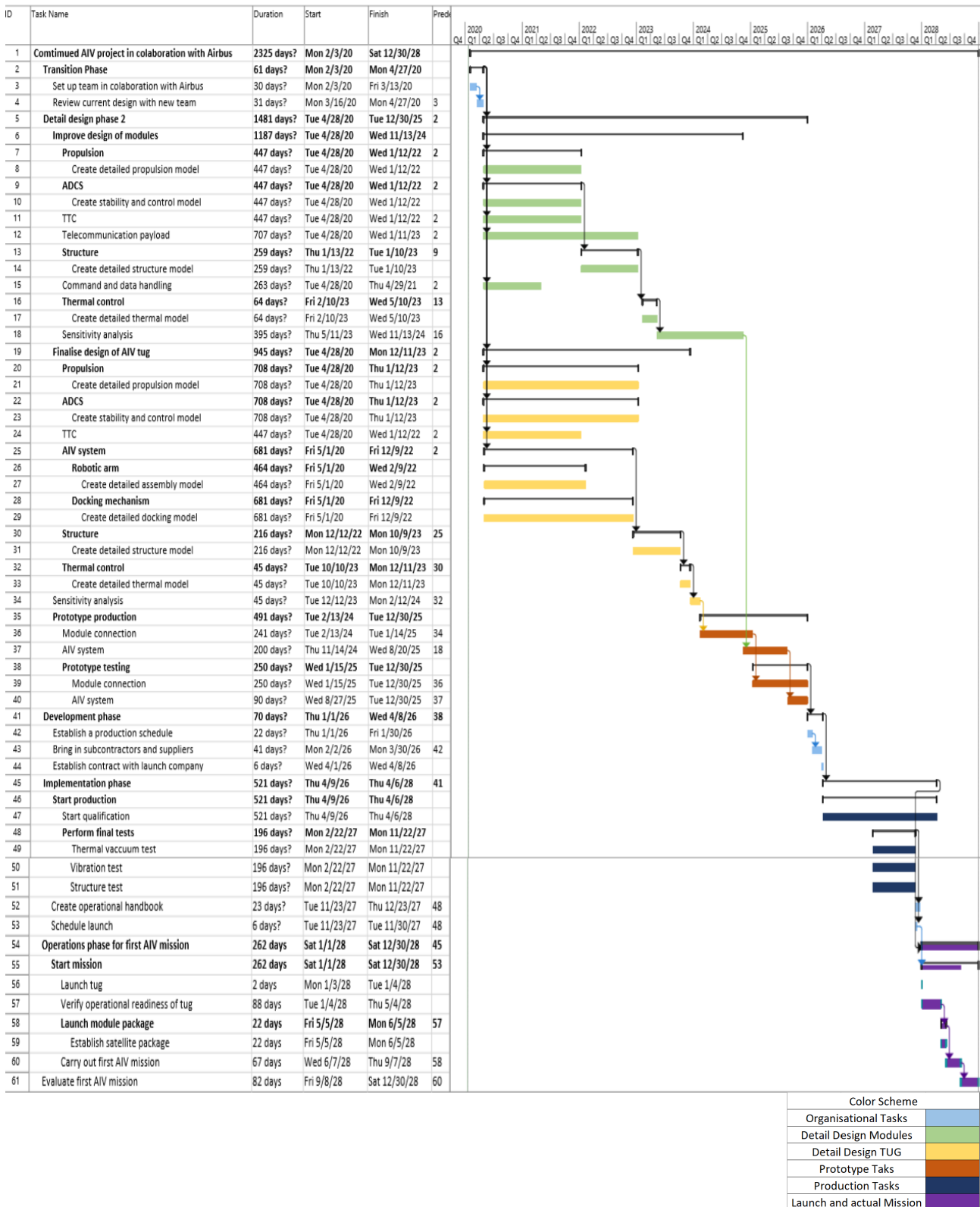


Figure 21.2: Project Gantt Chart

Manufacturing, Assembly, Integration & Validation Plan

A Manufacturing, Assembly, Integration & Validation (MAIV) Plan shows all the steps that need to be undertaken to construct a product, from manufacturing until its final form, in a diagram. In Project MANTIS both the tug as well as the satellite need a complete planning on what subsystems have to be manufactured, assembled and finally integrated and tested with one another to finalise the product. The MAIV plan is a great tool that can visualise all steps elaborately and neatly.

In this particular case, two plans will be created: one for the tug and another for the telecommunication satellite. These will be relevant for every satellite or tug to be produced for Project MANTIS.

Firstly, the MAIV plan for the tug was set up, as shown in fig. 22.1. A top level for the plan is established, which includes all actions to be performed per subsystem. These actions are visualised in yellow. From the top level flow-downs list all the subsystems affected by this action, visualising more detailed work to be done in blue. Next, tests per subsystem are displayed in green that will ensure verification of that particular subsystem.

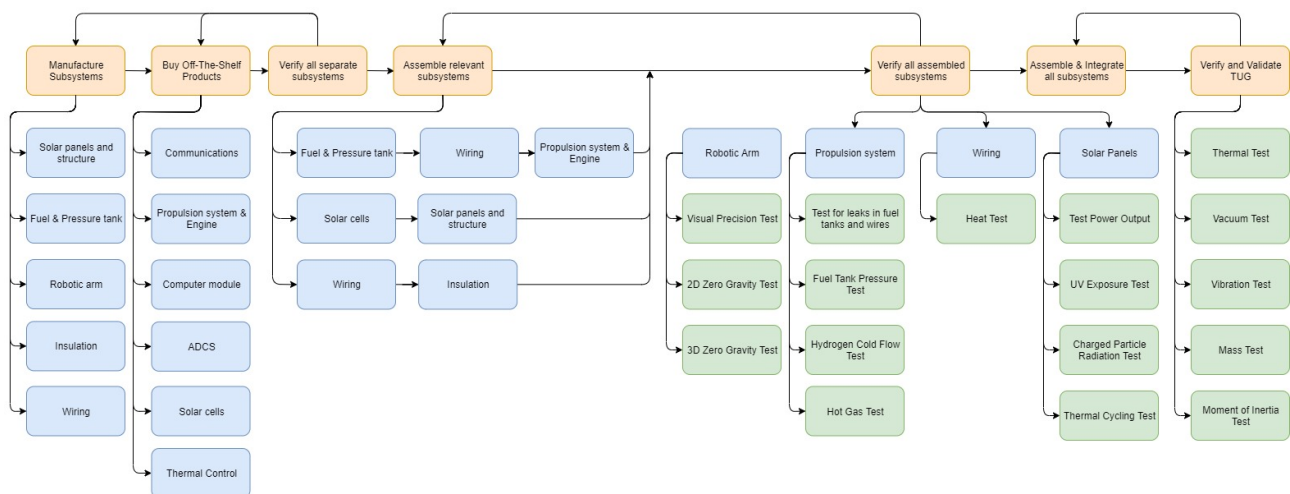


Figure 22.1: Manufacturing, Assembly, Integration and Validation Plan of the Tug

Lastly, in the right-most column of fig. 22.1, the fully manufactured, assembled and integrated tug has to pass the numerous tests listed to be fully verified and validated. For example, a thermal test must be conducted to confirm that the tug is able to maintain the defined temperature range and successfully withstand the extreme temperatures encountered in space.

During launch the tug will be subjected to serious vibrations. In order to remain functional, the tug will have to pass a test in which the probable vibrations during the mission are mimicked. A rather conventional but nevertheless very important test is determining the mass. After all, most calculations and the space mission envelop of the tug are highly dependent on how heavy the spacecraft is. Lastly, a Moment of Inertia test has to be performed too. This is necessary to align the inputs for software of for example the ADCS with the actual hardware situation. Facilities for most of these activities can be found in relative proximity, namely at the ESA ESTEC compound in Noordwijk.

Apart from the tug, the production of the telecommunication satellite has to follow its own MAIV plan as well. This consists of manufacturing, assembly, integration and validation on the ground as well as in space. First of all, the components of the modules are manufactured or ordered and separately tested afterwards. These components are eventually assembled to form the separate modules, which are then tested again. Once this is all done, the modules are all integrated into the LV and tested once more to verify structural strength. After successfully enduring that, the satellites are ready to be launched to space. As the modules

are standardised components, the verification and validation of these parts is a repeating process over time. Therefore, a learning curve applies to this stage, which causes the operational time and costs to go down as the project progresses.

After the MAIV on the ground, the two satellites are re-assembled in space as described in chapter 14. Every assembly and integration step between the modules is verified and validated. This will be done in two ways: First of all, the tug will check whether the module is safely mechanically connected. This is done by a visual check on all the connections and by applying a small tension force on the module. Secondly, a test signal will be send through the module to see whether the data and electric lines are coupled correctly. Assuming a failure is found in the assembly step, these steps will be repeated until the assembly is done correctly. Once the inspected connection is verified, the same procedure can start for another module. These assembled modules do not need to resist launch loads, because it is done in space. Therefore, it is not tested for this as well. This decreases the verification and validation costs again.

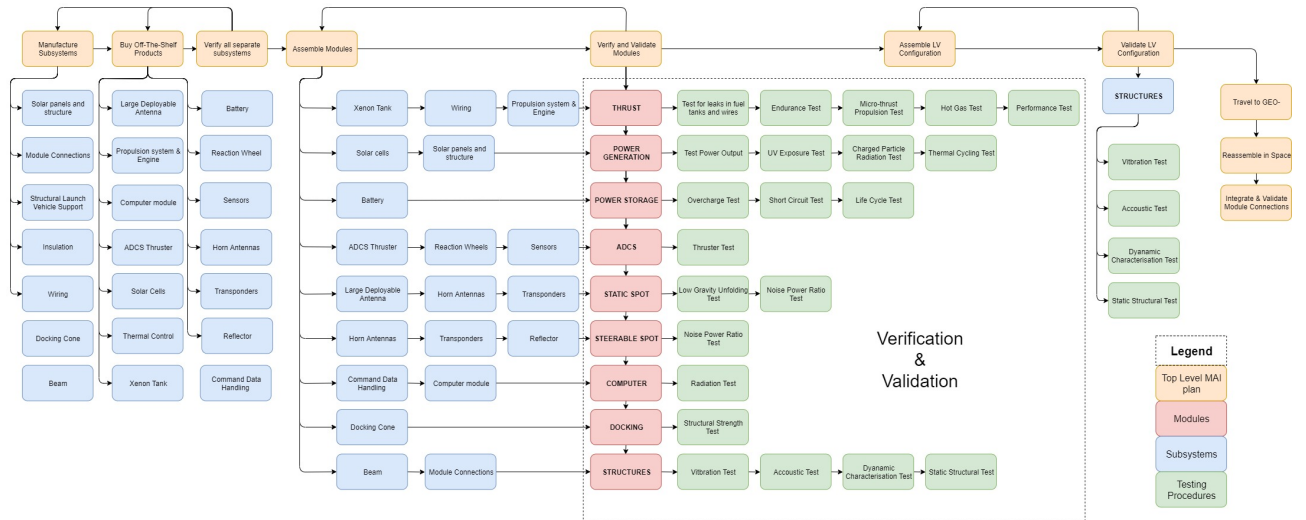


Figure 22.2: Manufacturing, Assembly, Integration and Testing Plan of the Satellite

Cost Breakdown Structure

To get an extensive view on how the cost of the satellite is built up, the total cost is broken down in multiple phases and parts in a Cost Breakdown Structure (CBD), as shown in fig. 23.1. Following that, these different phases are highlighted and explained starting with development continuing with production and ending with operations.

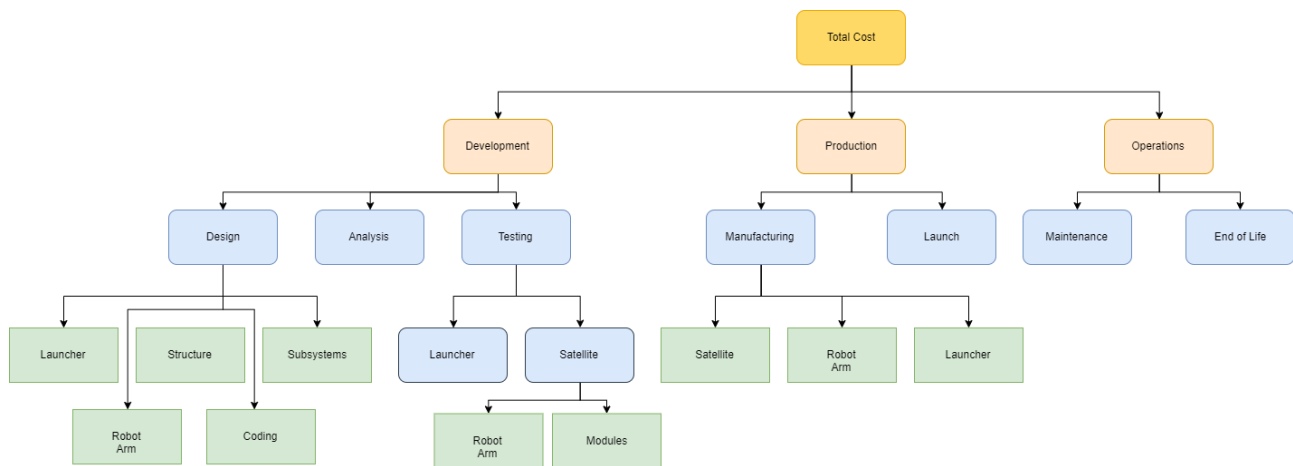


Figure 23.1: Cost Breakdown Structure

Development: In this phase, everything before the actual manufacturing is included. This begins with the first brainstorm session up until the detailed design and final testing. In the design phase, the launcher, tug and satellite should be addressed separate from each other when it comes to cost. All their different subsystems, both in the hardware as in the software coding, may differ a lot. Both the analysis and testing costs need to be included in development as well, as the products cannot go into the next phase before the analysis and testing have ended.

Production: After the development phase, the costs in the production phase should be estimated. The production consists of two major parts, being the manufacturing of the satellite and the tug. Finally the launcher to get satellites into orbit must be purchased.

Operations: After the launch is performed the operations phase is entered. This phase makes up for most of the mission time. Looking at this phase from a cost perspective, operations can be divided into maintenance to troubleshoot and ensure correct functioning in orbit and in an EOL part when servicing has finished.

23.1. Cost Estimation Model

At this moment, during the detailed design, some of the subsystems consist of already existing products. If the cost per product is available, that figure is preferred over a cost estimation model. When a cost estimation model is used though, mass is still one of the major inputs to determine the cost per subsystem. To determine which model in SMAD [58] should be used for the cost estimation, the differences between those models should be addressed. SMAD elaborates on the following cost estimation models: the Unmanned Space Vehicle Cost Model, version 8 (USCM8), Small Satellite Cost Model (SCCM), QuickCost Model, NASA Instrument Cost Model (NICM) and Cost Construction Model 1981 (COCOMO 81). Of these five models the USCM8 is thought to have the best tailored outcome for the MANTIS tug design and the modular satellites. For example, the SCCM model is not usable because it can only account for spacecraft with a maximum mass of 500 kg for satellites. The QuickCost model also does not fit the conditions because it is a more simple approach, in need of fewer inputs of which some are not even known at this stage.

23.1.1. Development

The designing, analysis and testing of all the systems and their subsystems will incur costs that have to be accounted for. The cost estimation of the development phase will also contain one qualification unit. The USCM8 for non-recurring costs will include the cost of that unit. Apart from the development beforehand, a certain budget for R&D in the coming years should also be anticipated. This is especially relevant for Project MANTIS because of the upgradable modularity of the satellites and the expected replacement of the tug per 7 years. The R&D budget will be discussed further in chapter 24.

Tug

For the development of the tug, the model distinguishes the detailed spacecraft bus, the integration, assembly and test phase, program level costs and the acquisition of aerospace ground equipment (AGE). Together, they make up the total estimated cost of the development phase for the tug, shown in table 23.1. The detailed spacecraft bus is estimated without its two robotic arms because those are already developed but they are included in the Integration, Assembly and Test as the system as a whole must be tested and functioning. In total, the tug is estimated to cost \$280m preliminary.

Table 23.1: Non-recurring Cost Estimation Tug

Tug Breakdown Element	Non-recurring cost (\$)
Detailed spacecraft bus	\$189,300,000
Integration, Assembly and Test	\$37,000,000
Program Level	\$53,100,000
Aerospace Ground Equipment	\$300,000
Total cost	\$279,700,000

Satellite

The development cost for the satellite are estimated with the model with an extra input for the Communications Payload integrated in the following table 23.2. The preliminary total cost for developing the telecommunications satellite is estimated to be \$630m.

Table 23.2: Non-recurring cost estimation satellite

Satellite Breakdown Element	Non-recurring cost (\$)
Detailed spacecraft bus	\$113,000,000
Communications Payload	\$298,000,000
Integration, Assembly and Test	\$80,000,000
Program Level	\$115,950,000
Aerospace Ground Equipment	\$21,500,000
Total cost	\$628,450,000

23.1.2. Production

After development, the costs for the next phase need to be determined. This will be the production of the tug and its robot arms, the satellite and the launcher. For the tug and the satellite the recurring costs in USCM8 is applied. However, because the launcher produced by another company and bought eventually, the actual price of that launcher is taken.

Tug

In table 23.3 all the estimated costs are written down to produce the tug. A robotic arm costs \$35m according to the client. Since the tug has two robotic arms, these costs are implemented in table 23.3 as well. The estimated cost to produce one tug (redesigned after seven years) is \$150m, of which almost half consists of the robotic arms cost.

Table 23.3: Recurring cost estimation tug

Tug Breakdown Element	Recurring cost (\$)
Detailed spacecraft bus	\$32,400,000
Robotic Arms	\$70,000,000
Integration, Assembly and Test	\$13,700,000
Program Level	\$26,900,000
Launch & Orbital Operations Support	\$5,850,000
Total cost	\$149,850,000

Satellite

The production cost per satellite is estimated in table 23.4. The Communications Payload is taken into account again, estimated by the model. The total cost of one satellite to produce is estimated preliminary to be around \$188m.

Table 23.4: Recurring cost estimation satellite

Satellite Breakdown Element	Recurring cost (\$)
Detailed spacecraft bus	\$40,450,000
Communications Payload	\$91,000,000
Integration, Assembly and Test	\$16,300,000
Program Level	\$34,600,000
Launch & Orbital Operations Support	\$5,850,000
Total cost	\$188,200,000

Launcher

The launcher that will be used can change ultimately, as the modular satellites are designed to fit the fairing of the Falcon Heavy. Ariane rockets could be considered in a later stage as well because they have a higher fairing volume than the SpaceX launcher. The Falcon Heavy will carry two MANTIS satellites per launch into GTO-. Dividing its probable cost of \$90m [99] over two satellites, this will contribute \$45m of recurring costs per satellite.

23.1.3. Operations

The costs to keep a MANTIS satellite and the tug running per year are have to be accounted for, as well. At this moment in the project phase, a very coarse estimation of a particular percentage of the total production cost per spacecraft is taken as anticipated operational cost per year. The tug has a versatile mission life and will have to be monitored and controlled extensively transferring and towing satellites from one orbit to another. Therefore, a 10% is of the tug production is taken to have a predicted \$15m operational cost for the tug per year. The telecommunication satellite however, will only have correctional commands and will not be controlled as heavily as the tug. The predicted percentage of the satellites production cost is therefore 5% resulting in a \$19m operational cost per year.

23.2. Conclusion

To conclude the preliminary costs in Project MANTIS for both the tug and telecommunication satellite, they are listed once more in table 23.5.

Table 23.5: All cost estimations

All costs	Tug	Satellite
Development	\$280,000,000	\$630,000,000
Production	\$150,000,000	\$188,000,000
Launch (per device)	\$90,000,000	\$45,000,000
Operations (per year)	\$15,000,000	\$19,000,000

Since it is still just a coarse estimate, the costs are rounded off to millions of dollars for simplicity. The development costs are high compared to the conventional satellites and might be estimated too pessimistically. The production costs are prone to decrease over time due to a learning curve, but that is not included in this preliminary estimation as of yet.

As this is still a very rough estimation of costs based on primarily mass with many assumptions, the actual costs are far from guaranteed. For example, the benefit in operational cost to keep the tug idle in GEO during vacant days. Furthermore, the replacement of the tug or space station after servicing for 7 years is not taken into account as of yet since it is still unclear after how many satellites that would take place.

Return on Investment

In this chapter, the financial model projecting return on investment is discussed. Firstly, the key characteristics of the model are discussed in section 24.1. Secondly, the assumptions used in this model and the base case scenario are discussed. Following the base case, various scenarios have been evaluated to consider which variables are most important and to be able to assess their corresponding impacts in section 24.3. Concluding the model discussion, all outputs and their meaning are discussed in section 24.4 and further value creation of Project MANTIS is discussed in section 24.5.

24.1. Model Characteristics and Use Case

The financial model is built to provide insight in the profitability of Project MANTIS. Since both revenue and cost are based on various assumptions, conducting a scenario analysis through an elaborate model clarifies many uncertainties that would remain if more simplistic calculation of the Return on Investment (ROI) was to be used. To provide a conservative and clear approach, the model is built accounting only for AIV-specific revenues and costs. Consequently, additional services such as removing space-debris, and the repair or refuelling of other satellites are not considered in revenue projections. Since satellite production, launch, and operations are not directly accounted to the AIV procedure (but accountable to other departments, possibly within Airbus), the AIV-service itself is only considered as revenues (in terms of a premium paid). Moreover, all costs considered are those directly related to developing and building the AIV system. This includes an initial investment (for preliminary development, production and launch), and various recurring costs (operating the tug, developing and producing future tugs and continuously developing the satellites and AIV system). Finally, these revenues and costs are projected as annual earnings. This is important since some years will account for significant costs such as new the production and launch of the next tug (after 7 and 14 years of operations). Therefore, the break-even point and ROI will differ per year.

24.2. Assumptions & Base Case Scenario

To build a valid model, a handful of assumption are made, concerning both revenues and costs. All base case assumptions are presented in table 24.1.

24.2.1. Revenues

Firstly, the main source of revenues, providing in-space AIV, must be projected. Therefore, volume, the market share, and pricing should be determined. Euroconsult projected approximately 150 GEO commercial telecom satellites built and launched in 2018-2027. Additionally, c.200 non-commercial GEO satellites will be launched in this period, and the average value in manufacturing and launch was estimated at nearly \$300m per satellite [20]. Considering Airbus' market share as discussed in Market Analysis, a market share of 15% is considered realistic. Moreover, after discussions with the client, the target volume was set at 3 to 4 satellites annually. The model is built accordingly, accounting 3 orders annually in the first 7 years. As the technology is projected to gain traction and the space industry is set to increase exponentially, the following years have been projected with 4 orders annually (which is still considered conservative). Finally the AIV will be priced at a 10% to 20% premium on current satellites costs: \$30m to \$60m. At this pricing, Project MANTIS creates value for the client through offering future upgradability, shorter throughput times and sustainability together with the initial cost savings. While pricing in the base case is set to \$45m, the sensitivity analysis will account for changes herein.

Secondly, upgrades of the previously assembled telecom satellites are assumed to be ordered at a conservative rate. This includes 2 upgrade orders annually from 2039 onward (10 years after operation start). Moreover, these have still been priced conservatively in the base case at a cost premium of \$5m per order.

Table 24.1: Base case assumptions for the financial model

Base Case Assumptions	
Preliminary tug development cost (\$m)	280
Tug production cost (\$m)	150
Preliminary satellite development cost (\$m)	630
Tug operation cost (\$m, annually)	15
Annual tug R&D (% of preliminary costs)	4,0%
Annual satellite R&D (% of preliminary costs)	4,0%
Upgrade price (\$m)	5
AIV price (\$m)	45

24.2.2. Costs

Development costs (of both the tug and satellites), tug production, and direct operational costs are derived from chapter 23. In addition to these costs, the tug is assumed to be launched on its own (therefore costing \$90m per flight). Furthermore, recurring R&D costs are considered for redesign and further development of both the tug and the AIV system (to maintain a market-leading technology). This is assumed to be a percentage of the preliminary tug development cost. In the base case, this is set to 4% - resulting in 100% throughout the lifetime of Project MANTIS. This will further be evaluated in the sensitivity analysis.

24.3. Sensitivity Analysis

To evaluate variables used in the model, two multi-parameter sensitivity analyses have been conducted. Both analyses comprise different variables, and therefore show the effect of changes in the model.

24.3.1. Sensitivity Analysis 1

Firstly, the AIV price is varied from \$30m to \$60m and the annual R&D cost is varied from 3% to 5%. These variables have been chosen because they are both key parameters in profitability projections. While pricing may vary in the future (due to market shifts), recurring development costs have not been accounted for in the cost analysis. As illustrated in tables 24.2 and 24.3, the results are given and sorted in terms of average ROI and in terms of break-even point (years). These results will be discussed in section 24.4.

24.3.2. Sensitivity Analysis 2

Secondly, a multi-parameter sensitivity analysis is conducted over the two main costs which are considered in chapter 23. Herein, a cost difference of \$350m in worst and best case scenario will be considered. Therefore, this sensitivity analysis serves as a basis to consider the profitability of the project if the cost budget is exceeded.

24.4. Model Outputs

Outputs have been generated of the base case and both sensitivity analyses. Firstly, the criteria will be discussed on which the outputs are assessed. Since the objective was to define a profitable business case, all scenarios are considered viable once they exceed the total costs throughout the lifetime of Project MANTIS. If this is not the case, the scenario will not be considered. Though an ROI of 4% will lead to profits, and ROI above 6% is considered safe, and only an ROI above 10% is considered a good investment. This is because profitability is based purely on earnings in this model, while cost of capital, inflation, tax, and other factors have been neglected for simplicity. Lastly, a break-even point reached after 15 years of operations is considered realistic. Significantly faster (i.e. 12 years or earlier) is considered good and significantly later (i.e. 20 years or later) is considered unfavourable.

The model of the base case is presented in fig. 24.1. The base case leads to an average ROI of 8.9% and a break-even point at 15 years. This is considered realistic, and would lead to substantial returns for Airbus. However, there are more factors to consider. Therefore, the sensitivity analyses show which variables are of

importance. Firstly, in tables 24.2 and 24.3, recurring R&D and AIV price show that many scenarios result in a viable business case. However, a significantly lower AIV price would have the largest impact. This is valuable to consider in final pricing of the system. Moreover, a price of \$35m or less is considered highly unlikely. In tables 24.4 and 24.5, the primary (investment) costs are evaluated. This clearly shows that with significantly higher development costs, Project MANTIS still results in a profitable business case.

Table 24.2: Multi-parameter sensitivity analysis of the recurring R&D costs versus AIV price in terms of ROI

		Recurring R&D (% of initial costs)				
		3.0%	3.5%	4.0%	4.5%	5.0%
AIV price (\$m)	30	4.9%	4.5%	4.1%	n/a	n/a
	35	6.5%	6.1%	5.7%	5.3%	4.9%
	40	8.1%	7.7%	7.3%	6.9%	6.5%
	45	9.7%	9.3%	8.9%	8.5%	8.1%
	50	11.3%	11.0%	10.6%	10.2%	9.8%
	55	13.0%	12.6%	12.2%	11.8%	11.4%
	60	14.6%	14.2%	13.8%	13.4%	13.0%

Table 24.3: Multi-parameter sensitivity analysis of the recurring R&D costs versus AIV price in terms of break-even point (years)

		Recurring R&D (% of initial costs)				
		3.0%	3.5%	4.0%	4.5%	5.0%
AIV price (\$m)	30	23	24	25	n/a	n/a
	35	19	20	21	21	23
	40	16	17	17	18	19
	45	13	13	15	16	16
	50	11	12	12	12	13
	55	10	11	11	11	12
	60	10	10	10	10	11

Table 24.4: Multi-parameter sensitivity analysis of the preliminary development costs in terms of ROI

		Preliminary Tug R&D				
		80	180	280	380	480
Preliminary Satellite R&D (\$m)	480	14.6%	12.5%	11.0%	9.5%	8.4%
	530	13.5%	11.7%	10.2%	8.9%	7.9%
	580	12.5%	10.9%	9.5%	8.4%	7.4%
	630	11.7%	10.2%	8.9%	7.9%	7.0%
	680	10.9%	9.5%	8.4%	7.4%	6.6%
	730	10.2%	8.9%	7.9%	7.0%	6.3%
	780	9.5%	8.4%	7.4%	6.6%	5.9%

Table 24.5: Multi-parameter sensitivity analysis of the preliminary development costs in terms of break-even point (years)

		Preliminary Tug R&D				
		80	180	280	380	480
Preliminary Satellite R&D (\$m)	480	10	11	12	13	16
	530	10	11	12	15	16
	580	11	12	13	16	17
	630	11	12	15	16	18
	680	12	13	16	17	18
	730	12	15	16	18	19
	780	13	16	17	18	20

24.5. Value Creation for Airbus Defence & Space

Besides offering direct financial results, Project MANTIS is set to offer Airbus Defence & Space a strategic asset which creates value in several different ways. Three of these considerations are mentioned below.

- Firstly, Project MANTIS puts Airbus ahead of the competition. By creating value through AIV for its customers, Airbus has an excellent possibility to increase its market share and maintain its market leading position. By offering a new generation of telecommunication satellites with attractive advantages, Airbus can distinguish itself once again from the competition.
- Secondly, Project MANTIS offers Airbus additional financial benefit. As the company can strengthen its end-to-end value chain coverage, this gives Airbus the possibility to gain extra business through cross-selling its services (launching the modules, manufacturing the modules, etc.). Moreover, only AIV-revenues have been projected, while extra business through additional services such as debris-removal and refuelling are also possible.
- Lastly, investing in the development of Project MANTIS will enable Airbus to further develop in-space AIV for various other purposes besides GEO telecom satellites. Consequently, Airbus can roll-out this technology on a larger scale and thus serve a larger customer base.

Therefore, besides its direct profitability, Project MANTIS is, a promising business case with high potential to strengthen Airbus' product portfolio.

Values presented in \$m		2028	2029	2030	2031	2032	2033	2034	2035	2036	2037	2038	2039	2040	2041	2042	2043	2044	2045	2046	2047	2048	2049	2050	2051	2052	2053
Year	0	1	2	3	4	5	6	7	8	9	10	11	12	13	14	15	16	17	18	19	20	21	22	23	24	25	
<i>Number of orders</i>		3	3	3	3	3	3	3	4	4	4	4	4	4	4	4	4	4	4	4	4	4	4	4	4	4	
<i>Additional earnings per order</i>		45	45	45	45	45	45	45	45	45	45	45	45	45	45	45	45	45	45	45	45	45	45	45	45	45	
<i>Number of upgrades</i>		0	0	0	0	0	0	0	0	0	0	2	2	2	2	2	2	2	2	2	2	2	2	2	2	2	
<i>Additional earnings per upgrade</i>		5	5	5	5	5	5	5	5	5	5	5	5	5	5	5	5	5	5	5	5	5	5	5	5	5	
AIV Revenues		135	135	135	135	135	135	135	180	180	180	190	190	190	190	190	190	190	190	190	190	190	190	190	190	190	
	<i>Tug</i>																										
Development		280																									
Production		150							150																		
Tug launch costs		90							90																		
R&D			11,2	11,2	11,2	11,2	11,2	11,2	11,2	11,2	11,2	11,2	11,2	11,2	11,2	11,2	11,2	11,2	11,2	11,2	11,2	11,2	11,2	11,2	11,2	11,2	
Operations			15	15	15	15	15	15	15	15	15	15	15	15	15	15	15	15	15	15	15	15	15	15	15	15	
Total Tug costs		520	26,2	26,2	26,2	26,2	26,2	26,2	266,2	26,2	26,2	26,2	26,2	26,2	26,2	266,2	26,2	26,2	26,2	26,2	26,2	26,2	26,2	26,2	26,2	26,2	
	<i>Satellite & System</i>																										
Development		630																									
R&D			25,2	25,2	25,2	25,2	25,2	25,2	25,2	25,2	25,2	25,2	25,2	25,2	25,2	25,2	25,2	25,2	25,2	25,2	25,2	25,2	25,2	25,2	25,2	25,2	
Total Satellite & System costs		630	25,2	25,2	25,2	25,2	25,2	25,2	25,2	25,2	25,2	25,2	25,2	25,2	25,2	25,2	25,2	25,2	25,2	25,2	25,2	25,2	25,2	25,2	25,2	25,2	
Total costs			51,4	51,4	51,4	51,4	51,4	51,4	291,4	51,4	51,4	51,4	51,4	51,4	51,4	291,4	51,4	51,4	51,4	51,4	51,4	51,4	51,4	51,4	51,4	51,4	
Initial investment		1150																									
Earnings	<i>ROI</i>		83,6	83,6	83,6	83,6	83,6	83,6	-156,4	128,6	128,6	128,6	138,6	138,6	138,6	-101,4	138,6	138,6	138,6	138,6	138,6	138,6	138,6	138,6	138,6	138,6	
			7,3%	7,3%	7,3%	7,3%	7,3%	7,3%	-13,6%	11,2%	11,2%	11,2%	12,1%	12,1%	12,1%	-8,8%	12,1%	12,1%	12,1%	12,1%	12,1%	12,1%	12,1%	12,1%	12,1%	12,1%	

Figure 24.1: Financial model in base case scenario

Conclusion & Recommendations

In the detailed design phase of the project, the focus shifted to the modules of the satellite and how they should be assembled to finally be an fully integrated spacecraft. The modules were designed and sized in detail to be able to fit in the fairing while still being able to fulfill their tasks. The subsystem modules are worked out as much as possible, some to the point that products were chosen but further investigation of how these modules will work in reality is necessary to ensure Project MANTIS' success. A more detailed design per module will give more insight on their interaction and other unanswered questions. Surprisingly, the final weight of the modular satellite was 2096.3 kg, lower than expected compared to a conventional one. This might result in a decrease of the cost of a satellite or increase the number of satellites per launch in the future.

The modules in the fairing should be able to be assembled to a fully functioning satellite once in orbit. It was proven that the expected assembly works in space when the modules are packed well in the fairing, using 3D renders to visualise the assembly. However, whether the tug will be able to assemble as intended with its two robotic arms, had to be investigated thoroughly. These robotic arms were designed and programmed to see if the system was able to move all modules around the satellite's bus. After extensive calculations, it is concluded that the robotic arms are 6.9 m long and can reach everywhere they have to without colliding. They even have a better prospected accuracy than the DARPA arm. The assembly time of the modular satellite is approximately 37 hours. Once a physical robotic arm is built, the computer model could be verified and validated for a real working case. However, this is outside the scope of the project.

The great benefit of using MANTIS over conventional spacecraft is the modularity of its satellites. Over the years, faulty or deprecated modules can easily be replaced without having to discard the whole satellite. The choices of modules as payload makes changing the total module package also conveniently easy. This variety in configurations in the LV is also a great example of beneficial features of this modularity as well as other possible functionalities of the tug. For example, the future upgradability of the tug to gather junk from the graveyard orbit is a great feature to contain pollution in space. Though space missions are rarely climate friendly, sustainability was kept in mind during the whole project whether any design choices would be polluting or not. The MANTIS satellite was found to be 125% more sustainable than its reference case, the Eutelsat 172b. The space mission's EOL procedure is one of those choices to at least get rid of the waste after the mission is finished.

Though financially multiple variables are still uncertain on both costs as well as revenue, the business case still seems to be promising with a great market potential, especially because the before mentioned services make the MANTIS project very versatile. The sensitivity analysis on the return of investment underlines that.

Due to time constraints, this project focused mainly on the feasibility of performing AIV in space. In order to follow up on this report, some future recommendations could be helpful. Apart from the above mentioned more detailed design of the modules, a deeper insight in the assembly process might make cuts in the weight and volume of the modular system possible. Extra thorough research on custom made robotic arms will shine some light on how to optimise them in combination with the tug they are attached to. This iterative process of optimising could result in more loss of weight. This raises new opportunities. For example, the loss of weight creates space to put more fuel or extra modules in the LV.

For now, the initial method to perform Assembly, Integration and Verification (AIV) in space is believed to work. It even seems, be it preliminary, effective to compete with conventional spacecraft.

References

- [1] Clean space. URL https://www.esa.int/Safety_Security/Clean_Space/.
- [2] Risk and reliability. URL https://www.nasa.gov/pdf/140639main_ESAS_08.pdf.
- [3] Responsibility and sustainability. URL <https://www.airbus.com/company/responsibility-sustainability.html>.
- [4] Airbus annual report 2018. April 2019. URL <https://www.airbus.com/content/dam/corporate-topics/financial-and-company-information/Airbus-Annual-Report-2018.pdf>.
- [5] Airbus. Share price & information. URL <https://www.airbus.com/investors/share-price-and-information.html>.
- [6] Airbus. Fiber optic gyroscopes. <https://spaceequipment.airbusdefenceandspace.com/avionics/fiber-optic-gyroscopes/astrix-120/>, 2019.
- [7] Airbus. Worldwide presence at home around the world. <https://www.airbus.com/company/worldwide-presence.html>, 2019.
- [8] ArianeSpace. About us arianespace is the world's leading satellite launch company, operating a full family of launchers. <https://www.arianespace.com/about-us/>, 2020.
- [9] Satellite Industry Association. State of the satellite industry report. 06 2016. URL https://brycotech.com/downloads/SIA_SSIR_2016.pdf.
- [10] Ball. Ct-2020. https://www.ball.com/aerospace/Aerospace/media/Aerospace/Downloads/D3408_CT2020_0118.pdf?ext=.pdf, 2019.
- [11] T. Benson. Ideal rocket equation. <https://www.grc.nasa.gov/WWW/K-12/rocket/rktpow.html>, 2014.
- [12] J.M. Bockel. The future of the space industry. 11 2018. URL <https://www.nato-pa.int/download-file?filename=sites/default/files/2018-12/2018%20-%20THE%20FUTURE%20OF%20SPACE%20INDUSTRY%20-%20BOCKEL%20REPORT%20-%2017%20ESC%2018%20E%20fin.pdf>.
- [13] S. Boddu. A Modular Telecommunication Satellite Demonstrating AIT in Space, 2018.
- [14] C. Bonnal. Research on space debris, safety of space objects with nuclear power sources on board and problems relating to their collision with space debris. February 2019. URL https://www.unoosa.org/res/oosadoc/data/documents/2019/aac_105c_12019crp/aac_105c_12019crp_7_0_html/AC105_C1_2019_CRP07E.pdf.
- [15] Bradford. Reaction wheel unit. <https://www.bradford-space.com/products-aocs-reaction-wheel-unit.php>, 2019.
- [16] Bradford. Coarse sun sensor. <https://www.bradford-space.com/products-aocs-coarse-sun-sensors.php>, 2019.
- [17] E.F Bruhn. *Analysis and Design of Flight Vehicle Structures*. Tri-State Offset Company, 1973.
- [18] I. Buchmann. What's the best battery? <http://tiny.cc/bophiz>, 2017.
- [19] Richard H. Byrd, Peihuang. Lu, Jorge. Nocedal, and Ciyou. Zhu. A limited memory algorithm for bound constrained optimization. *SIAM Journal on Scientific Computing*, 16(5):1190–1208, 1995. doi: 10.1137/0916069. URL <https://doi.org/10.1137/0916069>.
- [20] A. Chatterton. Satellite manufacturing & launch. Sep 2019. URL <http://www.euroconsult-ec.com/sat-manuf-launch>.
- [21] Chetverno. Phased array animation. <https://commons.wikimedia.org/w/index.php?curid=54005685>, 2016.
- [22] Cobham. Xenon propellant tank. <https://www.cobham.com/mission-systems/composite-pressure-solutions/space-systems/xenon-propellant-tank-datasheet/docview/>, 2009.
- [23] Rockwell Collins. Rdr 68 momentum and reaction wheels. <https://www.rockwellcollins.com/Products-and-Services/Defense/Platforms/Space/RDR-68-Momentum-and-Reaction-Wheel.aspx>, 2019.
- [24] Rockwell Collins. Ht-rsi high motor torque momentum and reaction wheels 14 – 68 nms with integrated wheel drive electronics. http://www.electronicnote.com/RCG/HT-RSI_A4.pdf, 2019.
- [25] P.B. de Selding. Spate of solar-array failures on ss/l satellites traced to manufacturing defect. January 2013. URL <https://spacenews.com/33046spate-of-solar-array-failures-on-ssl-satellites-traced-to/>.
- [26] Thomas Debus and Sean Dougherty. Overview and performance of the front-end robotics enabling near-term demonstration (frend) robotic arm. In *AIAA Infotech@ Aerospace Conference and AIAA Unmanned... Unlimited Conference*, page 1870, 2009.
- [27] M. D'heer, M. Rebhein, L. Peschke, and et al. *AIV Baseline Report Group 02*. IKEASPACE, 2019.
- [28] M. D'heer, M. Rebhein, L. Peschke, and et al. *AIV Midterm Report Group 02*. IKEASPACE, 2019.
- [29] L. Dreyer. *Falcon 9 User's Guide*. Space Exploration Technologies Corp, 2009.
- [30] B.R. Elbert. *The Satellite Communication Applications Handbook*. Artech House space technology and applications library. Artech House, 2004. ISBN 9781580538084. URL <https://books.google.nl/books?id=D9k5s2-mMKgC>.
- [31] eoPortal. Winds (wideband internetworking engineering test and demonstration satellite) / kizuna. <https://directory.eoportal.org/web/eoportal/satellite-missions/v-w-x-y-z/winds>, 2020.
- [32] ESA. Airbus's new feed array for next-gen multi-beam antennas. <http://tiny.cc/f9ohiz>, 2016.
- [33] ESA. Esa's e.deorbit debris removal mission reborn as servicing vehicle. <https://indico.esa.int/event/234/contributions/3742/contribution.pdf>, 2017.
- [34] ESA. T6 hpeps t6 high power electric propulsion system development and qualification. <https://artes.esa.int/projects/t6-hpeps>, 2019.
- [35] ESA. Estrack ground stations. https://www.esa.int/Enabling_Support/Operations/Estrack/Estrack_ground_stations, 2020.
- [36] Stéphane (Airbus) ESTABLE. Capturing and deorbiting envisat with an airbus spacetug. results from the esa e.deorbit consolidation phase study. <https://indico.esa.int/event/234/contributions/3742/contribution.pdf>, 2018.
- [37] Eutelsat. Reference document 2017-18. https://www.eutelsat.com/files/PDF/investors/2017-18/Eutelsat_Communications_Reference_Document_2017-18.pdf, 2019.
- [38] Espace & Exploration. "fiche technique: Falcon heavy". June 2019. URL <http://www.espace-exploration.com/fr/numeros/766-espace-et-exploration-n%C2%B050-2>.
- [39] W. Fehse. *Automated Rendezvous and Docking of Spacecraft*. Cambridge Aerospace Series. Cambridge University Press, 2003. ISBN 9780521824927.
- [40] Ferriauol B. Hertel T. Fisher, J. Next-c flight ion propulsion system development status. October 2017. URL https://iepc2017.org/sites/default/files/speaker-papers/iepc_2017-218_next-c_development.pdf.
- [41] M. Garcia. Space debris and human spacecraft. August 2017. URL https://www.nasa.gov/mission_pages/station/news/orbital_debris.html.

- [42] K. Glatre, Pascal Renaud, Robert Guillet, and Y. Gaudette. The eutelsat 3b top-floor steerable antennas. *IEEE Transactions on Antennas and Propagation*, 63:1301–1305, 2015.
- [43] HPS GmbH. Overview of hps antenna solutions. <http://www.hps-gmbh.com/en/portfolio/subsystems/reflector-antennas/>, 2020.
- [44] Ariane group/ Space Propulsion. 10n bipropellant thrusters. <http://www.space-propulsion.com/spacecraft-propulsion/bipropellant-thrusters/10-bipropellant-thrusters.html>, 2019.
- [45] Ariane group/ Space Propulsion. 1n monopropellant hydrazine thruster. <http://www.space-propulsion.com/spacecraft-propulsion/hydrazine-thrusters/1n-hydrazine-thruster.html>, 2019.
- [46] L3 Harris. Cirus — compact inertial reference unit for space. <https://www2.l3t.com/spacenv/products/cirus.html>, 2019.
- [47] Ali Hassani, Mehrdad Ghorbani, and Milad Pasand. A study of spacecraft reaction thruster configurations for attitude control system. *IEEE Aerospace and Electronic Systems Magazine*, 32, 10 2017. doi: 10.1109/MAES.2017.160104.
- [48] T. Helmenstine. Abundance of elements in earth's crust – periodic table and list. December 2018. URL <https://sciencenotes.org/abundance-of-elements-in-earths-crust-periodic-table-and-list/>.
- [49] C. Henry. Geo satellite orders continued to underwhelm in 2018. Feb 2019. URL <https://spacenews.com/geo-satellite-orders-continued-to-underwhelm-in-2018/>.
- [50] C. Henry. Geo satellite orders are up, but full rebound remains to be seen. Sep 2019. URL <https://spacenews.com/geo-satellite-orders-are-up-but-full-rebound-remains-to-be-seen/>.
- [51] S. Hernandez. International space station. <https://grabcad.com/library/international-space-station-iss-1>, 2014.
- [52] P.Q. Hien. Robot fd - h5 (daihain japan). <https://grabcad.com/library/robot-fd-h5-daihen-japan-1>, 2019.
- [53] General Dynamics Mission Systems Inc. Space qualified multi-mode standard transponder (mst). <https://gdmssystems.com/-/media/General-Dynamics/Space-and-Intelligence-Systems/PDF/space-multi-mode-standard-transponder-mst-datasheet.ashx?1a=en&hash=C31931BE393AB88BCA5A07EA45DEC45FCFD40AFD>, 2020.
- [54] ISIS. In-orbit verification of european space technologies. <https://ec.europa.eu/research/participants/documents/downloadPublic/bTR0eTZKU2ovWEhsQ1dwUy9FbUVQZklzb1pBalljNnhnMElpVGtSSUJCROVJdWlMK3N0N2VRPT0=/attachment/VFEyQTQ4M3ptUWVGbHhLbWV2VjBjMWRmak1hcHlzSGE=>, 2016.
- [55] Prof. Dr. Kai-Uwe Schroeder Joerg Kreisel, Thomas A. Schervan. A game-changing space system interface enabling multiple modular and building block-based architectures for orbital and exploration missions. <https://www.iboss.space/wp-content/uploads/2019/11/IAC-19-Presentation.pdf>, 2019.
- [56] Prof. Dr. Kai-Uwe Schroeder (VP Institutional Affairs) Joerg Kreisel (Chairman), Thomas A. Schervan (CEO). [iboss gmbh. https://www.iboss.space/](https://www.iboss.space/), 2020.
- [57] A. Jonas. Main trends and challenges in the space sector. July 2019. URL <https://www.morganstanley.com/ideas/investing-in-space>.
- [58] D.F. Everett J.R. Wertz and J.J. Puschell. *Space Mission Engineering: The New SMAD*. Microcosm Press, Hawthorne CA, 2015.
- [59] Tesat Spacecom GmbH & Co. KG. Data sheet ku-band ttc receiver and transmitter, 2010.
- [60] Müller J. & Kukies R. Killinger, R. Status of the rit-xt high performance rf-ion thruster development. *Spacecraft Propulsion, Third International Conference*, page 443, 10 2000. doi: 10.2514/6.2000-3272.
- [61] Leonardo. Autonomous star trackers. https://www.leonardocompany.com/documents/20142/3150068/Copia_di_A_STR_Autonomous_Star_Trackers_LQ_mm07786_.pdf?t=1538987562062, 2019.
- [62] Paul Marks. Defending the orbital internet. <https://cacm.acm.org/news/234198-defending-the-orbital-internet/fulltext>, 2019.
- [63] Prof. M. Martinez-Sanchez. Lecture 34: Performance to geo. <http://tiny.cc/1sphiz>, 2005.
- [64] Adcole Maryland. Mai-ss space sextant: Miniature star tracker. <https://www.maiaero.com/star-tracker-adacs-1>, 2019.
- [65] NASA. Nasa plan for commercial leo development. https://www.nasa.gov/sites/default/files/atoms/files/comleodevt_plan_6-7-19_final-links-new.pdf, 2019.
- [66] NASA. Tess - transiting exoplanet survey satellite. <https://www.nasa.gov/tess-transiting-exoplanet-survey-satellite>, 2020.
- [67] United Nations. Space law. URL <https://www.unoosa.org/oosa/en/ourwork/spacelaw/index.html>.
- [68] United nations development program. Human development data (1990-2018). <http://hdr.undp.org/en/data>, 2019.
- [69] L3 Space & Navigation. Rwa-15 — reaction wheel assembly. <https://www2.l3t.com/spacenv/pdf/datasheets/RWA-15.pdf>, 2019.
- [70] Time of change. Co2 emissions for shipping of goods. 2018. URL <https://timeforchange.org/co2-emissions-for-shipping-of-goods/>.
- [71] University of Maryland. Mass estimating relations. <https://spacecraft.ssl.umd.edu/academics/791S16/791S16L08.MERSx.pdf>, 2016.
- [72] University of Oregon. Space lecture 03. <http://abyss.uoregon.edu/~js/space/lectures/lec03.html>.
- [73] J.N. Pelton. *Satellite Communications*. SpringerBriefs in Space Development. Springer New York, 2011. ISBN 9781461419945. URL <https://books.google.nl/books?id=XWoEEasQqUkC>.
- [74] Prof. R. Currant et. al. Prof. E. Gill. Ae3211-i systems engineering & aerospace design, 2019.
- [75] Christian Rave and Arne F. Jacob. Architectures for efficient power sharing in active multiple-feed-per-beam satellite antennas. *2016 21st International Conference on Microwave, Radar and Wireless Communications (MIKON)*, pages 1–4, 2016.
- [76] Lens R&D. Bison64-et-b / 700s00401. <https://lens-rnd.com/sun-sensors/bison64-et-b/>, 2019.
- [77] Robin M. Pinson & Connie K. Carrington Richard T. Howard, Andrew Heaton. Orbital express advanced video guidance sensor. April 2008. URL https://www.researchgate.net/publication/224314684_Orbital_Express_Advanced_Video_Guidance_Sensor.
- [78] Aerojet Rocketdyne. In-space product data sheets; monopropellant and bipropellant engines. <https://www.rocket.com/sites/default/files/documents/In-Space%20Data%20Sheets%209.13.19.pdf>, 2019.
- [79] Aerojet Rocketdyne. RL10 propulsion system fact sheet. https://www.rocket.com/sites/default/files/documents/Capabilities/PDFs/RL10_data_sheet.pdf, 2019.
- [80] D Bailey S. Callery. Climate change: How do we know? January 2020. URL <https://climate.nasa.gov/evidence/>.
- [81] S. Sachdeva. The “new normal” in satellite manufacturing & launch. Aug 2019. URL <https://www.nsr.com/the-new-normal-in-satellite-manufacturing-launch>.

- [82] Saft. A global presence. <https://www.saftbatteries.com/about-us/who-saft/saft-worldwide>, 2019.
- [83] SpaceX Sales. *Falcon User's Guide*. Space Exploration Technologies Corp, 2019.
- [84] Satsearch. St200. <https://satsearch.co/products/hyperion-technologies-st200-star-tracker>, 2019.
- [85] Satsearch. St400. <https://satsearch.co/products/hyperion-technologies-st400-star-tracker>, 2019.
- [86] L. Scatteia. Satellites to be built & launched 2018-2027. Mar 2019. URL <https://www.globenewswire.com/news-release/2019/03/27/1774099/0/en/Satellites-to-be-Built-Launched-2018-2027-3-300-Satellites-Over-50-kg-to-be-Launched-Representing-a-Market-of-284-Billion.html>.
- [87] L. Scatteia. Main trends and challenges in the space sector. June 2019. URL <https://www.pwc.fr/fr/assets/files/pdf/2019/06/fr-pwc-main-trends-and-challenges-in-the-space-sector.pdf>.
- [88] M. Schneider, C. Hartwanger, E. Sommer, and H. Wolf. The multiple spot beam antenna project "medusa". pages 726–729, March 2009. ISSN 2164-3342.
- [89] Senosor. Stim 300. <https://www.senosor.com/products/inertial-measurement-units/stim300/>, 2019.
- [90] E.J. SMITH. How many times can spacex reuse a rocket? May 2018. URL <https://www.yoursurvivalguy.com/financial-security/how-many-times-can-spacex-reuse-a-rocket/>.
- [91] Hofer R. Polk J. et al. Snyder, J.S. Performance evaluation of the t6 ion engine. *Journal of Propulsion and Power*, 28(2), 3 2012. doi: 10.2514/1.B34173.
- [92] Azur Space. 32% quadruple junction gaas solar cell type: Qj solar cell 4g32c - advanced, . URL http://www.azurspace.com/images/0005979-01-00_DB_4G32C_Advanced.pdf.
- [93] RUAG Space. Command & data handling. . URL https://www.ruag.com/sites/default/files/media_document/2019-06/Command_Data_Handling_May202019.indd_.pdf.
- [94] RUAG Space. Next generation on board computer. . URL https://www.ruag.com/sites/default/files/media_document/2019-06/Next20generation20on20Board20Computer20May202019.pdf.
- [95] Spaceflight101. Eutelsat 172b. <http://spaceflight101.com/ariane-5-va237/eutelsat-172b/>, 2019.
- [96] SpaceX. SpaceX statistics. URL <https://spacexnow.com/stats.php>.
- [97] SpaceX. Making life multiplanetary. https://www.spacex.com/sites/spacex/files/making_life_multiplanetary_2016.pdf, 2016.
- [98] SpaceX. Falcon heavy. <https://www.spacex.com/falcon-heavy>, 2020.
- [99] SpaceX. Capabilities & services. <https://www.spacex.com/about/capabilities>, 2020.
- [100] TNO. Tno coarse sun sensor using european cells. <https://artes.esa.int/projects/tno-coarse-sun-sensor-using-european-cells>, 2019.
- [101] Transparency. Corruption perceptions index 2019. <https://www.transparency.org/cpi2019>, 2019.
- [102] U.C.S. Ucs satellite database. Sep 2019. URL https://s3.amazonaws.com/ucs-documents/nuclear-weapons/sat-database/5-9-19-update/UCS_Satellite_Database_4-1-2019.xlsx.
- [103] H. Ullah. *Buckling of thin-walled cylindrical shells under axial compression*. John Wiley & Sons Ltd., 2009.
- [104] Florida International University. Orbital mechanics. <http://faculty.fiu.edu/~vanhamme/ast3213/orbits.pdf>, 2020.
- [105] G. Warwick. 2015 delivery forecasts. *Aviation Week & Space Technology*, Dec 2014. URL https://aviationweek.com/defense/2015-delivery-forecasts#slide-8-field_images-1240791.